LATE-QUATERNARY PLUVIAL AND TECTONIC HISTORY OF PANAMINT VALLEY, INYO AND SAN BERNARDINO COUNTIES, CALIFORNIA

Thesis by

Roger Stanley Uhr Smith

In Partial Fulfillment of the Requirements

for the Degree of

Doctor of Philosophy

California Institute of Technology

Pasadena, California

1976

(Submitted August 3, 1975)

ACKNOWLEDGMENTS

I especially thank Dr. Robert P. Sharp, for supervising this thesis, and my wife, Suzan, for her forbearance during the gestation of this thesis and for typing its final draft. Drs. Arden L. Albee, Clarence R. Allen, Joseph H. Birman, George R. Rossman and George I. Smith ably served as members of the thesis committee.

Dr. Pierre Saint-Amand arranged for permission to do field work on Mojave Range "B" of the U.S. Naval Weapons Center, China Lake. Permission to collect samples in Death Valley National Monument was granted by Peter Sanchez.

Discussion and correspondence with many people have improved my understanding of the thesis problem, its context and its significance. In addition to those mentioned above and faculty and fellow Caltech graduate students, these include Jim Babcock, Roy Bailey, George Brogan, Clark Burchfiel, Malcolm Clark, Ronald Cooke, Greg Davis, Phil Durgin, Roger Hooke, Jim Kahle, Ken Lajoie, Glen Miller, Steve Moore, Ken Pierce, Bert Slemmons, Ted Snyder, Clyde Wahrhaftig, and participants in a Geological Society of America Reno to Los Angeles field trip through Panamint Valley in March, 1975. I appreciate their help and take sole responsibility for any misrepresentation of their views and the views expressed by others in the literature cited.

Costs of field work were largely defrayed by two Penrose Bequest Research Grants from the Geological Society of America. Funds for radiocarbon dating were provided by Dr. Sharp. Travel costs for defending the thesis were defrayed by the Geology Department, University

of Houston, whose facilities were used to complete the thesis. Graduate Teaching Assistantships supported the author during much of his tenure as a graduate student. All of this assistance is gratefully acknowledged.

Dedicated to the memory of my father,

H.T.U. Smith

ABSTRACT

Panamint Valley was filled to overflowing on five, possibly six, separate instances, fed largely by runoff from the Sierra Nevada discharged through Owens and Searles lakes. These high water levels are best represented by uplifted lake terraces and associated deposits at Pleasant Canyon on the west face of the Panamint Range, where shorelines at five, possibly six, levels have formed with respect to the level of Wingate Pass (present elevation 1977±1 feet) into Death Valley. The level of this sill seems to have been tectonically stable, but was permanently raised about 50 feet by a mudflow which poured into the pass during a long-lasting lake stage, herein named Gale Stage. Paired Gale-Stage shorelines, attributed to lake stands stabilized at pre- and post-mudflow sill levels are found throughout Panamint Valley. The lower shoreline is 1.26 times older than the higher, more prominent shoreline, based on 1.26 times greater tectonic deformation at most localities. On the rising range block at Pleasant Canyon, the higher shoreline seems superposed on the lower to form a composite shoreline at 2177±10 feet elevation. Shoreline elevations at Pleasant Canyon (and probable uplift they experienced) are: 2410±10 feet (480±25 feet); 2298±10 (368±25); 2265±10 (335±25); 2177±10 (247±25 to 200±11); 2127±10 (150±11); and 2040±40? (63±41?). If the long-term uplift rate has been constant, the age of each shoreline should be proportional to its height above its sill level. Relatively steady deformation rates throughout Panamint Valley are suggested by the constant proportion (1.26:1.00) of deformation between the older (lower) and younger (higher) Gale-Stage shorelines.

A radiocarbon age of 31,150±1400 B.P. on snail shells establishes a minimum age for the shoreline at 2127 feet. Extrapolation using steady uplift rates indicates the following youngest-possible ages (in thousands of years) for the other uplifted shorelines: 2410 ft: 100±17; 2298 ft: 77±14; 2265 ft: 70±13; 2177 ft: 52 to 42±7; and 2040 ft?: 14±10?. The probable age of each lake stage is about 20 per cent greater than its youngest possible age, a judgement based on correlation with the stages of Searles Lake (G.I. Smith, 1968).

The higher, younger Gale-Stage shoreline is prominent throughout Panamint Valley. Differential tectonic deformation of this feature amounts to about 370 feet, as established by a maximum elevation of 2190±10 feet on the central Panamint Range to a minimum of 1820±20 at Panamint Valley's north end. Deformation involves differential north-south warping of crustal block on both sides of the Panamint Valley and Ash Hill fault zones, which respectively define the east and west margins of Panamint Valley.

Right-lateral displacement of Quaternary features along the Panamint Valley fault zone exceeds their vertical offset. Sixty feet of right-lateral offset have occurred since desiccation of the last, low lake to occupy Panamint Valley (15,000±5,000 B.P.), and cumulative offset of a sheet of monolithologic (landslide?) breccia of Plio-Pleistocene age from its probable source in Wildrose Canyon may total 10,000 to 15,000 feet.

Panamint Valley is abruptly and massively closed at its north end, where valley-floor deposits appear to underthrust Mesozoic plutonic rocks of Hunter Mountain along a northwest-trending zone

which may represent the northwestward continuation of the Panamint Valley fault zone. Along the middle part of this reach of the zone, poorly-sorted (talus?) rubble of sound crystalline boulders underlies a 50 to 100-foot-thick zone of crushed crystalline rock which dips 17 to 35 degrees to the northeast beneath unshattered crystalline rocks. Thrusting may reflect a response to regional northwest-southeast right-lateral shear, possibly imposed upon classical Basin-Range bounding faults. The complex pattern of warping and faulting throughout the rest of Panamint Valley is also consistent with right-lateral shear, and the valley itself may have originated as a right-lateral "pull apart".

The unusually large volume of deposits along the 2177-foot shoreline suggests correlation with the Sierra Nevada Tahoe glaciation, which is distinguished by unusually large moraines. The small volume of 2127-foot shoreline deposits suggests correlation with the Tenaya glaciation, whose moraines are small. Thus the queried 2040-foot shoreline could represent the Tioga glaciation and the 2410-foot shoreline the Mono Basin glaciation. The 2265 and 2298-foot shorelines may represent early Tahoe events, suggesting that the Tahoe may be divided into early and late phases. Tentative ages of glaciations, based on correlation with pluvial events in Panamint Valley, are (in thousands of years B.P.): Mono Basin: 120±20; Tahoe (early): 92±15 to 78±15; Tahoe (late): 65±13 to 48±10; Tenaya: 38±6; Tioga?: 23±10?.

TABLE OF CONTENTS

Page

LIST OF ILLUSTRATIONS

LIST OF TABLES

1. INTRODUCTION 1

Purpose and Scope 1
Geography 2
Location and Access 2
Human Activity 2
Topographic Mapping and Aerial Photography 4
Climate 4
Flora and Fauna 6
Physiographic Setting 6
Geologic Setting 9
Tectonic Setting 12
Quaternary Geology 14
Sierra Nevada Glacial Chronology 14
The Owens-Manly Pluvial Lake System 14
Lake Panamint 21
Methods of Investigation 23
Geologic Mapping 23
Alluvial Mapping Units 24
Lacustrine Mapping Units 26
Criteria for Recognizing Shorelines 26
Criteria for Determining the Relative Ages of Shorelines 28

2. SOUTHERN PANAMINT VALLEY 30

Inlet and outlet of Lake Panamint 30
The inlet channel from Searles Lake 30
Lake sediments on valley floor near inlet 30
Wingate Pass 34
High Shorelines 45
Southernmost Panamint Valley 45
Southern Panamint Range 49
Slate Range 57
Correlation 57
Low shorelines 61
Tectonic deformation 63
Vertical movement 63
Lateral movement 65
The elevation of Wingate Pass during pluvial times .. 67

Page

3. CENTRAL PANAMINT VALLEY 71

High shorelines and lake deposits at Pleasant Canyon 71
Introduction 71
Nomenclature 78
Lacustrine succession and history of dissection 79
Deposits older than Gale Stage 82
Gale-Stage deposits and shorelines 85
Deposits younger than Gale Stage 93
High shorelines and lake deposits elsewhere on the central Panamint Range 96
South of Pleasant Canyon 96
North of Pleasant Canyon 100
High shorelines and lake deposits on the northern Slate Range and southern Argus Range 101
Introduction 101
Water Canyon 103
Shepherd Canyon 107
Bendire Canyon 107
Revenue Canyon (west of Ash Hill fault) 112
Revenue Canyon (east of Ash Hill fault) 113
Low shorelines 117
The Lake Panamint record in U.S. Geological Survey cores taken from south Panamint playa 117
Correlation 122
Lake-bottom sediments and lake-shore features .. 122
Shorelines 123
Tectonic deformation 124
Vertical movement 124
Lateral movement 127

4. NORTHERN PANAMINT VALLEY 128

High shorelines on the northern Argus Range 128
Ash Hill 128
Panamint Springs 133
North of Panamint Springs 133
High shorelines and lake deposits on the Wildrose segment 135
Introduction 135
Shorelines 137
Beach gravels 146
Dissection 148
Relative age 150
Absolute age 153

Page

High shorelines on the northern Panamint Range 155
Townes Pass Road 155
Lake Hill 155
Big Four Mine road (south) 160
Big Four Mine road (north) 164
Absolute age 167
Shallow lake stands 167
The Lake Panamint record in cores taken from north Panamint playa 168
Correlation 172
Tectonic deformation 173
Normal faulting 173
Warping 173
Folding 174
Thrust faulting 175
Right-lateral faulting 179

5. PALEOHYDROLOGY 182

Modern hydrology 182
Introduction 182
Precipitation 187
Runoff 197
Evaporation 199
Paleohydrology 204
The climate during pluvial times 204
The shallow late-Wisconsin lake in north Panamint Valley 207
Local runoff to southern Panamint Valley during pluvial times 212
The dependence of Lake Panamint's overflow on Sierra Nevada runoff 213
Runoff into Owens Valley during glacial times 213
Lake Manly not sustained by Sierra Nevada runoff 217

6. TECTONICS OF PANAMINT VALLEY 219

Summary of shoreline deformation 219
The small magnitude of isostatic deformation 221
Tectonic rates 226
Have uplift rates remained uniform through time? 227
The Sierra Nevada and elsewhere in California 227
Panamint Valley 229

Page

Quaternary right-lateral tectonics of Panamint Valley 233

7. PLUVIAL CHRONOLOGY AND CORRELATION 240

History of Lake Panamint 240
Bases for reconstruction 240
Composite lake history 243
Radiometric and extrapolated ages of lake stages 245
Youngest possible ages 245
Probable ages 248
Comparison with other pluvial-lake chronologies 251
Searles Lake 251
Lake Manly 252
Lakes Lahontan and Bonneville 254
Correlation with Sierra Nevada glaciations 256
Introduction 256
Relative duration of glaciations 256
Tentative correlation 259
Tentative ages of glaciations 262

APPENDIX A VALIDITY OF RADIOCARBON DATES ON CARBONATE MATERIALS 265

APPENDIX B PUBLISHED CORE LOGS FROM PANAMINT VALLEY 268

South Panamint Valley 268
SP-1 268
DH1,1a 269
DH3 271
North Panamint Valley 276
NP-1 276
NP-2 276
NP-3 277
DH2 278

REFERENCES CITED 282

LIST OF ILLUSTRATIONS

Figure		Page
1-1.	Political map of Panamint Valley and vicinity	3
1-2.	Topographic mapping of Panamint Valley.....	5
1-3.	Topographic map of Panamint Valley and vicinity.....	8
1-4.	Geologic map of eastern California.....	10
1-5.	Previously-published geological mapping of Panamint Valley.....	11
1-6.	Major pluvial-lake systems in the Great Basin.....	16
1-7.	The pluvial-lake system which sumped in Death Valley.....	18
1-8.	Late-Quaternary pluvial chronology of Searles Lake.....	20
1-9.	Area and volume of Lake Panamint as functions of lake-surface elevation.....	22
2-1.	Index map of Southern Panamint Valley and vicinity.....	31
2-2.	Garlock fault at south end of Panamint Valley.....	32
2-3.	Panamint Valley inlet channel.....	32
2-4.	Index map of southernmost Panamint Valley.....	33
2-5.	Dissected lake beds in southernmost Panamint Valley.....	35
2-6.	Lake beds on valley floor opposite Wingate Pass.....	35
2-7a.	Oblique air photo of Wingate Pass from west.....	36
2-7b.	Oblique sketch of Wingate Pass from west.....	36
2-8.	View up Wingate Wash, 4 mi. E of Wingate Pass.....	37
2-9.	View up Wingate Wash, 6 mi. E of Wingate Pass.....	37
2-10.	Geological map of Wingate Pass.....	39

Figure		Page
2-11.	View west through Wingate Pass.....	40
2-12.	View to NW from BM 1976 in Wingate Pass.....	41
2-13.	Lag deposit on south margin of Wingate Pass.....	41
2-14.	Typical sediments beneath Wingate Pass.....	42
2-15.	View to north across Wingate Pass.....	44
2-16.	Lake bench near Wingate Pass.....	46
2-17.	Lake gravel from bench in fig. 2-16.....	47
2-18.	Lake gravel on old monorail line.....	48
2-19.	Possible shoreline benches on northwest side of Hill 2200.....	50
2-20.	Geological map of southern Panamint Valley, Goler Wash south to 35° 45" N.....	51
2-21.	Nodose tufa mound near county line.....	52
2-22.	Geological map of southern Panamint Valley from Big Horn Canyon south to Coyote Canyon.....	54
2-23.	Geological map of area between Redlands and Manly Peak Canyons.....	55
2-24.	High shorelines at the mouth of Manly Pk Canyon.....	56
2-25.	Tufa and gravel at Manly Pk Canyon.....	56
2-26.	High shoreline at the mouth of Redlands Canyon.....	58
2-27.	High shorelines on the Slate Range south of Fish Canyon.....	59
2-28.	Low shorelines north of Redlands Canyon.....	62
2-29.	County line landslide.....	64
2-30.	Laterally-offset mudflow levees south of Manly Pk Canyon.....	66
2-31.	Possible lateral offset in older fan deposits.....	66

Figure		Page
2-32.	Fault(?) topography in northern end of Brown Mountain.....	69
3-1.	Index map of central Panamint Valley.....	72
3-2.	Diagrammatic sketch of the fluctuations in the level of Lake Panamint.....	73
3-3.	Index map of the region around Ballarat.....	74
3-4a.	Aerial view looking southeast toward lake shores and deposits north of Pleasant Canyon.....	75
3-4b.	Sketch of fig. 3-4a.....	75
3-5.	Geological map of the mouth of Pleasant Canyon.....	76
3-6.	Geological map of lake deposits on the north side of Pleasant Canyon.....	81
3-7.	Geological cross sections of lake deposits on the north side of Pleasant Canyon.....	83
3-8.	F_1 bench.....	84
3-9.	Lag boulders overlying F_4 gravel.....	86
3-10.	Foreset beds of basal Gale-Stage (G_1) gravel.....	88
3-11.	Deposit of G_2 gravel.....	90
3-12a.	Looking southwest at filled G_2 gully.....	92
3-12b.	Looking southwest at lower reach of G_2 gully.....	92
3-13.	Looking southwest at H_1 bar.....	95
3-14.	Geological map of the region between Middle Park and South Park canyons.....	97
3-15.	Profiles and correlation of shorelines on the central Panamint Range.....	98
3-16.	Geological map of region adjacent to lowermost Water Canyon.....	102
3-17.	Light-colored lake deposits from Water Canyon.....	104

Figure		Page
3-18.	Coquina, east end of deposits south of Water Wash	104
3-19.	Granitic lake gravel on the northeast side of volcanic hill 1960	106
3-20.	Geological map of the region between Shepherd Canyon wash and Bendire Canyon wash	108
3-21.	Cross sections of shorelines and lake deposits at Bendire Canyon wash	109
3-22.	Marl in lake deposits south of Bendire Canyon wash	111
3-23.	Geological map of the region near the mouth of Revenue Canyon	114
3-24.	Shoreline on Argus Range south of Revenue Canyon	115
3-25.	Shorelines east of Revenue Canyon	116
3-26.	Typical worn gravel on beach east of Revenue Canyon	116
3-27.	Map of deformation of highest low shoreline in central and southern Panamint Valley	118
3-28.	Map of south Panamint playa, showing the location of drill holes	120
3-29.	Graphic logs of cores from south Panamint playa	121
3-30.	Possible explanation for development of prominent Gale-Stage shoreline at Pleasant Cyn	125
4-1.	Index map of northern Panamint Valley	129
4-2.	Geological map of the north end of Ash Hill	130
4-3.	High shoreline at extreme south end of Ash Hill	131
4-4.	Geological map of region near Panamint Springs	134
4-5.	Index map of the Wildrose segment	136

Figure		Page
4-6.	Aerial view across the drainage divide between the north and south basins of Panamint Valley.....	138
4-7.	Geological map of the southeastern Wildrose segment.....	139
4-8.	Geological map of the northwestern Wildrose segment.....	140
4-9.	Northwest-southeast profiles of shorelines along the Wildrose segment.....	141
4-10.	Cut shoreline on the northern Wildrose segment.....	142
4-11.	Lake gravel overlying tufa on the northern Wildrose segment.....	142
4-12.	Lacustrine gravel deposits on northern Wildrose segment.....	144
4-13.	Dendritic tufa of the middle shoreline.....	145
4-14.	Steeply-dipping gravel of the lower shoreline.....	147
4-15.	Map of sources and distribution of gravel along the Wildrose segment.....	149
4-16.	Lake gravels of two ages north of Wildrose-Trona road.....	151
4-17.	Cemented lake gravel.....	152
4-18.	Geological map of region near Townes Pass Road.....	156
4-19.	Geological map of Lake Hill and the Big Four segment.....	158
4-20.	Shorelines on Lake Hill.....	159
4-21.	Aerial view of the southern Big Four segment.....	161
4-22.	Looking south across Station 2 of E.L. Davis.....	162
4-23.	Graphic logs of cores from north Panamint playa.....	170

Figure		Page
4-24.	Aerial view of Hunter Mountain from the southwest	176
4-25.	Looking west along thrust zone	176
4-26.	Geological map of thrust faults along the southern flank of Hunter Mountain	177
4-27.	Thrust zone marked by crushed crystalline rock	178
4-28.	Stereogram of right-lateral fault offset near Townes Pass road	180
4-29.	Aerial view to the southeast along the Panamint Valley fault zone	180
5-1.	Topographic setting of Panamint Valley's hydrologic basin	183
5-2.	Panamint Valley's hydrologic basin	184
5-3.	Map of precipitation in Panamint Valley and vicinity	186
5-4.	Topography of, and precipitation in, the Wildrose Canyon watershed	190
5-5.	Gage capture of incident precipitation as a function of wind speed	191
5-6.	Precipitation in Panamint Valley and vicinity as a function of elevation	192
5-7.	Evaporation in Panamint Valley and vicinity as a function of elevation	201
5-8.	The relationship between elevation and enclosed area for Panamint Valley's subbasins	209
5-9.	The relationship between evaporation and the runoff required to sustain shallow lakes in north Panamint Valley	210
5-10.	The pluvial-lake system which sumped in Death Valley	215
6-1.	Map of high shoreline deformation	220

Figure		Page
6-2.	Map of low-shoreline deformation.....	220
6-3.	North-south profiles of high-shoreline deformation.....	220
6-4.	The Owens-Searles-Panamint-Manly pluvial lake system.....	222
6-5.	Map of Panamint Valley showing mean water depth of the Owens-China-Searles-Panamint-Manly lake system.....	225
6-6.	Elevation of earliest Gale-Stage shoreline as a function of elevation of latest Gale-Stage shoreline.....	230
6-7.	Comparison between the pattern of uplifted Pleasant Canyon shorelines and the pattern of ostracod zones in core DH1,1a.....	232
6-8.	Diagrammatic map showing possible opening of Panamint Valley as a right-lateral "pull apart.".....	236
7-1.	Construction of the composite pluvial chronology of lake Panamint.....	241
7-2.	Youngest possible ages of lake stages.....	246
7-3.	Correlation of the pluvial chronologies of Lake Panamint and Searles Lake.....	249
7-4.	Comparison of pluvial chronologies of lakes Lahontan, Bonneville and Panamint.....	255

LIST OF TABLES

Table		Page
1-1.	Pleistocene glacial succession of the Sierra Nevada	15
3-1.	High and intermediate stands of Lake Panamint at Pleasant Canyon	80
4-1.	Published Radiocarbon Ages from the Wildrose Segment	154
4-2.	Published Radiocarbon Ages from Station 2 of E.L. Davis	165
4-3.	Published Radiocarbon Ages from Station 4 of E.L. Davis	166
4-4.	Published Radiocarbon Ages of the Shallow Lake in North Panamint Valley	169
5-1.	Monthly distribution of precipitation in Wildrose Canyon	188
5-2.	Seasonal variation in mean wind speed in Wildrose Canyon	195
5-3.	Evaporation rates at 5750 ft. elevation in Wildrose Canyon	200
5-4.	Evaporation data used in plotting figure 5-7	203
5-5.	Seasonal distribution of mean temperature in Panamint Valley and Vicinity	205
7-1.	Youngest possible, and probable, ages of stages of Lake Panamint	250
7-2.	Tentative ages of late-Pleistocene Sierra Nevada glaciations compared with published ages	261

CHAPTER 1

INTRODUCTION

Purpose and Scope

This study deals with the late Quaternary history of the succession of pluvial lakes which intermittently occupied Panamint Valley, with the relationship of this succession to the histories of other pluvial lakes in the western Great Basin and the glacial succession in the Sierra Nevada, and with the record and nature of late-Quaternary tectonic deformation within Panamint Valley. Because the valley's watershed is small and arid, pluvial lakes could only have filled Panamint Valley to overflowing when increased runoff from the Sierra Nevada caused the Owens-Searles lake chain to overflow into Panamint Valley. If glaciations are the result of cool, wet climates, periods of pluvial maxima should coincide with glacial maxima. Thus the age of episodes within the glacial succession of the Sierra Nevada can be established if the corresponding events in the pluvial history of Panamint Valley can be dated.

The nature of late-Quaternary tectonism in Panamint Valley can be determined from shoreline deformation, and it may be representative of tectonism elsewhere in the Basin-and-Range province where corresponding indicators are lacking. Fortunately, uplift has preserved older shorelines and lake deposits from obscuration by later younger lakes, so the pluvial history can be recovered in greater detail than would otherwise be possible. Furthermore, the amount of uplift is indicative of the approximate age of each shoreline where multiple shorelines are present.

This study involved a field reconnaissance of that part of Panamint Valley below 2500 feet elevation, designed to determine the location of shoreline remnants and to seek structural, stratigraphic and lithologic criteria by which they can be correlated. Localities where several shorelines of different ages could be differentiated

were mapped in detail.

Geography

Location and Access

Panamint Valley, California, is in the southwestern Great Basin at 35° 30' to 36° 30' N and 117° to 117° 30' W (fig. 1-1). It is a deep, north-trending valley separated by the Panamint Range from Death Valley to the east, by the Argus and Coso ranges from Owens Valley to the west, and by the Slate Range from Searles Valley to the southwest.

Panamint Valley is connected by paved highways to Trona (16 miles south), Lone Pine (45 miles west) and Furnace Creek (50 miles east) (fig.1-1). A network of gravel roads, dirt roads and jeep trails makes most parts of the area accessible except during wet weather. The southern part of Panamint Valley lies within the U.S. Naval Weapon Center's Mojave Range "B" and is closed to public entry without special permission. It is most easily reached by a dirt road which enters the south end of Panamint Valley from the paved Navy road from China Lake into Mojave Range "B". Much of the Panamint Range lies within Death Valley National Monument, where collecting of geologic specimens is prohibited without official permission.

Human Activity

Permanent habitation within Panamint Valley is sparse. In addition to habitation at Ballarat, Panamint Springs Indian Ranch, and Onyx Mine on the valley floor, an undetermined number of Park Rangers, hippies and prospectors inhabit canyons of the Panamint and Argus ranges. Although retail commercial activity is limited to the store at Ballarat and the gas station, motel and cafe at Panamint Springs, metal mines and a cat-litter plant are intermittently active. The limestone quarry at Revenue Canyon continually produces about 100,000 tons per year for the chemical plants at Trona (Gray,

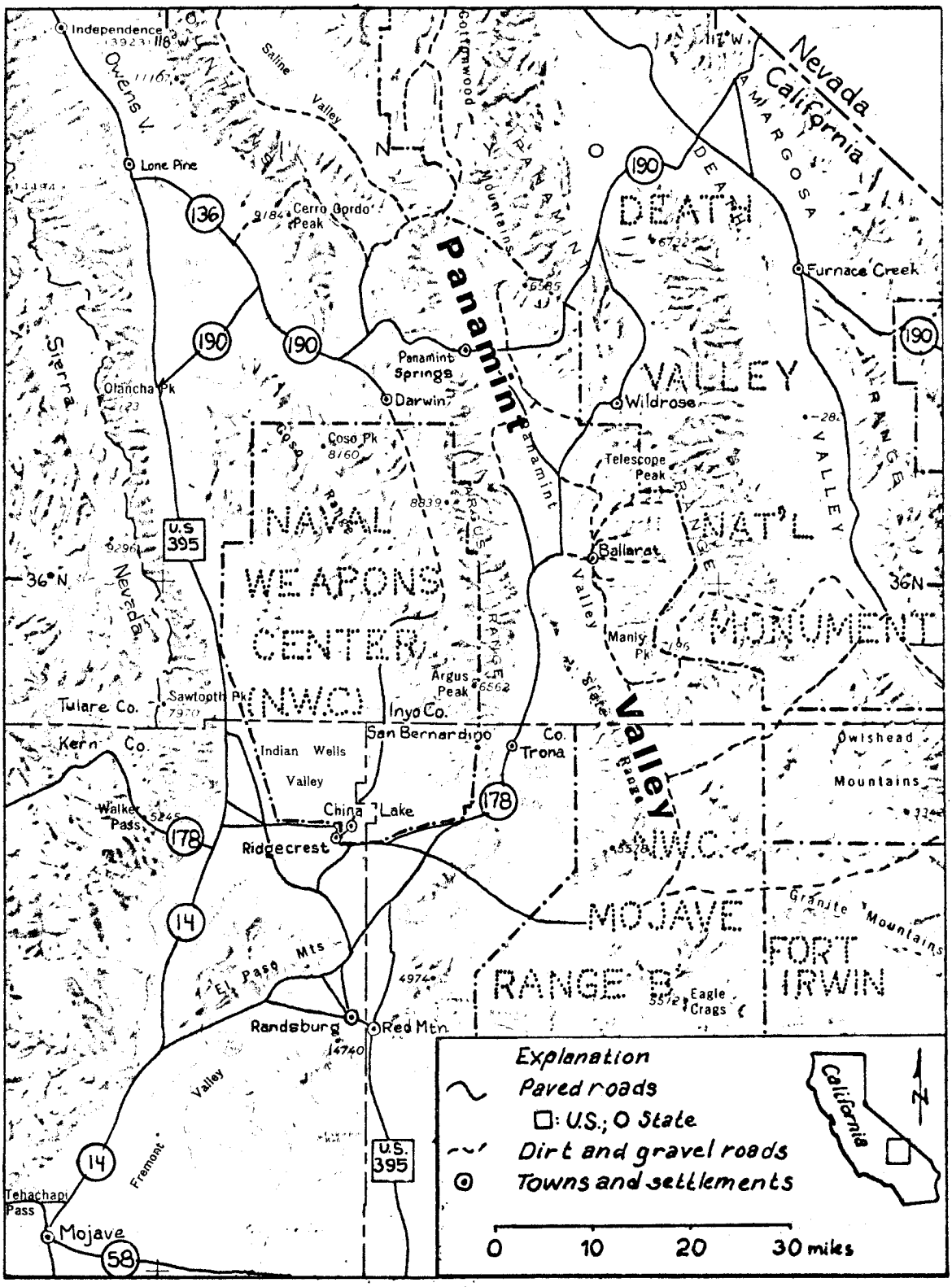

Figure 1-1. Political map of Panamint Valley and vicinity.

1962, p.5). A so-called Onyx Mine sells decorative slabs of Tertiary (?) travertine to rockhounds.

Topographic Mapping and Aerial Photography

The entire area tributary to Panamint Valley has been topographically mapped at 1:62,500 scale on modern, 15-minute quadrangles by the U. S. Geological Survey during 1948-1954 (fig. 1-2). The contour interval on the Telescope Peak sheet is 80 feet but it is 40 feet on the other quadrangles. The maps were prepared from aerial photographs taken during the late 1940's at scales of 1:37,400 to 1:56,100. The extreme northern and southern ends of the valley were photographed from high altitude by the U.S. Air Force during the late 1960's at scales of 1:120,000 to 1:140,000. Both types of photography are available from the U.S. Geological Survey.

Climate

The climate of Panamint Valley is arid with hot summers and cool winters. Annual precipitation probably averages three to four inches on the valley floor but increases with altitude in the Panamint Range at about one inch per thousand feet. About two thirds of recorded precipitation falls from Pacific maritime storms during November through April, and the rest comes from summer thundershowers fed by moist air from the gulfs of Mexico and California. The distribution of precipitation is erratic in both space and time, and wet years typically receive three to four times the precipitation of dry years. Winter precipitation of the mountains comes largely as snow, which may linger until May.

Temperatures in Panamint Valley are probably intermediate between those recorded at Death Valley (elevation -179 ft) and at Trona (elevation 1695 ft, fig. 1-1). During July and August, the daily maximum temperature averages 103-105° F at Trona and 113-114° at Death Valley, but nighttime minima average about 30°F cooler at both places. This pattern of sharp diurnal variations in temperature

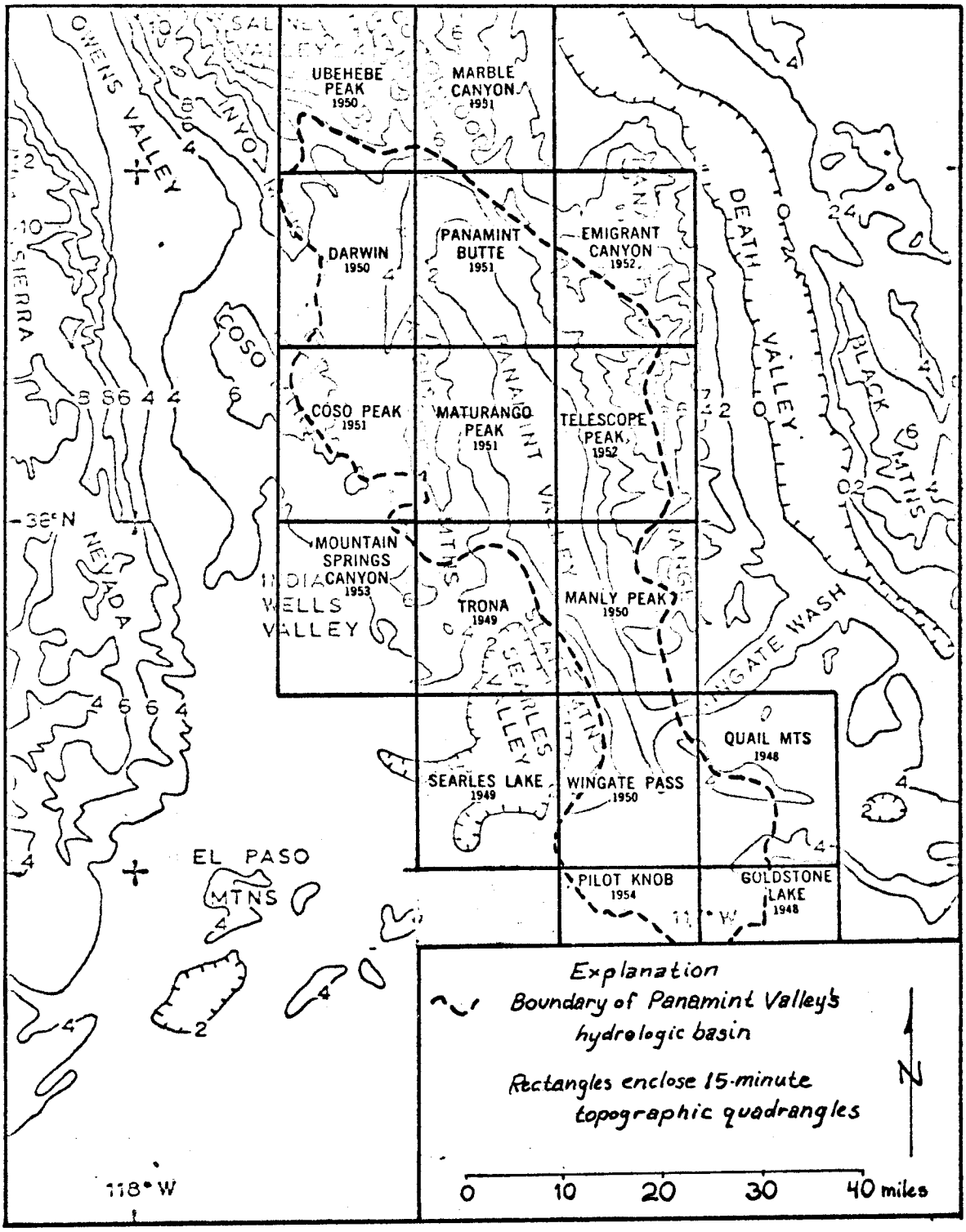

Figure 1-2. Topographic mapping of Panamint Valley.

persists throughout the year: December and January maxima are about 60°F and 65°F at Trona and Death Valley, respectively, with nighttime minima about 25°F cooler (U.S. Dept. Commerce, 1967-71).

In this climatic enviroment, evaporation is rapid and runoff infrequent. The mountain streams maintain perennial flow only where ground water is forced to the surface, and this flow typically reinfiltrates a short distance downstream. Intense, localized storms, usually during the summer, seem to be the principal source of significant runoff to the valley floor. The modern climate and hydrology of Panamint Valley and the pluvial counterparts will be described in greater detail in Chapter 5.

Flora and Fauna

Vegetation is sparse, largely creosote bush on the valley floor and the adjacent alluvial and mountain slopes. Places where the water table is high, as near Ballarat and for five miles north, are marked by groves of mesquite and a dense growth of other preatophytes. In the mountains, the sagebrush zone starts at 4000-5000 feet elevation and grades into pinyon-juniper woodland at 6000-7000 feet; Joshua trees are locally abundant in sandy soils in the sagebrush zone.

The only large animals seen in the area are coyotes and the ubiquitous feral burros.

Physiographic Setting

The Panamint Range possesses greater topographic relief than any other in the Basin and Range physiographic province. The crest of the range culminates in Telescope Peak, elevation 11049 feet,

which rises from -282 feet in Death Valley to its east and from 1021 feet in Panamint Valley to its west (fig. 1-3). Much of the rest of the range rises 6,000 to 8,000 feet above Panamint Valley, and the other bordering ranges are nearly as high--the Argus Range rises 6,000 to 7500 feet along the west margin and the Cottonwood Mountains 6,000 feet above its north end. This high relief moderates only along the southwestern valley margin, which lies 3,000 to 3500 feet below the crest of the Slate Range.

Elevated remnants of subdued topography characterize the physiography of some of the uplands bordering Panamint Valley; these include much of the area between Owens Valley and the Argus Range and parts of the Cottonwood and northern Panamint ranges. Radiometric dating of volcanic rocks (Evernden et al, 1964, p. 164, 177, 189; Hall, 1971, p. 45-8; Lanphere, Dalrymple and Smith, 1975) suggests that these upland surfaces of gentle topographic relief need not be the remnants of a regionally-continuous Pliocene erosion surface as proposed by Hopper (1947, p. 401, 415-6) and Maxson (1950, p. 101-3).

The physiography of Panamint Valley is dominated by tectonic landforms rather than by lacustrine features. Fresh fault scarps abound along both east and west valley margins and reach hundreds of feet in height. The steep, high planar front of the southern Panamint Range has been interpreted as a rilled fault scarp (Maxson, 1950, p. 106). These tectonic landforms are easily discerned within the coarseness of 40-foot contours, which only locally reveal the subtler lacustrine landforms, mostly beach cliffs and beaches.

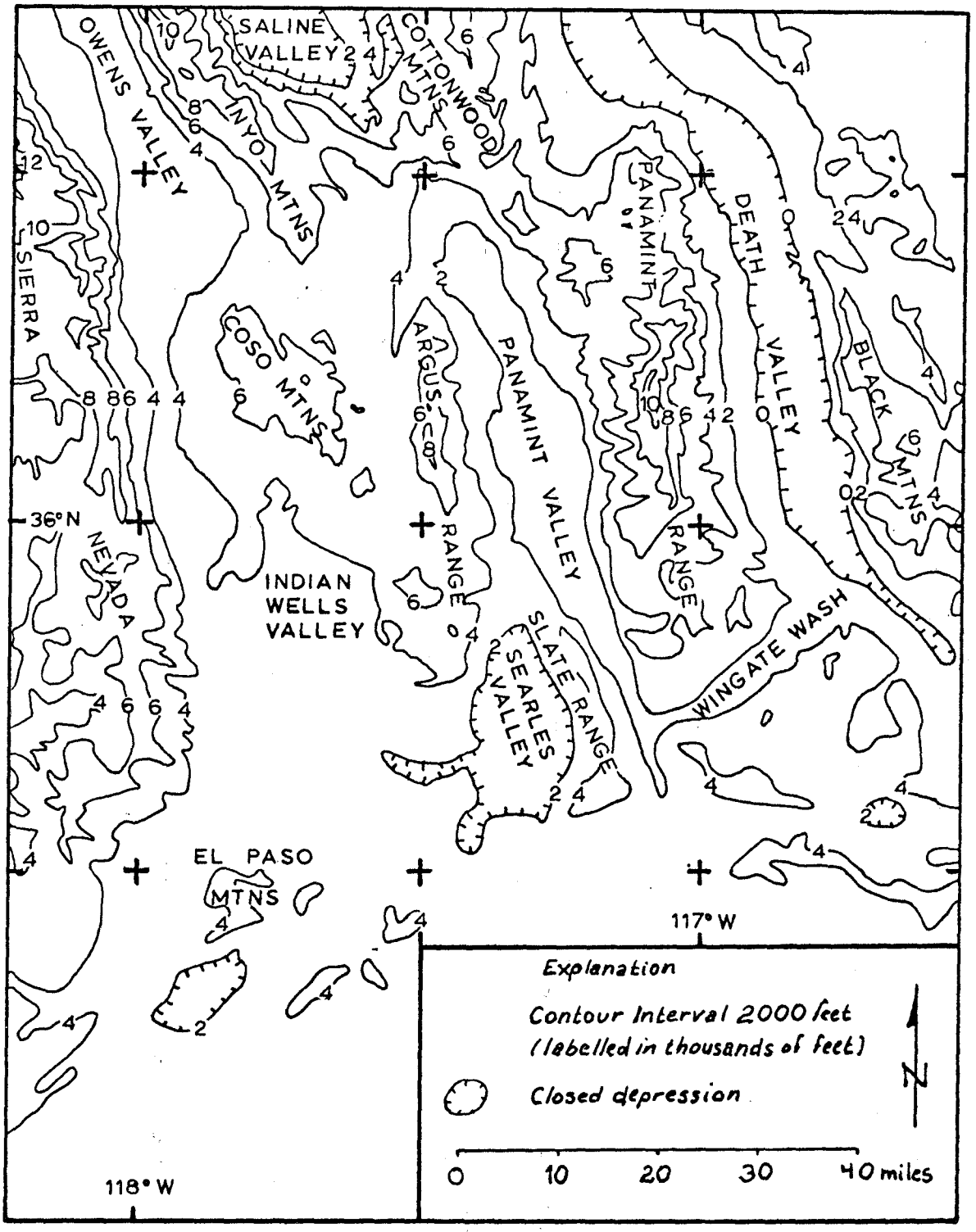

Figure 1-3. Topographic map of Panamint Valley and vicinity.

Geologic Setting

Panamint Valley lies on the boundary between a largely-Precambrian geologic terrane to the east and a terrane of Paleozoic rocks pervasively intruded by Mesozoic plutons to the west (fig. 1-4). Both terranes are overlain by late-Cenozoic volcanic rocks and continental sediments which are generally thin but locally reach 10,000 feet in thickness (Hall, 1971, p. 5). Faulting, which has continued since late-Tertiary time, is responsible for delineating the modern closed valley and for the large amount of topographic relief between the valley and its bordering ranges.

All of the area within Panamint Valley's watershed has been mapped geologically, much of it at scales of 1:48,000 and 1:62,500; the largest-scale published map for each part of the valley is shown on Figure 1-5. Except for the northern part of the area, much of this mapping is of a reconnaissance nature and variable in quality.

Much of the previous geological mapping of Panamint Valley is not shown on Figure 1-5 because of antiquity, small scale or lack of publication, for example, theses. Ball (1907) mapped a large area, mostly of southwestern Nevada, which included part of the northern Panamint Range. Murphy (1932) prepared a generalized map of the central Panamint Range at the latitude of Telescope Peak. Hopper (1947) mapped a swath six miles wide extending from Owens Valley to Death Valley at the latitude of Darwin. Wright and Troxel (1954) made a reconnaissance map in conjunction with a road log along the highway from Trona to Emigrant Canyon. Knox (1963) and Thompson (1963)

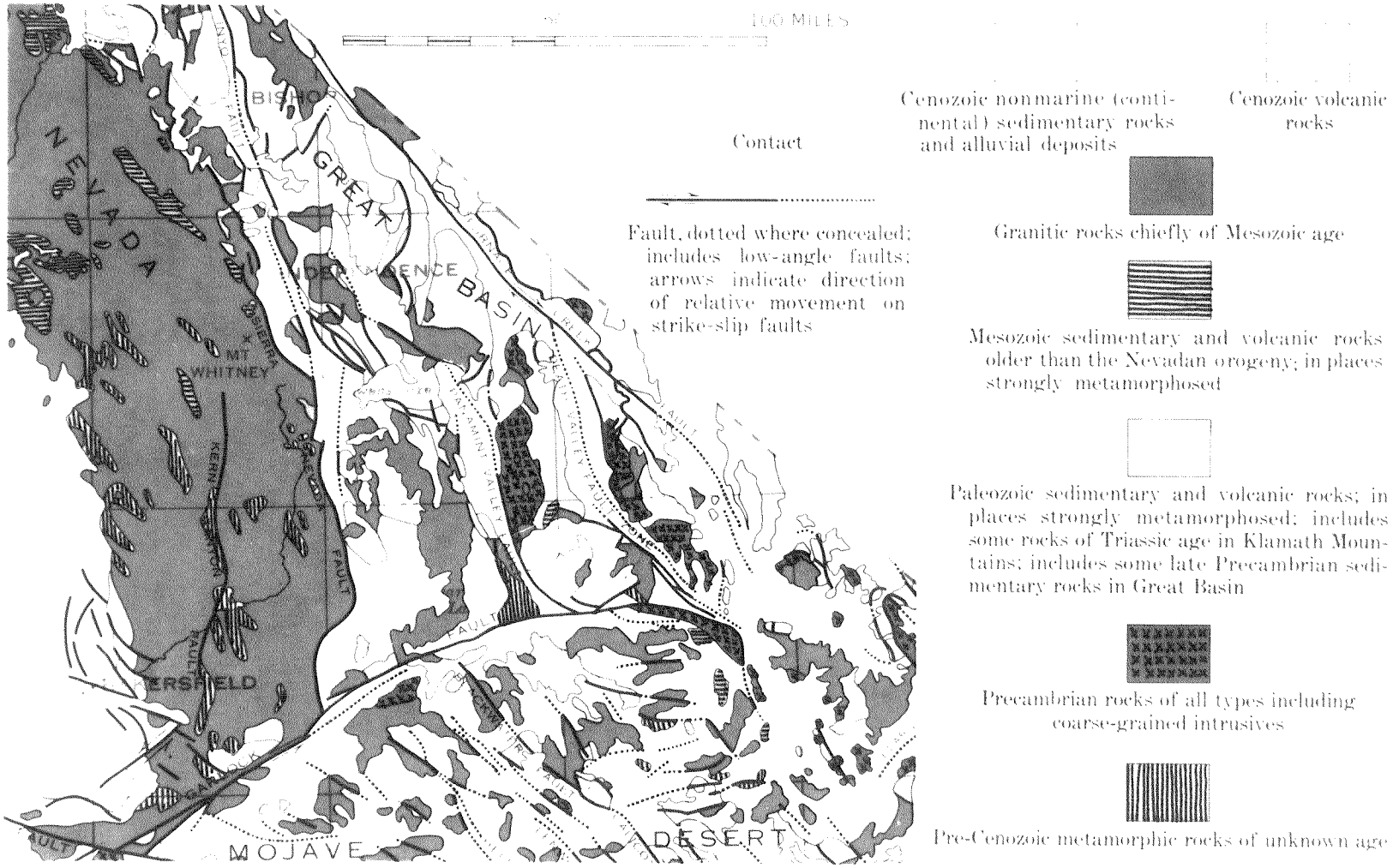

Figure 1-4. Geologic map of eastern California (after U.S. Geol. Surv. Map I-512).

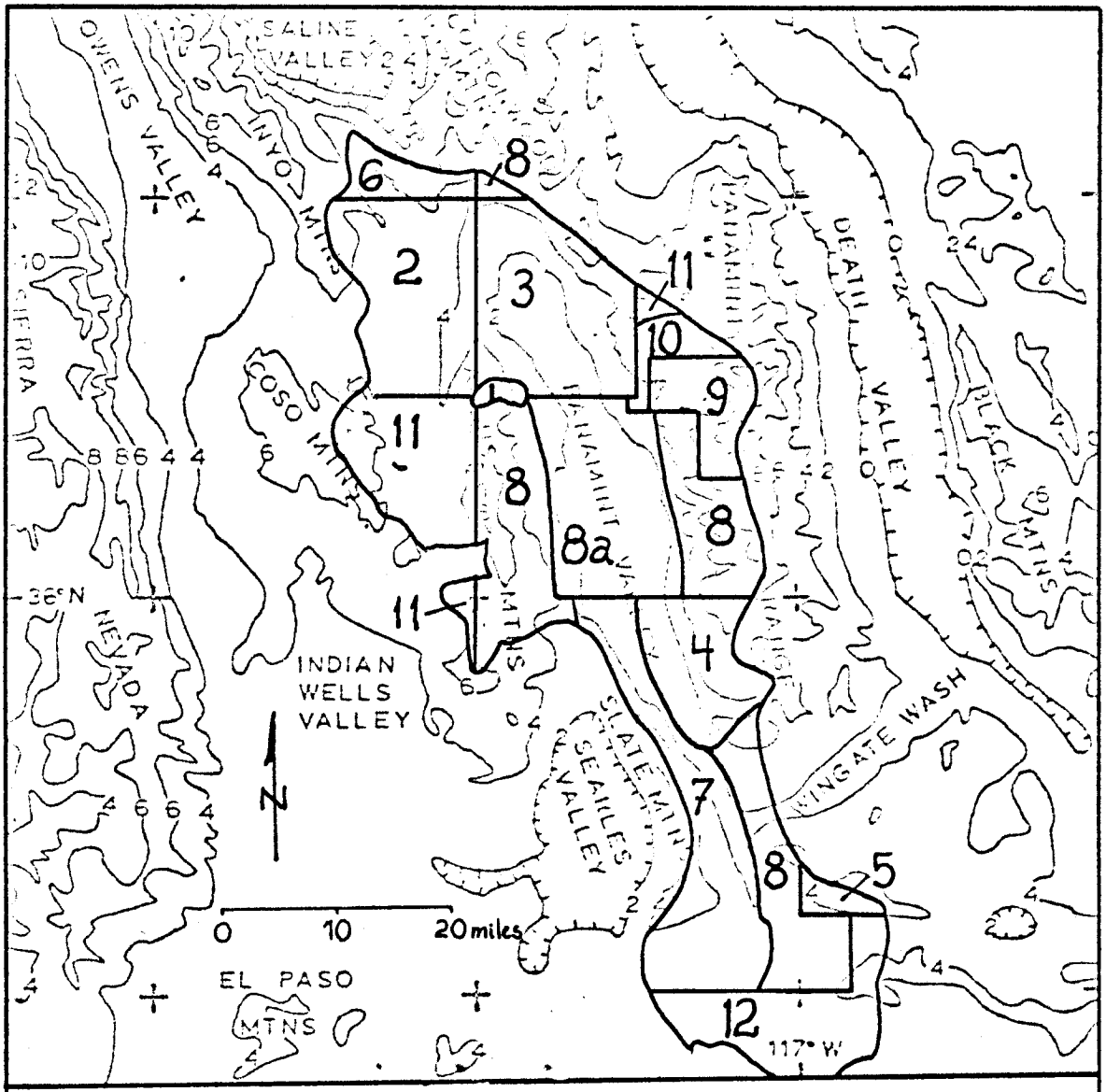

KEY:

1:24,000
1) Hall & Stephens, 1963

1:48,000
2) Hall & Mackevett, 1962
3) Hall, 1971
4) Johnson, 1957
5) Muehlberger, 1954

1:62,500
6) McAllister, 1956
7) Smith et al, 1968
8) Moyle, 1969
8a) " , after Carranza, 1965

1:125,000
9) Murphy, 1932

1:220,000
10) Hopper, 1947

1:250,000
11) Jennings, 1958
12) Jennings et al, 1962

NOTE: Only the largest-scale, most-recent mapping of each area is shown.

Figure 1-5. Previously-published geological mapping of Panamint Valley.

mapped the Cenozoic and pre-Cenozoic deposits, respectively, of Emigrant Canyon and produced a joint thesis map, scale 1:24,000. Albee (1971) compiled the geology of the Telescope Peak quandrangle at 1:62,500 based on unpublished work by him and theses by Lanphere (1962) and McDowell (1967, 1974). Carranza's (1965) thesis map at 1:24,000 covers a large area about Ballarat in reconnaissance fashion. James A.Babcock (1975) is now mapping volcanic rocks west of the Argus Range for a Ph.D. thesis at the University of California at Santa Barbara and Stephen C. Moore (1974) is mapping the Argus Range for a Ph.D. thesis at the University of Washington.

Tectonic Setting

Panamint Valley lies in the southwest corner of the Basin-and-Range structural province, an area of active lateral and vertical faulting. The valley's south end butts against the Garlock fault, whose cumulative left-lateral displacement totals 30 to 45 miles (G.I. Smith, 1962; Michael, 1966; Dibblee, 1967, p. 115; and Smith and Ketner, 1971).

Both vertical and right-lateral movement seem to characterize the displacement along the major north-to northwest-trending faults which lie within Panamint Valley and its neighbors, Death Valley to the east and Owens Valley to the west. A large right-lateral component of the movement along the Death Valley-Furnace Creek fault zone is generally accepted (Curry, 1938; Noble and Wright, 1954; Hill and Troxel, 1966; Burchfiel and Stewart, 1966; Wright and Troxel, 1967, 1970; Stewart, 1967; Stewart, Albers and Poole, 1968, 1970;

and McKee, 1968). The preponderance of evidence favors a right-lateral sense of the strike-slip movement which has accompanied vertical movement along the Sierra Nevada frontal fault (Bateman, 1961), but a left-lateral sense has been offered as an alternative (Pakiser, Kane and Jackson, 1964, p. 55-6). Right-lateral movement along the Panamint Valley fault zone was recognized by Hopper (1947, p. 399) and Maxson (1950, p. 107), and along its southward extension (the Brown Mountain fault) by Clark (1973). Others who have suggested that this lateral movement might have large magnitude have not cited supporting evidence (Hill, 1954, p. 10; Saint-Amand et al, 1963, p. 88; and G.I. Smith et al, 1968, p. 57).

The seismicity of Panamint Valley has been low during historic times. The maps of epicentral locations during 1932-1972 (Hileman, Allen and Nordquist, 1973, p. 55-65) show no events of Richter magnitude greater than four centered in the valley, although several events of magnitude four to five were reported from the adjoining ranges. The earthquake of 4 November 1908 in the Death Valley region (Townley and Allen, 1939, p. 151) was assigned a queried location in the south-central Panamint Range and a queried magnitude of 6 1/2 by Richter (1958, p. 469).

The low level of seismic activity during historic times is probably not representative of the level over longer periods of time. Young-looking fault scarps abound in the valley, and the average rate of offset of late-Quaternary features may reach 4.5 feet per thousand years (vertical) and may exceed six feet per thousand years (right-lateral).

Quaternary Geology

Sierra Nevada Glacial Chronology

Blackwelder (1931) established the classical basis for the chronology of the Pleistocene glaciation along the eastern escarpment of the Sierra Nevada. From oldest to youngest, he (p. 870, 918-9) named the glacial stages McGee, Sherwin, Tahoe and Tioga, which he correlated respectively with the Nebraskan, Kansan, "Iowan" (early Wisconsin), and Late Wisconsin glacial stages of the midcontinental United States. He suspected the presence of deposits correlative with the Illinoian stage but was unable to differentiate them from the others.

More recent work has been ably summarized by Wahrhaftig and Birman (1965, p. 305-310), Bateman and Wahrhaftig (1966, p. 158-165) and Porter (1971, p. 315-318); see Table 1-1). Sharp and Birman (1963) recognized two additional stages: Mono Basin (between Sherwin and Tahoe) and Tenaya (between Tahoe and Tioga). Neither stage is recognized in many canyons; the Tenaya because of the small volume of its deposits and possible overriding by Tioga glaciers; the Mono Basin because of overriding by Tahoe glaciers and burial beneath their extremely massive moraines.

The Owens-Manly Pluvial Lake System

Large, interconnected pluvial-lake systems filled many of the closed basins between the Sierra Nevada and the Wasatch Range during some parts of Pleistocene time (fig. 1-6). Although the lake system

Table 1-1.

Pleistocene glacial succession of the Sierra Nevada.

Midcontinent Correlative	Sierra Nevada Stage	Age (years B.P.)	References
		9,990±800	Adam, 1967
Wisconsin	Tioga		Blackwelder, 1931
	Tenaya		Sharp & Birman, 1963
	Tahoe		Blackwelder, 1931
		60,000±50,000 90,000±90,000	Dalrymple, 1964
		62,000±13,000[1]	Bailey et al, (in press)
Illinoian?	Mono Basin		Sharp & Birman, 1963
		126,000±25,000[1]	Bailey et al, (in press)
? ? ?	Casa Diablo[1]	400,000±40,000?	Curry, 1971
		710,000	Dalrymple. Cox & Doell, 1965; Sharp, 1968
Kansan?	Sherwin		Blackwelder, 1931
Nebraskan?	McGee		Blackwelder, 1931
		2.6 m.y.	Dalrymple, 1963
? ? ?	Deadman Pass	2.7-3.1 m.y.	Curry, 1966

[1] Bailey, Dalrymple and Lanphere (in press) ran new K-Ar dates on basalt flows which overlie and underlie the type Casa Diablo till; these new dates lead them to suggest that Casa Diablo till is equivalent in age to Mono Basin till. Curry's (1971) 400,000-year age of the type Casa Diablo till was based on K-Ar dates of 441,000±40,000 on the underlying flow and 280,000±67,000 on the upper flow, respectively redated at 126,000±25,000 and 62,000±13,000 by Bailey et al (in press).

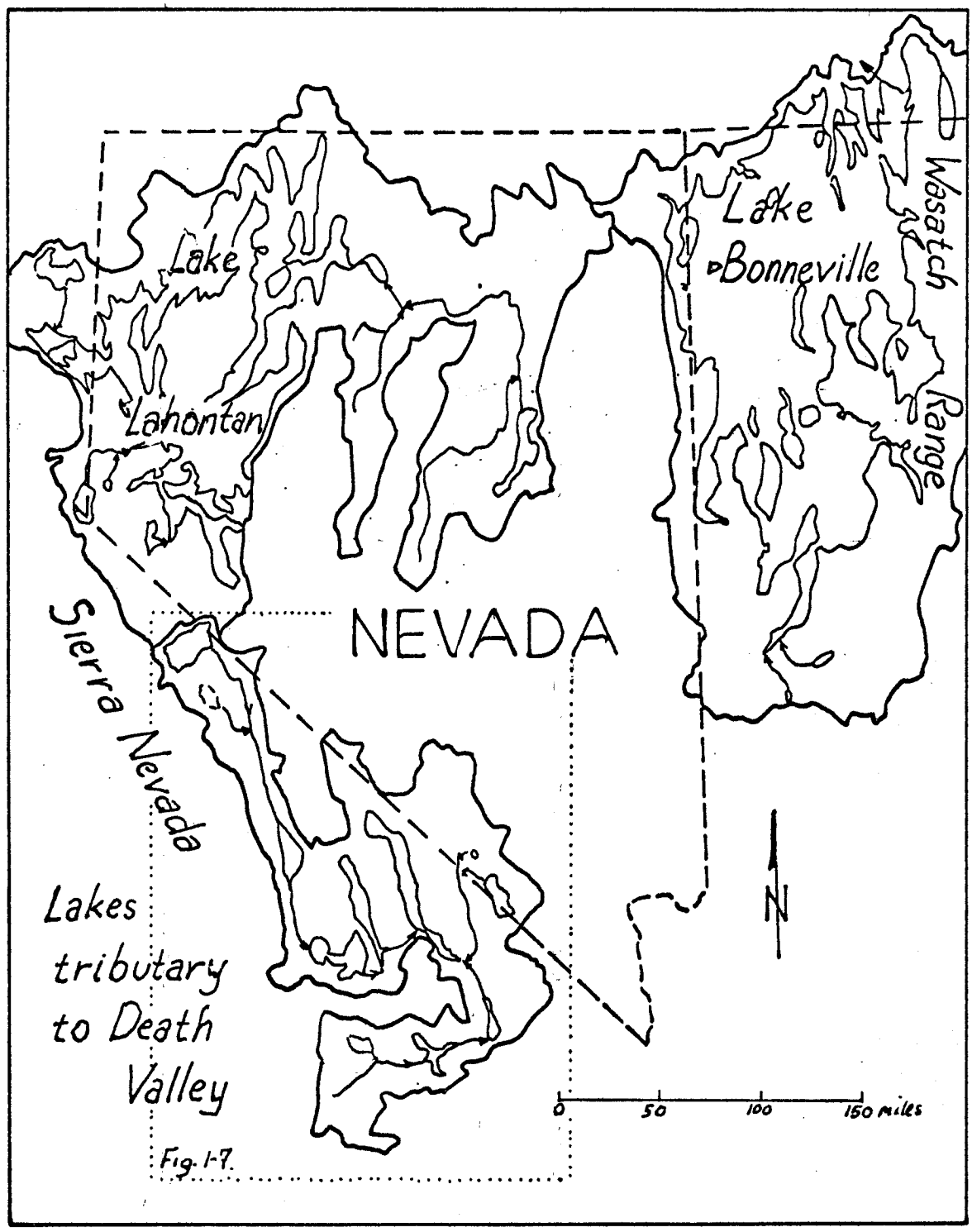

Figure 1-6. Major pluvial-lake systems in the Great Basin. (Modified from Morrison, 1965b, p.266).

sumping in Death Valley never coalesced into a single lake, its drainage area was exceeded only by that tributary to lakes Lahontan and Bonneville (fig. 1-6). The historic remnants of this lake system are Owens Lake (now dry from water diversion) and Mono Lake.

During Tahoe time, water overflowing from Lake Russell (ancestral Mono Lake, Putnam, 1949, p. 1295-6) is judged to have reached Death Valley as Owens, China, Searles and Panamint lakes filled in succession and spilled into the next basin in line; Lake Panamint overflowed into Lake Manly (Blackwelder, 1933) in Death Valley (fig. 1-7). Lake Manly also received discharge from the Amargosa River, draining southwestern Nevada, and from the Mojave River, including lakes Manix and Mojave, draining the San Bernardino Mountains south of the Mojave Desert.

The pluvial lakes in Searles, Panamint and Death valleys were first shown on Russell's (1885, pl. 1) map of "Quaternary Lakes of the Great Basin," but no mention of them was made in the text. Bailey (1902, p. 12, 16-17) postulated that all these lakes were desiccational remnants of an enormous Quaternary lake, covering most of the Mojave Desert. Campbell (1902, p. 20) noted the high shorelines of Lake Panamint near Ballarat but did not recognize that they stood at an elevation near that of the basin's lip. Lee (1906, p. 7) cited the first evidence for Owens Lake's having formerly overflowed southward into Indian Wells Valley. Free (1914, p. 39-41) likewise recognized that Searles Lake had been fed by overflow of Owens Lake, but thought that Lake Panamint had been a small lake fed mainly by local runoff, which never approached overflow levels and only

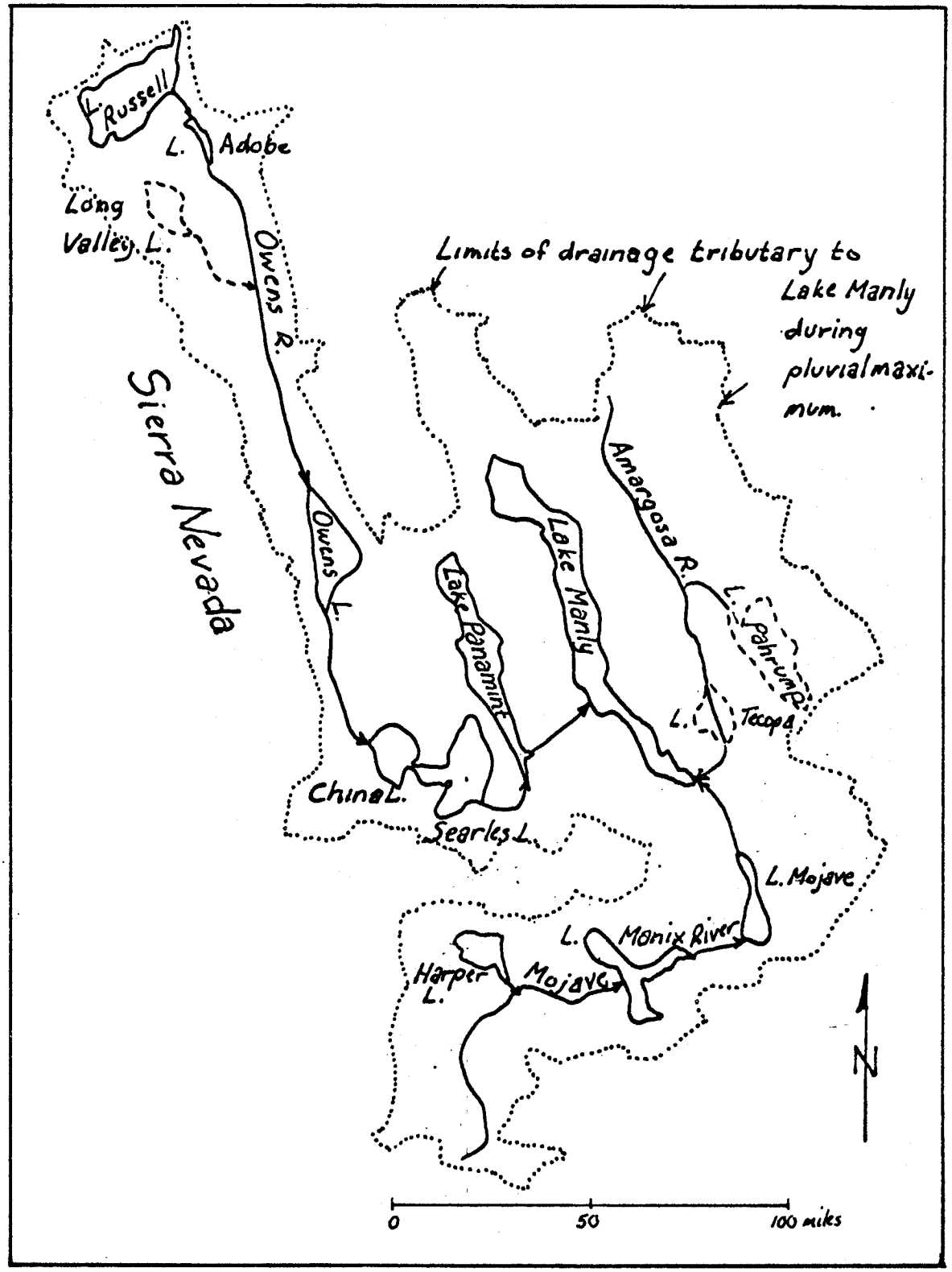

Figure 1-7. The pluvial-lake system which sumped in Death Valley (Modified from Snyder et al, 1964).

briefly received discharge from Searles Lake.

In what is still the most detailed study of many aspects of this lake system, H.S. Gale (1915, p. 315-7) proposed that Lake Panamint has overflowed into Death Valley via Wingate Pass, whose elevation coincided with that of shorelines farther north. Although Gale did not visit Wingate Pass, Thompson (1929, p. 186-7) accepted the likelihood of overflow through the pass after finding rounded gravel both there and downstream in Wingate Wash. In the first thorough description of Lake Manly in Death Valley, Blackwelder (1933, p. 468-9) agreed that it was fed by overflow from Lake Panamint during Tahoe time, but thought that its major tributary had been the Amargosa River. In later papers, Blackwelder (1941, 1954) persisted in this belief because he found evidence for overflow of Searles Lake only during Tahoe time. During Tioga time, he thought that the depth of Lake Panamint was only 200 feet (compared with 950 feet during Tahoe time, when it overflowed) and that the depth of Lake Manly was 400 feet (compared with 600 feet during Tahoe time). However, recent work by G.I. Smith (1968, p. 307) has shown that Searles Lake did indeed overflow during Tioga time. From the earlier studies of the Searles Lake cores and their radiocarbon ages, as reported by Flint and Gale (1958) and Stuiver (1964), and supplemented by his own exhaustive work on the exposed lake deposits, G.I. Smith has constructed a curve of the fluctuations of the level of Searles Lake for the last 130,000 years (fig. 1-8).

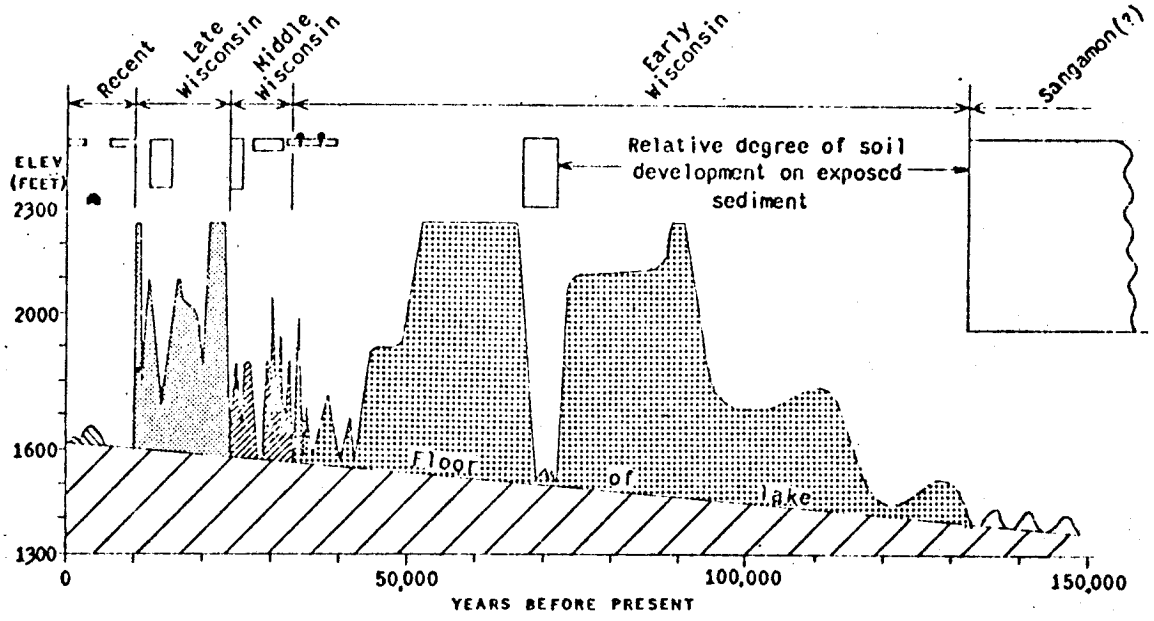

Figure 1-8. Late-Quaternary pluvial chronology of Searles Lake (after G.I. Smith, 1968, p.300).

Lake Panamint

Lake Panamint was a deep lake in a flat-bottomed basin with gentle to steep sides. Its paleobathymetry can be approximated by the topography of the modern basin below 1977 feet elevation. On this basis, the lake's area and volume increased with surface elevation as shown on Figure 1-9. At its overflow level, its depth exceeded 950 feet, its area was about 300 square miles and its volume about 92 million acre feet. The lake basin is divided into north and south basins by a drainage divide at about 1715 feet elevation. This contour encloses an area about three times greater in the south basin than in the north and a volume about 12 times greater (fig. 1-9).

Lake Panamint could have had long-enduring stands at any of three stable elevations: 1) low stands, elevation <1165 feet in the south basin and 1540-1560 feet in the north basin; 2) Intermediate stands in the south basin, elevation about 1715 feet; and 3) high stands, elevation 1977±1 feet.[1] The elevation of the low stands depended on how large a surface of evaporation could be sustained primarily by local runoff. Evidence for low stands is seen in both south and north basins. The elevation of the intermediate stands was controlled by overflow of Sierra Nevada water from the south basin into the north basin through the 1715-foot divide between them. The stability of this lake level depended on the ability of evaporation

[1]Early high lake stands were probably stabilized at the level (1930 ± 15 feet) of the bedrock lip beneath Wingate Pass, whose level seems to have been raised to its present elevation by a mudflow which buried the bedrock lip during the early history of the high lake stand which cut the most prominent shoreline.

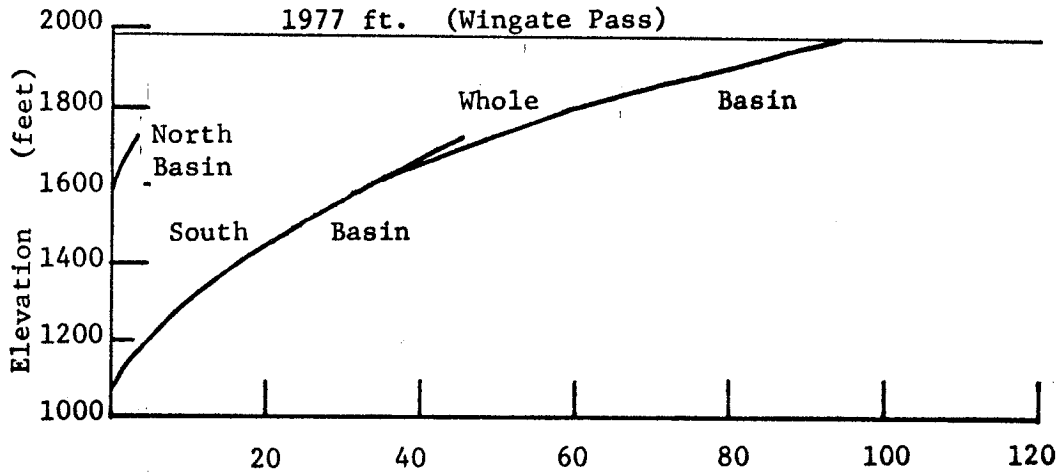

(computed from modern topography using methods of Hutchinson, 1957, p. 166.)

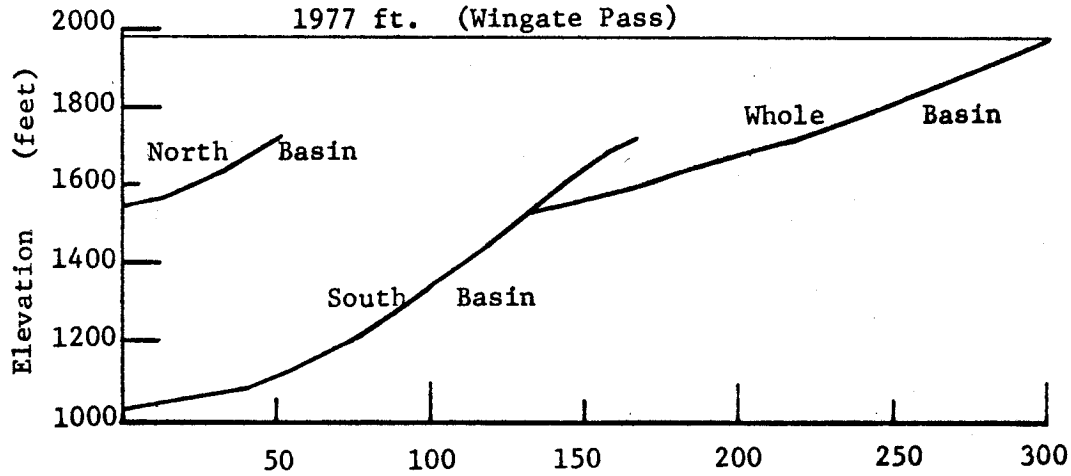

(Planimetered from modern topography)

Figure 1-9. Area and volume of Lake Panamint as functions of lake-surface elevation.

to consume all the water which overflowed into the north basin. Because of the delicacy of this required balance between inflow and evaporation, this level was probably not continuously occupied but, rather, intermittently occupied by both rising and falling lakes. The evidence for shorelines attributable to this level is largely equivocal. The elevation of the high stands was controlled by overflow of runoff into Death Valley (Lake Manly) through Wingate Pass. Shorelines traceable to this level are the most prominent ones seen in Panamint Valley today.

Methods of Investigation

Geologic Mapping

Mapping was primarily on aerial photographs enlarged to scales of 1:12,500 to 1:18,700, although some areas were mapped on contact prints of these photos, at scales of 1:37,400 and 1:47,200. Some detailed mapping was on low-altitude oblique air photos and ground photos taken by the author. In general, little attention was devoted to Quaternary deposits which predated or postdated the lake deposits. Approximately four months were spent in field study.

Shoreline elevations were determined primarily by a combination of altimetry and hand levelling to bench marks. Paulin altimeter readings, taken in closed traverses, were corrected to a calibration temperature of 60°F using methods adapted from Lahee (1952, p. 480-483). Most elevations are considered accurate to $\pm$10 feet, and some are accurate to $\pm$2-3 feet. Some shoreline elevations were interpolated from 40-foot contours of the 15-minute topographic

maps; these are considered accurate to ±20 feet generally and locally to ±10 feet. Elevations of some shorelines on gentle, even slopes were interpolated to greater precision by using a Salzman projector to transfer their mapped trace on air photos onto a 1:24,000 enlargement of the topographic map. Other information was transferred from the photos to the 1:24,000 map using a combination of inspection and the Salzman projector. Page-sized geologic maps of critical areas, scale 1:24,000, are interleaved with the thesis text.

Alluvial Mapping Units

Three alluvial units are mapped: 1) Oldest fan gravel (Qog) into which high shorelines have been cut; 2) Older fan deposits (Qof), which bear no trace of shorelines at high elevation (1800 to 2200 feet) but which underlie mounds of nodose tufa at intermediate elevation (1500 to 1800 feet); and 3) Fan deposits (Qf) which postdate all lake deposits. Relationships between alluvial and lacustrine units are best seen along the foot of the Argus Range (figs. 3-15, 3-19, 3-22).

The surface of the oldest fan gravel (Qog) is mantled by well-developed desert pavement of stones deeply stained by desert varnish. Granitic boulders are rare on the surface, even if abundant in the subsurface. The pavement is interrupted by streaks of unvarnished granule-and smaller-sized clasts which occupy gentle swales at the heads of broad, shallow, closely-spaced dendritic drainage channels. These fine-grained clasts may have been eroded from disintegrating

granitic clasts in the pavement adjacent to the swales. Spots of similar debris, mostly ten feet across, may be the remnants of disintegrated granitic boulders. East of the Ash Hill fault, the oldest fan gravel has been dissected to depths of 40 to 80 feet by streams heading entirely within the oldest gravel, and to depths of several hundred feet by seemingly-antecedent streams heading in the Argus Range to the west.

The surface of older fan deposits (Qof) is in most places mantled by well-developed desert pavement of deeply-varnished stones. Granitic boulders are locally abundant on the surface, whose older parts display (in less pronounced form) the streaks and spots of finer clasts which characterize the surface of the oldest gravel (Qog). The surface of the older fan deposits has been dissected to depths of less than 20 feet by streams heading within the unit, and parts of the surface retain degraded distributary channels of the original fan. Locally (eg, fig. 3-19, NE 1/4 sec 34, T 21 S, R 43 E), mounds of nodose tufa, which elsewhere overlie older fan deposits, have been buried beneath gravel whose surficial appearance is identical with that of the older fan deposits (Qof).

The surface of fan deposits (Qf) is topographically irregular with abundant cobbles and small boulders lying on the surface rather than within it. Older segments present a smoother appearance with poorly-developed desert pavement of slightly-varnished stones. Original fan channels are numerous and prominent on the surface of this unit. Alluvium in modern stream channels is included in this unit.

Lacustrine Mapping Units

Lacustrine units are mapped solely on the basis of lithology except at Pleasant Canyon, where stratigraphic relationships allow the relative ages of units to be determined. Four lithologies of lacustrine deposits are recognized: 1) Tufa (t); 2) gravel (g); 3) sand (s); and 4) marl (m). Three different types of tufa are locally mapped: lithoid (t_l); dendritic (t_d) and nodose (t_n). Where each unit completely covers the ground surface, its extent is mapped; scattered remnants of each unit are indicated by a symbol within parentheses (eg, scattered lithoid tufa and rounded gravel on a beach are indicated by (t_l, g)).

Criteria for Recognizing Shorelines

Cut shorelines are best identified by: 1) a broad, gently-sloping topographic bench surmounted by a steeper slope; 2) presence of dendritic and/or lithoid tufa on these benches; 3) presence of rounded and/or sorted gravel; and 4) local presence of a boulder and cobble lag along the bench beneath colluvium. The cut bench is partly masked, along most high shorelines, by a wedge of later colluvium, analogous to the alluvial coverhead on marine terraces. The surface of this colluvial deposit typically slopes basinward at 2.5° to 6°, compared to basinward slope of the underlying cut surface of only 2 to 4 degrees. The cut surface is exposed, if at all, only in gullies or at the distal edge of the colluvial deposit. At the base of the beach cliff, the colluvial wedge typically is 5 feet thick. The surmounting beach is usually 15 to 40 feet high,

and its surface has been degraded to a slope between 8 and 24 degrees.

Where present, lithoid and dendritic tufa occupy only a narrow vertical range, which extends no higher than 5 feet below the nip between the beach and beach cliff and no lower than 20 feet below the nip. This tufa typically contains some fresh-water snail shells and forms rinds up to a foot thick around boulders. Some encased boulders have disintegrated from within these tufa rinds. The tufa rinds are thickest near the sharp upper boundary of their vertical range and thinner downslope toward the lower boundary of their range. This range should represent the lake's photic zone if lithoid and dendritic tufa are formed in association with algal growths as suggested by Scholl (1960, p. 426-7). On some heavily-colluviated slopes the distinctiveness of tufa as float suggests the presence of buried beach benches. Locally the hummocky topography of tufa causes it to project through the thin distal margin of a colluvial wedge.

Rounded gravel is seen only on some of the high benches, being generally lacking from narrow benches perched on precipitous slopes. In places, it can be seen only because the colluvial blanket has been dissected down to the beach level. Because well-rounded gravel is generally lacking in present stream beds debouching into the valley, it is regarded as a product of reasonably long-enduring processes within the surf zone along the lake shore. Deposits of rounded gravel typically have a loose, sandy matrix and moderate sorting by layers. Such features are lacking in the angular gravels of both

ancient and modern fan deposits. In some places, beds of rounded beach gravel interfinger with beds of sand, silt and marl which locally can be seen to contain snails, ostracods and/or diatoms. In other places, steeply-dipping foreset and backset gravel beds are found within constructional features such as bars.

Many of the foregoing criteria are not, by themselves, unequivocal evidence for a lake stand, but in combination they carry considerable weight. Usually, only the beaches of the most-prominent shoreline display all the features described. Other high stages have been identified using at least two of the criteria. The low shorelines generally lack both tufa and rounded gravel, but their freshness makes them easier to identify than the high shorelines.

Criteria for Determining the Relative Ages of Shorelines

Three criteria are used for determining the relative ages of the various shorelines and associated near-shore deposits: 1) Stratigraphic relationships; 2) Degree of tectonic deformation; and 3) Degree of erosion and colluviation. Stratigraphic relationships between deposits associated with shorelines of the various stages are rarely found, but at Pleasant Canyon they confirm the relative ages postulated from the degree of tectonic deformation, erosion and colluviation, as well as providing evidence for substages within the lake's overflow stages. The degree of tectonic deformation can be used only where two or more shorelines at different elevations exist in close proximity; it is based on several assumptions which may locally lead to erroneous results. The degree of erosion and

colluviation is used mainly to relate the ages of the very oldest and very youngest shorelines to the age of the most-prominent high shoreline.

CHAPTER 2

SOUTHERN PANAMINT VALLEY

Inlet and Outlet of Lake Panamint

The Inlet Channel from Searles Lake

Water spilling southeastward from Searles Lake circled the south end of the Slate Range, crossed Pilot Knob Valley and then flowed north across the Garlock fault into the south end of Panamint Valley (fig. 2-1, 2-2). The inlet channel north of the fault has a representative width of less than 200 feet, a bouldery bottom and only slightly incises adjoining fan surfaces (fig. 2-3). The channel gradient is about 12 feet per mile down to 2000 feet elevation and then steepens to about 35 feet per mile between 2000 and 1660 feet elevation where the channel is entrenched 40 to 60 feet below the surface of the lake beds which mantle the valley floor. The gentler gradient of the channel's upper reach may be relict from the pluvial channel graded to the overflow level of Lake Panamint.

Lake Sediments on Valley Floor near Inlet

Dissected lake beds are continuously exposed on the valley floor within a swath about a mile wide extending 7 miles north from hill 2200 to hill 1800 opposite Wingate Pass (fig. 2-4). Their gently-sloping upper surface descends northward from slightly above 1960 feet (1.5 miles north of hill 2200) to 1720-1760 feet (opposite Wingate Pass). The slope of this surface is probably very nearly

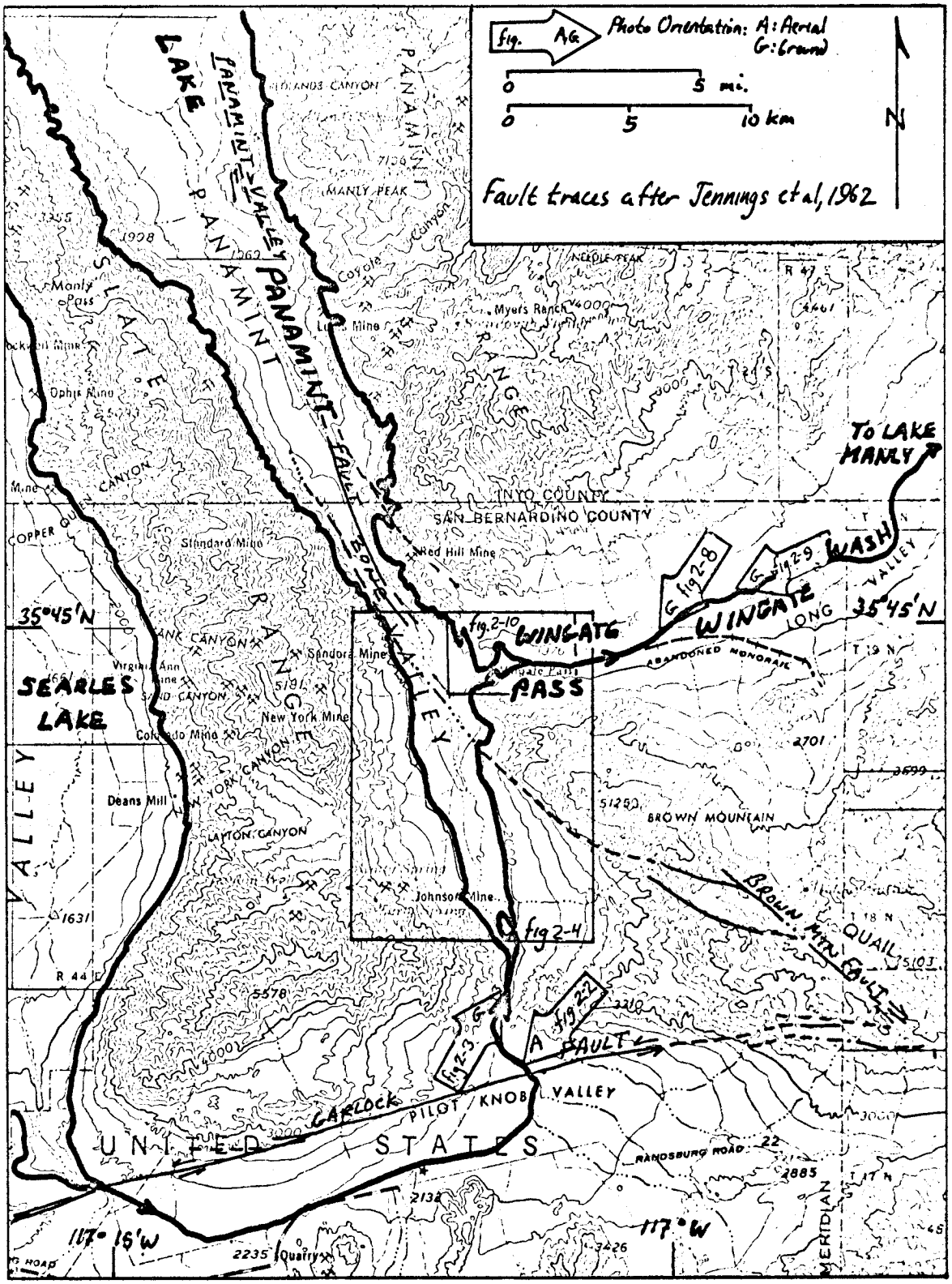

Figure 2-1. Index map of Southern Panamint Valley & vicinity.

Figure 2-2 Garlock fault at south end of Panamint Valley.
Looking southwest across Panamint Valley inlet channel into Pilot Knob Valley. Ground trace of Garlock fault after Clark (1973).

Figure 2-3 Panamint Valley inlet channel.
Looking northeast down the broad, bouldery channel with water ponded in it at lower right; stream gradient about 12 ft/mi. Location about 2 miles north of Garlock fault. Brown Mountain forms the left skyline.

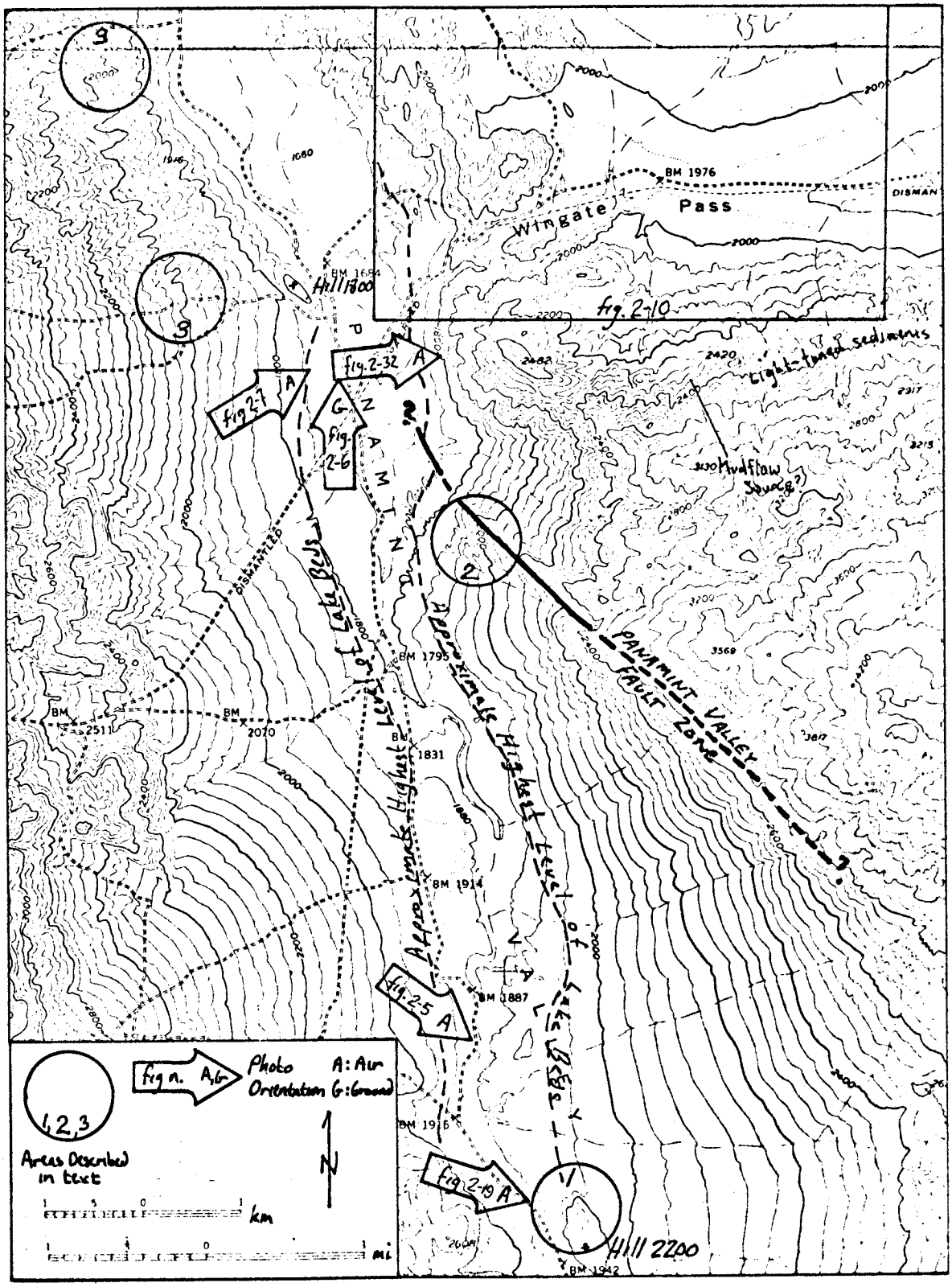

Figure 2-4. Index map of southernmost Panamint Valley.

that of the original depositional surface.

The deposits in the swath's southern half are typically fine-grained, indurated grayish mud overlain by a subequal thickness of well-sorted fine-grained sand which may represent a prograding delta, although foreset bedding has not been seen (fig. 2-5). Mud predominates in the deposits in the northern half of the swath, where the lower elevation of the valley floor permits greater water depth than in the southern half (fig. 2-6). Thin beds of poorly-sorted sand and granules interbedded in deposits of both parts of the swath probably represent recessional phases of the lake. Erosion before a later transgression is suggested by the low-angle unconformity within the deposits shown in Figure 2-6. Traces of meandering channels, which now seem to be filled with lake deposits, may indicate dissection during a still-earlier episode of dissection. These deposits have been studied only in reconnaissance fashion, and a detailed history comparable to that derived from the inlet stratigraphy of Searles Lake (G.I. Smith, 1968) has not been worked out.

Wingate Pass

Wingate Pass, elevation 1977 $\pm$ 1 feet, is the lowest gap in the mountains which encircle Panamint Valley (figs. 2-1, 2-4, 2-7a,b). It lies at the head of Wingate Wash, an ephemeral, northeast-flowing tributary of Death Valley. The upper part of this wash is broad (100-300 feet) and alluviated (fig. 2-8). Its gradient is fairly gentle (17 ft/mi) for the first 5 miles, but steepens progressively downstream to nearly 150 ft/mi as the channel becomes more incised

Figure 2-5. Dissected lake beds in southernmost Panamint Valley. Thirty feet of sand here overlie 20 feet of mud; this stratigraphy is typical for the area. Highest lake beds (middle distance) lie at 1960 ft. elev., 70 feet above wash in foreground. This view looks southeast, about five miles south of Wingate Pass.

Figure 2-6. Lake beds on valley floor opposite Wingate Pass. This knob, elev. 1720-1760 ft., is predominantly mud. A low-angle unconformity within the right-hand spur is not visible in this view, looking north.

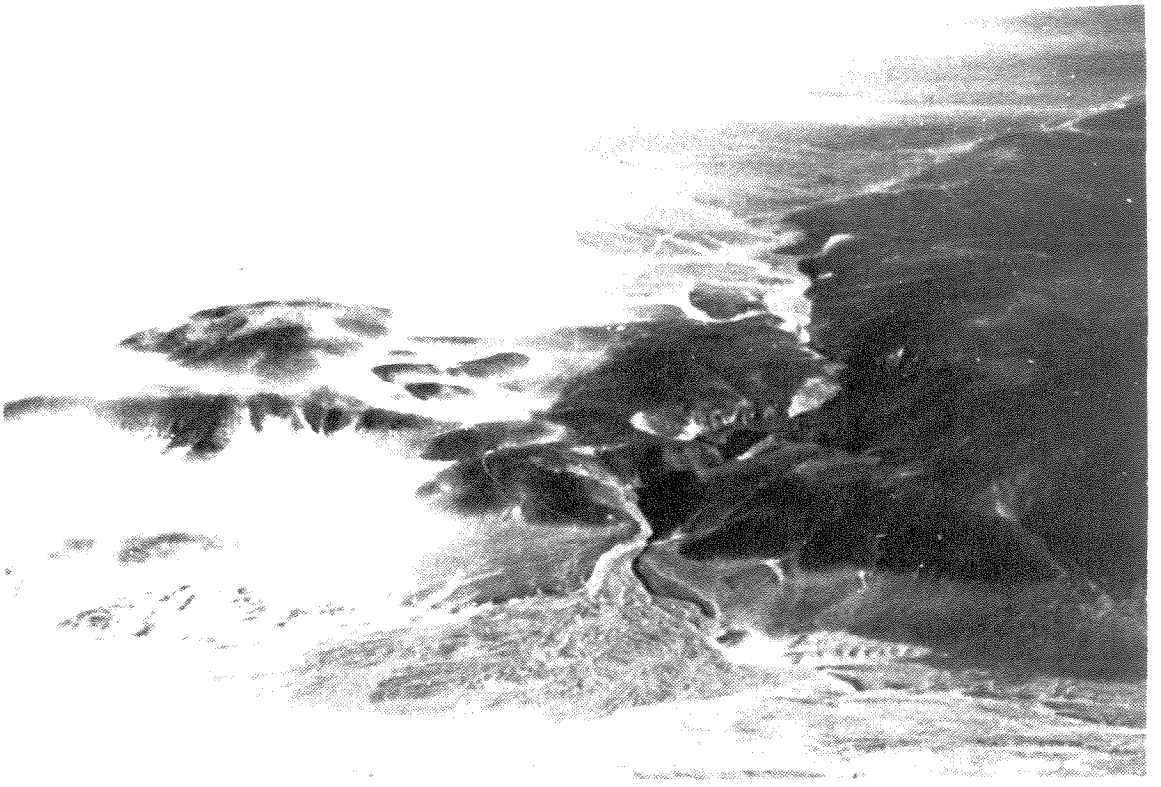

Figure 2-7a. Oblique air photo of Wingate Pass from west.

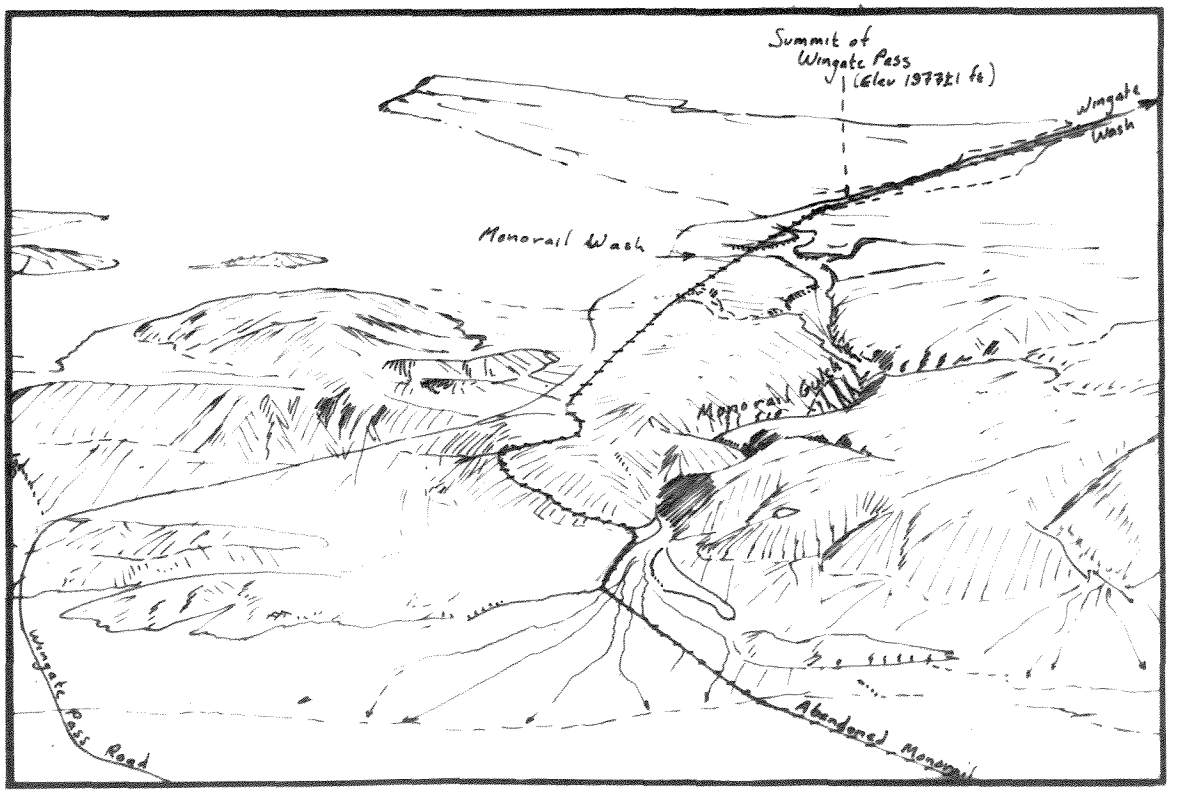

Figure 2-7b. Oblique sketch of Wingate Pass from west.

Figure 2-8. View up Wingate Wash, 4 mi. E of Wingate Pass.
Note the broadness of the wash (200-300 feet), the abundance of fine deposits and the absence of any single well-defined channel. Grade is about 17 ft/mi. Brown Mountain forms the left skyline.

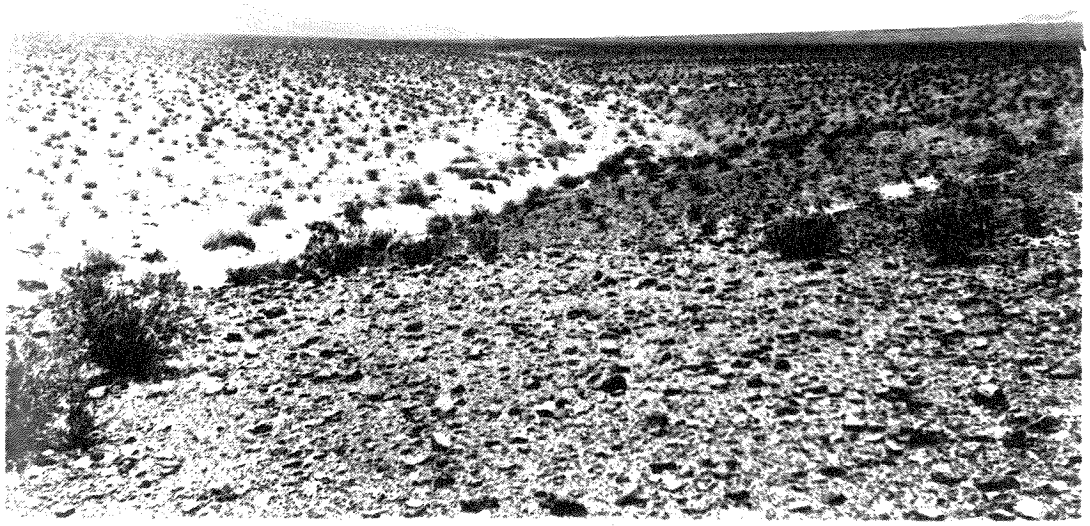

Figure 2-9. View up Wingate Wash, 6 mi. E of Wingate Pass.
Note that the wash has become narrower and more incised than in fig. 11, 2 mi upstream. Grade is about 30 ft/mi. The subrounded volcanic clasts in the foreground resemble those in Wingate Pass but are part of an older unit which antedates pluvial runoff through Wingate Pass.

and narrows to 100 feet (fig. 2-9). Water from the west side of the pass now flows westward into Panamint Valley through the sharply-incised gulch of Monorail Wash (herein named), much of whose gradient is steeper than 100 ft/mi.

The summit of Wingate Pass lies within a broad, slightly-sinuous, flat-bottomed channel about 400 feet wide between low, subdued banks 5 to 10 feet high (figs. 2-10, 2-11). This channel is the westward extension of Wingate Wash. Younger alluvium from tributaries to the wash fills the eastern part of the channel. The floor of the channel is mantled by a veneer of subrounded pebbles, cobbles and small boulders which may represent a lag deposit formed during channel erosion, but lag cobbles also cover the slopes along and above the channel margins (fig. 2-13). The floor of the pass slopes gently west for about 300 feet west from the summit to the brink of an abrupt five-foot drop into a modern, cross-cutting wash tributary to Monorail Wash (fig. 2-12).

The materials composing the floor and walls of the channel are lithologically distinct from the subangular fluvial gravels of the modern bordering fans. They are muddy, very-poorly-sorted fine sand containing pebbles and cobbles, mostly subrounded (fig. 2-14). A prominent columnar structure lends a honeycombed, mudcracked appearance to the channel floor, particularly where the surficial lag gravel has been disrupted, as along roads (figs. 2-11, 2-12). Such exposed surfaces are easily gullied where they border lower-lying washes along the west end of the channel (fig. 2-12).

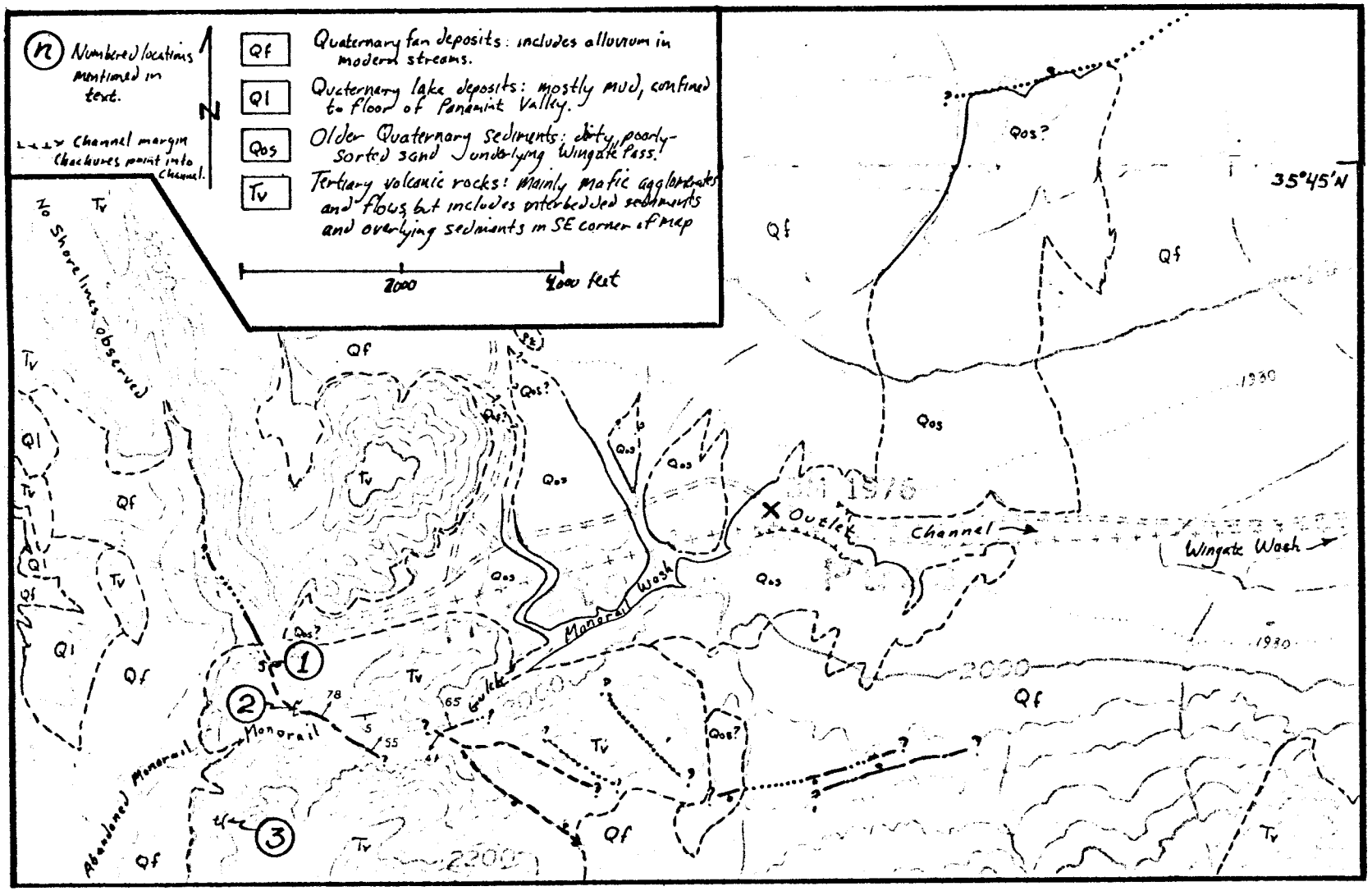

Figure 2-10. Geological Map of Wingate Pass.

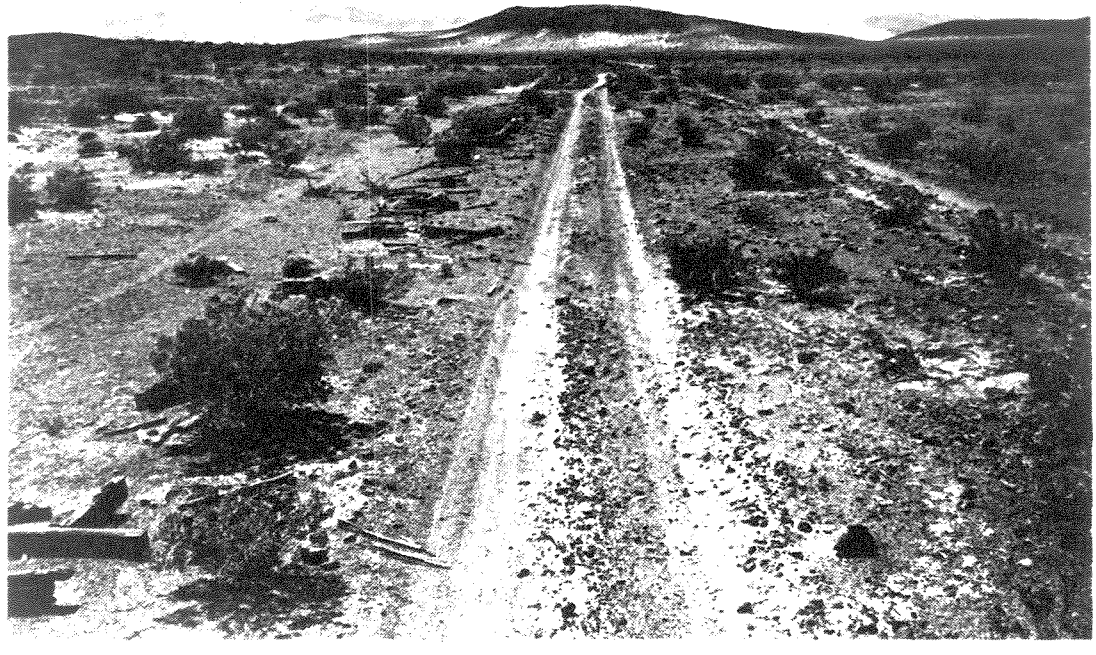

Figure 2-11. View west through Wingate Pass.
Taken from a point 500-1000 feet east of BM 1976; Slate Range forms skyline. Note the flatness of the channel floor and the fine-grained sediments beneath the surficial lag gravel. Timbers to left of road are remains of uprights which supported the abortive epsom-salts monorail constructed during 1922-4; the rails were scrapped in 1939 (Jahns, 1951).

Figure 2-12. View to NW from BM 1976 in Wingate Pass.
In the middle left, the road descends a 5-ft erosional scarp into a branch of Monorail Wash. Note the gully which has formed along the former trace of the road. Erosion was probably initiated by the road's disrupting sediments underlying the pass.

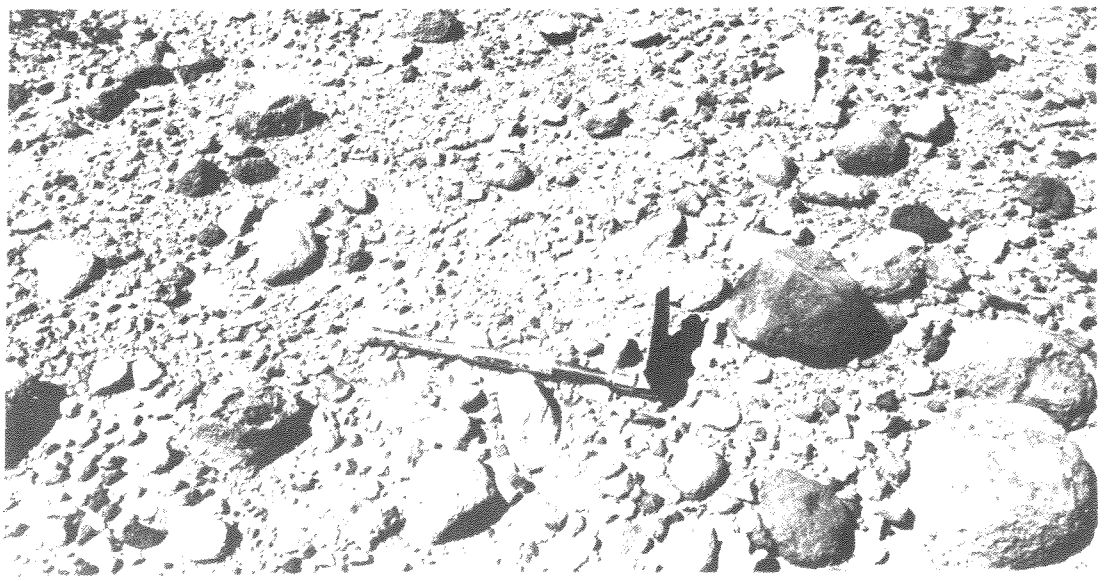

Figure 2-13. Lag deposit on south margin of Wingate Pass south of BM 1976.
Most of the clasts are subrounded volcanic rocks.

Figure 2-14. Typical sediments beneath Wingate Pass.
Note the strong columnar structure and surficial armor of lag gravel. Looking at N wall of gully in fig. 2-12; this is the "Qos" mapped on fig. 2-10.

Similar sediments underlie much of the area extending a mile west from the pass, where they have been deeply dissected by Monorail Wash (fig. 2-10). These sediments occur mostly below 2000 feet elevation and their greatest exposed thickness is about 20 to 30 feet. They seem to overlie an irregular topography on underlying Tertiary volcanic rocks, whose highest exposed elevation beneath the pass is 1930±15 feet. South of the channel, the gently-sloping upper surface of these deposits intersects the steeper slope of the modern fans and is mantled by a veneer of subangular clasts (fig. 2-15).

The fine-grained texture and poor sorting of these sediments into which the channel has been incised suggest that they formed as a mudflow whose source was probably about one mile south of Wingate Pass (fig. 2-4). Here, an ampitheater between Hills 2482 and 2420 forms a mile-wide gap in an east-trending ridge of north-dipping questas of Tertiary sediments which have light photo tone (fig. 2-32). This ridge of questas can be traced continuously eastward for 4 miles from Hill 2420 and forms the south limb of the syncline occupied by Wingate Pass and Wingate Wash. The sediments in the ridge were mapped as "Tertiary continental" sediments on the Trona sheet of the state geologic map (Jennings et al, 1962). "Plio-Pleistocene nonmarine" sediments, exposed six miles east of the pass, contain abundant subrounded clasts like those found in the presumed mudflow deposits at the pass (fig. 2-9). The probable source area of the presumed mudflow was not visited.

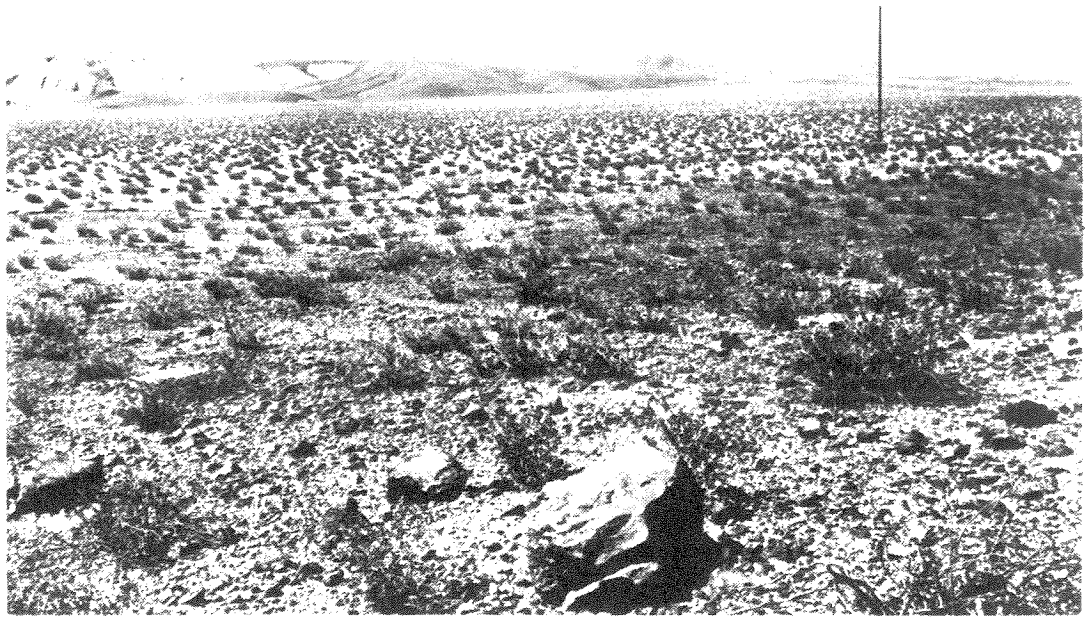

Figure 2-15. View to north across Wingate Pass.
Jeep (arrow) is marked at BM 1976. The subangular rocks in the light-colored foreground overlie the darker-colored, subrounded lag gravels in the middle distance (fig. 2-13). In mapping (fig. 2-10) this veneer is not differentiated from the underlying sediment.

High Shorelines

Southernmost Panamint Valley

There is but sparse evidence for high shorelines in southernmost Panamint Valley, despite nearly continuous exposures of lake sediments on the valley floor. The only firm evidence for a high shoreline was found 1.5 miles west-southwest of Wingate Pass, ③ on fig. 2-10. Here, lithoid tufa mantles boulders on a steep bench attaining 1980±10 feet elevation (fig. 2-16). Sparse subrounded gravel occurs about 20 feet below this tufa line (fig. 2-17), and 15 to 20 feet below that are fragments of lithoid tufa, possibly float.

Although no shorelines were found on the gentler slopes of the hills just to the northeast, lake gravel and tufa crop out at a slightly lower elevation just north across Monorail gulch. At 1925±5 feet elevation, cuts along the monorail line expose gravel of subrounded-to-rounded gravel in a sandy matrix (① on fig. 2-10; fig. 2-18). Scattered, six-inch fragments of lithoid tufa reach 1940 feet elevation on a southwest-facing slope about 500 feet southwest of here, (② on fig. 2-10), but no associated shorelines were found on the adjoining hills or on any of those within a mile's distance to the northwest.

Three other locations (numbered on fig. 2-4) seemed initially promising in terms of prospective shorelines, but no firm evidence was found at them. The best lies on the northwest slopes of hill

Figure 2-16. Lake bench at elev 1980±10 ft, 1.5 miles west-southwest from Wingate Pass.
View looks east. Note tufa rinds in lower right.

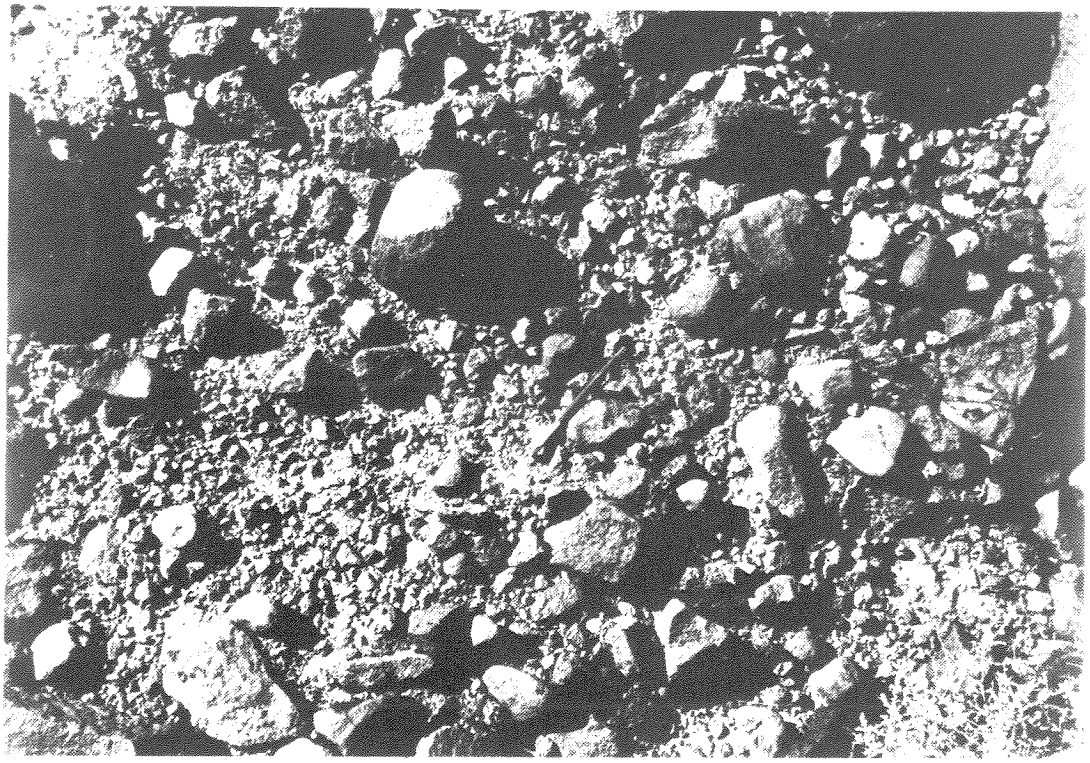

Figure 2-17. Lake gravel from bench in fig. 2-16.
This sparse, subrounded, volcanic gravel occurs about 20 feet below the high tufa line in fig. 2-16. Pencil gives scale.

Figure 2-18. Lake gravel at 1925±5 ft elevation on old monorail line. These pebbles and cobbles are better-rounded and have a coarser-sand matrix than those of the lag gravel in the Wingate Pass outlet channel, 1.5 miles to the east.

2200, where the highest of several benches reaches 2000±10 feet elevation (①on fig. 2-4; fig. 2-19). However, no tufa or rounded gravel was found on these benches. Some large, well-rounded quartzite boulders seen here may be a beach lag but they are much larger and more rounded than clasts elsewhere associated with Lake Panamint's beaches and probably were derived from an underlying unit correlative with a Tertiary conglomerate mapped in the Slate Range by G.I. Smith et al, (1968, p. 12-13).

No tufa was found on weakly-developed benches on the surface of old dissected and faulted fan deposits at other locations (②, ③, & ④on fig. 2-4). The benches at locations ③& ④are not traceable from one spur to the next, and those at location ②are not horizontal. Sparse well-rounded pebbles of welded tuff at location ②may come from the underlying fan deposit rather than from lacustrine deposits.

Southern Panamint Range

Shoreline remnants along the Inyo-San Bernardino county line lie at 1940±20 feet elevation on hill 2504 and at 1935±15 on hill 2000+ (①and ②on fig. 2-20). They are marked by abundant, snail-bearing lithoid to locally nodose tufa with associated accumulations of well-rounded pebbles. However, no prominent bench has been cut at this level. A shelf 10 to 15 feet below the tufa line on hill 2504 may be of lacustrine origin, but no lake deposits were found on it. A prominent knob of nodose tufa crops out at 1720±20 feet elevation on the west side of hill 2000+ (fig. 2-21), but a weakly-

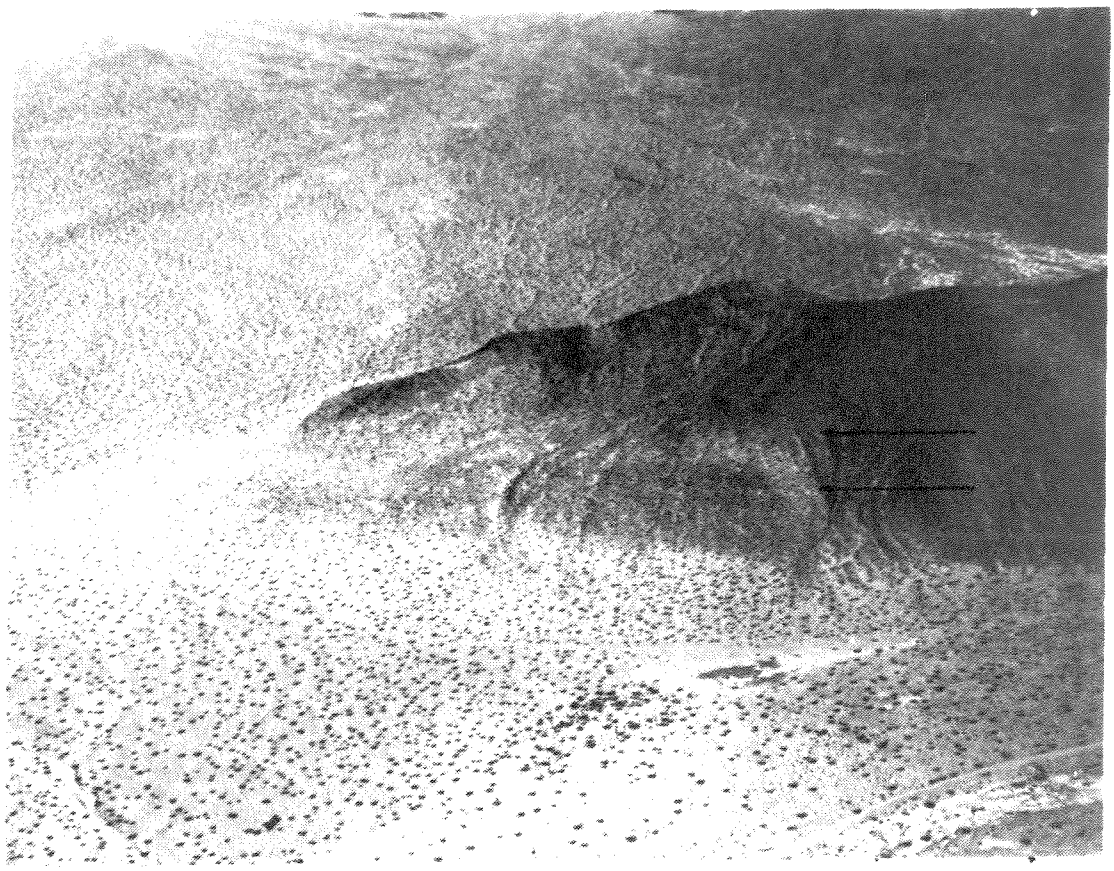

Figure 2-19. Possible shoreline benches on northwest side of Hill 2200. Horizontal arrows indicate possible shoreline benches. The highest bench (elev. 2000±10 ft.) bears sparse, well-rounded quartzite boulders but no tufa or rounded gravel. The boulders are probably not related to Lake Panamint, but rather were derived from Tertiary conglomerate interbedded with the volcanic rocks of the hill.

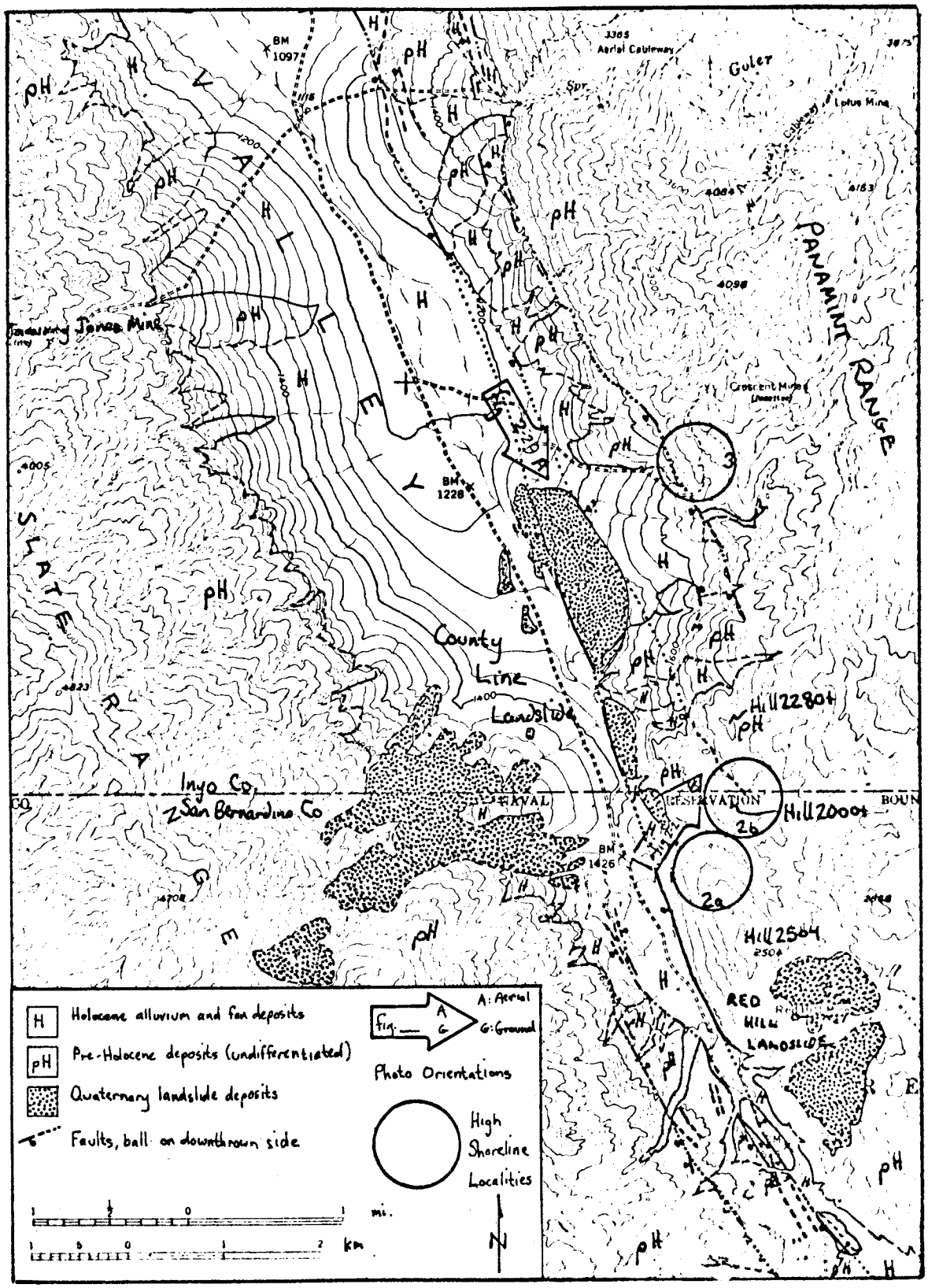

Figure 2-20. Geological map of southern Panamint Valley, Goler Wash south to 35° 45' N.

Figure 2-21. Nodose tufa mound near county line.
This outcrop, elevation 1720±20 feet, is not related to any specific shore features and is thought to be sublacustrine in origin. Hammer and pack give scale.

developed bench extending northward at slightly lower elevation bears neither tufa nor rounded gravel.

Thin rinds of snail-bearing lithoid tufa along the Crescent Mine trail (elev. 1900±20 ft, ③on fig. 2-20) and at Coyote Canyon (elev. 2000±40 ft, ④on fig. 2-22) are the only evidence for high shorelines in the six-mile stretch north from the county line. Very-sparse, fresh-looking snail shells found on hillslopes between 2000 and 2200 feet elevation at Coyote Canyon are judged to be of terrestrial species since: 1) no shorelines, tufa or rounded gravel were found associated with them; 2) seemingly identical snail shells were later found scattered on steep hillslopes of the Big Maria Mountains north of Blythe, California, where exterior drainage makes inundation by any pluvial lake unlikely.

A prominent band of dense dendritic tufa and subrounded gravel, elevation 1910±20 feet, is the best shoreline evidence at Manly Peak Canyon (herein named), three miles north of Coyote Canyon (⑤on fig. 2-22; fig. 2-23). This band lies on a steep slope (figs. 2-24, 2-25), as does a fainter band of tufa at 1945±20 feet elevation. At 1980±20 feet elevation is a gravel deposit containing mostly sub-angular clasts in beds which dip steeply south. Across a gully to the north, the highest of a series of benches is accordant in elevation, but its questionable tufa contains no snail shells. No evidence for shorelines was found above this 1980-foot bench on the gently-sloping hills up to 2400 feet elevation.

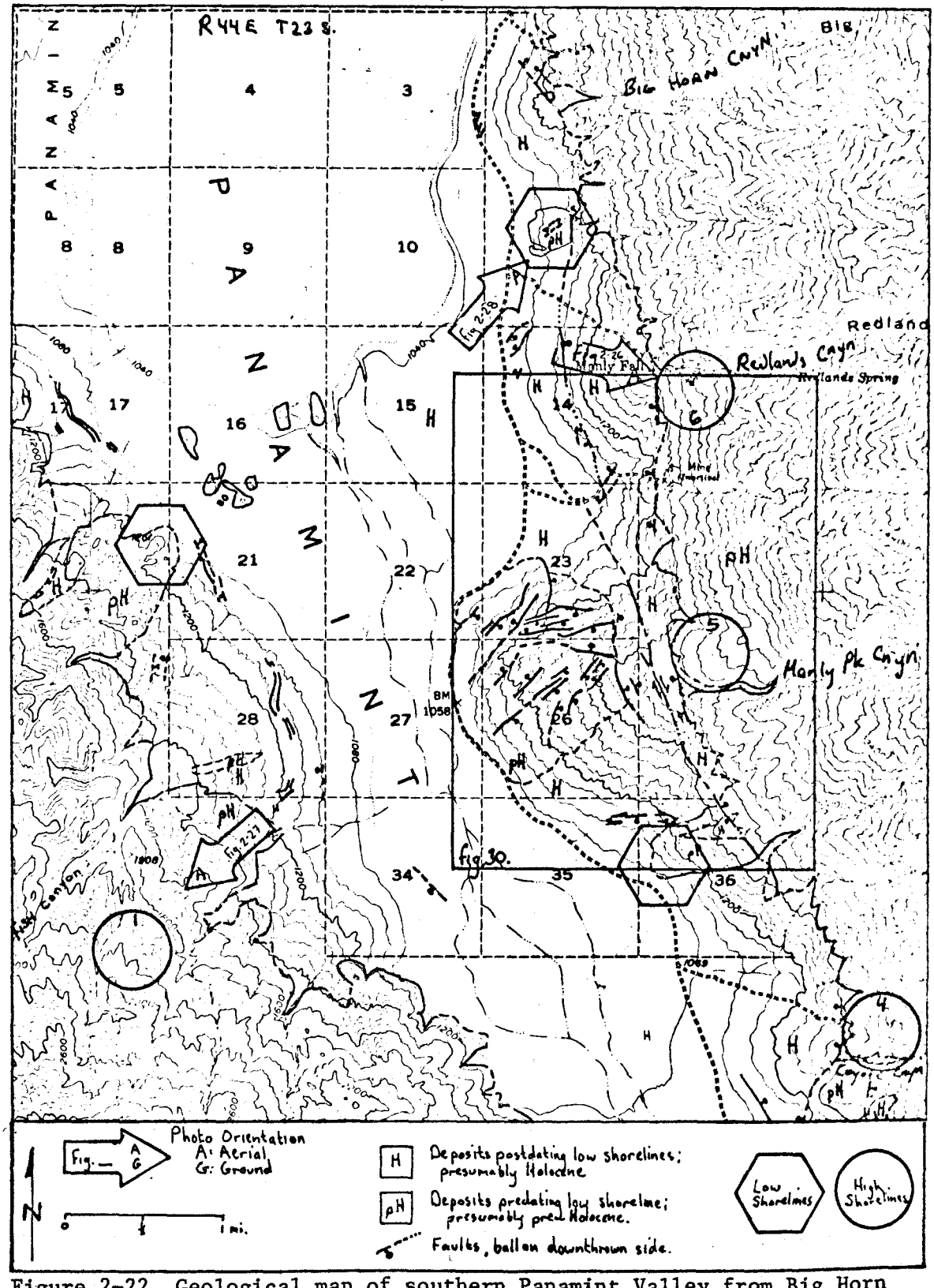

Figure 2-22. Geological map of southern Panamint Valley from Big Horn Canyon south to Coyote Canyon.

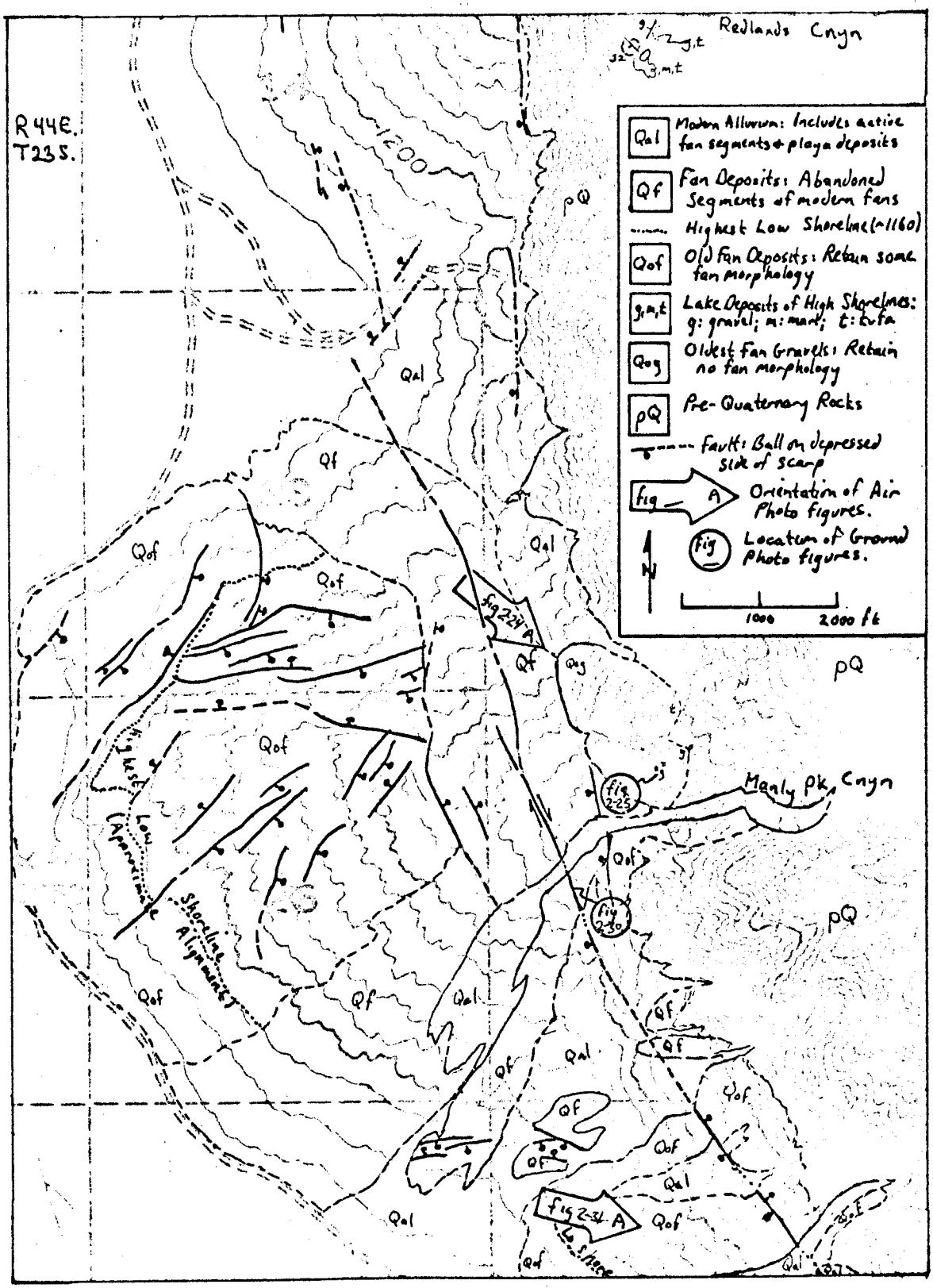

Figure 2-23. Geological map of area between Redlands and Manly Peak Canyons.

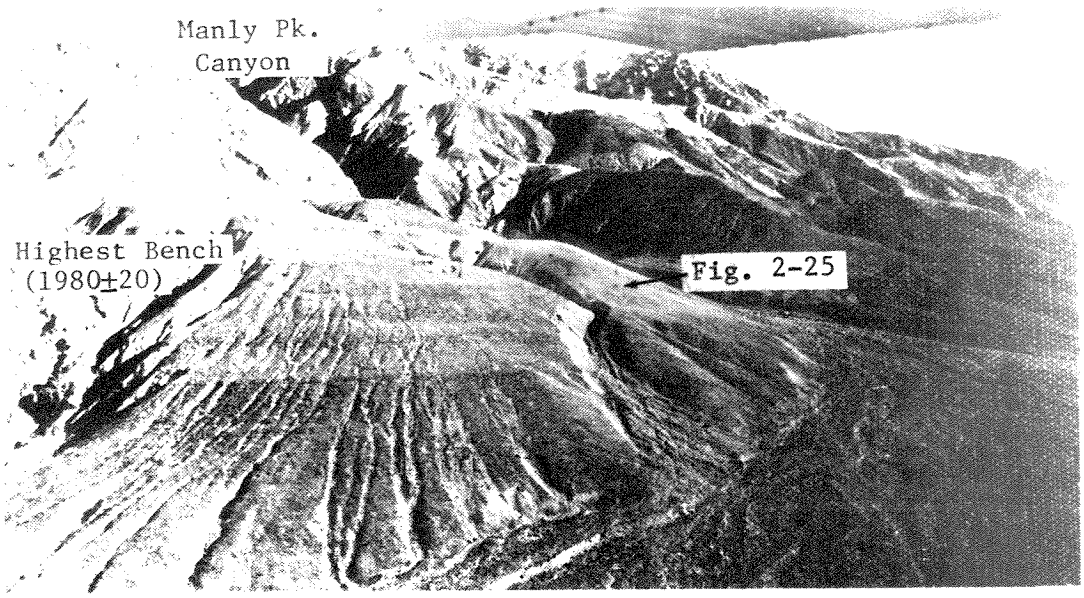

Figure 2-24. High shorelines at the mouth of Manly Pk Canyon. View looks southeast from about 2000 feet elevation.

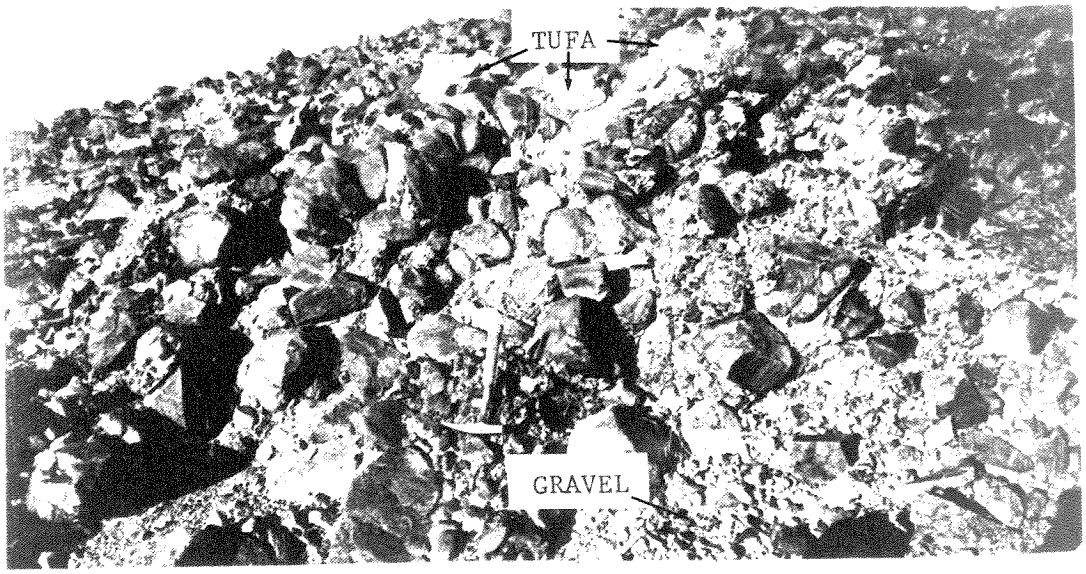

Figure 2-25. Tufa and gravel at 1910±20 feet elevation, Manly Peak Canyon.

The shoreline at Redlands Canyon, two miles north of Manly Peak Canyon, lies at much higher elevation than any of those to the south (⑥on fig. 2-22; figs. 2-23, 2-26). The base of a prominent beach cliff lies at 2140±20 feet elevation, dendritic to lithoid tufa litters the bench below the cliff up to 2135 feet, and a deposit of subrounded to rounded gravel underlies the northern part of the bench. On slopes southwest of the bench, subrounded to rounded gravel dips southwest at the angle of repose and underlies marl at 2060±20 feet elevation. Above the gravel lies a zone of probable weathering, containing some subangular to angular clasts in a matrix of reddish sand. Sandy, friable tufa covers one boulder directly beneath the marl.

Slate Range

High shorelines on the central and southern Slate Range were found only in a range-front embayment just south of Fish Canyon (①fig. 2-22). Here, a cut bench at the highest shoreline level attains 1980±10 feet elevation and is littered with abundant rounded gravel and much snail-bearing, lithoid and dendritic tufa (fig. 2-27). Nodose tufa,barren of snail shells, crops out prominently at lower elevation (1540 to 1640 feet) on a series of steep benches also littered with sparse rounded cobbles.

Correlation

These high, prominent shorelines are thought to have formed with respect to the overflow level of Lake Panamint through Wingate

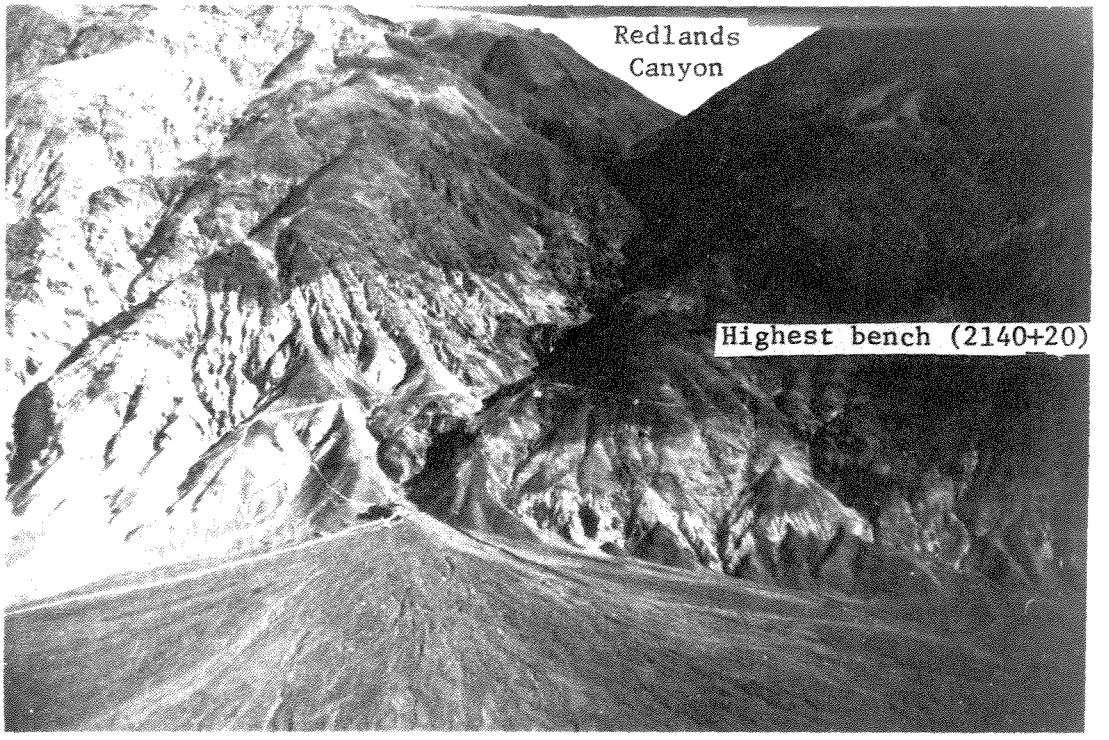

Figure 2-26. High shoreline at the mouth of Redlands Canyon
View looks east from about 2000 feet elevation.

Figure 2-27. High shorelines on the Slate Range south of Fish Canyon. View looks southwest from an elevation of about 2000 feet. The dotted line marks the position of the highest shoreline (elevation 1980±10 feet).

Pass or across the bedrock lip now buried 47±16 feet beneath the pass. This is because it seems unlikely that the lake's surface would have been very stable at any other level within 250 feet below the pass elevation. The highest shoreline near Wingate Pass, at Fish Canyon, at Coyote Canyon and (?) on Hill 2200 all lie at essentially this elevation (1980-2000 feet) and are attributed to the same high lake stand which overflowed through Wingate Pass. Where paired shorelines are seen, as near Wingate Pass and at Manly Peak Canyon, the higher one is attributed to a lake stand which overflowed through Wingate Pass and the lower one to an earlier stand which overflowed across the bedrock lip beneath the pass. The high shoreline at Redlands Canyon may represent superposition of the higher lower shoreline as diagrammed on Figure 3-30. Single shorelines below the level of Wingate Pass (county line, Crescent Mine trail) bear tufa which is megascopically indistinguishable from tufa of the Wingate-Pass shorelines but could correlate instead with the bedrock-lip shorelines. Their low elevation, like the high elevation of shorelines at Redlands Canyon, seems best explained by tectonic deformation.

The highest (1980-ft.) gravel at Manly Peak Canyon may represent the undeformed shoreline of a lake stand, younger than those described above, which was stabilized by overflow through Wingate Pass. The rounded gravel at intermediate elevation (1540-1640 ft.) at Fish Canyon suggests that a lake stand persisted within this elevation range without control by an overflow lip. The higher (1700-1720 ft.) bench on the county line could have been cut at a level

controlled by a continuing overflow from the south basin of Panamint Valley into the north basin. However, the multiplicity of benches at places like Fish Canyon suggests that at various stages the lake lingered long enough at many different elevations to cut poorly-developed benches. The nodose tufa at Fish Canyon and the county line is devoid of snail shells and is thought to be the product of sublacustrine springs rather than of a near-shore evironment.

Low Shorelines

Fresh and abundant remnants of low shorelines are found along three, possibly four segments of the Slate Range and southern Panamint Range (figs. 2-20, 2-22, and 2-23). Typically, a series of closely-spaced cut benches extends as high as 1165 feet elevation (fig. 2-28), but no shoreline features have been found between this level and the 1500-foot elevation of the lowest of intermediate to high-level benches described in the previous section. These low shorelines are devoid of tufa and generally lack both rounded gravel and constructional features. The highest of the multiple shorelines is typically the most prominent, and locally bears deposits of subrounded gravel. The fresh appearance of these shorelines compared with the subdued aspect of the higher shorelines suggests that they are much younger.

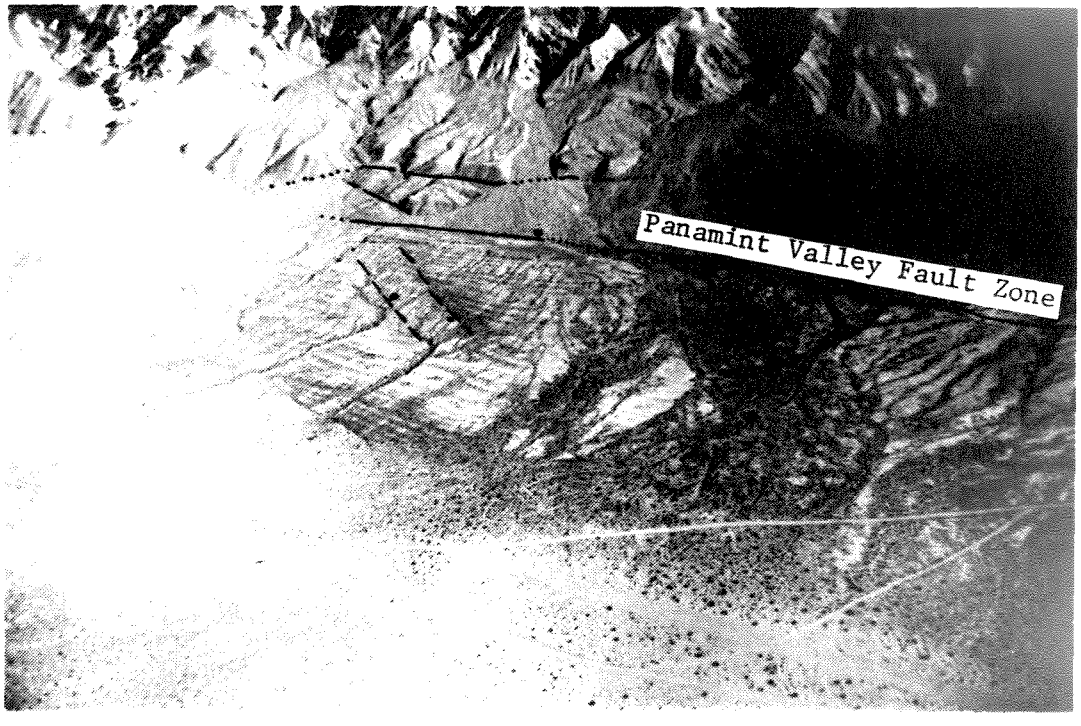

Figure 2-28. Low shorelines north of Redlands Canyon.
The highest low shoreline may be absent on this segment of older fan deposits, truncated by the Panamint Valley fault zone along its eastern margin at about 1160 feet elevation. Note the subdued graben, oblique to the trend of the fault zone, which appears to have been modified by wave action along the low shorelines. View looks northeast from about 2000 feet elevation.

Tectonic Deformation

Vertical Movement

Fault scarps abound along the foot of the Panamint Range, and, where continuous, roughly parallel the range front, facing either toward or away from it (figs. 2-20, 2-22, 2-23). Less continuous scarps trend mostly northeasterly, oblique to the range front. Fault scarps are less abundant along the foot of the Slate Range, there being a discontinuous series of north-to northwest-trending gräben near Fish Canyon and some more-continuous scarps paralleling the range front south of the county line (figs. 2-20, 2-22)

Difference in elevation of the high shorelines have been interpreted as evidence for tectonic deformation in a preceding section (High Shorelines: Correlation). Stability of the Slate Range block is suggested by accordance between the Fish Canyon high shoreline and Wingate Pass and by the absence of vertical deformation of Searles Lake shorelines as reported by G.I. Smith et al (1968, p. 25); these reach within three miles of Fish Canyon (fig. 2-1). Deformation of the Panamint Range has involved uplift in some parts and downdropping in other parts. Along the county line, the most prominent shoreline appears to have been warped down below the level of Wingate Pass, although prominent west-facing fault scarps indicate uplift relative to the adjacent part of the valley (fig. 2-29). This suggests that both valley and range sank, but that the valley sank more than the range. In other places, range-facing scarps

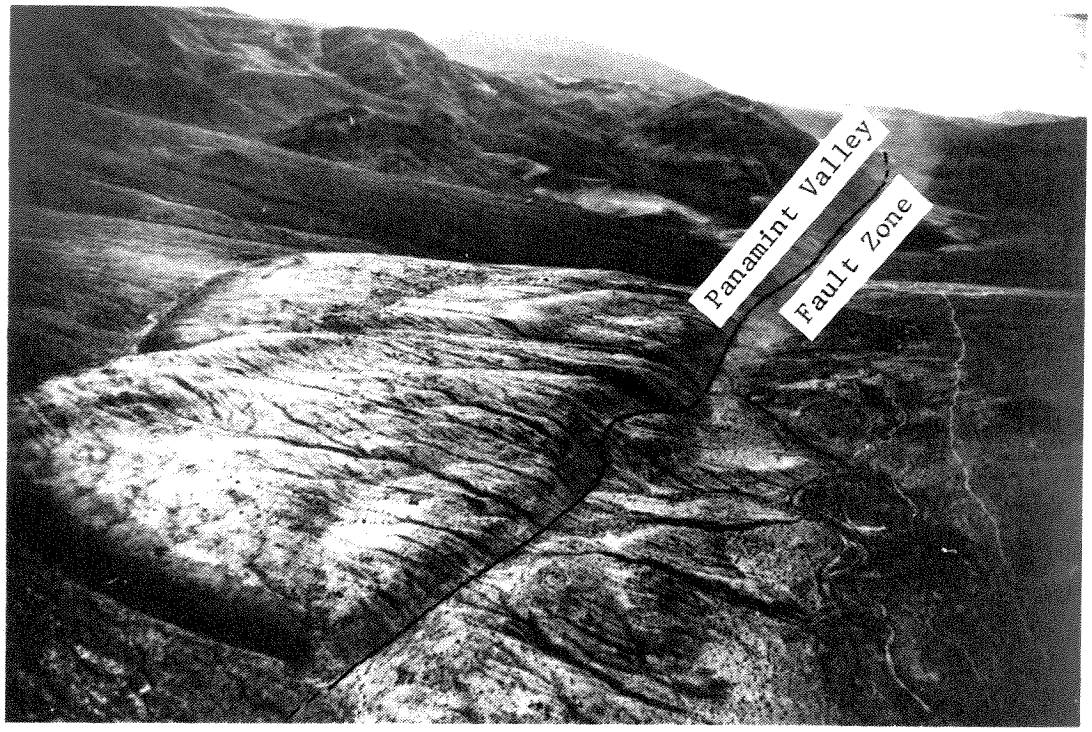

Figure 2-29. County Line landslide.
Looking south over the toe of the slide along the Panamint Valley fault zone. The source of this slide is off the picture to the right in the Slate Range.

suggest uplift of the valley relative to the mountains, both at places where shorelines appear to have been depressed (Manly Peak Canyon) and at places where they have been uplifted (Redlands Canyon).

Lateral Movement

The trend of discontinuous fault scarps along the foot of the Panamint Range is generally oblique to the range front in a clockwise sense, which is consistent with extension related to right-lateral shear along the Panamint Valley fault zone (fig. 2-23). The best evidence for such movement is found just south of Manly Peak Canyon, where a mudflow levee at 1500±20 feet elevation has been offset 60 feet right-laterally, juxtaposing the right bank on the east (range) side with the left bank on the west (valley) side (figs. 2-23 and 2-30). Deposits believed to be associated with this mudflow descend to about 1100 feet elevation, but bear no traces of the low series of shorelines, suggesting that they postdate the low shorelines. About 2000 feet south of the mudflow's distal end, faint traces of the low shorelines are preserved on the surface of an older fan deposit (fig. 2-31). Antithetic fault scarps parallel to the range front cut off the head of this unit. Tentative correlations of old, abandoned fan channels crossing the fault suggests about 400 feet of dextral movement since deposition of this fan. These relationships set maximum and minimum limits of 400 and 60 feet, respectively, on right-lateral movement along the Panamint Valley fault zone since low shorelines were formed.

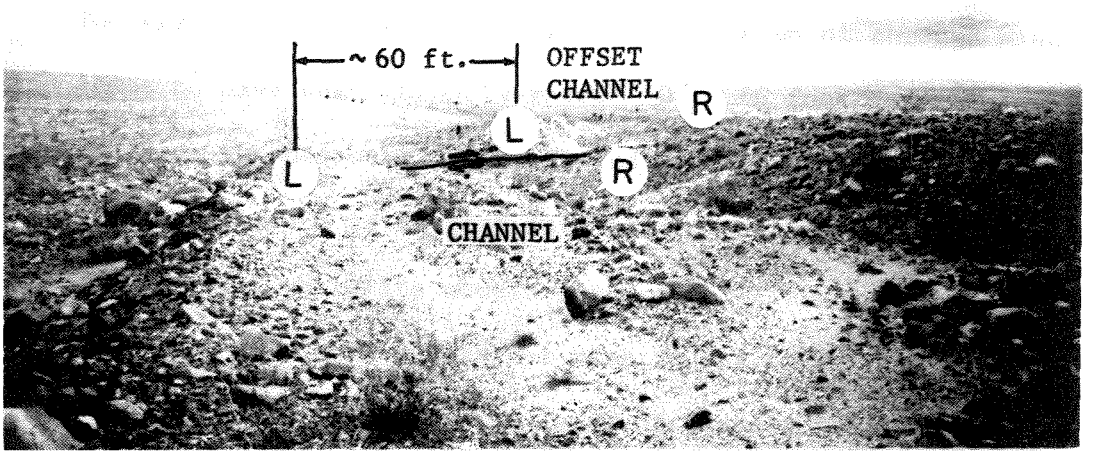

Figure 2-30. Laterally-offset mudflow levees south of Manly Peak Canyon.
Looking south-southwest down channel between mudflow levees; note that the right-hand levee east of the fault is juxtaposed against the left-hand levee across the fault.

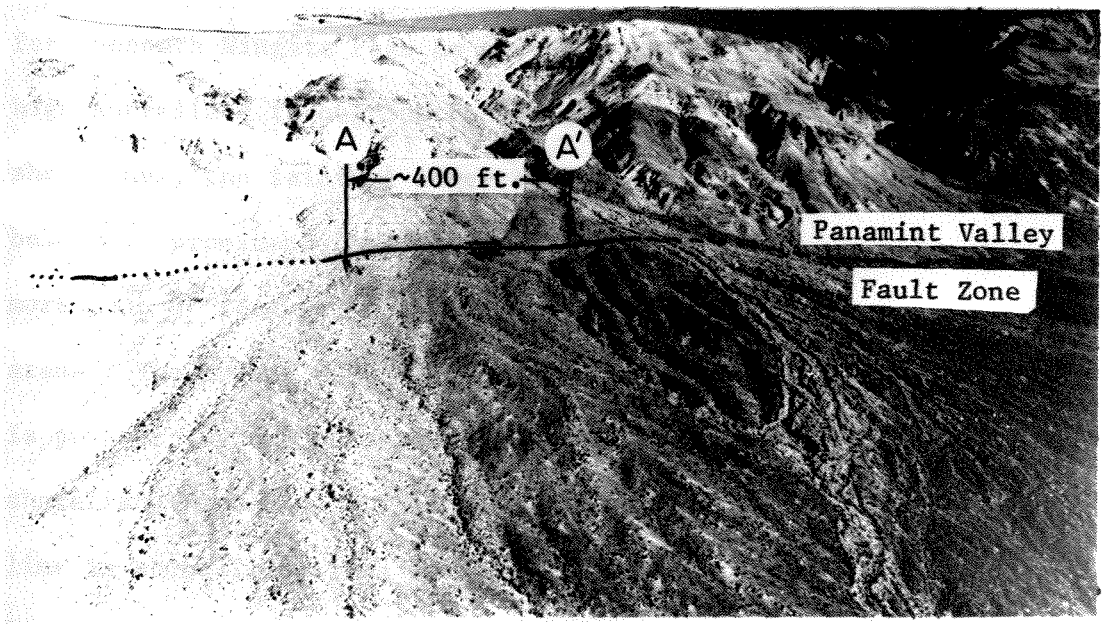

Figure 2-31. Possible lateral offset in older fan deposits one mile south of Manly Peak Canyon.
The channels at A and A' abut against the Panamint Valley fault zone on opposite sides. Their breadth and subdued character suggest that they are original distributary fan channels, unlike the sharp, narrow gullies now dissecting the deposit. If correlative, they indicate 400 feet of dextral offset.

The Elevation of Wingate Pass during Pluvial Times

The elevation of the outlet lip of Lake Panamint through Wingate Pass seems to have been abruptly raised 50 to 60 feet during pluvial times because the bedrock lip was buried beneath a mudflow. A channel was incised 5 to 10 feet into the top of the mudflow and probably eroded down to its modern level (1977±1 feet) during this period. Aside from this one abrupt rise in the outlet level and slight, slow, later lowering, the level of Wingate Pass seems to have been little altered by erosion, alluviation or tectonic deformation.

Evidence for overflow across the bedrock lip now buried 47±16 feet beneath Wingate Pass is provided by the ubiquity of paired high shorelines throughout Panamint Valley. For almost all paired shorelines, the fainter, lower shoreline lies less than 47 feet below the prominent, higher shoreline in uplifted areas but lies more than 47 feet below the prominent, higher shoreline in downwarped areas. The amount of tectonic deformation of the lower shoreline is greater (1.26x) than the amount of deformation of the higher shoreline (fig. 6-6). This suggests that the age of the lower shoreline is about 1.26 times greater than the age of the higher shoreline. Because formation of the lower shoreline ceased when the mudflow filled Wingate Pass, the age of the mudflow is probably slightly less than 1.26 times more than the age of the prominent, higher shoreline. All high shorelines which formed before the mudflow are are attributed to lake stands stabilized by overflow across the

bedrock lip.

The eastern end of the outlet channel is now being aggraded, but this aggradation has not yet reached within a horizontal distance of about 1000 feet from the pass. Aggradation within the summit part of the channel is probably the result of colluviation from the channel walls, and is so small that it could not have significantly raised the level of the pass.

Erosion has lowered the level of the summit of Wingate Pass by 5 to 10 feet below the general level of the land surface to the north and south, judging by the height of the walls of the overflow channel. No terraces were found at higher levels to document greater erosion. Because the channel retains its broad, flat bottom and is now beheaded on its west end, most or all erosion probably occurred during lake overflow through the channel.

Evaluation of the possibility of tectonic deformation is more difficult. Several splinter faults of the Panamint Valley fault zone trending directly into Wingate Pass from the north have been previously mapped (Jennings et al, 1962; G.I. Smith et al, 1968). Directly southwest of the pass, the northern extension of Brown Mountain is cut by northwest-trending aligned stream segments, and small playas and lithologic contacts seen on air photos also probably mark fault traces (fig. 2-32). Several northwest-trending faults cut the volcanic rocks exposed in the gulch of Monorail Wash, where one of them has subhorizontal slickensides on its plane (fig. 2-10). These faults do not seem to break the modern alluvium and are expressed on the hills above the gulch only by zones of calichification.

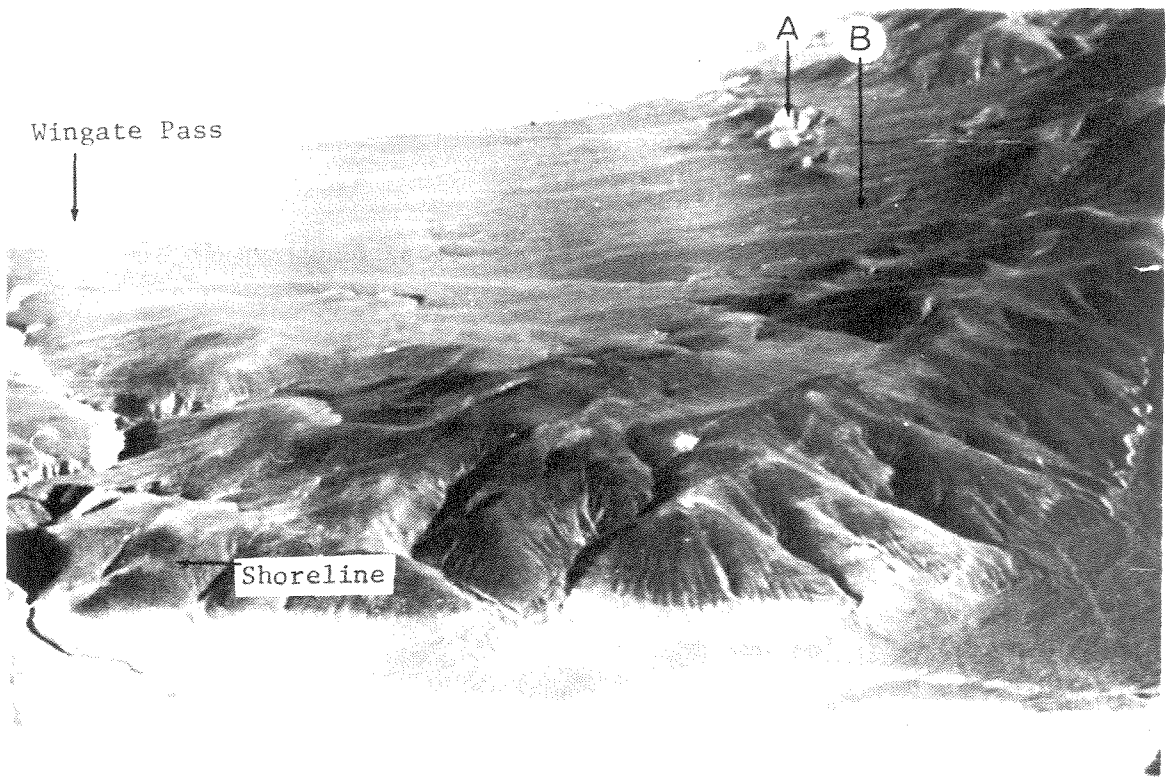

Figure 2-32. Fault (?) topography in northern end of Brown Mountain. View looks east; Wingate Wash is at upper left and Brown Mtn. is at upper right. Note the pronounced northwesterly grain in the topography, probably created by faults parallel to the Panamint Valley fault zone and the Brown Mtn. fault. The light-toned sediments (A) on the north slope of Brown Mtn. appear to overlie volcanic rocks and dip northward under Wingate Wash. The gap (B) in the ridge of sediments is probably the source area of the mud-flow which covered Wingate Pass and raised its level during pluvial times.

East-trending fault scarps break fan deposits south of Wingate Pass.

The accordance in elevation between Wingate Pass and the observed shoreline a mile and a half west suggests that there has been little vertical movement on the faults lying between them. The highest lake deposits crop out five and a half miles south of Wingate Pass and less than 17 feet lower in elevation; this establishes an upper limit for differential uplift of the pass relative to southern Panamint Valley across the Panamint Valley fault zone. The depth of water overlying these lake beds could easily have been equal to this difference unless the valley has been uplifted relative to the pass. The absence of prominent scarps along this part of the Panamint Valley fault zones argues against large vertical movement since deposition of the lake beds. Tectonic stability of the level of Wingate Pass is further suggested by the accordance in level between the pass and the highest shoreline at Fish Canyon on the Slate Range. Thus a reasonable case can be made for altitudinal stability of the level of Wingate Pass in an absolute sense as well as relative to the adjoining part of Panamint Valley.

CHAPTER 3

CENTRAL PANAMINT VALLEY

Central Panamint Valley extends from five miles south of Ballarat to ten miles north (fig. 3-1). The uplifted shorelines and associated lake deposits athwart the mouth of Pleasant Canyon in the Panamint Range east of Ballarat provide a more complete and detailed record of the history of Lake Panamint than is found anywhere else in the valley. This record, presented schematically on Figure 3-2, forms the basis for the summary discussion of Panamint Valley's pluvial chronology (Chapter 7).

High Shorelines and Lake Deposits at Pleasant Canyon

Introduction

The north side of lowermost Pleasant Canyon is the type locality for the lake stages and substages described in this section (figs. 3-2, 3-3, 3-4, 3-5). The stratigraphy of lake deposits is more complete, dissected and informative on the canyon's north side than on its south side. Progressively older lake deposits are stratigraphically associated with shorelines at progressively higher elevations. All shorelines with present elevations from 2040 to 2410 feet were probably formed by lake stands stabilized by overflow through Wingate Pass (present elevation 1977±1 feet; elevation of buried bedrock lip 1930±15 feet). Three intermediate-level shorelines with present elevation from 1890 to 2025 feet were probably formed

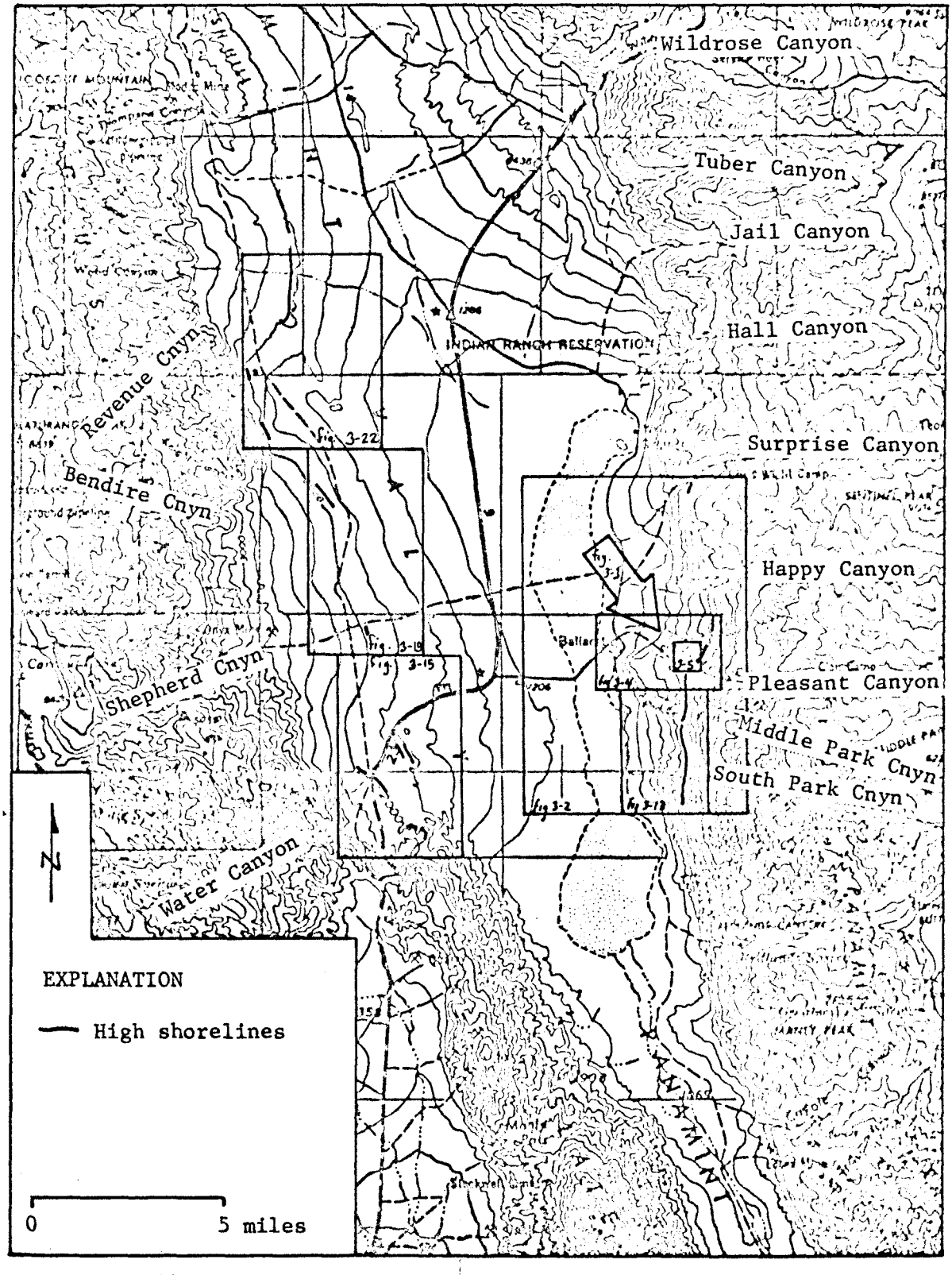

Figure 3-1. Index map of central Panamint Valley.

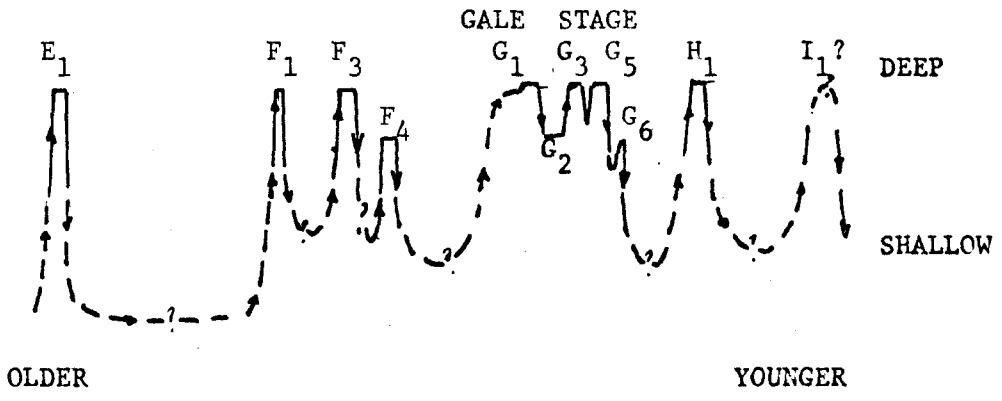

Figure 3-2. Diagrammatic sketch of the fluctuations in the level of Lake Panamint inferred from shoreline and stratigraphic relationships at Pleasant Canyon.

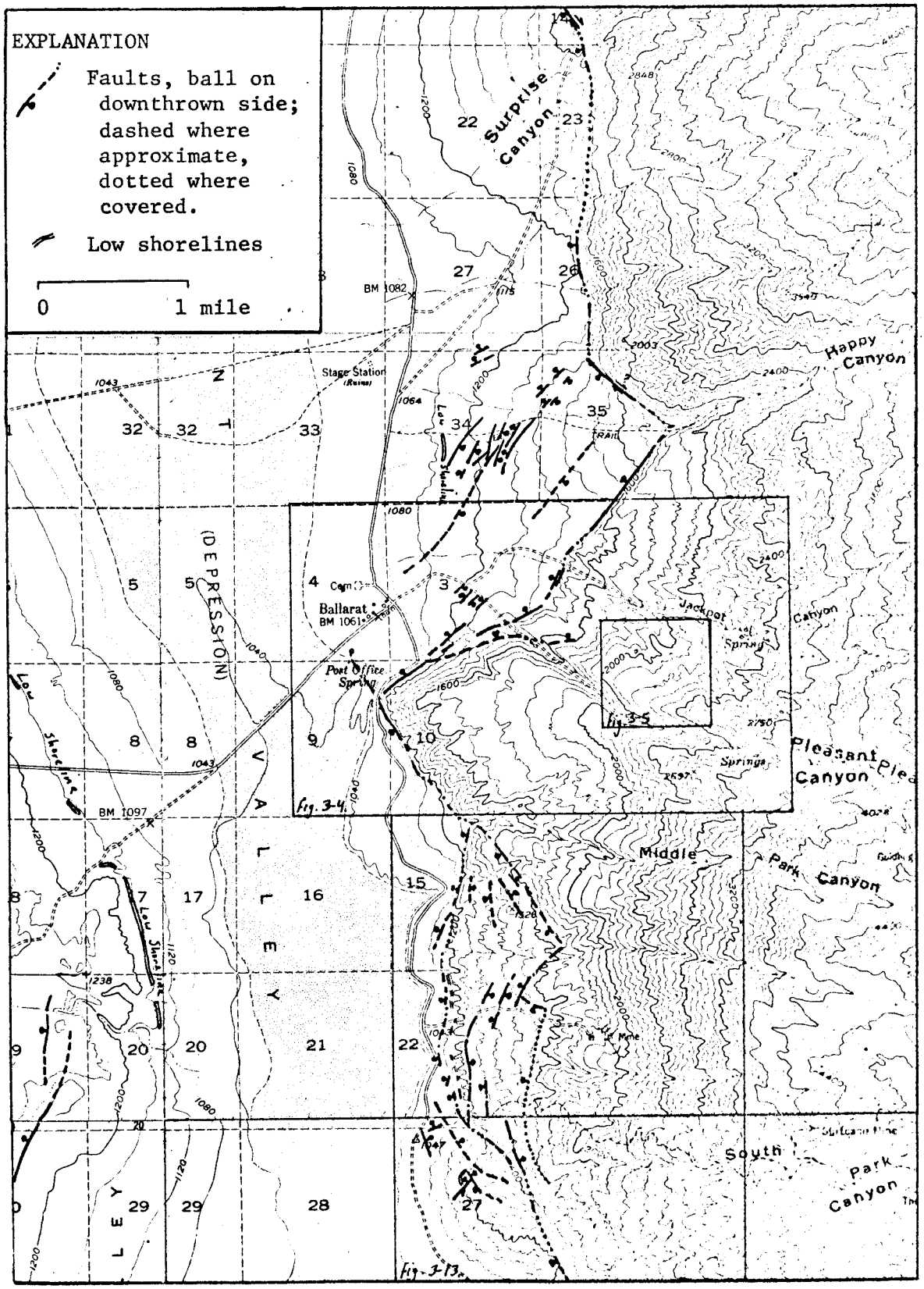

Figure 3-3. Index map of the region around Ballarat, showing shorelines and late-Quaternary fault traces.

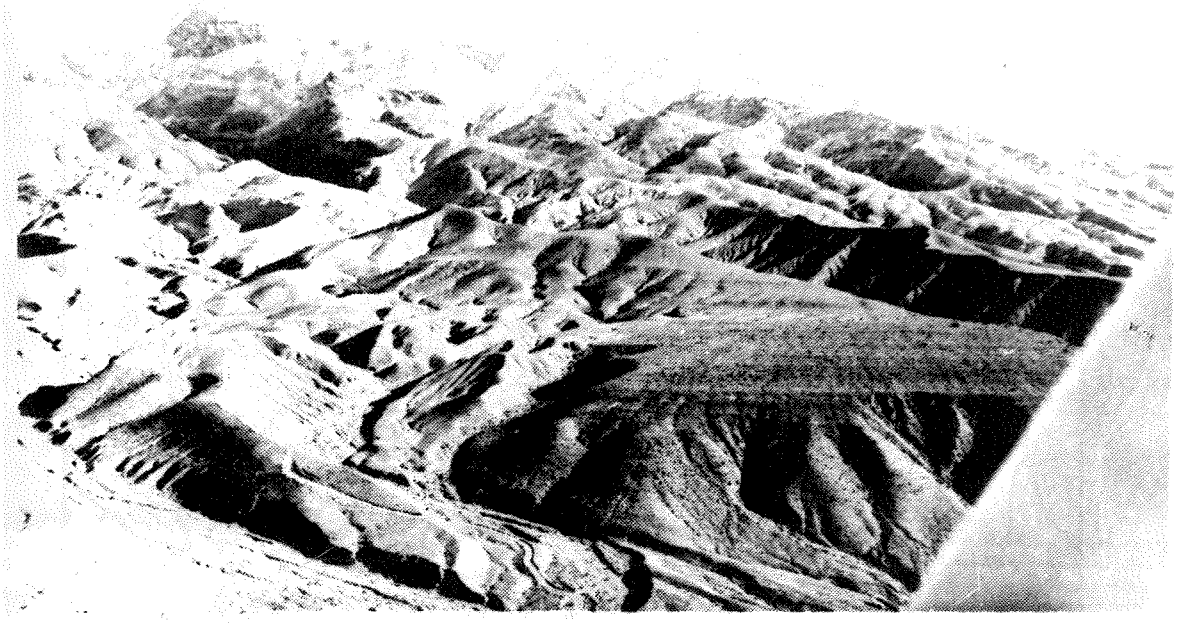

Figure 3-4a. Aerial view looking southeast toward lake shores and deposits north of Pleasant Canyon.

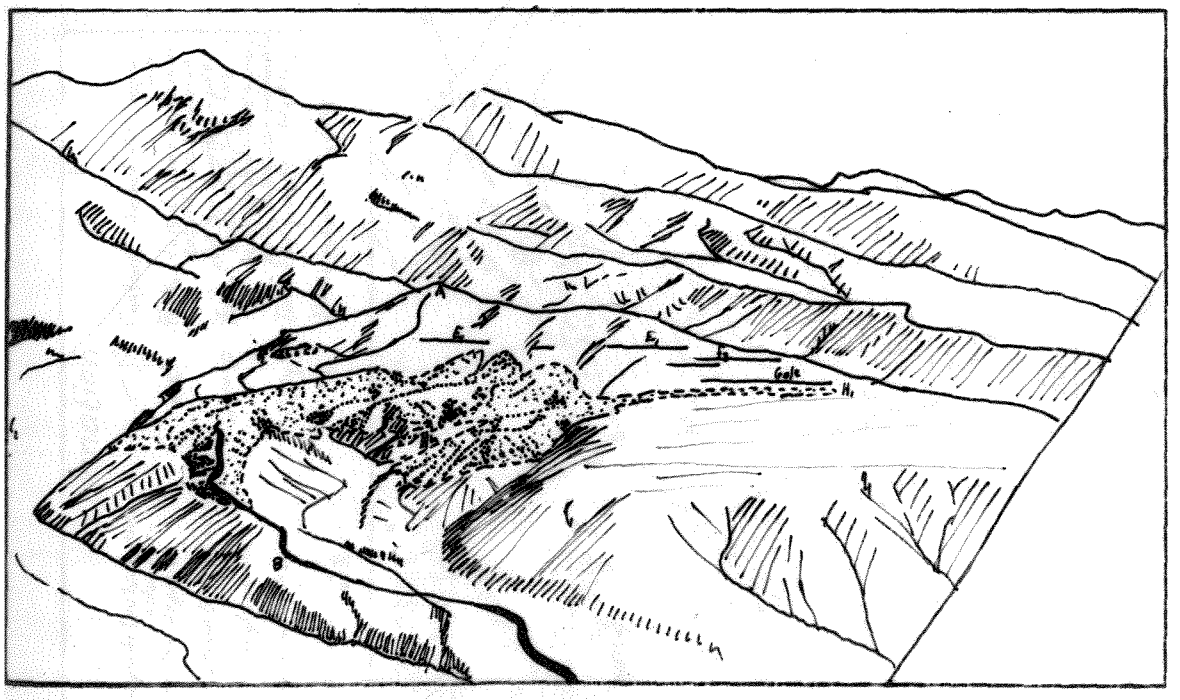

Fig. 3-4b. Sketch of fig. 3-4a. Lake deposits are stippled.

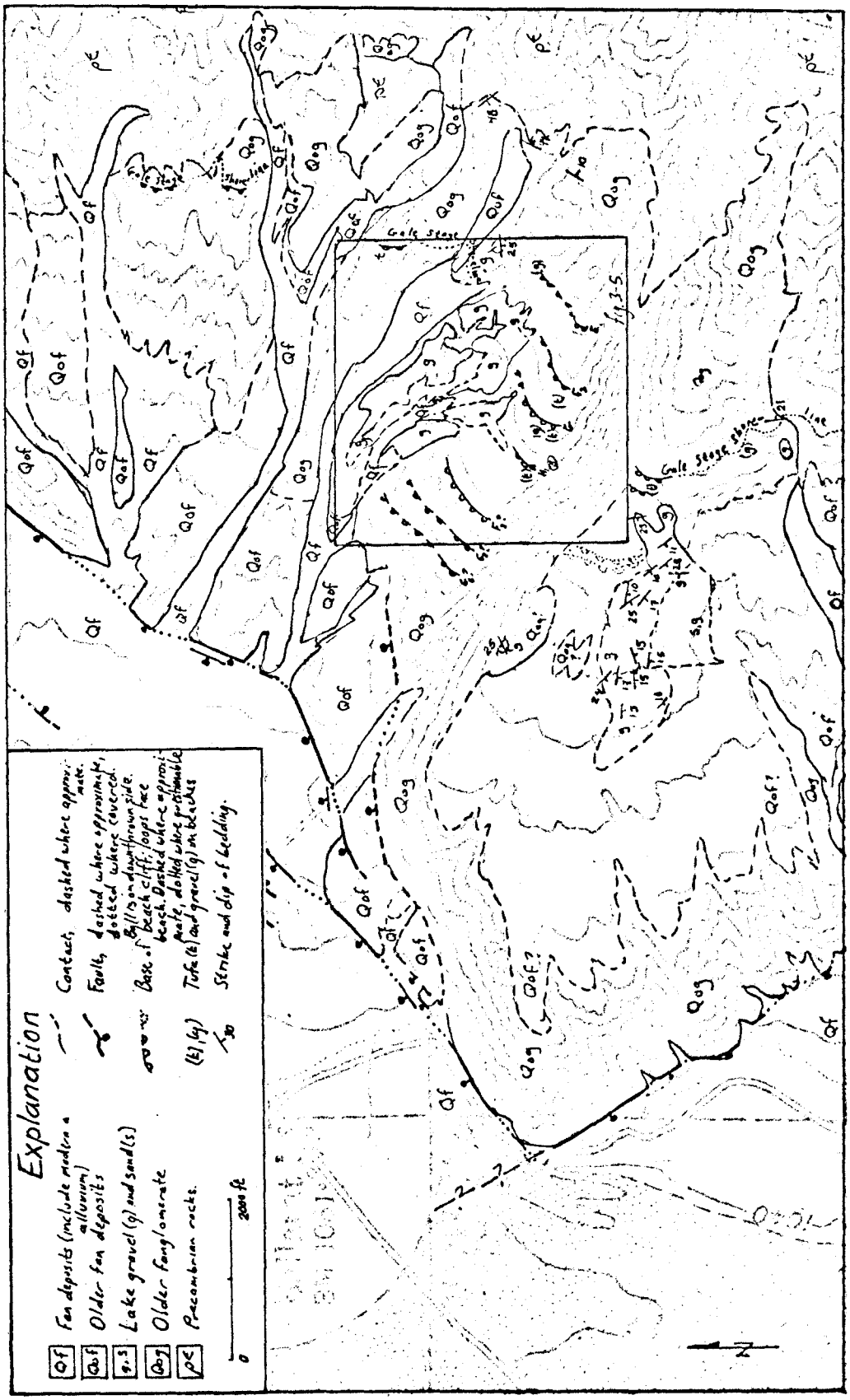

Figure 3-5. Geological map of the mouth of Pleasant Canyon.

by lake stands stabilized by overflow from Panamint Valley's south basin into its north basin (present pass elevation 1715±5 feet). Differential vertical movement is suggested by the difference in elevation of these shoreline levels and their overflow sill levels.

If a modern, intermediate-level shoreline formed in Panamint Valley, its level (1715 feet) would be 262 feet below the level of a modern high shoreline formed with respect to the level of Wingate Pass (1977 feet). If both shorelines were uplifted, the vertical separation between them would be preserved. By analogy, an ancient, intermediate-level shoreline should lie about 262 feet below an ancient, high shoreline of the same age formed with respect to the modern elevation of Wingate Pass, regardless of how much the two shorelines have since been uplifted. Similarly, an older ancient, intermediate-level shoreline should lie about 215 feet below an ancient high shoreline which formed with respect to the bedrock lip buried beneath Wingate Pass (elevation 1930±15 feet).

Distinctive shorelines were probably cut only at lake levels stabilized by overflow through Wingate Pass or (at lower level) by overflow across the sill into north Panamint Valley. Lake stands at other levels were not stabilized by overflow and thus fluctuated too sharply and were too ephemeral to leave identifiable records.

The shorelines at Pleasant Canyon are situated near the north end of a band of high shorelines which extends along the foot of the Panamint Range from South Park Canyon five miles north almost to Happy Canyon (fig. 3-3). The topographic form of these shorelines

is distinct and they can usually be clearly discerned from the west side of Panamint Valley. They were recognized by Campbell (1902, p.20), one of the earliest workers in the area, and have attracted comment from others (Maxson, 1950, pl. 10; Wright and Troxel, 1954, p. 23; Johnson, 1957, p. 412; Carranza, 1965, p. 58; Shelton, 1966, p. 357). Hoyt Gale's (1915, p. 314-6) pioneering study has been the most thorough previously-published investigation of these shorelines.

Nomenclature

The most prominent shoreline at Pleasant Canyon was formed during a high lake stand herein named "Gale Stage" in honor of Hoyt Gale. This shoreline can be traced almost continuously from South Park Canyon to Pleasant Canyon. Its beaches are broader, its beach cliffs higher, and the bulk of associated lacustrine gravel deposits far greater than corresponding features associated with any other stage of Lake Panamint. Gale-Stage beaches are abundantly littered with tufa, generally rare on beaches attributed to other stages. Prominent high shoreline remnants seen elsewhere in Panamint Valley were probably formed during Gale-Stage time.

All lake stages recognized are alphabetically designated E, F, G, H, I from oldest to youngest, with "G" being Gale Stage. All substages of Lake Panamint thought to have been stabilized by overflow through Wingate Pass are designated by odd subscripts, and non-overflow substages are designated by even subscripts regardless of whether or not the lake's level may have been stabilized at the

spillway elevation into north Panamint Valley. The recognized stages and substages of Lake Panamint are tabulated on Table 3-1 and will be described from oldest (E_1) to youngest (I_1).

Lacustrine Succession and History of Dissection

The sequence, amount of deposition and degree of dissection of lakeshore sediments of pre-Gale levels is poorly known compared to that of Gale and later levels. Contact relationships between E_1, F_1, and F_3 deposits are poorly exposed, but the basal G_1 contact on fanglomerate and F-stage gravel is extensively exposed in modern gullies, as is the internal stratigraphy of Gale-Stage deposits. A prominent bottomset G_1 sand and an overlying deltaic(?) gravel filled a system of northwest-draining gullies which had been incised 50 to 100 feet into fanglomerate and older lake deposits (F and E?). The pattern of these gullies resembled that of the modern drainage, but modern gullies are about 10 feet deeper. During the following low stand of the Gale-Stage lake (G_2), the G_1 deposits were dissected by a shallow set of gullies which drained northeast, parallel to the shoreline, and emptied into the large, northwest-draining wash which now runs along the northeast margin of the entire Pleasant Canyon deposit of lake sediments (fig. 3-6). These gullies were filled with gravel during the lake's next overflow stand (G_3). The G_3 deposits were not discernibly dissected prior to deposition of G_5 gravels, but slight dissection of G_5 gravels by broad, shallow northeast-draining gullies preceded deposition of H_1 beds. This

Table 3-1. High and intermediate stands of Lake Panamint at Pleasant Canyon.

High Stands		Intermediate Stands		C^{14} Age
Stage	Elevation	Stage	Elevation	
I_1?	2040±40 ft. ?			
H_1	2127±10			>31,150±1400 BP
Gale Stage		Gale Stage		
		G_6?	1890±25	
G_5, G_3, G_1	2177±10	G_2	>1920±20	
		F_4	2025±15 ?	
F_3	2265±10			
F_1	2298±10			
E_1	2410±10			

Oldest

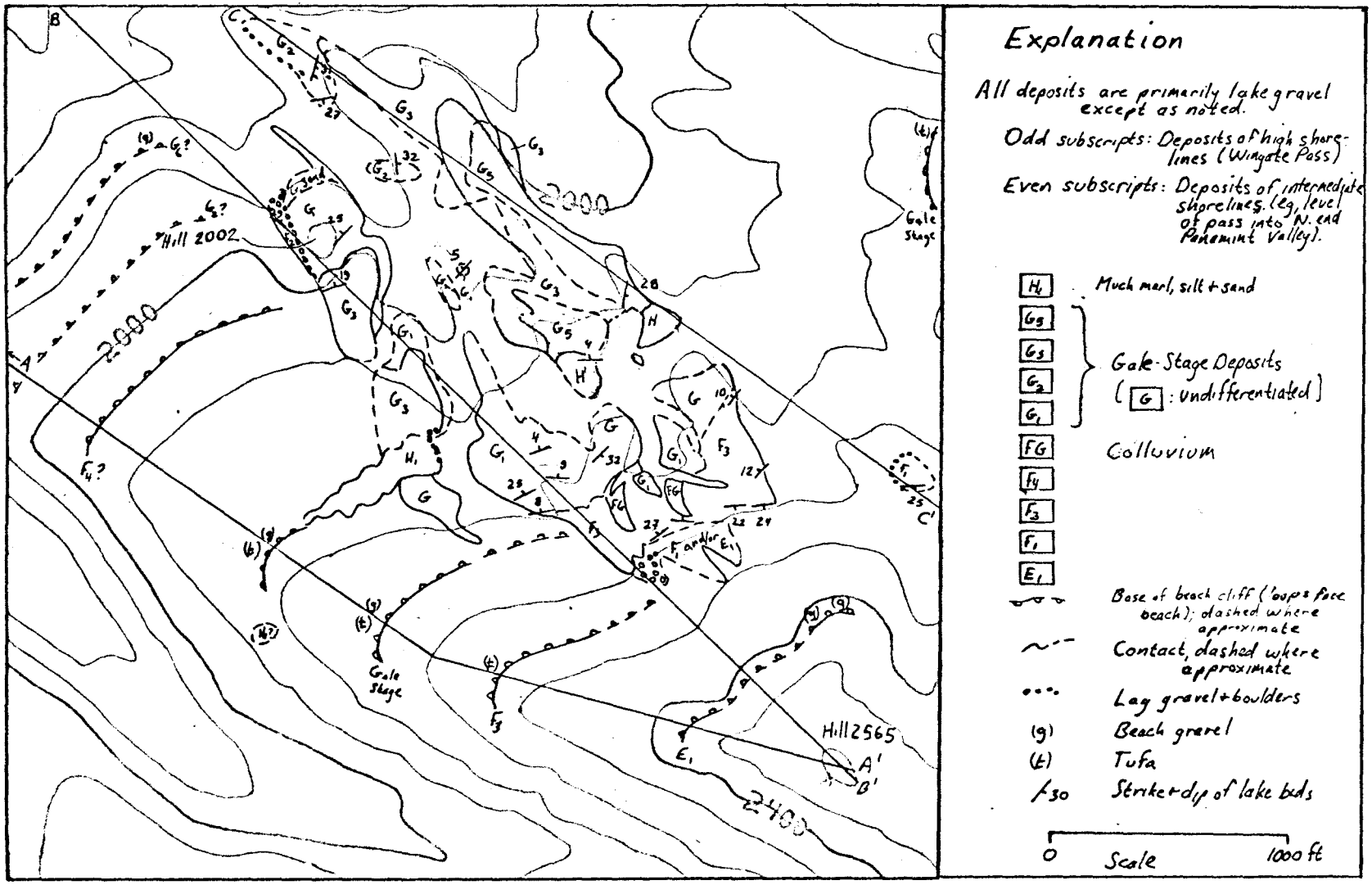

Figure 3-6. Geological map of lake deposits on the north side of Pleasant Canyon.

succession of deposits is mapped on Figure 3-6 and shown in cross section on Figure 3-7.

Deposits Older than Gale Stage

All pre-Gale high stands of Lake Panamint were probably stabilized by overflow across the bedrock lip (1930±15 feet) now buried beneath Wingate Pass.

E_1 (elevation 2410±10 ft.). Evidence for this stage is confined to abundant subrounded gravel exposed along the distal edge of a deeply-dissection topographic bench which slopes 10-13° valleyward (fig. 3-6). One head-sized block of calcareous material found along the upper margin of this bench does not resemble any of the tufa found on lower shorelines and contains no snail shells. Topographic benches at similar elevation between Pleasant and Middle Park canyons lack rounded gravel and tufa but may correlate with this feature (fig. 3-15).

F_1 (elevation 2298±10 ft.). Evidence for this substage is a cut bench armored by a lag accumulation of boulders and cobbles and overlain by up to 15 feet of backset beds of subrounded gravel (fig. 3-8). This exposure is now separated by a 50-foot gully from the principal sequence of beaches and gravel deposits on the north side of Pleasant Canyon, where no shoreline can be found at a corresponding elevation. Deposits of subrounded gravel in the principal sequence at a proper elevation may represent an eroded E_1 deposit rather than an F_1 deposit.

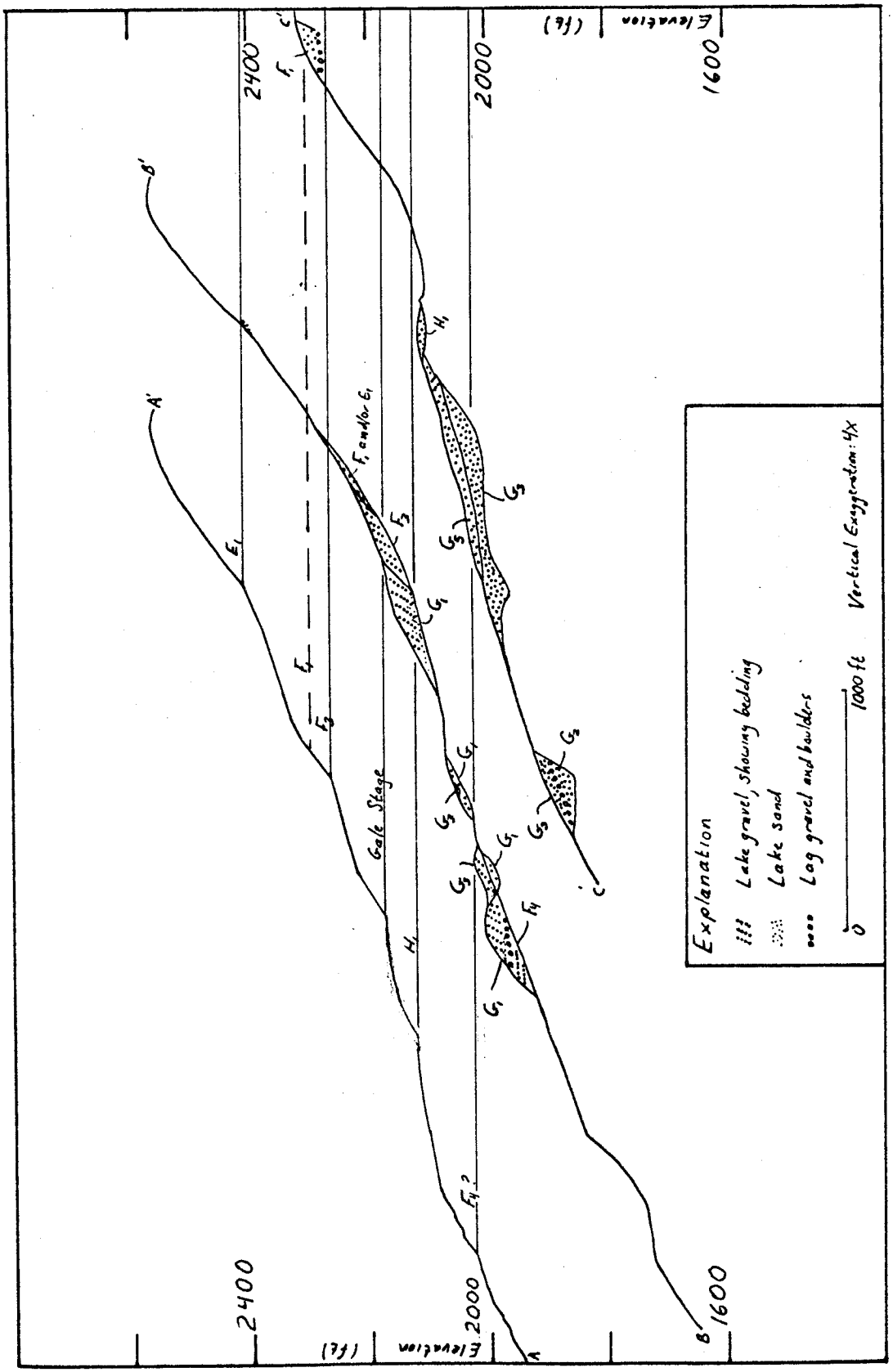

Figure 3-7. Geological cross sections of lake deposits on the north side of Pleasant Canyon.

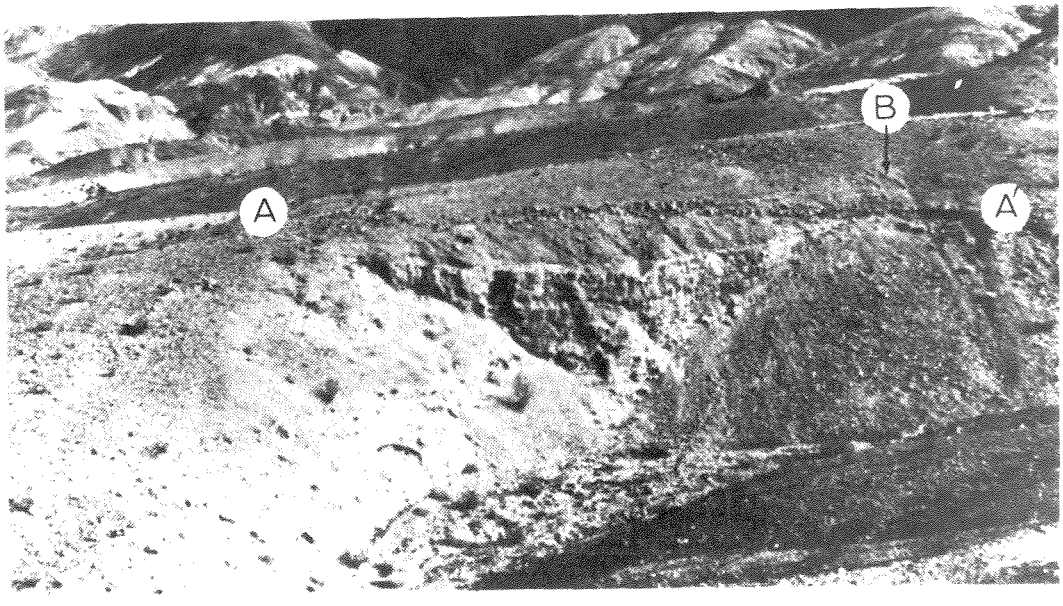

Figure 3-8. F_1 bench. Looking northeast at the type locality north of Pleasant Canyon (fig. 3-6). Note the coarse lag boulders (A-A') on the cut bench (which has no topographic expression) and the backset bedding in lake gravel at the head of the bench (B). The gully in the foreground is about 50 feet deep and isolates this only outcrop of F_1 from all lake deposits of other stages.

F_3 (elevation 2265±10 ft.). Evidence for this substage is a wide bench, sloping seven degrees valleyward, from which a prominent gravel bar extends northeastward (fig. 3-6). This bar, of sub-rounded gravel, unconformably overlies a lag accumulation on the surface of a gravel deposit attributed to E_1 and/or F_1 substage. Nodose to lithoid tufa found along the distal edge of the F_3 bench contains no snail shells.

F_4 (elevation 2025±15 ft.?). Northeast-dipping lake gravel attributed to this substage is 15 feet thick, reaches 1990 feet elevation and is capped by a four-foot-thick lag deposit of boulders (figs. 3-7, 3-9). The F_4 gravel is older than the bottom-set G_1 sand which overlies the boulders. The F_4 shoreline may be along the nip (elevation 2025±15 ft.) of a bench cut into fanglomerate to the south (fig. 3-7), but this bench bears neither rounded gravel nor tufa and the F_4 gravel cannot be traced up to this bench. The F_4 gravel was probably deposited in a lake whose level was stabilized by overflow into north Panamint Valley. The possible F_4 shoreline lies about 240 feet below the F_3 shoreline, which suggests that the F_3 shoreline had been uplifted about 25 feet before the lake again rose and occupied the F_4 shoreline (240 feet modern elevation difference minus 215 feet difference in elevation of overflow sills equals 25 feet uplift of F_3 shoreline).

Gale-Stage Deposits and Shorelines

The prominent, high Gale-Stage shoreline was cut during lake stands whose level was stabilized by overflow through Wingate Pass.

Figure 3-9. Lag boulders overlying F_4 gravel. Looking south-southeast at hill 2002 from a point on its northern spur at about 1940 feet elevation (fig. 3-6). Bedding in the F_4 gravel dips nearly 30° to the northeast. Bottomset sand of basal Gale-Stage (G_1) is exposed at the shovel (A). This sand overlies the lag boulders and interfingers upward with the foreset G_1 gravel beds, which dip to the northwest at about 25°. The gully on the right side of the photo now isolates the F_4 gravel from the F_4(?) shoreline above.

The earliest part of G_1 substage was probably stabilized by overflow across the 1930-foot bedrock lip beneath Wingate Pass and the rest of G_1, plus G_3 and G_5 substages, were probably stabilized by overflow through the modern 1977-foot outlet channel in Wingate Pass. The fainter, intermediate-level Gale-Stage shorelines were probably cut during lake stands whose level was stabilized by overflow across the sill (now 1715 ft.) into north Panamint Valley. The water level of lake stands at intervening elevations fluctuated too much and too often to leave identifiable records. Gale Stage is divided into five substages: three high substages (G_1, G_3, G_5) and two intermediate substages (G_2, G_6). With one possible exception (G_3-G_5) the high substages are separated by distinct falls of water level from the Wingate Pass stabilization to the north Panamint sill stabilization.

G_1 (elevation 2177±10 ft.). Gale-Stage gravels lie along and downslope from a shoreline at this elevation (fig. 3-7). On the north side of the mouth of Pleasant Canyon, basal Gale-Stage gravels are nearly everywhere underlain by a bottomset sand which mantles an eroded surface (figs. 3-9, 3-10). This sand bed persists over an altitudinal range of more than 300 feet and is useful both as a marker for the base of Gale-Stage deposits and to distinguish them from deposits of other stages. In most places, the sand bed directly overlies eroded fanglomerate rather than older lake deposits, but at low elevation (~1900-1950 feet) it locally overlies a lag deposit of boulders developed on F_4 gravel (fig. 3-9). At high elevations

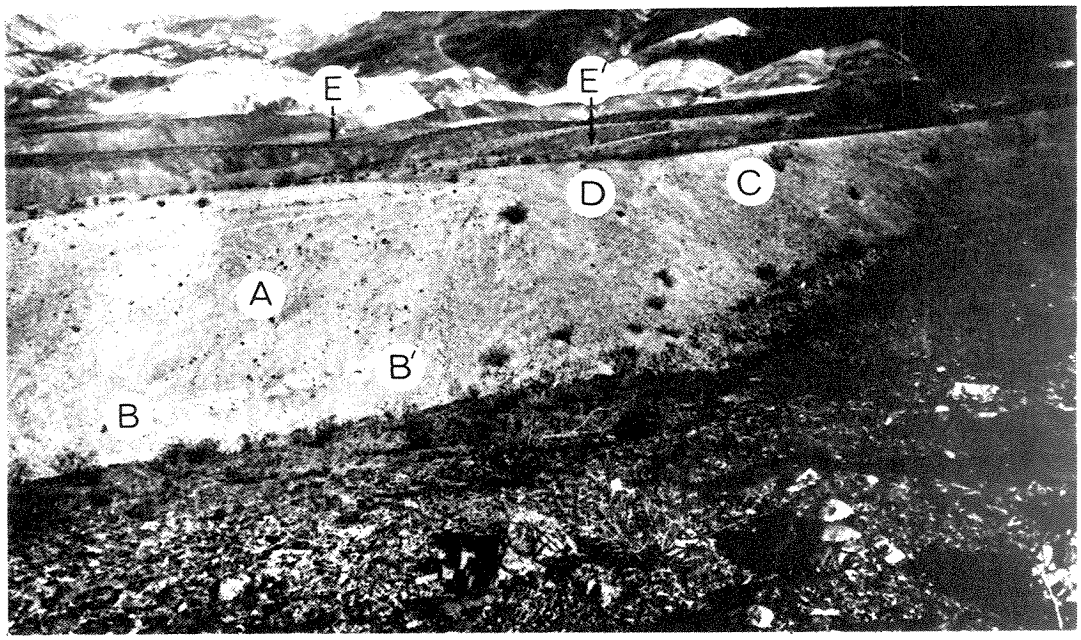

Figure 3-10. Foreset beds of basal Gale-Stage (G_1) gravel. Looking northeast along the Gale-Stage shoreline north of Pleasant Canyon (fig. 3-6). The foreset G_1 gravel (A) interfingers with bottomset G_1 sand (B-B') in a gully wall about 30 feet high. These Gale-Stage deposits overlie F_3 gravel (C); this contact is covered but lies somewhere on the slope below (D). Note the accordance in elevation between the top of the G_1 gravel and the Gale-Stage shoreline in the distance (E-E').

(~2140-2170 feet) the sand locally overlies subaerially-eroded F_3 gravel (fig. 3-10). The foreset beds of G_1 gravel interfinger with the bottomset sand (fig. 3-10) and at their highest extent rest directly on F_3 gravel or overlie a thin (one foot thick) layer of compact colluvium which locally mantles F_3 gravel.

Voluminous deposits of foreset gravel are found 500 to 2,000 feet south of Pleasant Canyon (fig. 3-5). They are continuously exposed from about 1800 to 2130 feet elevation but cannot be traced higher to the prominent Gale-Stage bench because they are mantled by a thick layer of bouldery mudflow debris. These deposits are attributed to Gale Stage because they lie at an elevation comparable to that of Gale-Stage deposits on the north side of Pleasant Canyon, and are assigned to G_1 substage because of their great bulk and relationships to probable G_2 deposits described below.

G_2 (elevation 1920±20 ft.). Downgully, near its lowest exposed elevation (~1870 ft.), the bottomset G_1 sand underlies two distinct bodies of backset (east- and south-dipping) gravel (G_2) which underlie G_3 gravel (figs. 3-6, 3-7). The upper part of the G_2 gravel overlies a lag deposit developed on the top of lower G_2 gravel beds, and both parts terminate against a gully wall cut into fanglomerate during pre-G_1 time (fig. 3-11). The highest elevations of the lower and upper G_2 bodies (1900 and 1920 feet, respectively) lie 277 feet and 257 feet, respectively, below the Gale-Stage shoreline. This suggests that they were deposited during a Gale-Stage phase stabilized by overflow into north Panamint Valley. The

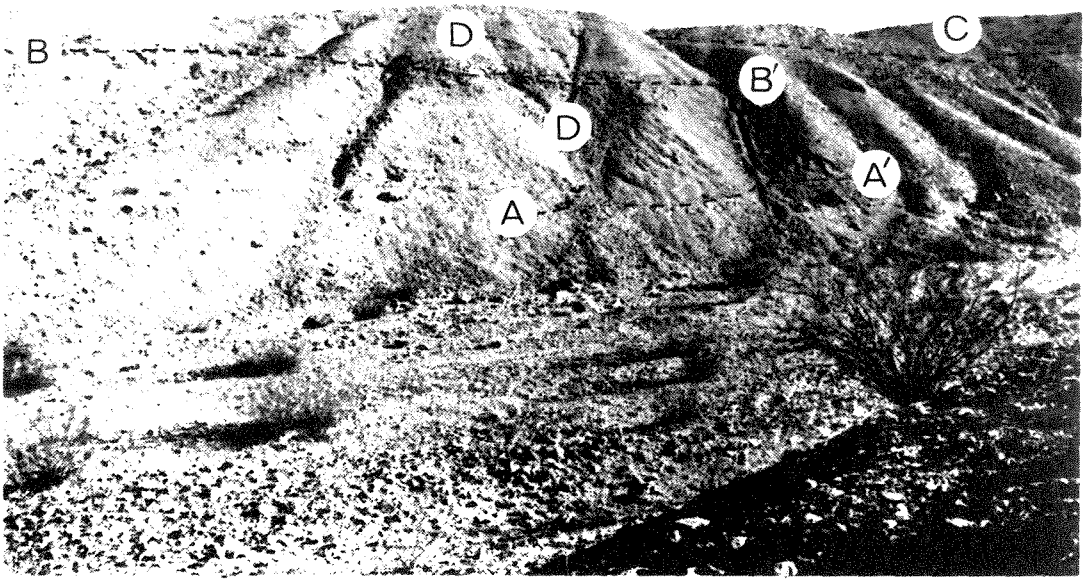

Figure 3-11. Deposit of G_2 gravel. Looking east at exposure in gully wall, about 60 feet high, whose brink lies at about 1920 feet elevation (fig. 3-6). Bottomset G_1 sand (A-A') underlies the lower of two G_2 gravel bodies, which are separated by a lag deposit (B-B') and overlain by G_3 gravel (C). Note the backset bedding in both the upper and lower G_2 bodies (D). Both bodies are interpreted as bars which formed across the gully mouth.

G_2 deposits may be remnants of bars formed across the gully mouth, and this substage lasted long enough for gullies to cut more than 30 feet into G_1 gravel and underlying fanglomerate (figs. 3-12a, b). A shoreline bench at 1950±20 feet elevation may be related to the G_2 gravels, but the latter cannot be traced up to it (figs. 3-7, 3-15) Shoreline benches at similar elevation (1930±20 and 1950±20 feet) on the south side of Pleasant Canyon were cut into debris which may in part mantle G_1 (?) gravel. Deposits of subrounded gravel attributed to the 1930 and 1950 shorelines continuously exposed from 1800 to 1930 feet elevation are attributed to G_2 substage (fig. 3-5).

G_3 (elevation 2177±10 ft. (?)). Deposits of lake gravel (G_3) which overlie G_2 gravel are laterally continuous with gravel fillings in a northeast-draining gully cut during G_2 time (fig. 3-12a, b). Here, G_3 gravel is underlain by up to 10 feet of G_3 sand, silt and marl above a thin, hard, calcareously-cemented crust on G_1 deposits exposed on the old gully wall. Elsewhere, G_3 gravel is underlain by silt above a coarse lag accumulation which marks the top of G_2 gravels. Although G_3 gravel cannot be traced with certainty higher than 2080 feet elevation, it is thought to have been deposited in a lake whose level was stabilized by overflow through Wingate Pass. Lacustrine gravel, either G_3 or G_5, overlies G_1 gravel and extends up to the Gale-Stage shoreline (elevation 2177 feet).

G_5 (elevation 2177±10 ft.). Deposits representing G_5 substage overlie G_3 gravel along a contact which is fairly smooth and marked

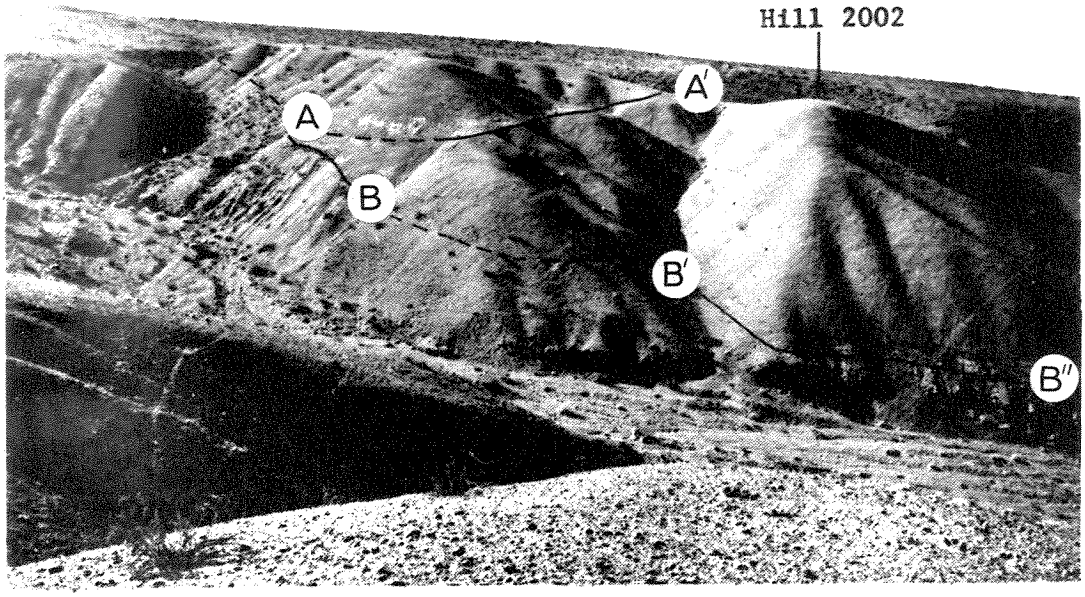

Figure 3-12a. Looking southwest at filled G_2 gully. This gully (A-A'), about 30 feet deep, was cut into foreset beds of G_1 gravel during an intermediate (G_2) stand of Lake Panamint and later filled with G_3 deposits (fig. 3-6). The bottomset G_1 sand (B-B'-B'') descends westward (right) almost to the floor of the modern gully, here about 100 feet deep.

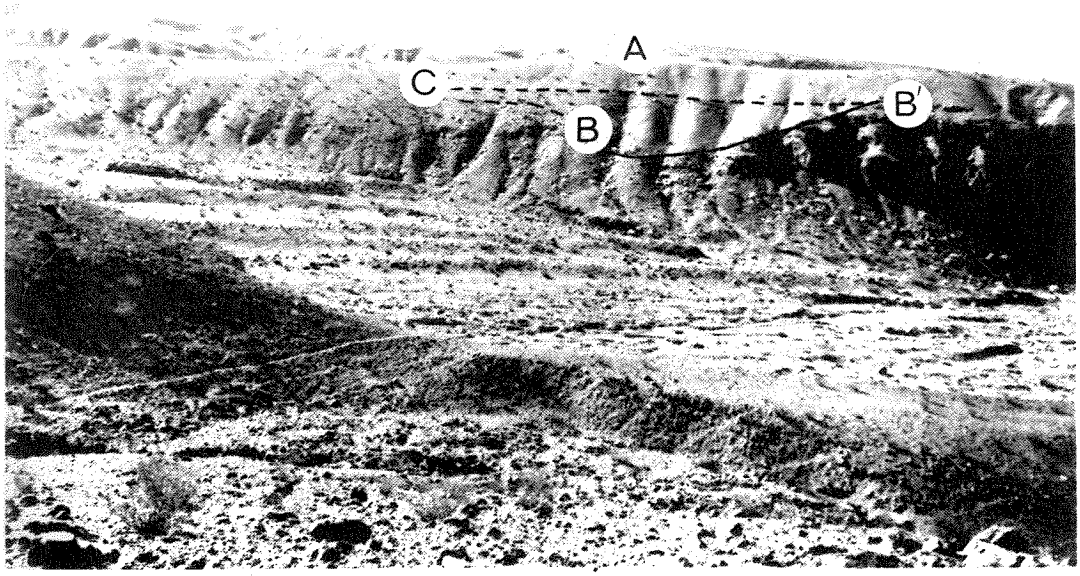

Figure 3-12b. Looking southwest at lower reach of G_2 gully. Figure 3-12a was taken from point A. The gully (B-B') is here cut into fanglomerate. The G_3-G_5 contact (C-B') is slightly accentuated by erosion and some lag gravel.

by a slight topographic bench that probably represented differential erodibility of the two units (fig. 3-12b). This contact is locally identified by a lag deposit. Elsewhere it cannot be seen in shallow trenches cut through it. Because of the subtle nature of the G_3-G_5 contact and the absence of any identified G_4 deposits, G_3 and G_5 may both be deposits of high-lake stands, uninterrupted by any lower lake level. In any case, the G_3-G_5 interval was too short for noticeable erosion of G_3 deposits, and much shorter than the G_1-G_3 interval of erosion.

G_6 (?) (elevation 1890±25 ft.). A shoreline at 1895±20 feet has been cut partly into gravels below the 1930-ft. shoreline on the south side of Pleasant Canyon. It is associated with a gravel deposit on the brink of Pleasant Canyon and lies at similar elevation to a cut bench (elevation 1885±20 feet) on the north side of the canyon. This bench is littered with subrounded gravel (figs. 3-5, 3-7). These features and a shoreline at 1895±20 feet elevation at South Park Canyon, may represent the youngest stand of the Gale-Stage lake, a stand probably stabilized by overflow into north Panamint Valley.

Deposits Younger than Gale Stage

H_1 (elevation 2127±10 ft.). A narrow beach bar which overlies Gale-Stage deposits (G_3, G_5) on the north side of lowermost Pleasant Canyon grades southwestward into a tufa-littered bench cut into fanglomerate (figs. 3-6, 3-7). The bar's composition is pea gravel,

marl, sand and silt, with locally-abundant snail shells. It occupies a broad, shallow, northeast-draining trough, cut mainly along the contact between fanglomerate and G_5 lake gravels, and is floored by a thin, hard unit of calcareously-cemented sand (fig. 3-13). This trough represents shallow (about 10 feet) dissection of Gale-Stage deposits by a broad, northeast-draining gully. This G_5-H_1 interval of subaerial exposure and dissection was probably shorter than the G_1-G_3 interval, if relative duration can be measured by relative depth of dissection.

The minimum age of the H_1 bar is 31,150±1400 B.P. (I-6543), based on the radiocarbon age of its contained snail shells of the general Carnifex and Lymneae. Preparation of the sample for dating and reasons for considering this a minimum age are discussed in Appendix A.

I_1 (?) (elevation 2040±40 ft. ?). Evidence for an overflow stand of the I-Stage lake is equivocal, despite the abundance of I-Stage nodose tufa at intermediate elevation (1500-1800 feet) along the foot of the Argus Range. Similar tufa locally overlies Gale-Stage deposits up to 1890 feet elevation south of lowermost Pleasant Canyon, where the I-Stage shoreline may be indicated by benches at 2020±20 and 2040±20 feet elevation (fig. 3-5). These weakly-developed benches are on the surface of the bouldery mudflow debris which covers both the Gale-Stage gravels and the H_1 shoreline. They bear neither tufa nor rounded gravel and may not be of lacustrine origin. The topographic scarp above the lower bench diverges from a scarp of

Figure 3-13. Looking southwest at H_1 bar. Slope at left is in older fanglomerate; the topset(?) beds at right are G_5.

unknown origin which retains its height as it descends to the southwest. A more likely example of an I_1 shoreline is a sharply-incised bench (nip elevation 2065±20 feet) at South Park Canyon to be described later. A narrow bench on the north side of Pleasant Canyon lies at this elevation (fig. 3-15) but cannot be traced to the south side. This 2065 bench might have been buried beneath the debris which covers all older units on the south side.

High Shorelines and Lake Deposits elsewhere on the Central Panamint Range

South of Pleasant Canyon

Prominent high shorelines extend about three miles south from Pleasant Canyon to South Park Canyon (figs. 3-3, 3-14). The Gale-Stage shoreline is best developed at South Park Canyon, where the nip of a bench cut partly onto bedrock lies at 2190±20 feet elevation (figs. 3-14, 3-15). This bench, sloping two to three degrees westward, is overlain by tufa-encrusted lag boulders and subrounded to rounded gravel. These underlie a wedge of colluvial material, 20 feet thick at the old beach cliff, which is eroded at its distal edge to expose a beach littered with snail-bearing lithoid, dendritic and nodose tufa. The Gale-Stage shoreline between South Park and Pleasant canyons is marked by broad bench remnants littered with lithoid to dendritic tufa and subrounded to rounded gravel. The nip of these bench remnants lies at 2180±20 feet elevation.

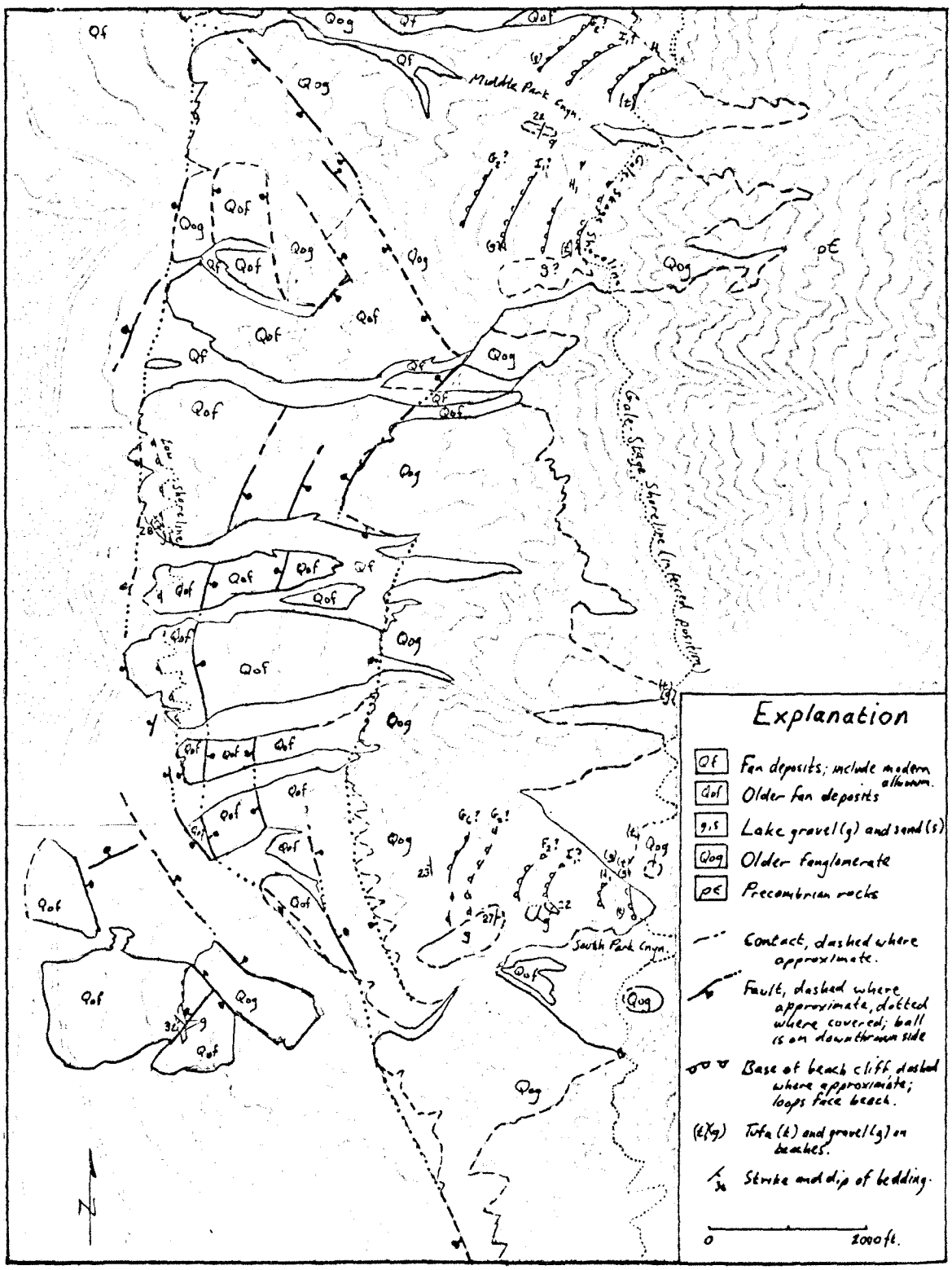

Figure 3-14. Geological map of the region between Middle Park and South Park canyons.

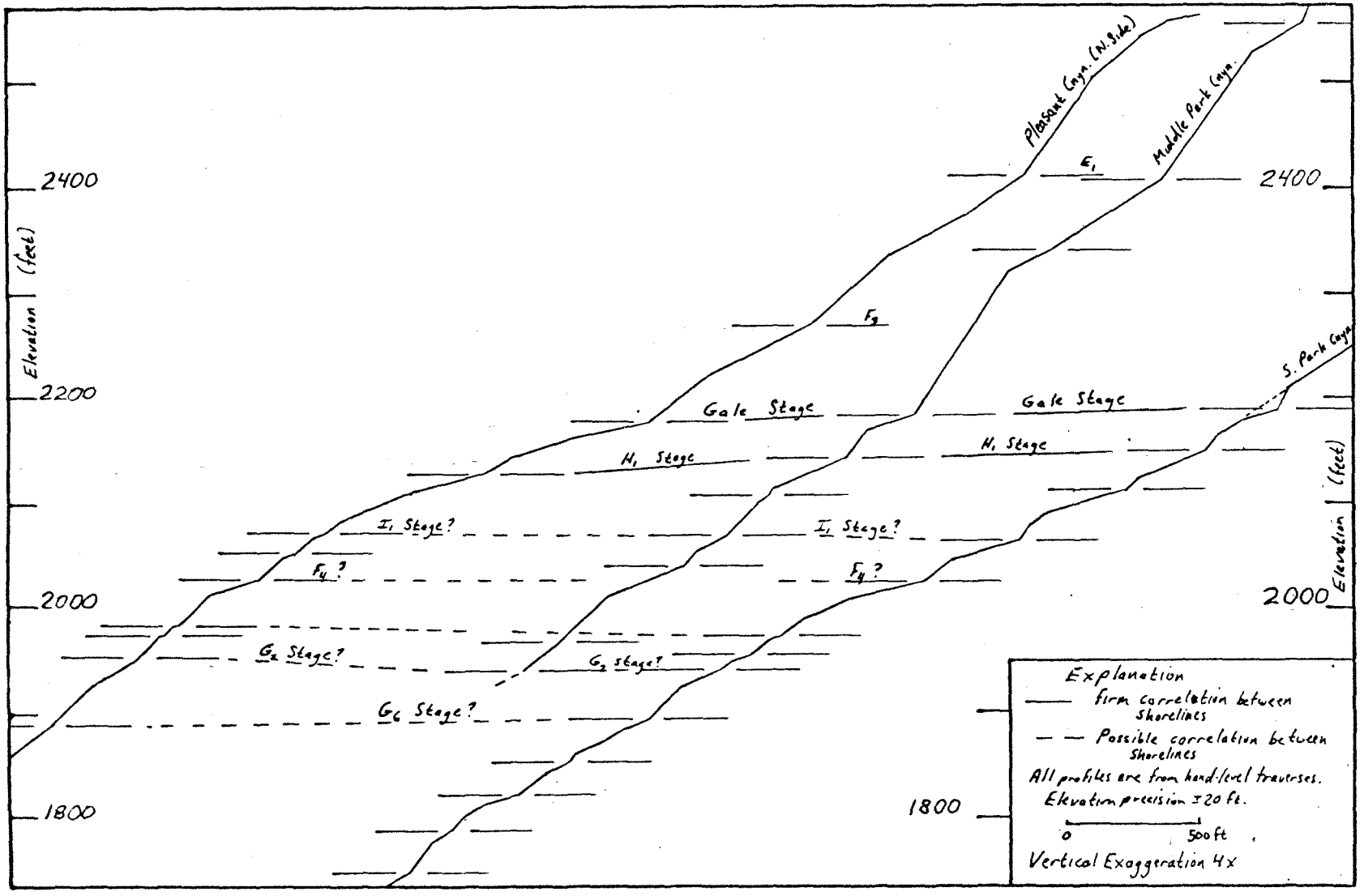

Figure 3-15. Profiles and correlation of shorelines on the central Panamint Range.

No shorelines higher than the Gale-Stage level were identified with any certainty in this area, but fairly abundant subrounded gravel was found on a bench at Middle Park Canyon at 2555±20 feet elevation, which is substantially higher than the oldest, highest (E_1, 2410±10 feet) shoreline at Pleasant Canyon and thus possibly substantially older. Scattered subrounded pebbles were found on benches at 2400±20 and 2340±20 feet elevation, overlying a lag deposit of boulders on the lower bench (fig. 3-15). Neither tufa nor deposits of gravel with lacustrine depositional structures were found on any of these three bench remnants.

The F_4 shoreline may be indicated at South Park Canyon by a bench at 2027±20 feet elevation, slightly above a large body of lake gravel which is capped by lag boulders (figs. 3-14, 3-15). The gravel body is made up of alternating beds of cobbles and pebbles which dip steeply (27°) to the east and extend down to about 1700 feet elevation in South Park Canyon. A bench which lies at elevation 2038±20 feet at Middle Park Canyon may also correlate with F_4 (fig. 3-15).

Evidence for the H_1 stage was found at South Park Canyon, where snail-bearing lithoid-to-dendritic tufa encrusts lag boulders one foot in diameter on a bench which reaches 2150±20 feet elevation, 40 feet below the Gale-Stage shoreline (figs. 3-14, 3-15). Likewise, 40 feet below the Gale-Stage shoreline on the north side of Middle Park Canyon, lag boulders mantle a bench whose continuation south of the canyon bears tufa overlying a lacustrine(?) deposit of gravel

which extends upward only to the Gale Stage shoreline. Clasts within this deposit are subrounded near its uppermost extent but elsewhere are mostly subangular, so the deposit may be partly non-lacustrine in origin.

An I_1 shoreline may be present at South Park Canyon, where a bench reaching 2065±20 feet elevation is surmounted by a beach cliff that retains a much steeper slope (21°) than any other degraded beach cliff (8°-16°) on the broad, smooth slopes from 1800 to 2200 feet elevation (figs. 3-14, 3-15). Its steeper slope suggests that it has experienced a much shorter interval of degradation than even the H_1 cliff (14°). At the south end of this I_1(?) bench is a deposit of subangular gravel which is moderately sorted into beds which dip 22° southwest. The gravel deposit is locally overlain by a lag deposit which may either be lacustrine or colluvial in origin.

North of Pleasant Canyon

The Panamint Range front extending northward from Pleasant Canyon is largely devoid of evidence for high stands of Lake Panamint (fig. 3-3). Only in Surprise Canyon do probable bottomset sands extend upward and eastward from an elevation of about 2000 feet to scattered subrounded gravels that reach a maximum elevation of 2180±40 feet. No tufa was found with these deposits, but a lag accumulation seems to underlie their higher part. They lie at about the same elevation as the Gale-Stage deposits at Pleasant Canyon and

may be correlative. Lag boulders overlain by subrounded gravel lie at 1950±40 and 1875±40 feet elevation on steep slopes on the south side of Surprise Canyon, and subrounded gravel with sand lies at 1800±40 feet elevation.

Shorelines were sought but not found at Happy Canyon, Hall Canyon and Jail Canyon, both on the rocks of the range front and on the fanglomerate and older fan deposits flanking the range front (figs. 3-1, 3-3).

High Shorelines and Lake Deposits on the Northern Slate Range and Southern Argus Range

Introduction

Discontinuous remnants of a prominent high shoreline, tentatively attributed to Gale Stage, can be traced from Water Canyon at the north end of the Slate Range 15 miles northward to Revenue Canyon in the central Argus Range (fig. 3-1). West of the Ash Hill fault, it is marked mainly by large, but separated, bodies of lacustrine gravel, sand and marl, and a few cut shoreline benches. East of the Ash Hill fault (east and north of Revenue Canyon), it is expressed by a prominent cut bench, littered with tufa and rounded gravel, which can be traced with few interruptions ten miles northward to Ash Hill (fig. 3-1). Shorelines on both sides of the Ash Hill fault have been tilted northward. Shorelines east of the fault are more continuous than those west of the fault because uplift of the east side has diverted streams, thus preserving the shoreline on the east

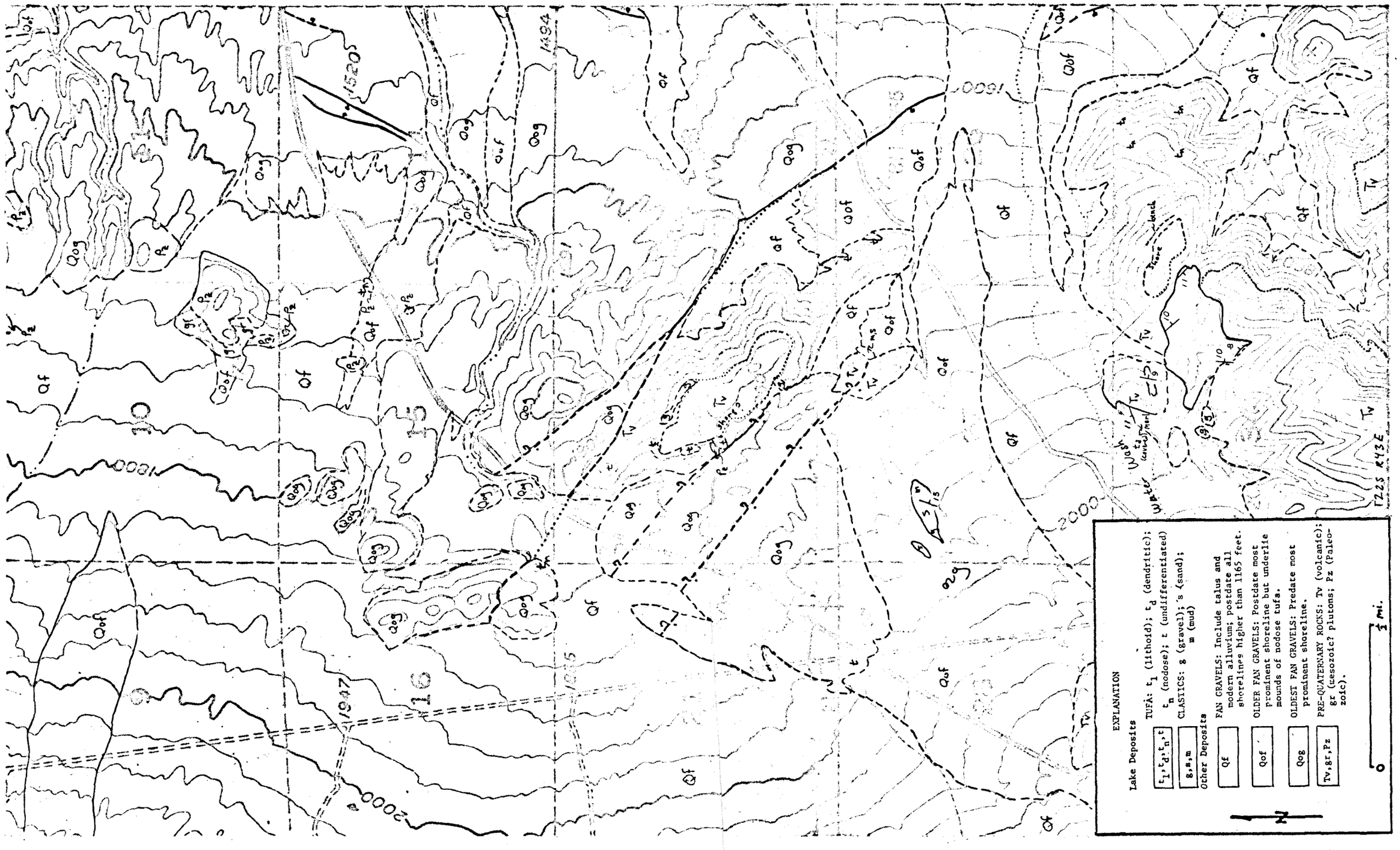

Figure 3-16. Geological map of region adjacent to lowermost Water Canyon.

side from dissection.

Water Canyon

Voluminous lake deposits, preserved south of lowermost Water Canyon in an embayment in the northern Slate Range, reach an elevation of 2005±5 feet (fig. 3-17; fig. 3-16, NE 1/4 sec. 34). At this level a narrow bench cut into basalt encircles Hill 2074 (fig. 3-15). No tufa was found on this bench or on a fainter one 40 feet lower (1965±15 feet). Dendritic tufa found at 1960±20 feet elevation on the west side of Hill 2000+ underlies marl. Both tufa and the lower bench are attributed to the shoreline of the early G_1 substage lake, whose level was stabilized by overflow across the bedrock lip now buried beneath Wingate Pass.

Marl and thinly-bedded (varved?) silt, ten feet thick, are exposed from about 1900 to 1970 feet elevation and form the basal unit of the main body of lake sediments (fig. 3-17). Coquina is locally abundant in the upper part of the basal unit (figs. 3-17, 3-18).

A hard, irregular mantle of calcareously-cemented sand and granules caps the basal unit and was probably deposited on an erosional surface cutting the basal unit. Heads of dendritic tufa are locally found directly above this mantle. The upper unit, 40 to 80 feet of lacustrine sand and gravel, directly overlies the mantle and local tufa. The upper unit is flat-topped and bedding within it dips moderately, about ten degrees, towards the center of the deposit. Clasts of volcanic rocks from the hills above the deposit

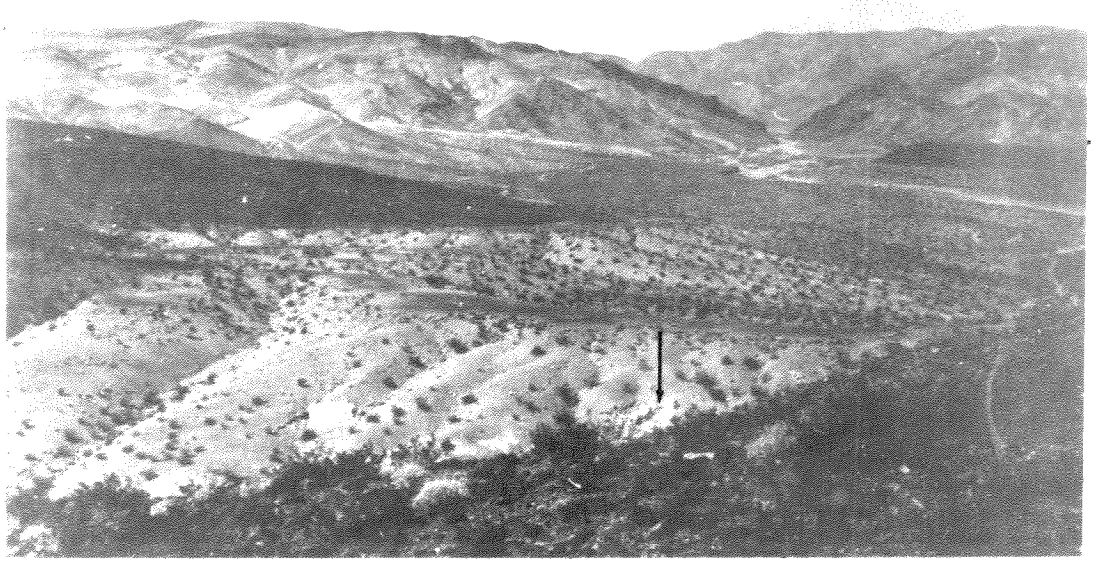

Figure 3-17. Looking west from hill 2074 at light-colored lake deposits from Water Canyon (upper right). Arrow points to coquina locality (fig. 3-18).

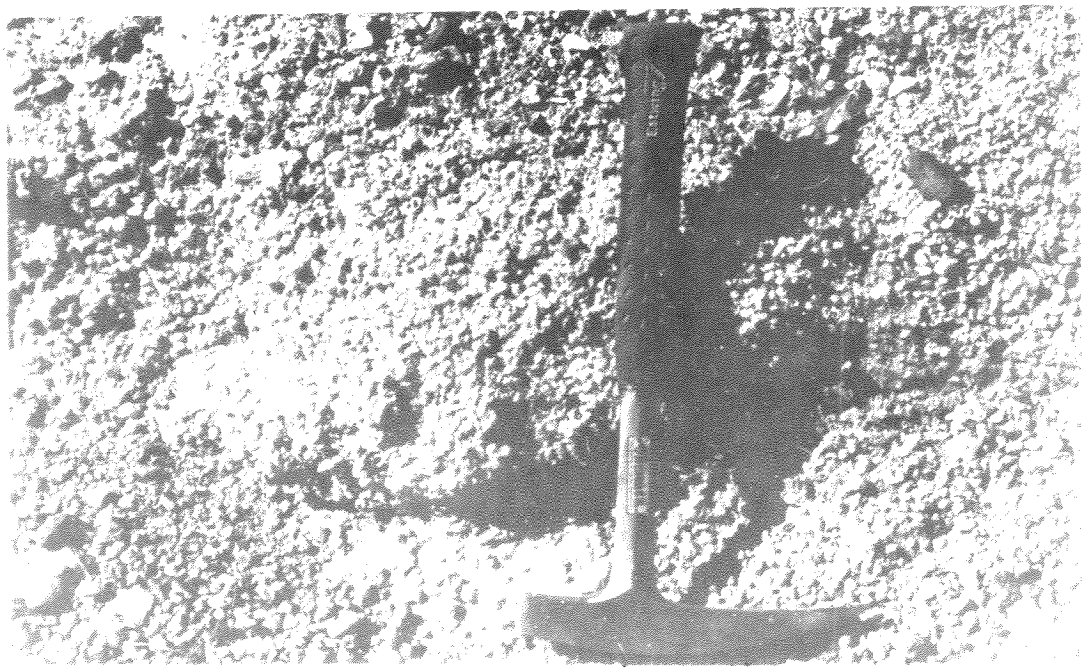

Figure 3-18. Coquina, east end of deposits south of Water Wash. Largely composed of gastropod genera Carnifex and Lymnaea.

are rare; almost all clasts are of plutonic and metamorphic rocks, like the clasts now found in Water Canyon but better rounded.

Sparse tufa and lake gravel reach 1980 to 1990 feet elevation on the north side of lowermost Water Canyon (fig. 3-16, NE 1/4 sec 28), but a shoreline of dendritic tufa and pebbles and cobbles of granitic rock reaches only 1880±20 feet elevation on the northeast-facing slopes of volcanic Hill 1960 (fig. 3-19; fig. 3-16, sec 22). This shoreline probably correlates with the prominent high shoreline to the south and west, but has been dropped 100 to 125 feet by graben-like movement along a pair of northwest-trending faults which bound Hill 1960 (fig. 3-16).

The present distribution of lake gravel with plutonic and metamorphic clasts suggests that a large delta, more than a mile wide and up to 200 feet thick, occupied lowermost Water Canyon during Gale-Stage time. The shoreline configuration suggests that longshore drift could not have deposited such gravel on volcanic Hill 1960 unless the lower flanks of the hill were buried beneath a delta constructed mostly from metamorphic and plutonic clasts (fig. 3-19). The principal body of the delta at the north end of the Slate Range has been dissected to depths of more than 80 feet and isolated from outliers by still deeper gullies, but concordance of the upper surface of all these remnants indicates that the delta once extended over the entire area and reached across Water Canyon to Hill 1960.

Isolated knobs of nodose tufa, locally more than ten feet high, are found only between 1600 and 1800 feet elevation. They are most prominent on volcanic-rock slopes on the east side of Hill 2074 and

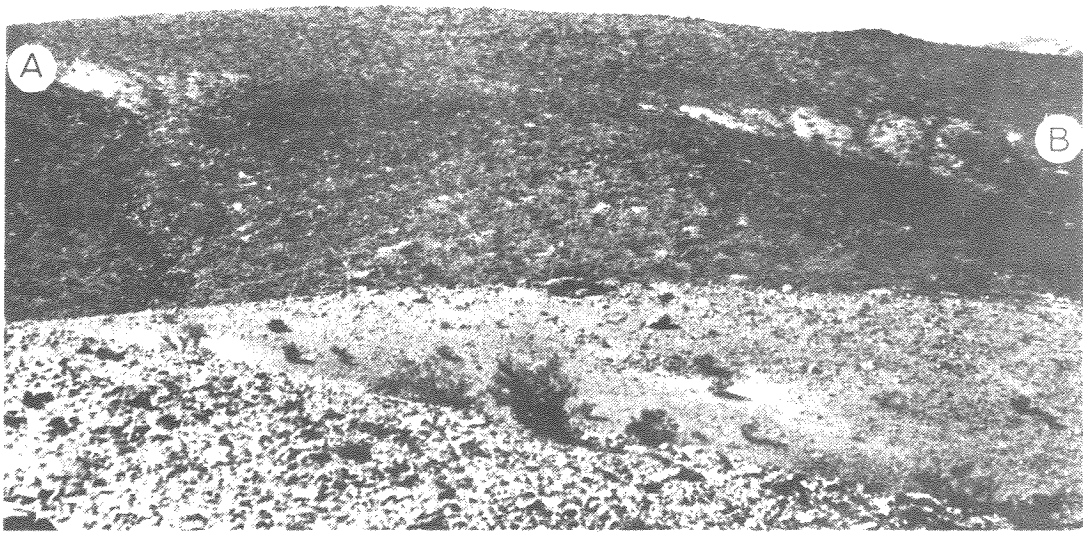

Figure 3-19. Granitic lake gravel on the northeast side of volcanic hill 1960.

Looking southwest at a gravel line, attributed to the prominent high shoreline, whose highest elevation descends northward from about 1880 feet on the left (A) to about 1860 feet on the right (B). This gravel was probably carried northward from a delta which is thought to have filled lowermost Water Canyon during development of the prominent high shoreline.

on the southeast end of Hill 1960 (fig. 3-16, N 1/2 sec 35 and NW 1/4 sec 26, respectively). Local knobs of nodose tufa are found on gentler surfaces of older gravel and older fan deposits, but no shoreline features are associated with them.

Shepherd Canyon

Two small deposits of foreset gravel below the mouth of Shepherd Canyon reach 1990±10 feet elevation and are correlated with the high prominent shoreline (fig. 3-20, SE 1/4 sec 4). Subrounded pebbles of the igneous and metamorphic lithologies found in the modern wash are moderately sorted by beds. These deposits are surrounded by modern fan deposits and no cut shoreline features were found associated with them.

Bendire Canyon

The nip of a tufa-bearing wave-cut shoreline lies at 1940±10 feet elevation on the north side of the wash which exits Bendire Canyon three miles to the west (fig. 3-21; fig. 3-20, NE 1/4 sec 20). On the south side of the wash, lake deposits extend outward from the 1940-foot shoreline and descend to 1720 feet elevation. A thin zone of lake gravel and lag cobbles at 1800 to 1825 feet elevation divides this deposit into a lower body of gravel (1720 to 1800) and a higher body of marl (bottom) and sand and gravel (top) (1825 to 1940) (figs. 3-20, 3-21). The age relationship between the higher and lower bodies has not been determined because beds from neither

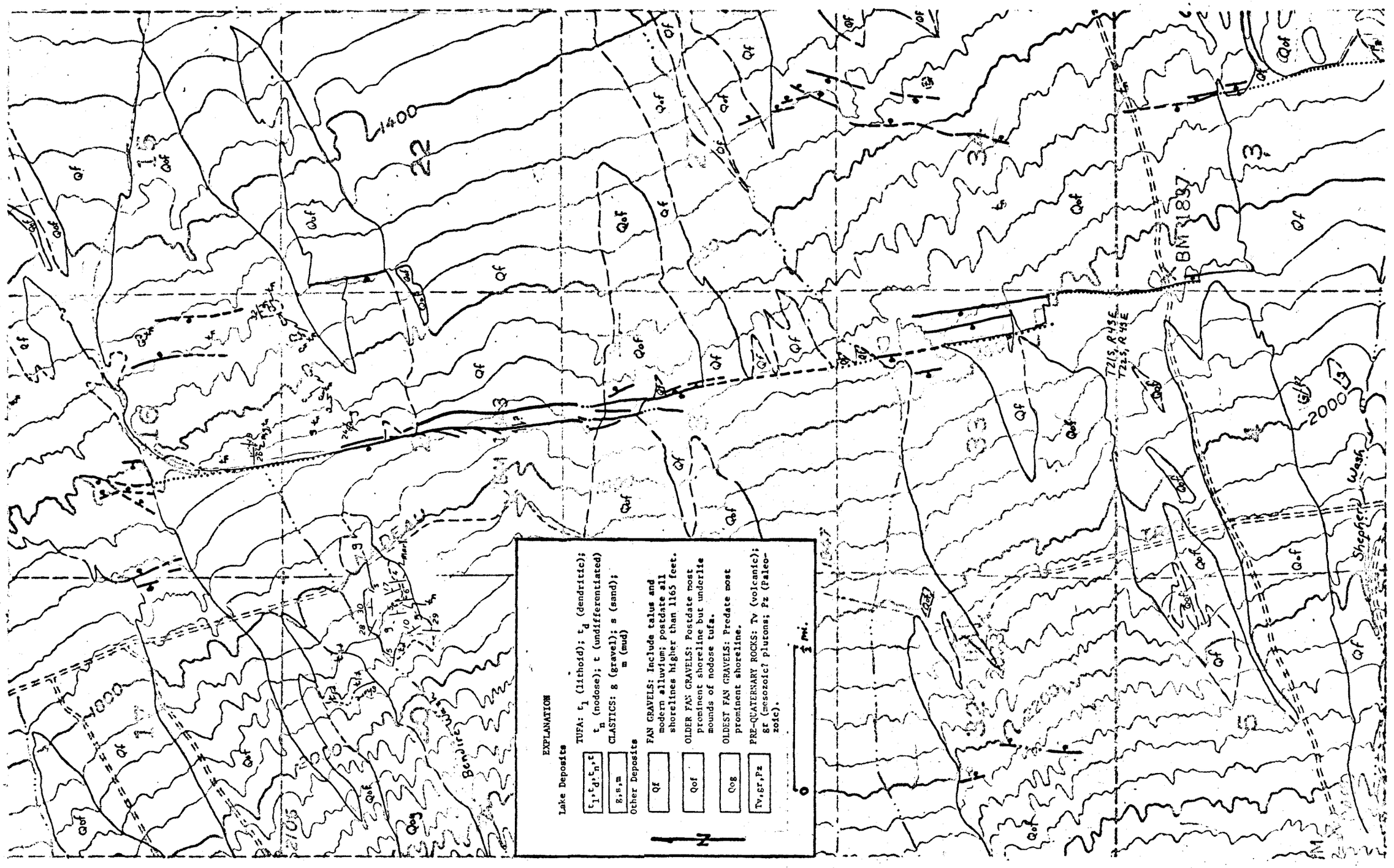

Figure 3-20. Geological map of the region between Shepherd Canyon wash and Bendire Canyon wash.

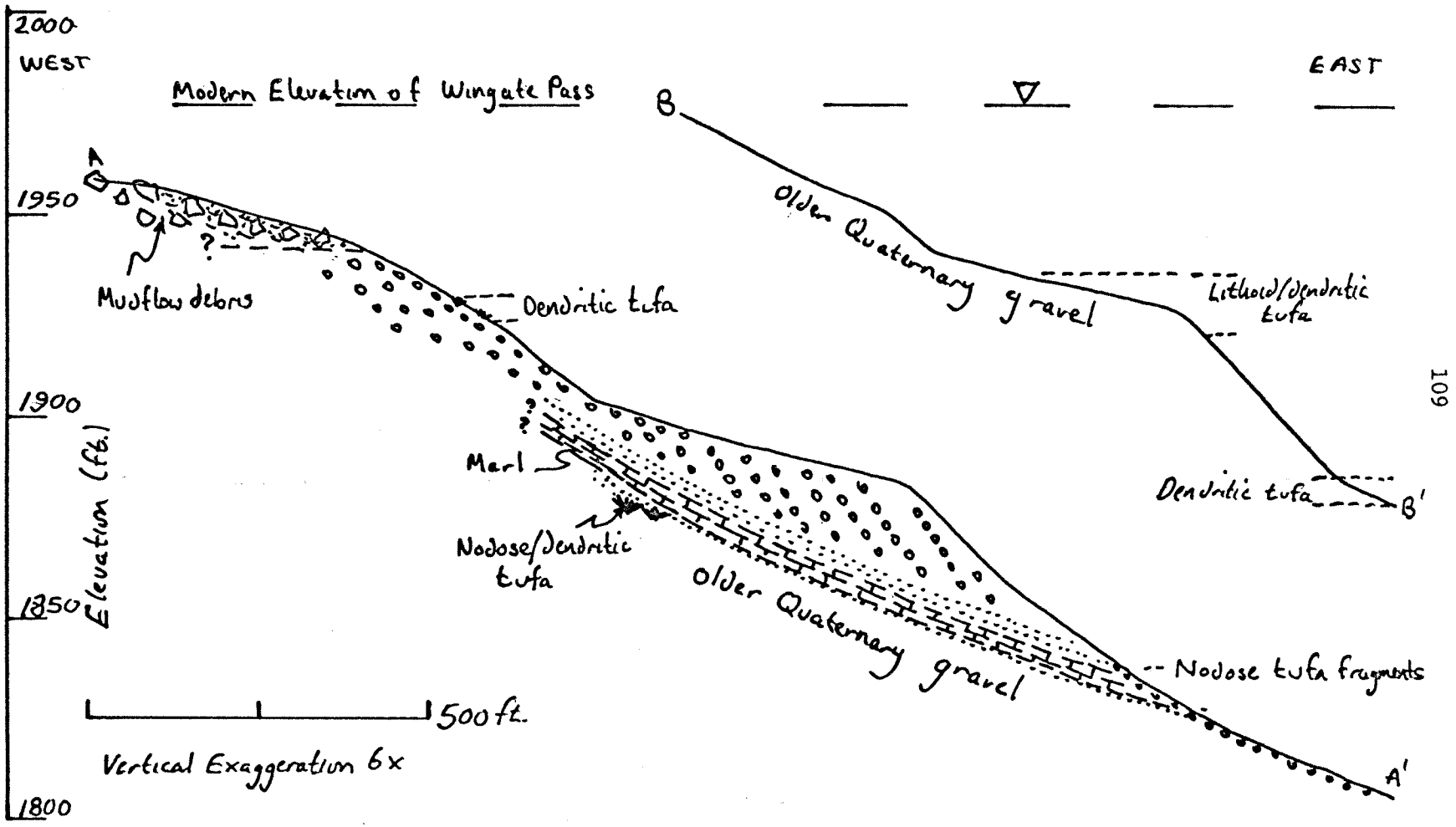

Figure 3-21. Cross sections of shorelines and lake deposits at Bendire Canyon wash.

body can be traced onto the other.

Mounds of nodose to dendritic tufa at 1875 to 1880 feet elevation underlie the basal part of the higher body, whose abundant gastropods and diatoms have been described by Hanna (1963) and Wornardt (1964) (figs. 3-21, 3-22). Foreset beds of gravel form the bulk of the higher body and are overlain by bouldery mudflow debris above 1940 feet elevation.

A cut bench (nip elevation 1885±10 feet) on the north side of the wash bears dendritic tufa which may correlate with the tufa beneath marl south of the wash (fig. 3-21). This suggests that the 1885-foot shoreline is older than the 1940-foot shoreline, which, south of the wash, lies at the head of gravel deposits which overlie the 1875-1880-foot tufa. The lower (1885) shoreline is tentatively correlated with the earliest part of G_1 substage, whose level was stabilized by overflow across the bedrock lip beneath Wingate Pass. The higher (1940) shoreline probably formed during the remainder of Gale Stage in lake stands (later G_1, G_3, G_5) stabilized by overflow through the outlet channel in Wingate Pass.

Separated bodies of lake deposits between 1490 and 1690 feet elevation east of the Ash Hill fault are probably younger than lake deposits at higher elevation because the surface of older fan deposits beneath these separated bodies can be traced continuously upslope to 2800 feet elevation without finding any trace of high shorelines on it (fig. 3-20, secs. 16, 17, 20, 21). These bodies are mostly mounds of nodose tufa, typically arranged in rows orthogonal to contour

Figure 3-22. Marl in lake deposits south of Bendire Canyon wash. Looking north at nodose to dendritic tufa exhumed from beneath marl.

lines. At 1520 feet elevation a mound of nodose tufa rests on the crest of a bar made of subangular gravel (fig. 3-20, extreme SE 1/4 sec. 16). At higher elevation (between 1640 and 1680 feet) are a few small, widely-scattered bodies of crossbedded, calcareously-cemented subangular gravel, one associated with silt containing snail shells.

Revenue Canyon (West of Ash Hill Fault)

Shoreline remnants extending to 1940 feet elevation and marked mainly by tufa were found in two places: 1) 2.5 miles south of Revenue Canyon's mouth and 2) one mile south (fig. 3-23, west edge sec 7, and NE 1/4 sec 1, respectively). At the southern site, two bands of tufa cling to marble bedrock which forms the steep basal slope of the Argus Range; 1) a prominent band of snail-bearing lithoid tufa at 1940±15 feet elevation, and 2) a faint band of dendritic tufa and local coquina with a tufa matrix 55 feet lower at 1885±15 feet. No cut bench or rounded gravel was found along either tufa band. At the northern site, rounded cobbles and one-to-two-foot blocks of lithoid tufa lie at the same elevation as a tufa band which nearly reaches the summit (elevation 1930±10 feet) of an isolated bedrock hill 0.2 miles to the northeast (fig. 3-24).

Lake or playa beds just west of the Ash Hill fault at 1560 feet elevation were probably deposited in a depression dammed by fault uplift and may be unrelated to Lake Panamint (fig. 3-2, S 1/2 sec 5). These beds, lying at the head of the canyon of a seemingly-

antecedent stream, have been dissected to a depth of 10 to 15 feet. No snail remains were found in them.

Revenue Canyon (East of Ash Hill Fault)

A prominent high shoreline opposite the mouth of Revenue Canyon lies at 2020±15 feet elevation, 90 feet higher than the presumably correlative high shoreline west of the Ash Hill fault (fig. 3-23, E 1/2 secs 23, 24). This shoreline is marked by extensive deposits of lithoid tufa and is surmounted by a wave-cut cliff 10 to 20 feet high (fig. 3-25). The shoreline wraps around spurs and penetrates gullies, suggesting that these features anteceded the shoreline. Rounded gravel is locally abundant on the shoreline (fig. 3-26), which can be traced almost continuously ten miles northward to the north end of Ash Hill.

A band of rounded gravel, with associated dendritic tufa downslope and subangular colluvial(?) debris upslope, is found locally at elevations 25 to 30 feet below the highest extent of lithoid tufa on the high shoreline at this locality. No cut benches were found on the smooth, gentle slopes which lie below this slightly-lower shoreline, whose relative age cannot be determined because its deposits are not extensive enough to be stratigraphically related to those deposits of the high shoreline. This slightly-lower shoreline may correlate with the shoreline of the lake stage which formed dendritic tufa 50 to 65 feet below the highest level at Water Canyon, Bendire Canyon and 2.5 miles south of the mouth of Revenue Canyon, and is tentatively attributed to earliest G_1 substage.

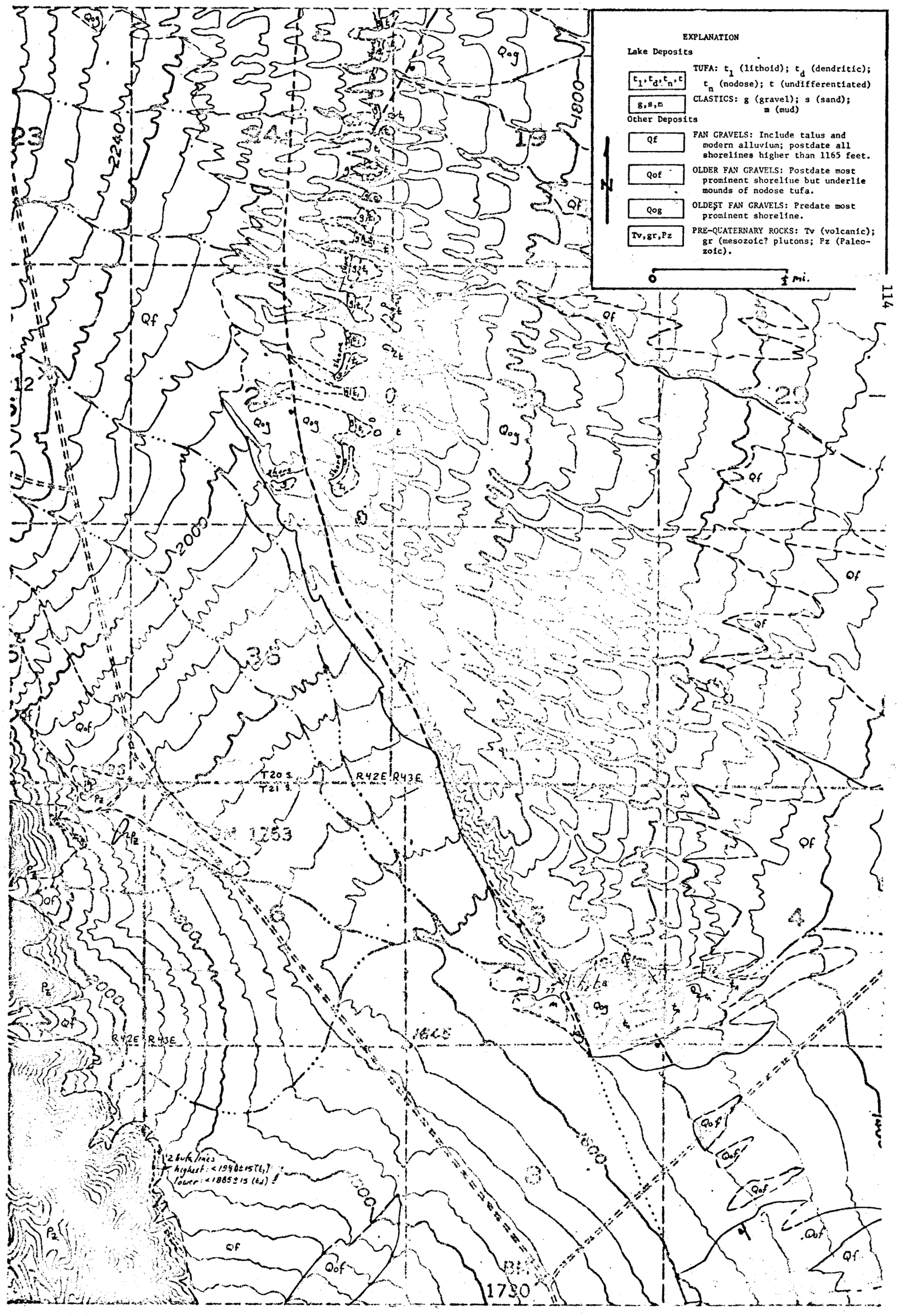

Figure 3-23. Geological map of the region near the mouth of Revenue Canyon.

Figure 3-24. Shoreline on Argus Range south of Revenue Canyon. Looking northeast at isolated, tufa-capped hill in NE 1/4 sec 1, T21S, R42E. Note large tufa block in left foreground.

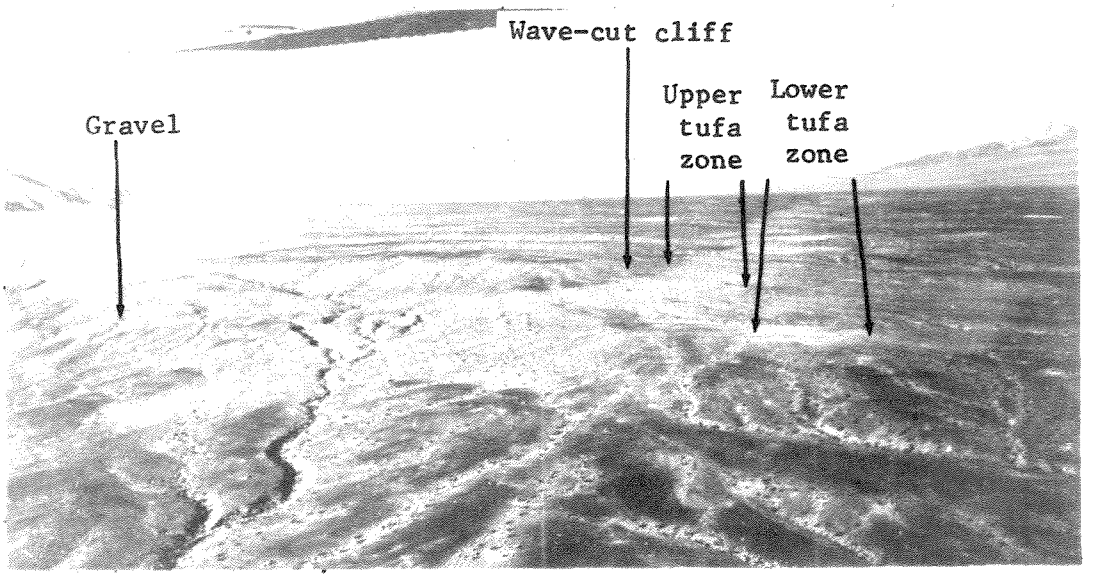

Figure 3-25. Looking north at shorelines east of Revenue Canyon. (Sec. 25, T20S, R42E)

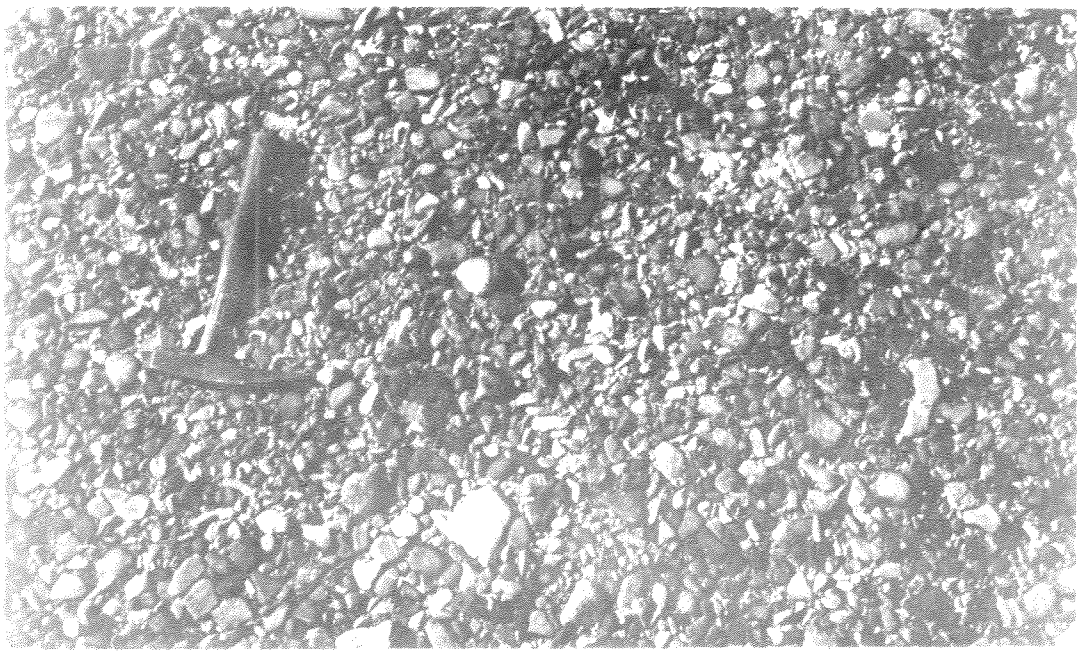

Figure 3-26. Typical worn gravel on beach east of Revenue Canyon. Location is in center of fig. 3-25.

Low Shorelines

The highest low shoreline is the most prominent of the low shorelines and is variously marked by wave-cut cliffs five to ten feet high, by bars of subangular gravel, by deposits of silt and clay, and by benches broader than those of lower shorelines (figs. 3-3, 3-14). This shoreline has an elevation of about 1165 feet on both sides of Panamint Valley except where it has been deformed near the Panamint Valley fault zone (elevation range here is 1145 to 1186 feet, fig. 3-27). No water levels above this shoreline can be found below the 1520-foot gravel bar at Bendire Canyon (fig. 3-21). On steep slopes, like those at South Park Canyon, up to 20 shorelines can be found below the highest low shoreline, but on gentle slopes, like those on the west side of Panamint Valley, less than three can be found (fig. 3-3). No tufa or snail shells have been found along any of the low shorelines, but a few blocks of nodose tufa were found along the Happy Canyon road at 1080 feet elevation (fig. 3-2). The low shorelines are by far the freshest-looking in Panamint Valley and are probably the youngest.

The Lake Panamint Record in U.S. Geological Survey Cores Taken from South Panamint Playa

Smith and Pratt (1957, p. 51-62) have logged cores taken from two deep holes drilled in south Panamint playa by the U.S. Geological Survey. These holes were designated DH1, 1a (500 feet deep, one mile southwest of Ballarat) and DH3 (995 feet deep, six miles south of

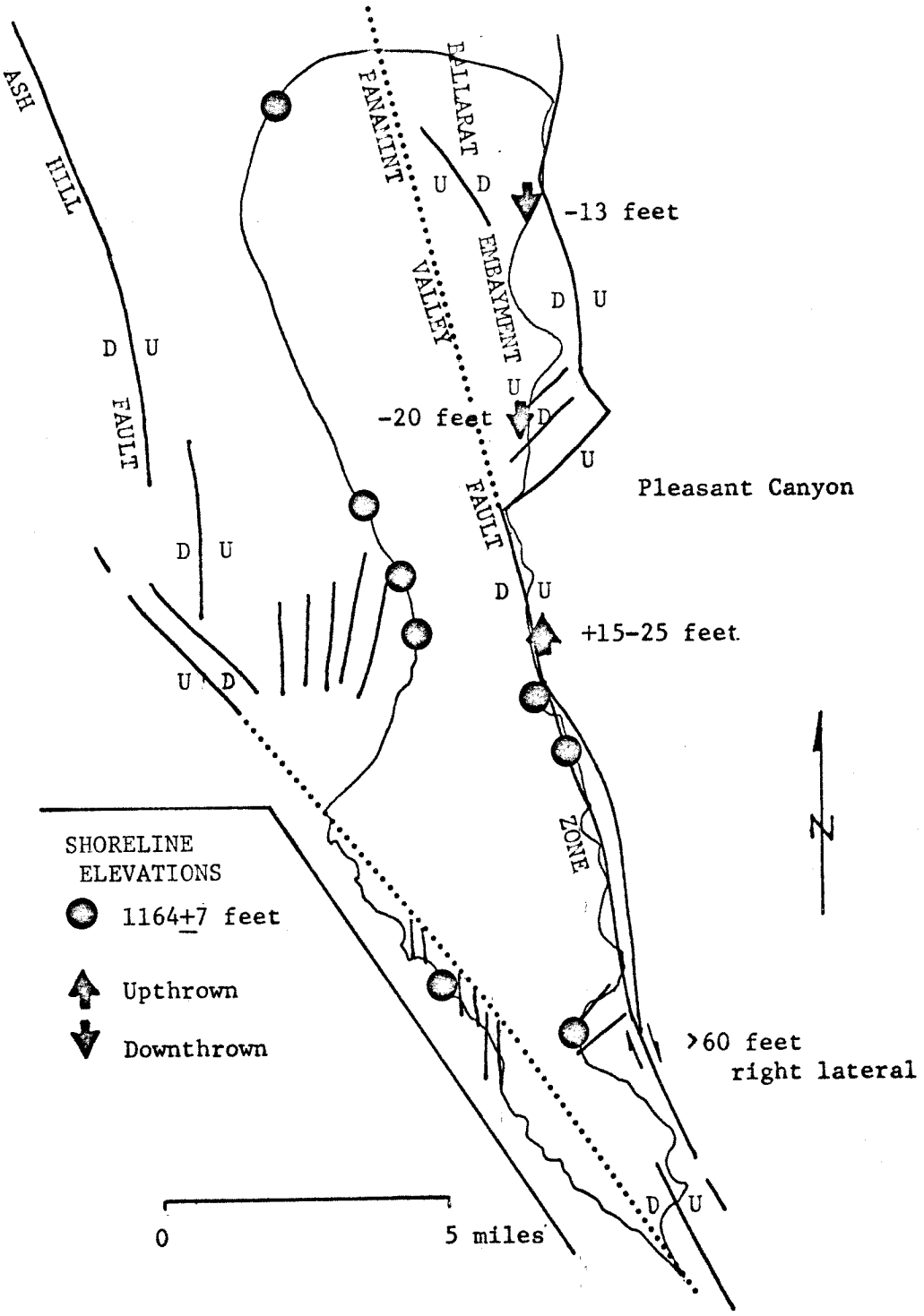

Figure 3-27. Map of deformation of highest low shoreline in central and southern Panamint Valley.

Ballarat)(fig. 3-28). Additionally, Motts and Carpenter (1968, p. 44-46) have logged the core from a shallower hole SP-3 (83 feet deep, five miles north of Ballarat)(fig. 3-28). Detailed logs of all three cores are reproduced in Appendix B; only the data from DH1, 1a and DH3 are used in the following discussion because SP-3 is too shallow.

The logs of these cores cannot be correlated by fossils or evaporites because ostracods and diatoms (diagnostic of high lake stands) were reported only from DH1, 1a and halite (diagnostic of very low lake stands) was reported only from DH3,where it forms half of the section above 500 feet depth.[1] To facilitate stratigraphic correlation between DH1,1a and DH3, the halite-rich beds in DH3 were compressed to the thickness of their clastic content (for example, a 10-foot bed of 70% halite and 30% clay is reduced to three feet of compressed section on fig. 3-29). Rates of clastic sedimentation in the lake at the sites of both holes should have been roughly comparable, independent of rates of halite precipitation, so the logs can be approximately correlated on the basis of thickness of layers (fig. 3-29).

---

[1] The absence of halite in DH1,1a could be explained in two ways: 1) The lake was deeper at DH3, and the salinity of lake water was not high enough to precipitate halite until the lake's shoreline receded past DH1,1a, leaving its site subaerially exposed during halite deposition at DH3; 2) Sublacustrine springs along the front of the Panamint Range may have kept the lake water at DH1,1a too fresh for halite to precipitate.

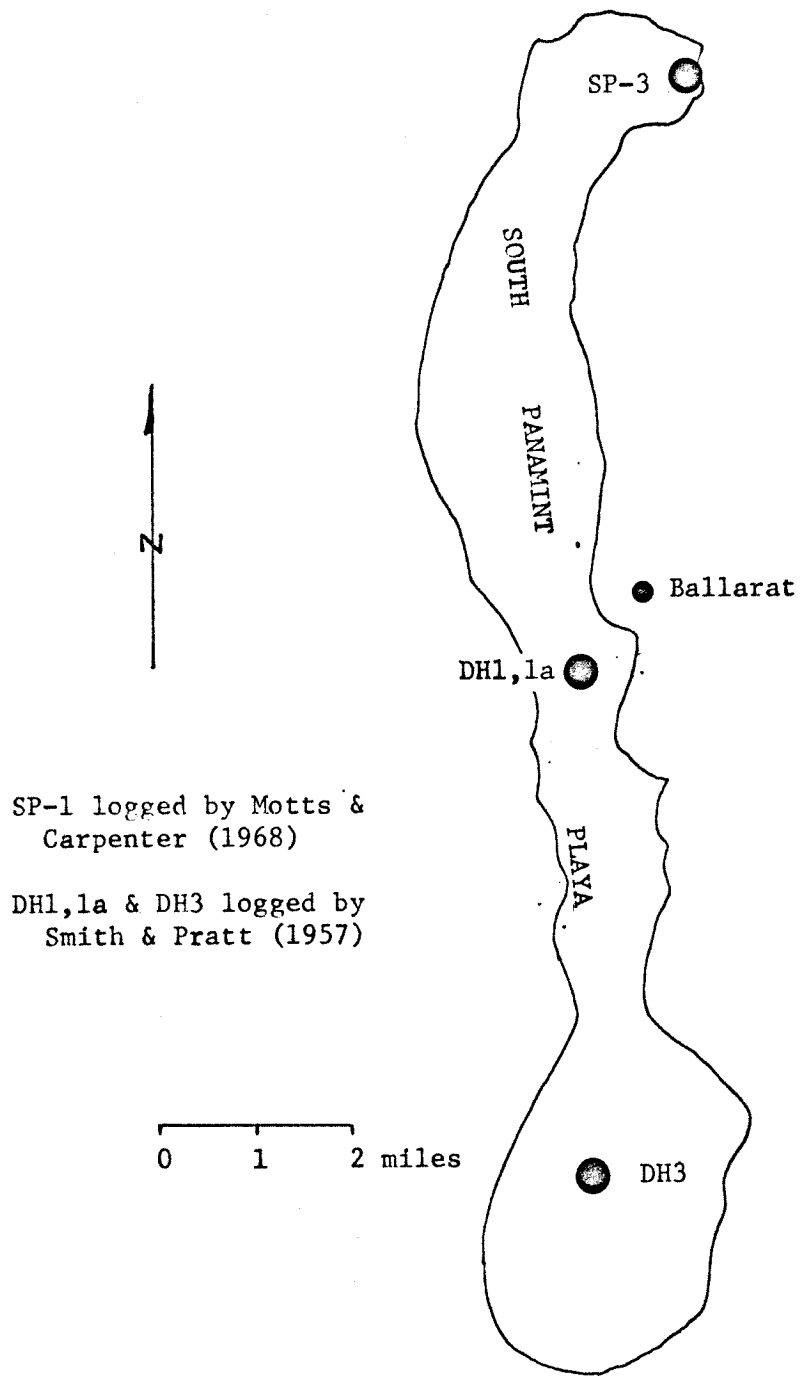

Figure 3-28. Map of south Panamint playa, showing the location of drill holes from which logs have been published.

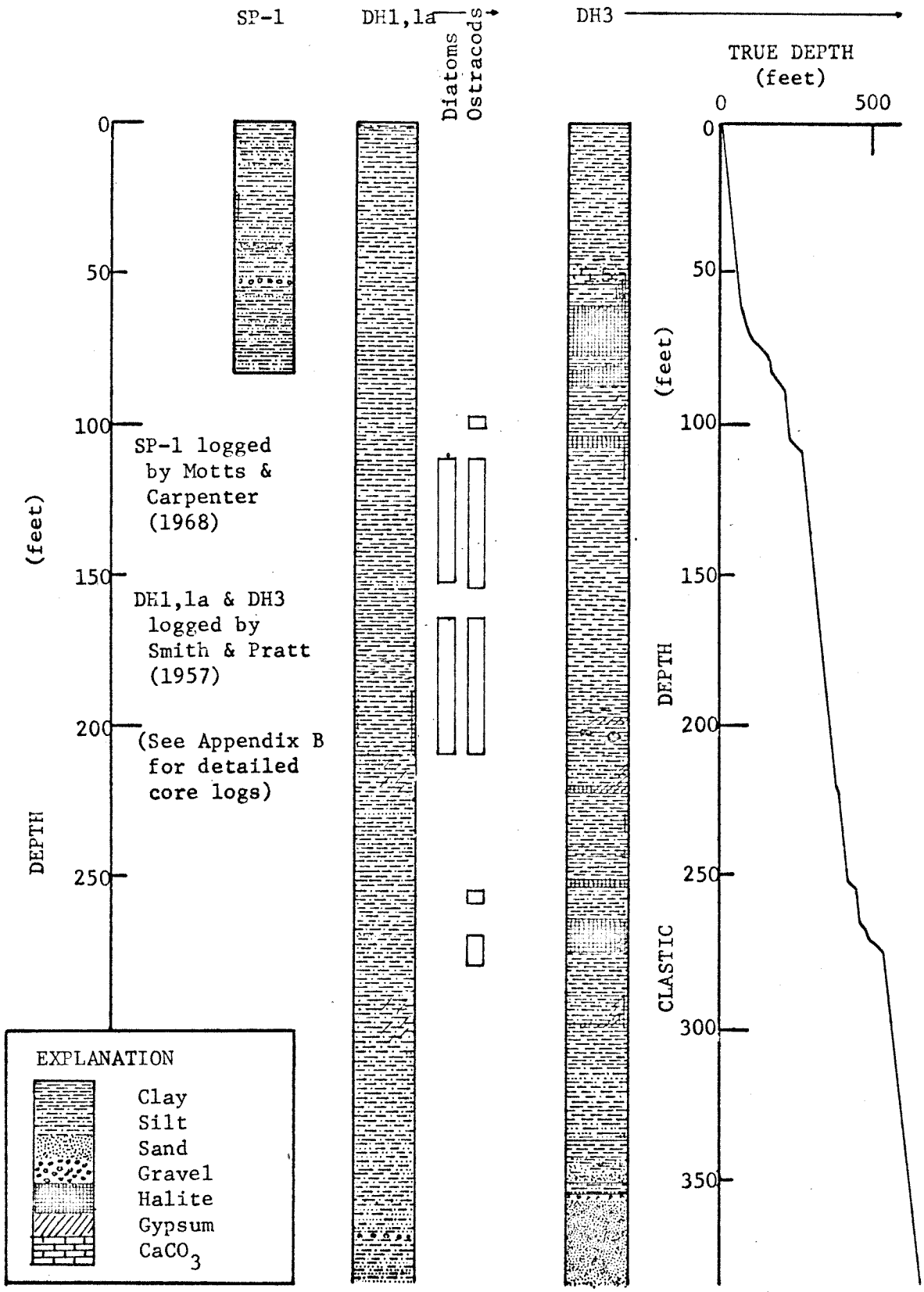

Figure 3-29. Graphic logs of cores from south Panamint playa published by Smith and Pratt (1957) and Motts and Carpenter (1968).

Correlation

Lake-Bottom Sediments and Lake-Shore Features

Tentative correlation between the high lake stands recognized in the logs of deep drill holes in south Panamint Valley and lake stages recognized within nearshore deposits at Pleasant Canyon is presented in Table 3-2. This correlation suggests that high lake stages E and H were short compared to the long duration of the combined F and Gale stages. These two stages appear to represent the older and younger parts of a long period of lake level continuously high enough to prevent halite deposition. No obvious correlative of the queried I_1 shoreline at Pleasant Canyon has been found in the core logs.

Table 3-2.

Tentative correlation between high shorelines at Pleasant Canyon and ostracod zones in the log of DH1,1a

Pleasant Canyon		DH1,1a	ostracod zones
Stage	Elevation (feet)	Thickness (feet)	Depth (feet)
I_1	2040±40 ?	-----	-----
H_1	2127±10	4	98-102
$Gale_{1,3,5}$	2177±10	43	112-155
F_3	2265±10	45	165-210
F_1	2298±10		
E_1	2410±10	4	255-259
		10	270-280

Shorelines

The highest shoreline on the Argus and northern Slate ranges is correlated with the Gale-Stage shoreline at Pleasant Canyon on the basis of its prominence and the large volume of deltaic (?) sand and gravel associated with it.

The shoreline 25 to 65 feet below the highest shoreline on the Argus and northern Slate ranges is largely marked by tufa which is overlain by deposits attributed to the highest shoreline at lowermost Water and Bendire canyons. Thus, this lower shoreline is older than the highest shoreline. The persistence of this lower shoreline, and the local development of benches along it, suggest that it formed in a lake whose level was stabilized by overflow, but at a level below that of the present outlet channel through Wingate Pass. This lower shoreline was probably stabilized by overflow across the bedrock lip (elevation 1930±15 feet) now buried beneath mudflow deposits into which the modern outlet channel is cut.

The lower shoreline is correlated with the early part of G_1 substage of Gale Stage despite there being only one, not two, discrete high Gale-Stage shoreline at Pleasant Canyon. The absence of paired shorelines at Pleasant Canyon can be explained if this single shoreline is a composite feature, first occupied during the early part of G_1 substage. Later G_1, and G_3 and G_5 lake stands were stabilized at higher level and their shoreline was cut into fanglomerate which was being uplifted during shoreline incision. Eventually, before the end of Gale Stage, the early G_1 shoreline was raised into

the surf zone of a later lake zone and only a single composite shoreline remains. The full sequence of hypothesized events is presented on Figure 3-30.

Tectonic Deformation

Vertical Movement

Most vertical movement has been down to the west on faults in central Panamint Valley. Along the valley's east side, the most prominent low shoreline lies 20 feet higher on the east side of the Panamint Valley fault zone than it does on the west, and the high Gale-Stage shoreline on the valley's east side now lies about 200 feet above the basin's modern lip at Wingate Pass (figs. 3-3, 3-5, 3-14, 3-27). Along the valley's west side, the prominent high Gale-Stage (?) shoreline at Revenue Canyon lies 90 feet higher on the east side of the Ash Hill fault than it does on the west, which is consistent with west-facing scarps which characterize the Ash Hill fault along much of its length (figs. 3-16, 3-20, 3-23, 4-2). Abundant fault scarps between Water Canyon and south Panamint playa also face mostly to the west (fig. 3-27). Half of the offset at Revenue Canyon must represent absolute uplift of the east side, and half must represent absolute downthrow of the west side, if the high shoreline there formed with respect to the modern elevation of Wingate Pass.

Shorelines have been lowered along subsidiary normal faults which strike obliquely to the northerly trend of both the Panamint

(1) Cutting of G_1 bench at 1930-foot level of bedrock lip in Wingate Pass. Deposition of G_1 gravel below bench.

(2) Mudflow buries bedrock lip in Wingate Pass. Lake level rises, overtops mudflow and cuts modern outlet channel into top of mudflow (elevation 1977±1 ft).

(3) New bench cut at higher level of new outlet channel.

(4) Width of new bench and height of new wave-cut cliff increase as wave erosion tries to keep pace with range uplift.

(5) Old G_1 bench uplifted to level of new bench and its width is added to the width of the new bench, making the prominent composite bench seen today.

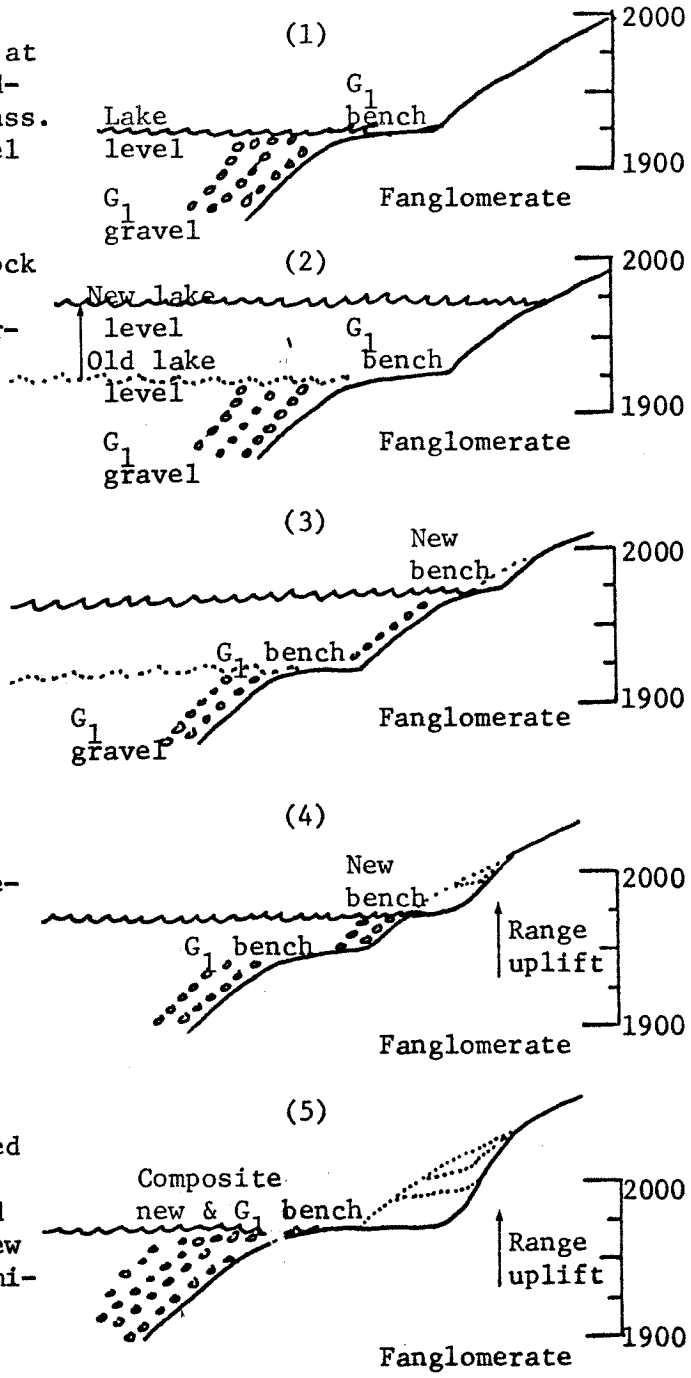

Figure 3-30. Possible explanation for development of prominent Gale-Stage shoreline at Pleasant Canyon.

Valley fault zone and the Ash Hill fault (figs. 3-16, 3-27). Northeast-striking faults form the south wall of the Ballarat embayment, the prominent range-front embayment which extends from Pleasant Canyon five miles north past Surprise Canyon (fig. 3-27). Within the embayment, the prominent low shoreline at Happy Canyon lies about 40 feet below its general elevation on the east side of the Panamint Valley fault zone and about 20 feet below its elevation everywhere west of the fault. On the west side of the valley north of Water Canyon, high shorelines on Hill 1960 have been dropped 100 to 125 feet in a graben bounded by northwest-trending faults (fig. 3-16). These faults line up with, and are probably related to, the postulated zone of faulting to the southeast along the northeast margin of the Slate Range.

Northward tilting of the high Gale-Stage (?) shoreline west of the Ash Hill fault is the only major late-Quaternary tilting detected in central Panamint Valley. This shoreline descends about 75 feet in the 13-mile segment from Water Canyon north to Revenue Canyon (fig. 3-1). North-south tilting of shorelines on the central Panamint Range appears to be slight, probably less than 15 feet in the seven-mile stretch from South Park Canyon to Surprise Canyon (fig. 3-15).

No north-south or east-west tilting of the prominent low shoreline has been detected (fig. 3-27). This shoreline lies everywhere at the same elevation (within measurement errors) except where it has been obviously faulted on the east side of the Panamint Valley fault zone and in the Ballarat embayment. The age of eastward

tilting of the oldest fan deposits at Revenue Canyon (present dip 8-12° E) and of old lake deposits three to four miles southwest of Ballarat (present dip 6° E) has not been determined (fig. 3-23).

Lateral Movement

The geometry of faults subsidiary to the Panamint Valley fault zone and to the Ash Hill fault is consistent with right lateral offset along these faults even though no firm evidence for such displacement has been found in central Panamint Valley. Fractures which feather into the Ash Hill fault at Bendire Canyon strike about 30 degrees clockwise to its trend. This is consistent with a right-lateral component of offset but not a diagnostic indicator of right-lateral offset (fig. 3-20). Faults within the Ballarat embayment strike about 45 degrees clockwise to the Panamint Valley fault zone south of Ballarat (fig. 3-3). Downthrow of the prominent low shoreline along these faults suggests that the Ballarat embayment marks a zone of northwest-southeast extension en echelon to the trend of the Panamint Valley fault zone, whose buried trace may extend northward about through Ballarat, two miles west of the range front (figs. 3-3, 3-27). The Ballarat embayment, the orientation of faults within it, and the extension and sense of downthrow within the embayment are all consistent with right-lateral shear along the Panamint Valley fault zone.

CHAPTER 4

NORTHERN PANAMINT VALLEY

Northern Panamint Valley extends from Jail Canyon in the Panamint Range and Snow Canyon in the Argus Range to Hunter Mountain which closes the north end of Panamint Valley (fig. 4-1). Two high shorelines, the higher being the more prominent, are nearly continuously exposed along much of both east and west valley margins in the southern part of northern Panamint Valley, but shoreline remnants are more fragmentary in the central and northern parts where only one shoreline is usually recognizable. Shorelines along both valley margins have been tilted northward.

High Shorelines on the Northern Argus Range

Ash Hill

The prominent high shoreline is almost continuously exposed along the six-mile length of Ash Hill and descends from about 1980 feet elevation at the hill's south end to about 1910 at the north end (figs. 4-1, 4-2). This shoreline zone is marked by a broad, gentle beach bench on the southern half of Ash Hill, where it has been cut into smooth, gentle slopes underlain by fan gravel, and by a steep, narrow bench on the northern half of Ash Hill, where it has been cut into steep slopes in volcanic rocks (fig. 4-3). Subrounded gravel is common along the shoreline on Ash Hill's southern half but very sparse on its northern half. Dense lithoid tufa containing snail

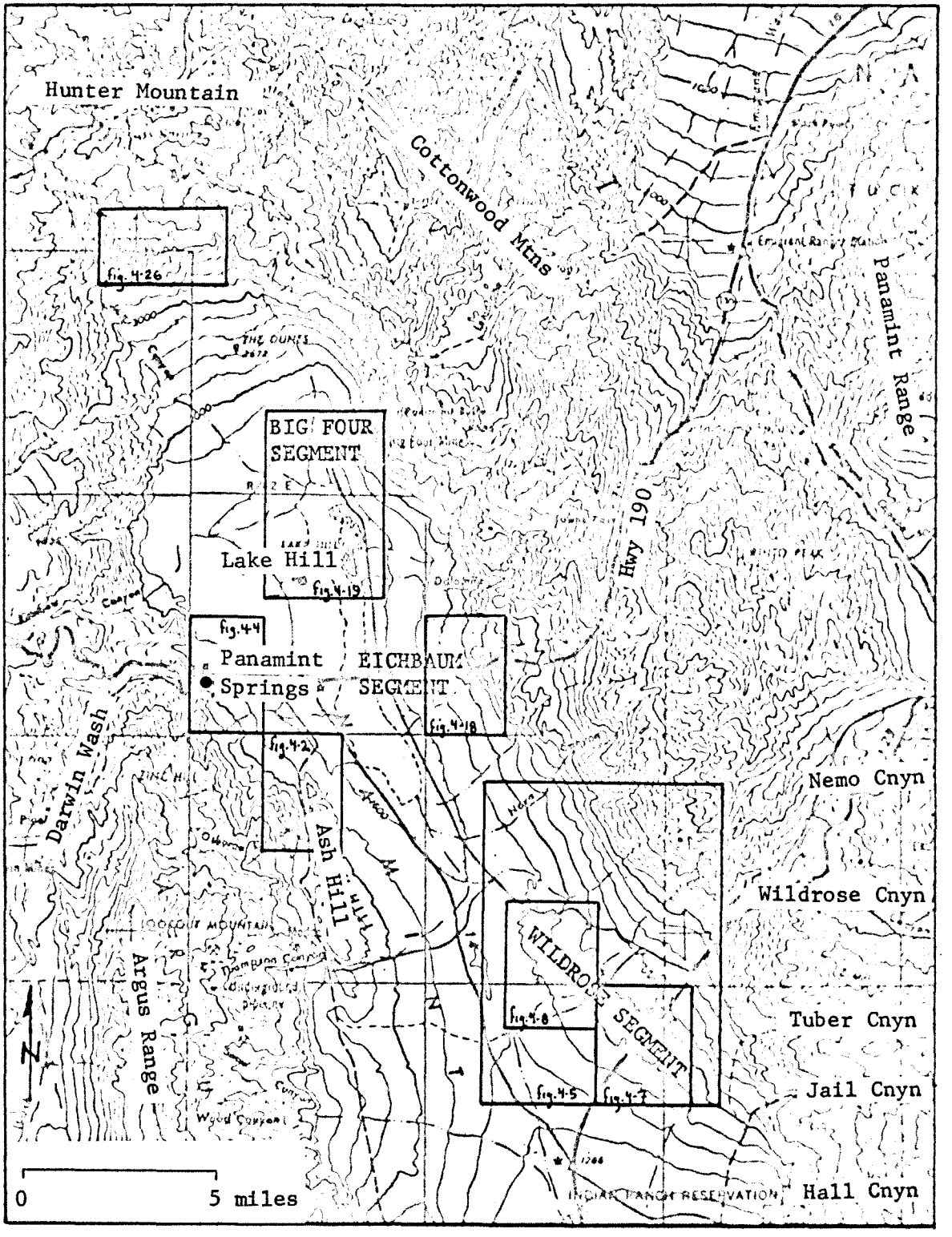

Figure 4-1. Index map of northern Panamint Valley.

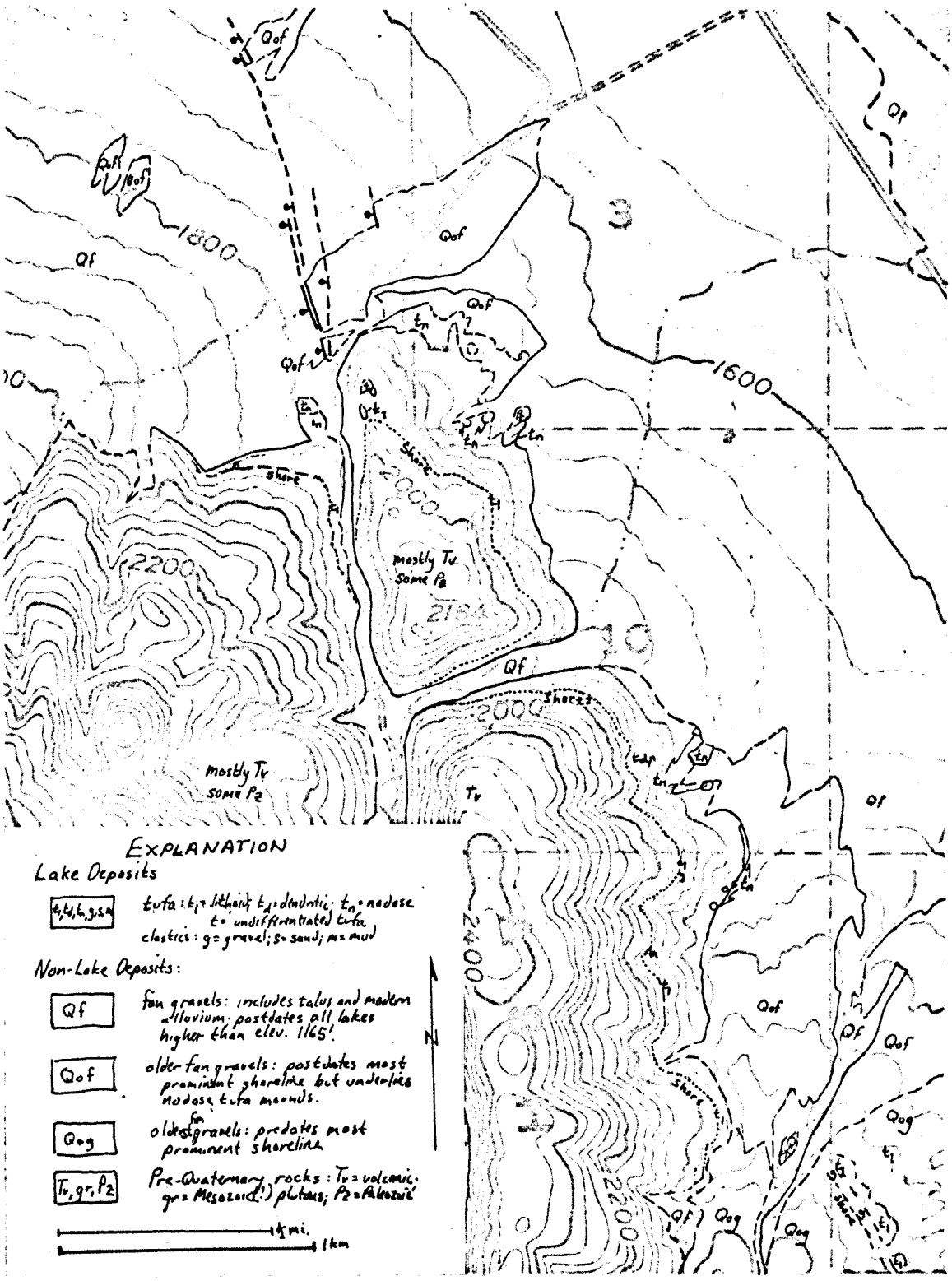

Figure 4-2. Geological map of the north end of Ash Hill.

Figure 4-3. High shoreline at extreme south end of Ash Hill
Looking northwest across light-colored tufa band, dark beach and gray, pre-lake gravel beyond beach. Note absence of beach cliff. (SW 1/4 sec 1, NW 1/4 sec 12, T20S, R42E).

shells is found at most points along the shoreline and sandy dendritic tufa is locally interspersed with lithoid tufa at the north end of Ash Hill. This high shoreline is also present on the volcanic slopes west of Ash Hill across the Ash Hill fault, where a narrow bench at 1880±10 feet elevation is locally littered with fragments of lithoid tufa and is thinly mantled by subrounded pebbles of Paleozoic (?) rocks (fig. 4-2).

A faint band of tufa is locally present 25 to 45 feet below the prominent high shoreline (fig. 4-2). This tufa contains snail shells and is generally lithoid to nodose in character but is locally dendritic. On the southern half of Ash Hill a surface composed mainly of subrounded gravel contains scattered six-inch-blocks of lithoid tufa 35 to 45 feet below the highest lithoid tufa (SW 1/4 sec 14, fig. 4-2). At the north end of Ash Hill, the lower tufa band is more prominent than elsewhere and consists of nodose to lithoid tufa 25 feet below the highest lithoid tufa.

Large tufa mounds at 1640-1760 feet elevation at the north end of Ash Hill have been described by Hall (1971, p. 51). Here, nodose tufa, devoid of snail shells, forms knobs three to ten feet high. The internal structure of this nodose tufa is much less dense than that of nodose tufa below the highest shoreline. Similar tufa reaches 1800 feet elevation west of Ash Hill. The thickest deposits of nodose tufa lie near the break in slope between the steep slope in volcanic rocks and the gentle slope on fan deposits below.

Panamint Springs

A remnant of a possible deltaic deposit fed by Darwin Wash extends nearly a mile east from Panamint Springs, its upper surface descending from about 1880 feet elevation to 1750 feet from west to east (fig. 4-4). This deposit consists primarily of foreset sand beds dipping 10 to 23 degrees northeast to southeast, with gentler, bottomset (?) beds at the east end dipping five degrees northeast. The upper surface of this deposit is mantled by a lag accumulation of subrounded cobbles. K.E. Lohman (in Hall and Stephens, 1963, p. 20) identified diatoms from this deposit as having been deposited "...in a fairly saline lake..."

North of Panamint Springs

The highest shoreline descends northward from 1880±10 feet elevation at Panamint Springs to 1820±20 feet at its northernmost exposure, five miles distant. This shoreline is marked principally by snail-bearing lithoid tufa, although downslope float contains some dendritic tufa. The shoreline is only locally marked by narrow benches and subrounded gravel, probably because it lies on steep slopes in most places. A gravel deposit extending 60 feet below the tufa line lies on the border of SE 1/4 sec 35, SW 1/4 sec 36, T 17 S, R 41E. Here, subrounded, moderately-sorted pebbles and cobbles of volcanic rocks are overlain by a one-foot bed of subangular debris in a silty matrix, which is in turn overlain by a veneer of subrounded to rounded cobbles and boulders of volcanic rocks.

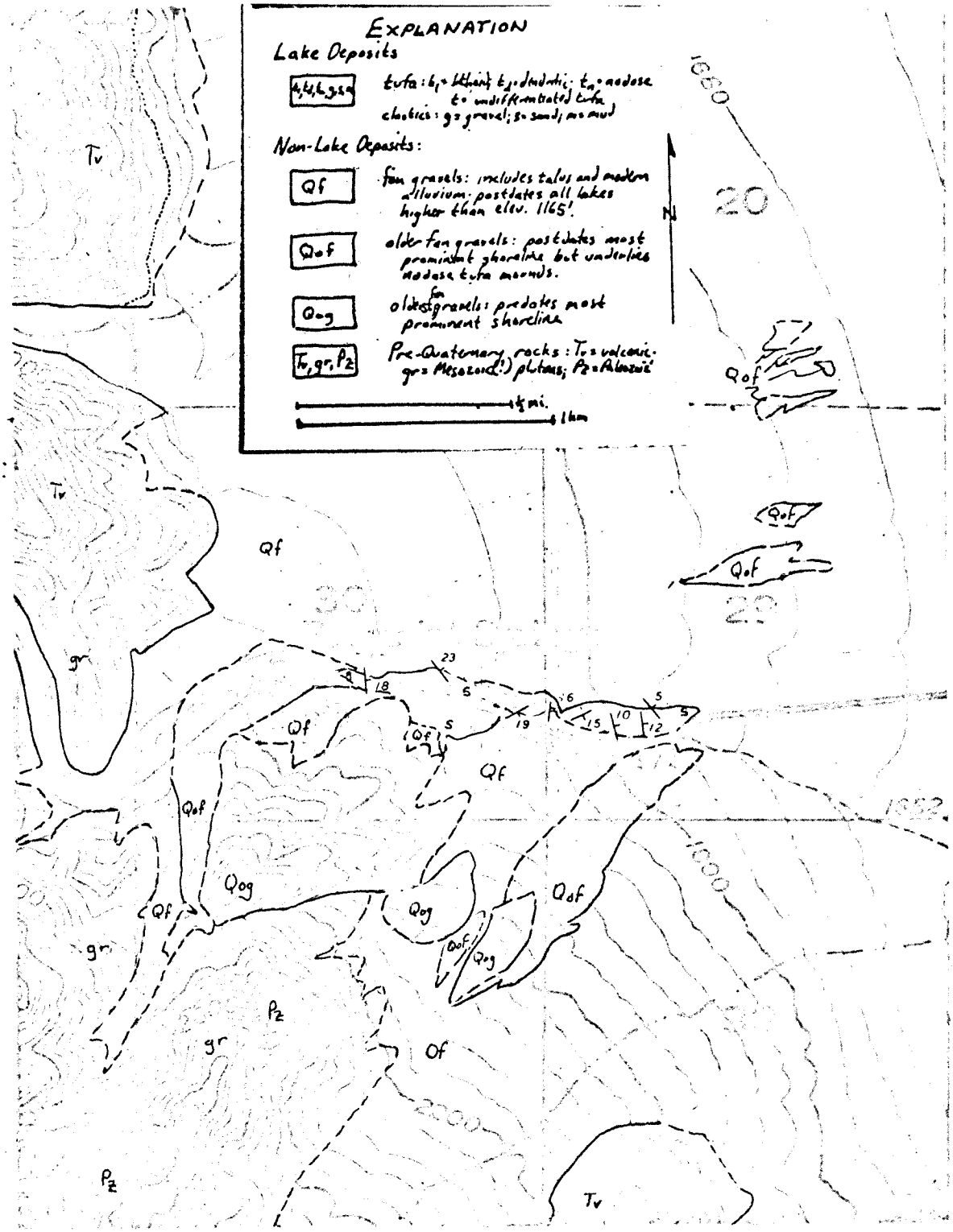

Figure 4-4. Geological map of region near Panamint Springs.

The lower tufa line was not identified north of Panamint Springs, nor were any shorelines seen above the prominent one. Float of dendritic tufa downslope from the prominent shoreline might have been deposited at this lower level, as a lower bed of subrounded gravel lies at corresponding elevation on the border of sections 35 and 36.

High Shorelines and Lake Deposits on the Wildrose Segment

Introduction

The Wildrose segment is a large, island-like remnant of tilted and dissected fan deposits which lies west of the Wildrose graben and whose length is about eight miles parallel to the northwest-trending front of the Panamint Range (figs. 4-1, 4-5). Relative downdrop of the Wildrose graben has beheaded several deep, wide stream channels which once transected the segment. This displacement has diverted these and other streams around the north and south ends of the segment (fig. 4-5). Thus isolated from the range front, the segment has been protected from both the depositional and erosive activity of energetic streams heading in the Panamint Range, and shoreline remnants have been preserved along much of the segment's length. Absolute uplift of the Wildrose segment is suggested by the present elevation of these shoreline remnants which in most places is higher than the present elevation of Wingate Pass. Dissection of the segment before streams were defeated and diverted also indicates absolute uplift.

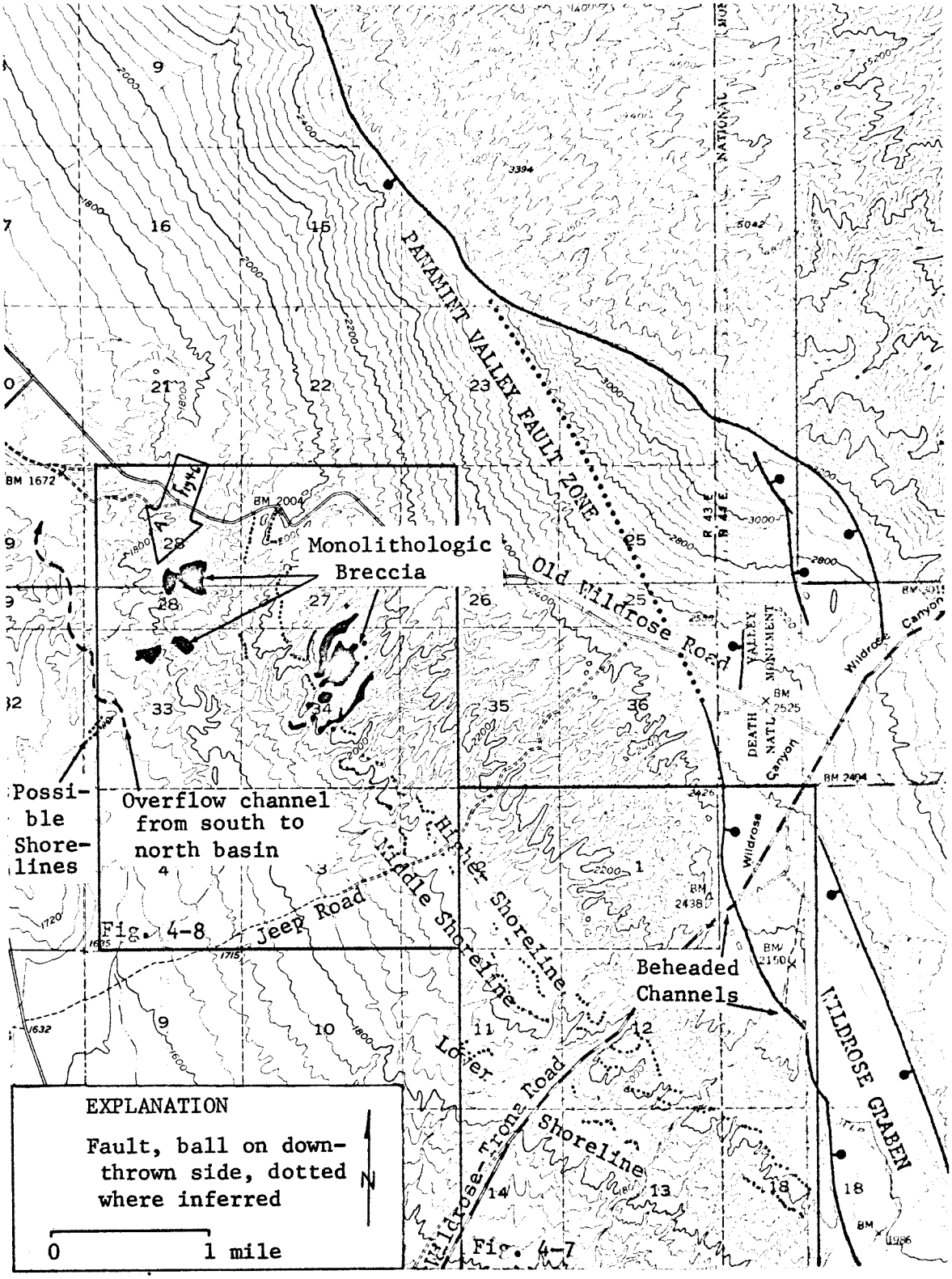

Figure 4-5. Index map of the Wildrose segment.

The pass at 1715±5 feet elevation between Panamint Valley's south and north basins lies at the northwest edge of the Wildrose segment, and possible shoreline remnants were found southwest of the pass at this elevation (fig. 4-5). A broad, sinuous, mile-long channel descends northward from the pass (figs. 4-5, 4-6). These features suggest that, as it filled, Lake Panamint overflowed from its south basin through this channel. This overflow probably allowed the level of Lake Panamint in the south basin to be stabilized at the pass elevation until the rate of discharge through the pass exceeded the evaporation rate from the lake in the north basin and allowed the north basin to fill to the pass level.

Shorelines

The Wildrose segment bears features of three tectonically-deformed high shorelines: 1) the higher (present elevation range 2012 to 2085 feet) has prominent wave-cut benches and cliffs, extensive gravel deposits and lithoid tufa; 2) the middle (present elevation range 1955 to 2045 feet) has few wave-cut features but displays locally-extensive deposits of worn and sorted gravel, and it bears dendritic tufa; and 3) the lower (present elevation range 1880 to 1930 feet) has no wave-cut features, bears no tufa and has only local sparse gravel deposits (figs. 4-7, 4-8).

Wave-cut cliffs along the higher shoreline are five to ten feet high on the southeast part of the segment and 15 to 30 feet high on the northwest part (fig. 4-10). These cliffs truncate spurs

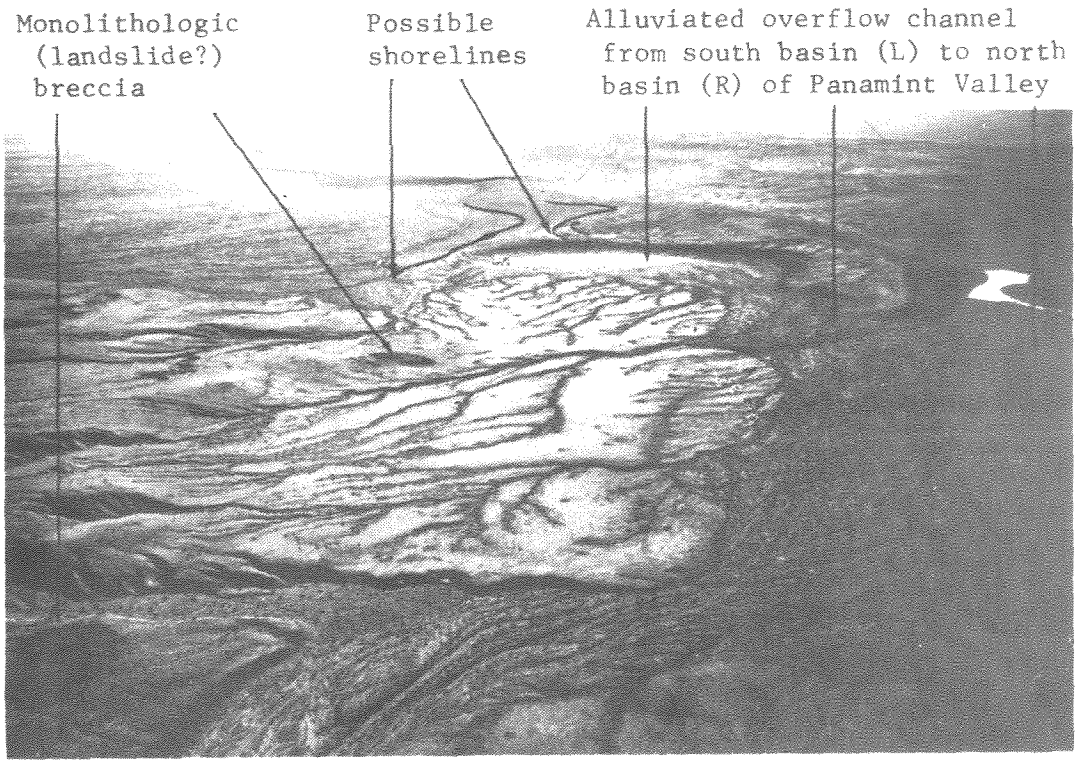

Figure 4-6. Aerial view to the south-southwest across the drainage divide between the north and south basins of Panamint Valley.

Lake overflow was probably from the south basin into the north basin. The light-toned areas on the photo represent reflection from desert pavement (center) and playas (right).

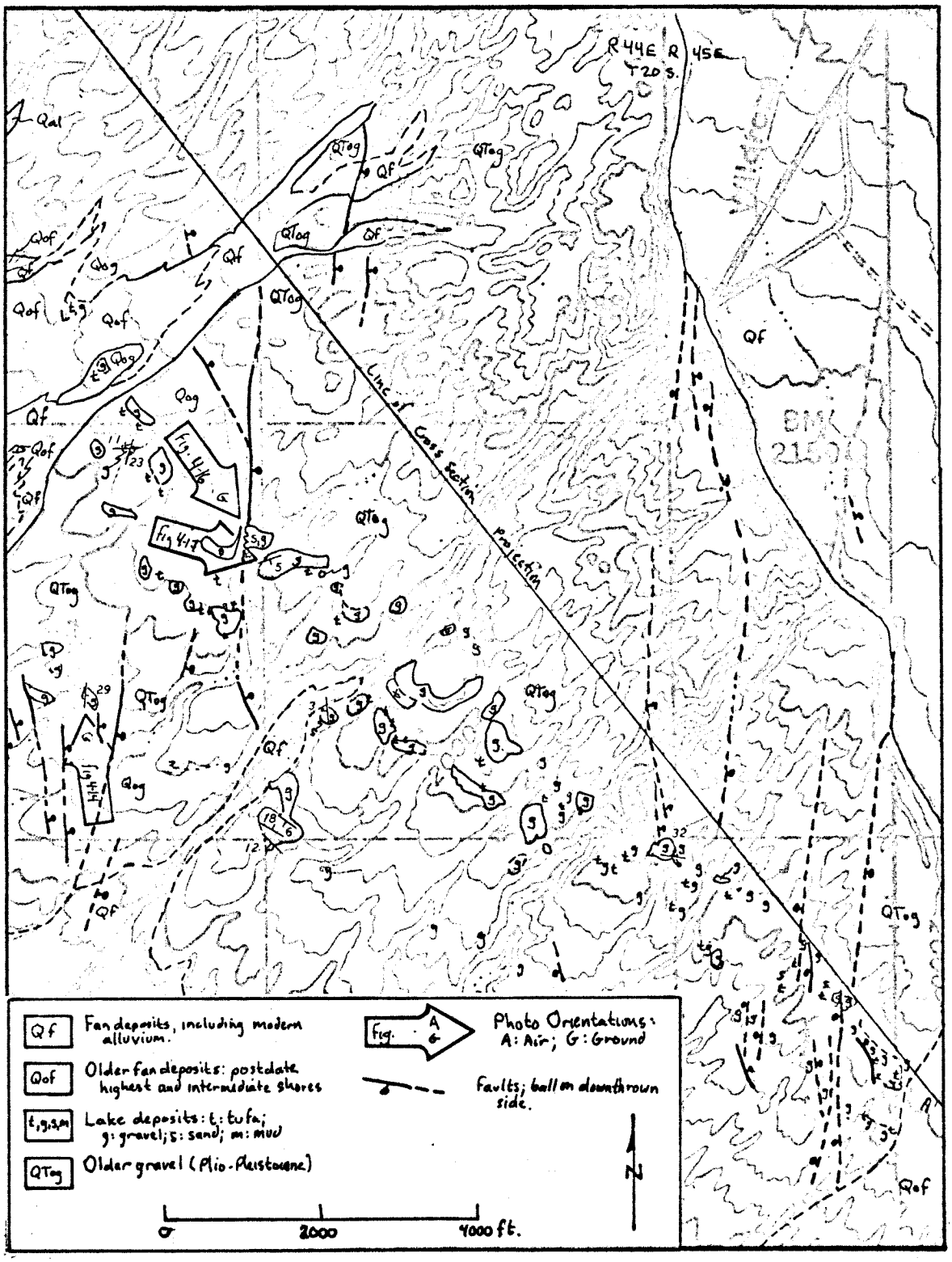

Figure 4-7. Geological map of the southeastern Wildrose segment.

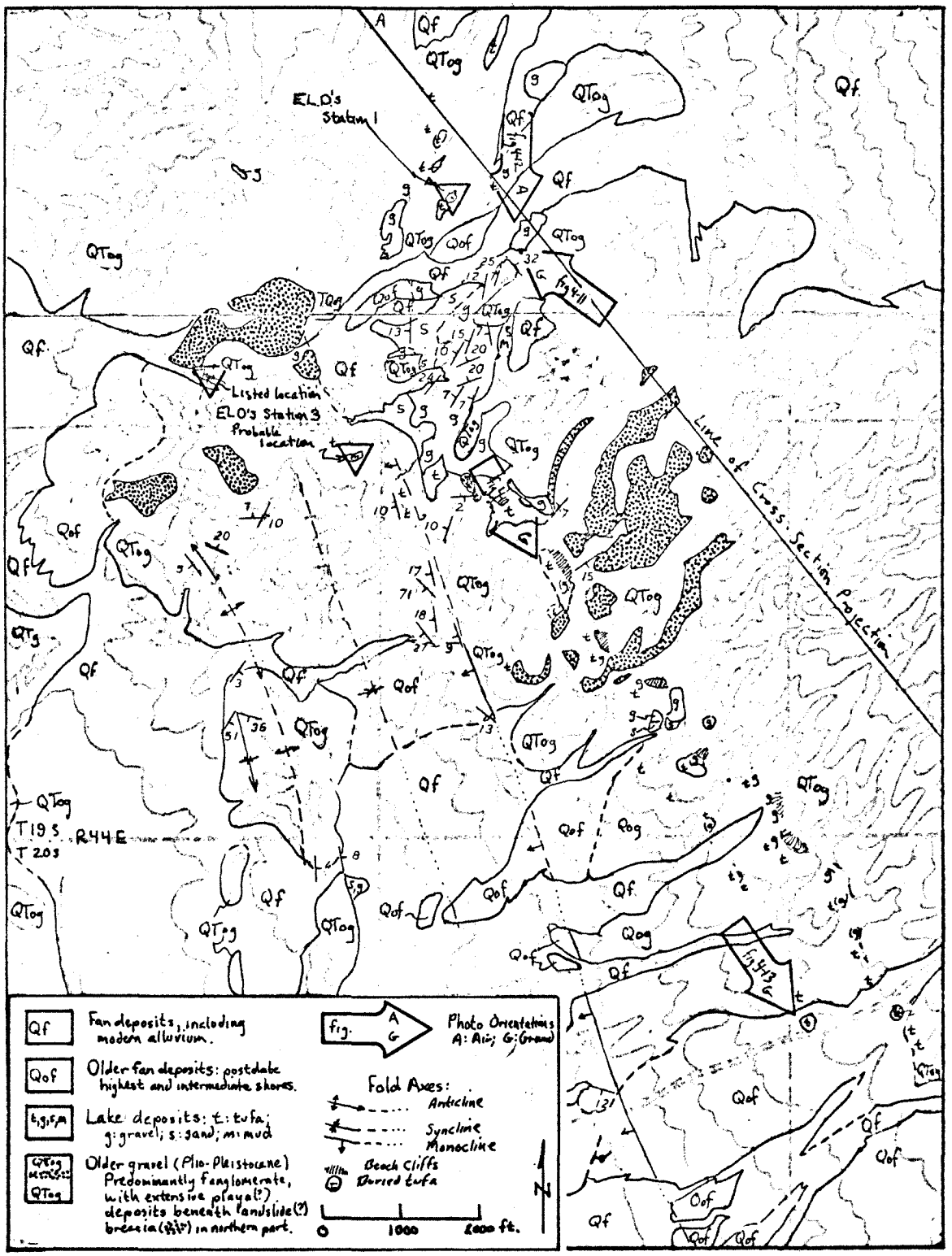

Figure 4-8. Geological map of the northwestern Wildrose segment.

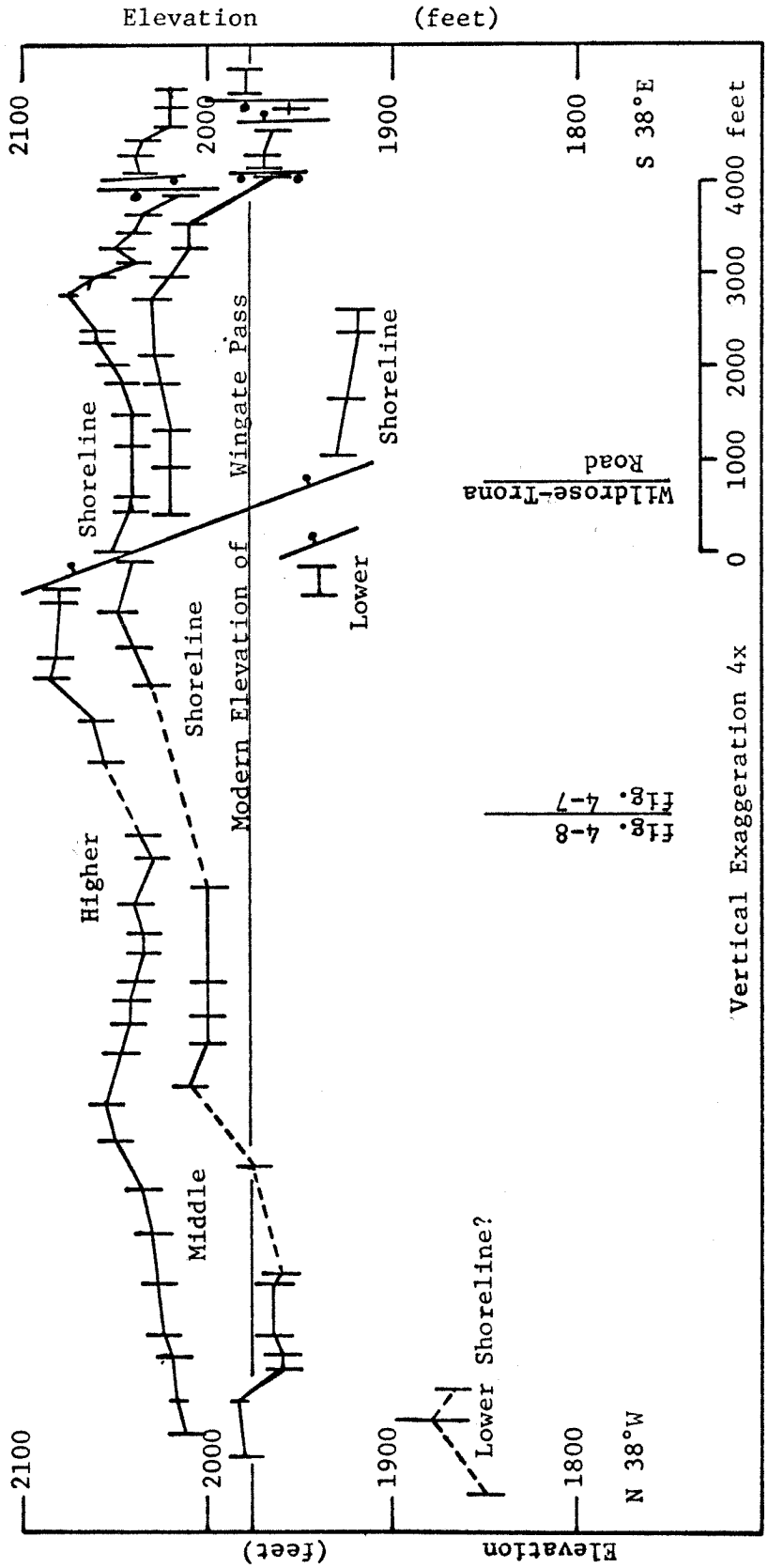

Figure 4-9. Northwest-southeast profiles of shorelines along the Wildrose segment.

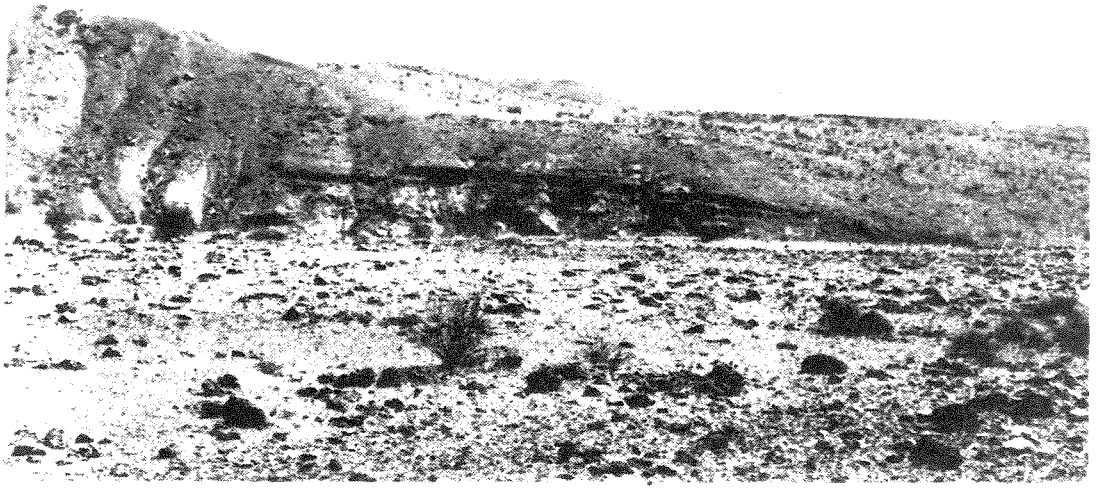

Figure 4-10. Cut shoreline on the northern Wildrose segment.
Looking south at a beach cliff above higher shoreline about 30 feet high cut into fanglomerate and playa (?) sediments. The shoreline below the cliff is at the same level as the tufa-littered bench in the foreground.

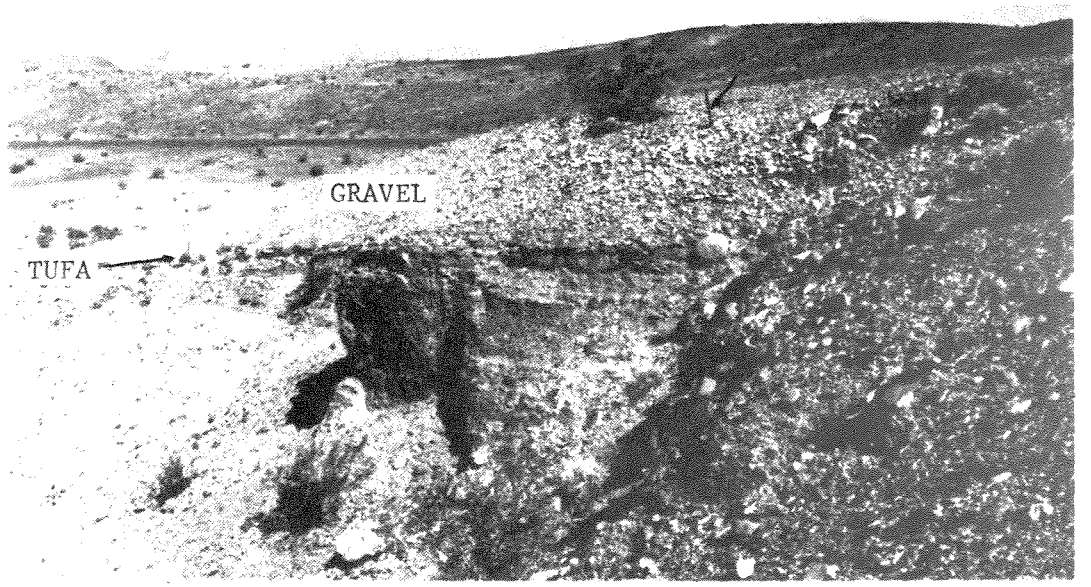

Figure 4-11. Lake gravel overlying tufa on the northern Wildrose segment.
Tufa of the higher shoreline grew on the lag boulders on top of the fanglomerate before they were buried by rounded gravel. Entrenching tool (arrow) gives scale.

40 to 80 feet high between major drainage channels. The beach zone below the cliffs has a vertical range of about 20 feet and contours around the spurs. Locally the upper half of the beach zone is littered with subrounded to rounded pebbles and cobbles, but at most places these round stones underlie angular clasts within a wedge of colluvium whose thickness reaches five feet at the cliff base. The lower half of the beach zone is littered with six-to-12-inch rinds of lithoid tufa that formerly coated decomposed lag boulders. This snail-bearing tufa locally has a nodose or coarsely dendritic internal structure. Rounded gravel typically overlies well-developed tufa heads where both gravel and tufa are exposed together (fig. 4-11). At its northwest end, this shoreline level coincides with the upper surface of a broad, thick, areally-extensive accumulation of lacustrine sand and gravel (figs. 4-8, 4-12).

The middle shoreline is marked by a band of lake gravel and an adjacent, but slightly lower, band of dendritic tufa. These features typically lie 25 to 45 feet below similar features on the higher shoreline (fig. 4-9). Gravel on the middle shoreline resembles gravel on the higher shoreline in size, rounding and parent lithology. The tufa contains abundant snail shells and is coarsely dendritic with dense lithoid walls (fig. 4-13). Locally it is lithoid or cellular. Like tufa of the higher shoreline, this tufa locally underlies lakeshore gravel. Few wave-cut features were seen along this shoreline, which rests on a broad, smooth surface that slopes gently up to the higher shoreline. Lag accumulations of boulders are locally developed on the substrate.

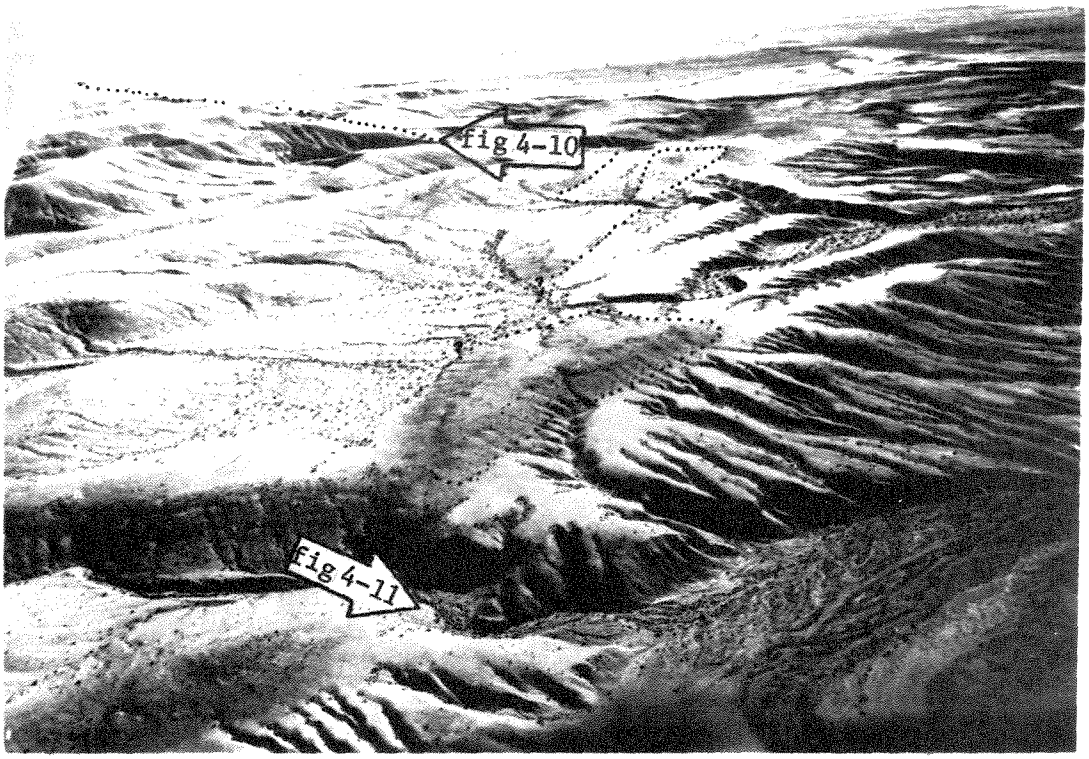

Figure 4-12. Lacustrine gravel deposits on northern Wildrose segment. Aerial view towards the south. Broad benches mark the upper surface of nearshore sand and gravel deposits which have buried much of the subdued pre-lake topography. The dotted line shows the position of the highest shoreline.

Figure 4-13. Dendritic tufa of the middle shoreline. This tufa head was buried beneath the older fan gravels and later exhumed, accounting for the good preservation of its dendritic form.

The lower shoreline bears no tufa but displays scattered patches of subrounded gravel locally lying on steeply-dipping subangular bar gravel (fig. 4-14). Stratigraphic relationships between deposits of this shoreline and the higher and middle shorelines have not been determined, but the fresh appearance of the lower shoreline suggests that it is younger than the other two. The lower shoreline may not represent a single, continuously-traceable tectonically-deformed feature but rather sparse remnants of several short-lived lake stands at different elevations.

Beach Gravels

The beach gravels on this segment consist primarily of subrounded to rounded pebbles and cobbles of metasedimentary and gneissic parentage. On the higher shoreline, these round-stone gravels commonly overlie calcareously-cemented accumulations of sand, granules and subangular to angular pebbles like those of the underlying fanglomerate. These cemented deposits typically lie at steep dips and were probably deposited along the higher shoreline before the lake had eroded beaches or established longshore drift. Similar deposits are more sparsely distributed along the middle shoreline. Uncemented deposits of steeply-dipping subangular clasts underlie rounded gravel of the lower shore (fig. 4-14).

Clasts of strongly-banded muscovite gneiss predominate within most well-worn gravel deposits along the higher and middle shorelines, but are absent both in the underlying fanglomerate and in the

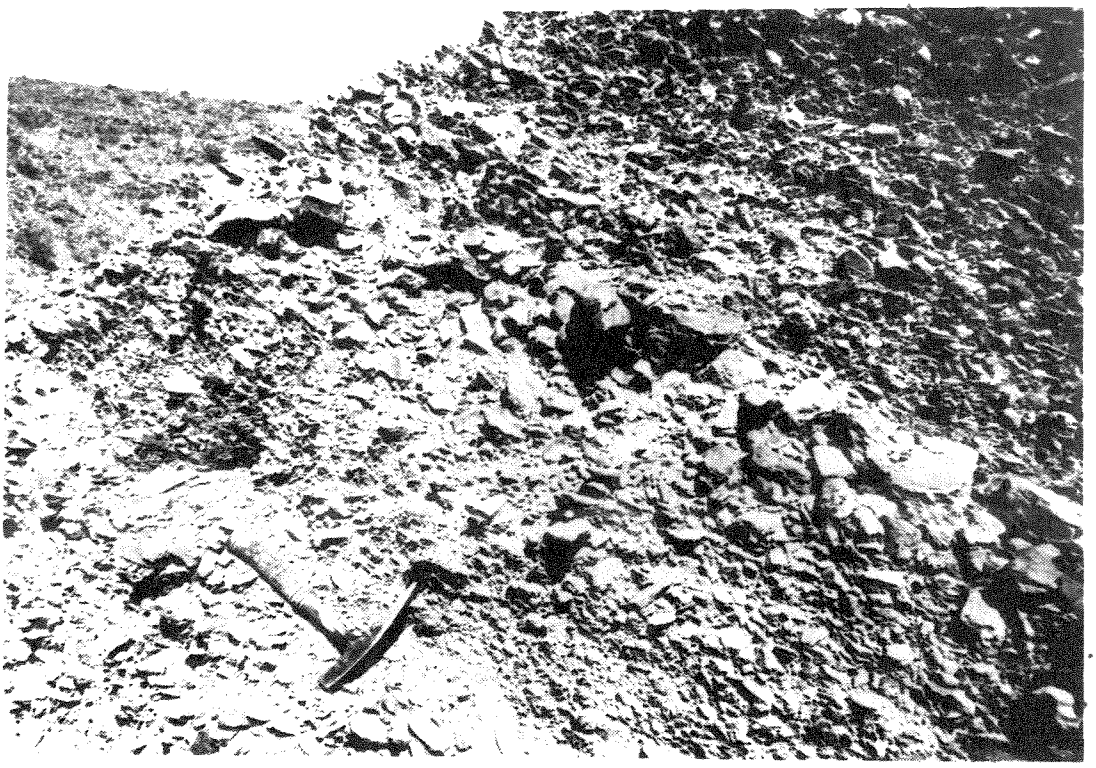

Figure 4-14. Steeply-dipping gravel of the lower shoreline. Looking north at a dissected beach bar of subangular clasts whose primary dip is 29 degrees east. This bar is overlain by a thin deposit of subrounded gravel.

drainage basins of Wildrose, Nemo and Tuber canyons, which debouche from the range along the Wildrose segment (fig. 4-15). To the south, Hall and Jail canyons each transect a large body of "...coarsely banded gneiss, composed of feldspar, quartz, muscovite, and more rarely biotite." (Murphy, 1930, p. 33-34, plates VIIB & IX; 1932, p. 339). Although rocks of similar composition crop out in Wildrose and Tuber canyons, they are unfoliated (Lanphere, 1962, p. 75, 80-81), and are represented rarely as clasts in the fanglomerate underlying the shorelines.

Clasts of gneiss form much of the beach gravels, even at the Wildrose segment's north end, 7.5 and 10 miles from the mouths of Jail and Hall canyons, respectively (fig. 4-15). This relationship suggests significant longshore drift northward along the Wildrose segment. Streams draining Hall and Jail canyons were seemingly more proficient in providing abrasion-resistant debris to the lake than were streams draining Wildrose, Nemo and Tuber canyons. Despite their resistance to abrasion, clasts of gneiss succumb quickly to granular disintegration by weathering after deposition, so clasts of metasediments predominate on the surface.

Dissection

The Wildrose segment appears to have been uplifted and dissected to a depth of 40 to 80 feet before deposition of the lake deposits described above. Lacustrine sand and gravel form a thin blanket on the floor and walls of gullies cut 40 feet below the level of the

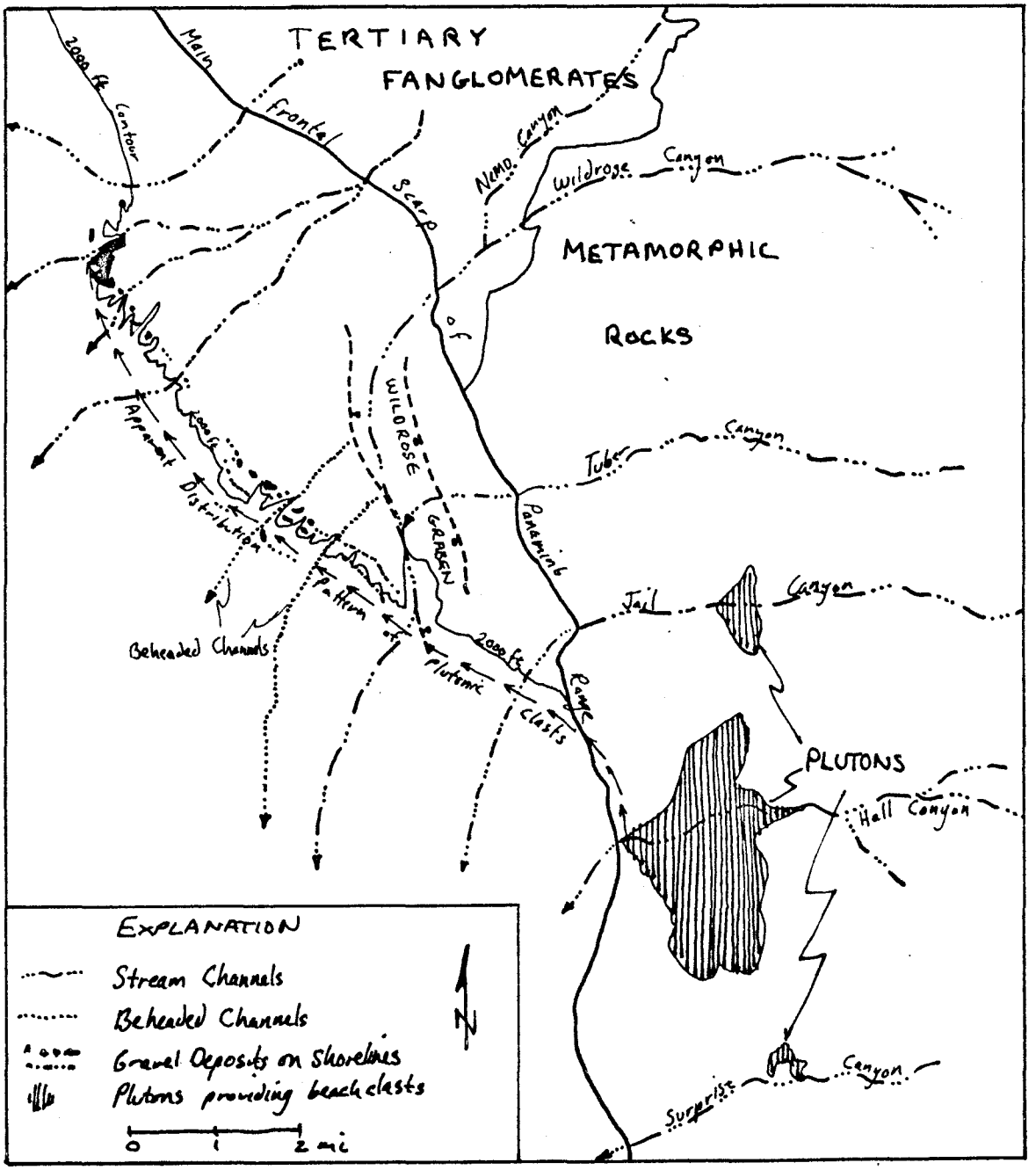

Figure 4-15. Map of sources and distribution of gravel along the Wildrose segment.

higher shoreline. Similar deposits another 40 feet lower, in deeper gullies, cannot be traced up to the higher shoreline and may have formed at lower, younger lake stands. Some of the lakeshore gravel deposits are probably remnants of the bars or deltas which dammed each gully allowing longshore transport of gneissic clasts to the segment's northwest end (fig. 4-15). The higher and middle shorelines each represent a lake stage which endured long enough at one level to allow bar and delta construction uninterrupted by significant episodes of erosion.

Relative Age

Greater age of the middle shoreline than of the higher shoreline is suggested by greater deformational relief of the middle shoreline than of the higher shoreline (90 feet vs. 73 feet, fig. 4-9).

Stratigraphic relationships also suggest greater age of the middle shoreline than of the higher shoreline. A body of lacustrine gravel, separated by a colluvial or alluvial layer into upper and lower units, is found in the S 1/2 NW 1/4 sec. 12 (fig. 4-7). The upper lacustrine unit, whose lowest exposed elevation is 2000±10 feet, extends eastward and upward to the higher shoreline at 2040±10 feet elevation (fig. 4-16). This upper unit is about five feet thick, cemented by calcium carbonate and made of subrounded pebbles and cobbles, 70 per cent of which are muscovite granite gneiss (fig. 4-17). The colluvial or alluvial layer, made of subangular pebbles, is poorly exposed but may reach a thickness of five or ten feet.

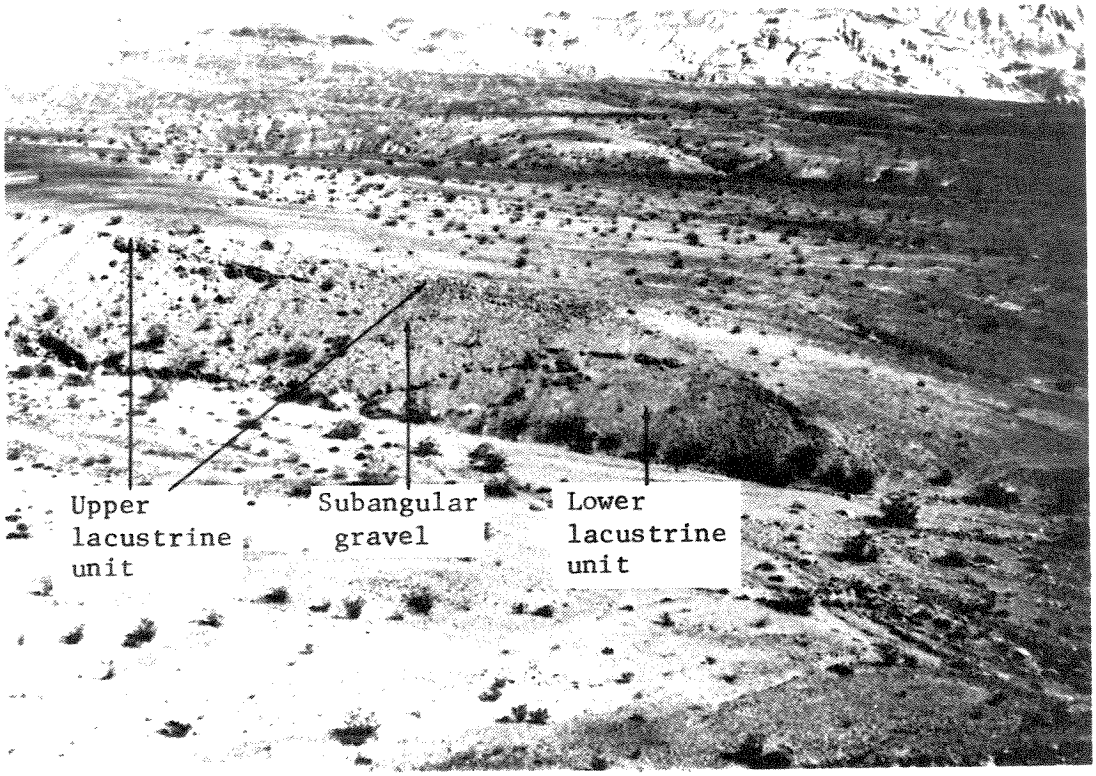

Figure 4-16. Lake gravels of two ages north of Wildrose-Trona road. View is southeast towards a gravel body which extends from below the level of the middle shoreline up to the higher shoreline. The lower lacustrine unit contains abundant subrounded to rounded pebbles, none of which are gneiss. Subangular colluvial or alluvial gravel overlies the lower unit. The upper lacustrine unit is of cemented gravel whose subrounded to rounded cobbles are largely of gneiss (fig. 4-17).

Figure 4-17. Cemented lake gravel.
This is the upper unit in Figure 4-16, attributed to the higher shoreline. Note the abundance of light-colored gneiss cobbles.

The lower lacustrine unit, about 10 feet thick, is cemented by calcium carbonate only in its upper part and is made of subrounded pebbles, all of metasedimentary rocks but none of gneiss (fig. 4-16). The highest elevation (2000±10 feet) reached by this lower unit is 20 feet lower than the middle shoreline (2020±10 feet). The age of the lower unit is probably the same as the age of the middle shoreline. The absence in the lower unit of clasts of gneiss so common elsewhere on the middle shoreline suggests that the lower unit represents a remnant of a body of locally-derived gravel which filled the gully before gneissic gravel reached this point.

Both the middle and higher shorelines are attributed to Gale Stage. The middle shoreline was probably cut during early G_1 substage by a lake stand stabilized at the level of the bedrock lip now buried beneath Wingate Pass, and the higher shoreline cut during later substages of Gale Stage stabilized at the level of Wingate Pass, 47±16 feet higher than the level of the bedrock lip.

The lower shoreline is arbitrarily regarded as younger than its higher associates because the sparse, well-rounded gravel found along it could have been reworked from their deposits.

Absolute Age

The age of the higher shoreline is greater than 45,000 years, judging from published radiocarbon ages of materials taken from the northwest end of the Wildrose segment (Hubbs, Bien & Suess, 1965, p. 93-96; table 4-1). This date, from snail shells in a deposit of

Table 4-1.

Published Radiocarbon Ages from the Wildrose Segment

(Samples from various stations collected by E.L. Davis and dated by Hubbs, Bien & Suess, 1965, p. 93-6)

Lab No.	Sta. No.	Elevation (feet)*	Location	Material Dated	Age (B.P.)	Notes
LJ-980	1	2018	36°15'14"N 117°18'36"W	Lithoid tufa	>35,000	1
LJ-982	1	"	"	Lithoid tufa	18,600±1,000	1
LJ-985	3	1854	36°14'54"N 117°19'16"W	Snails	45,000	2
LJ-989	3	1801	"	"Red tufa"	22,530±1,200	2
LJ-990	5	1650	36°15'39"N 117°20'20"W	Lithoid tufa	31,480±1,600	3

*Elevations were reported in meters, here converted to feet.

1) These samples both represent tufa from the higher shoreline. The older date is from a sample thought to represent the outer part of a thick tufa rind (LJ-990) and the younger from a sample thought to represent the inner part of the same tufa rind; Hubbs et al explained the discrepancy as an error in sample identification in the field or lab.

2) The only calcareous material at this location is possible 1-2" rinds of lithoid tufa (probably caliche) at 1860±20; no snails are present. At least one of the listed elevations is in error (tufa is supposed to directly overlie shells of Carnifex newberryi). A more likely locality for this station is: 36°14'44"N, 117°18'52"W, elev. 1960±20 feet. Here, dendritic tufa of the middle shoreline caps a knob (1970±10) and forms a lag deposit over shell-rich marl five feet thick in an adjoining saddle (1950±10). This marl seems a reasonable correlative of marl which elsewhere interfingers with deposits of the higher shoreline. The tufa here has a reddish cast.

3) This "tufa" does not seem related to any shoreline but rather to represent calcareously-cemented ground litter along the lower part of the inlet channel from south Panamint.

marl attributed to the higher shoreline, is probably more reliable than two dates from tufa on the higher shoreline (see Appendix A for discussion of the difficulties of dating calcium carbonate, particularly tufa). These dates from the "inner" and "outer" parts of a rind of lithoid tufa are 18,600±1,000 and >35,000 B.P., respectively (Table 4-1). The age obtained on tufa from the middle shoreline (22,530±1,200) is probably also unreliable because the evidence presented in the previous section suggests that the middle shoreline is older than the higher shoreline.

High Shorelines on the Northern Panamint Range

Townes Pass Road

A well-developed shoreline, marked by tufa, rounded gravel, a beach bench and a beach cliff is preserved about one and a half miles south of the Townes Pass Road (fig. 4-18) on the east side of Panamint Valley. The base of the wave-cut cliff, mantled by four to five feet of colluvium, lies at 1955±10 feet, and marks the highest extent of rounded gravel and tufa. The tufa contains snail shells and is weakly dendritic to slightly nodose in character; its highest extent is marked by mushroom-shaped bodies of friable tufa extending two feet above lag boulders which anchor them.

Lake Hill

The highest shoreline on Lake Hill lies athwart its south ridge at 1889±3 feet elevation and is defined by a wave-cut cliff rising

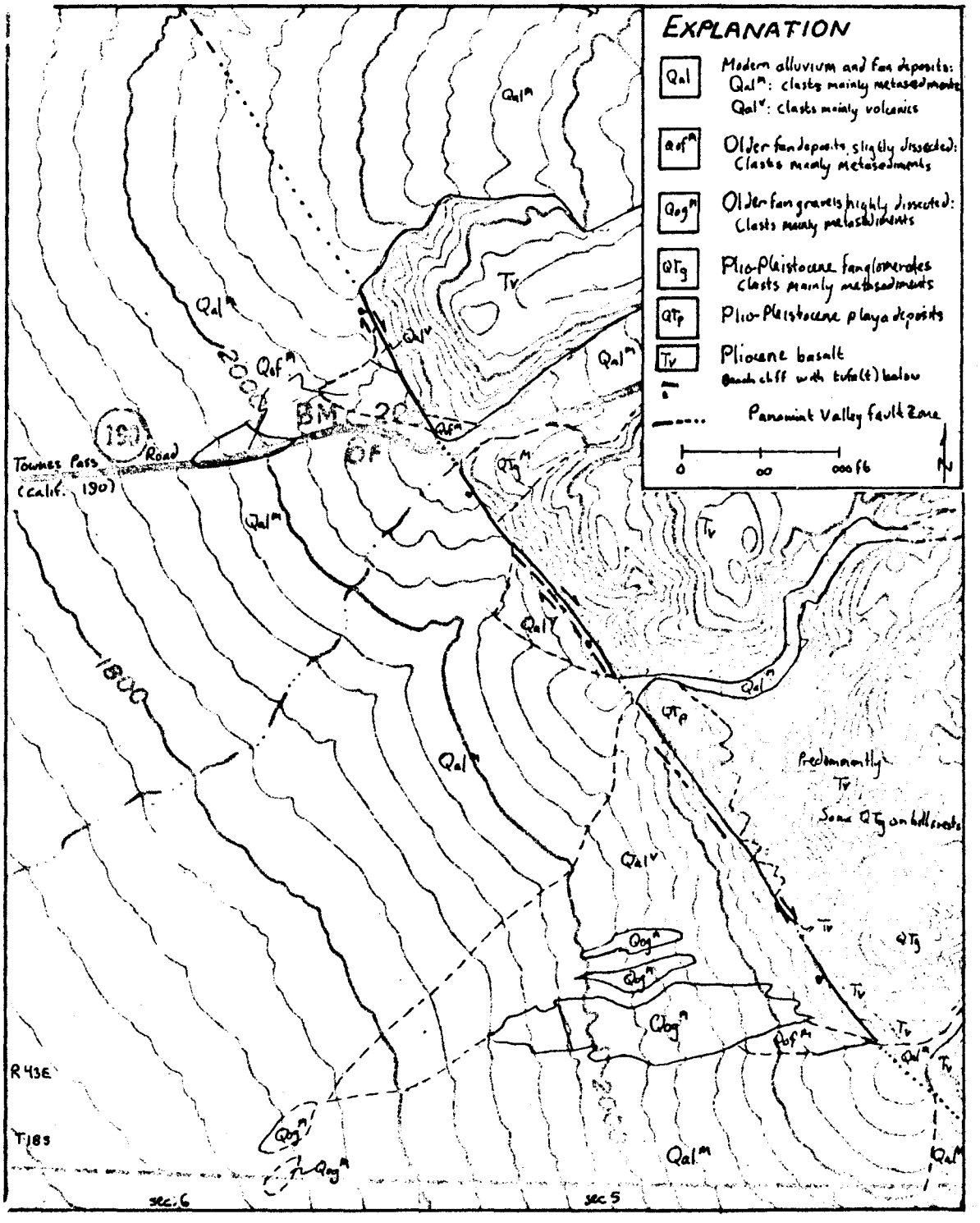

Figure 4-18. Geological map of region near Townes Pass Road.

above a south-sloping bench (figs. 4-19, 4-20). This bench, whose vertical extent is about 15 feet, is covered with tan-colored lithoid tufa which forms rinds up to two feet thick on boulders and can be traced to Lake Hill's west side, where it forms 18-inch rinds up to 1882±5 feet elevation. Tufa has been found neither on the hill's gentle north ridge nor on its steep east side.

Below this highest shoreline, several other tufa bands lie at elevations down to about 1800 feet (fig. 4-20). Although some of the higher tufa may be float, the 1810±10-foot tufa band appears to be in place because similar tufa also occurs on an isolated knob (1800+) to the south and on a flat-topped hill (1800+) one mile to the north (fig. 4-19). This tufa is coarsely dendritic to locally nodose, contains snail shells and is typically found as scattered three-to-six-inch blocks locally associated with subrounded gravel.

Intermediate in elevation between the 1800-foot and the 1889-foot shorelines on the south end of Lake Hill are a band of nodose tufa (upper limit 1848-1853 feet) and a band of dendritic tufa (upper limit 1865-1870 feet) of a character dissimilar to that of the highest shoreline.

No stratigraphic relationships were found between deposits on different shorelines, but, on the basis of position, the 1810-foot shoreline is tentatively attributed to early G_1 substage and the 1889-foot shoreline to late Gale Stage (probably G_5). The tufa bands at intervening elevation are attributed to mid-Gale Stage.

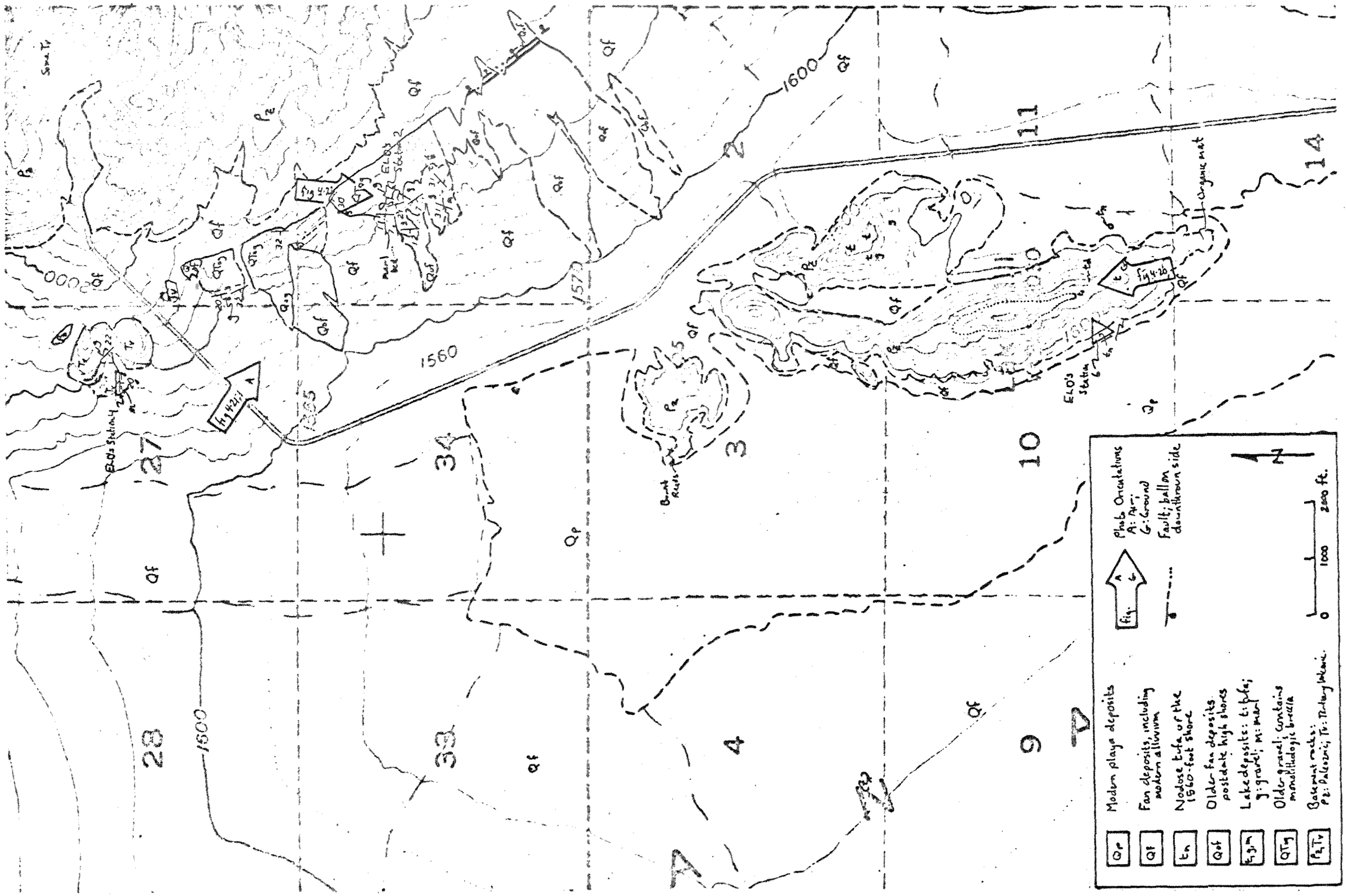

Figure 4-19. Geological map of Lake Hill and the Big Four segment.

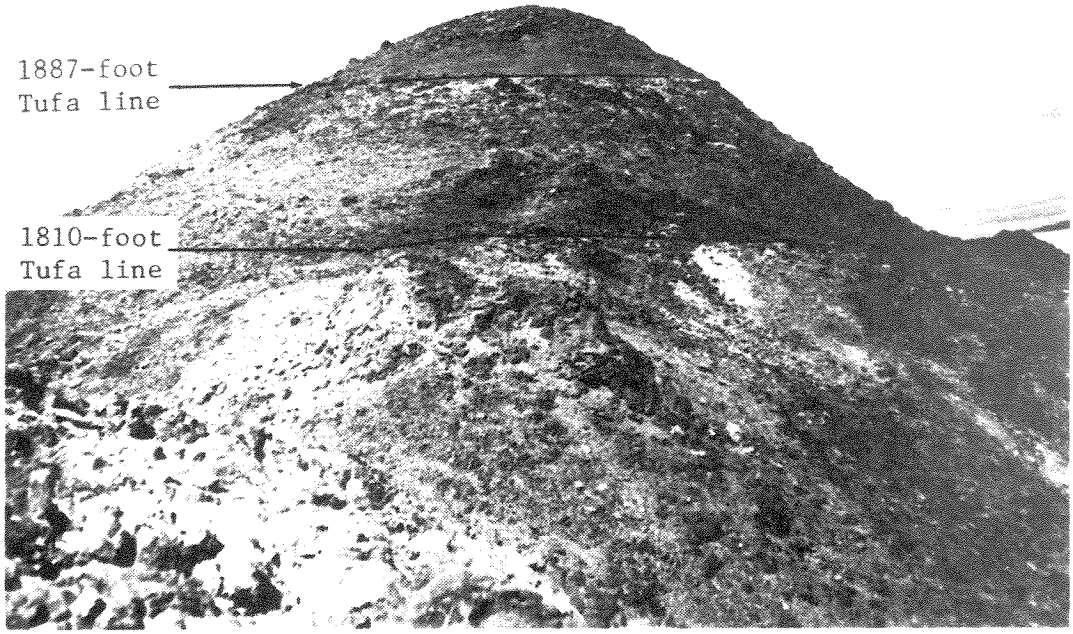

Figure 4-20. Shorelines on Lake Hill.
View north towards the hill's south ridge from about 1800 feet elevation. Note that only the 1887-foot and 1810-foot tufa lines show up clearly and have associated benches.

Big Four Mine Road (South)

South of the Big Four Mine road, shorelines and lake deposits lie along the west side of a series of hills which marks the west side of the Panamint Valley fault zone (figs. 4-19, 4-21). A prominent marl bed draped upon the southernmost hill is overlain by silt, sand and gravel, and is surmounted by two cut (?) benches and a faint tufa line (fig. 4-22). This is probably Station 2 of E.L. Davis as recorded in Hubbs et al (1965, p. 94-96). The topographic and stratigraphic and relationships which they describe are shown in Figure 4-22.

The marl is varved, encompassing nearly 400 sets of thin alternating calcium carbonate and silt beds in its four-foot thickness, contains snail shells and has wavy, possibly rippled, bedding. It is underlain by up to five feet of highly calcareous fine-grained sand and silt which contain abundant snail shells in an indurated upper foot and shell fragments throughout. The marl is overlain by 15 feet of fine-to-very-fine-grained sand and silt, containing some snail shells, two beds of loose gravel and several thin (1/4 inch) marl beds. The sand is overlain by nine feet of slightly crossbedded subrounded pebbly gravel with a sandy matrix; the upper foot has been strongly cemented by calcium carbonate.

Bedding in all these units is parallel to the steep, west-facing slope of the fanglomerate beneath the deposits and they are truncated by a gently west-sloping bench (fig. 4-22). The marl crops out in a gentle saddle just east of the highest point (1850±10 feet)

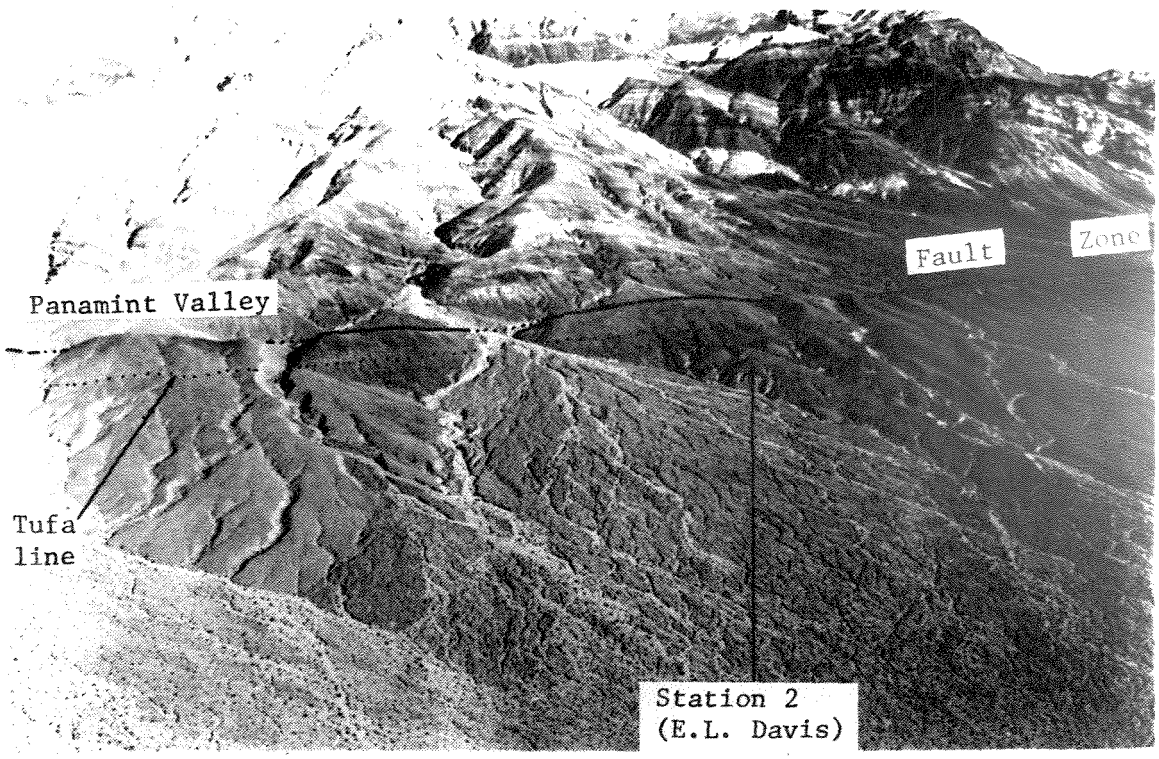

Figure 4-21. Aerial view of the southern Big Four segment. Looking southeast toward Station 2 of E.L. Davis. Note that these hills seem to have been uplifted along the Panamint Valley fault zone relative to the northern Panamint Range, despite the fact that they have been depressed in an absolute sense based on deformed shorelines.

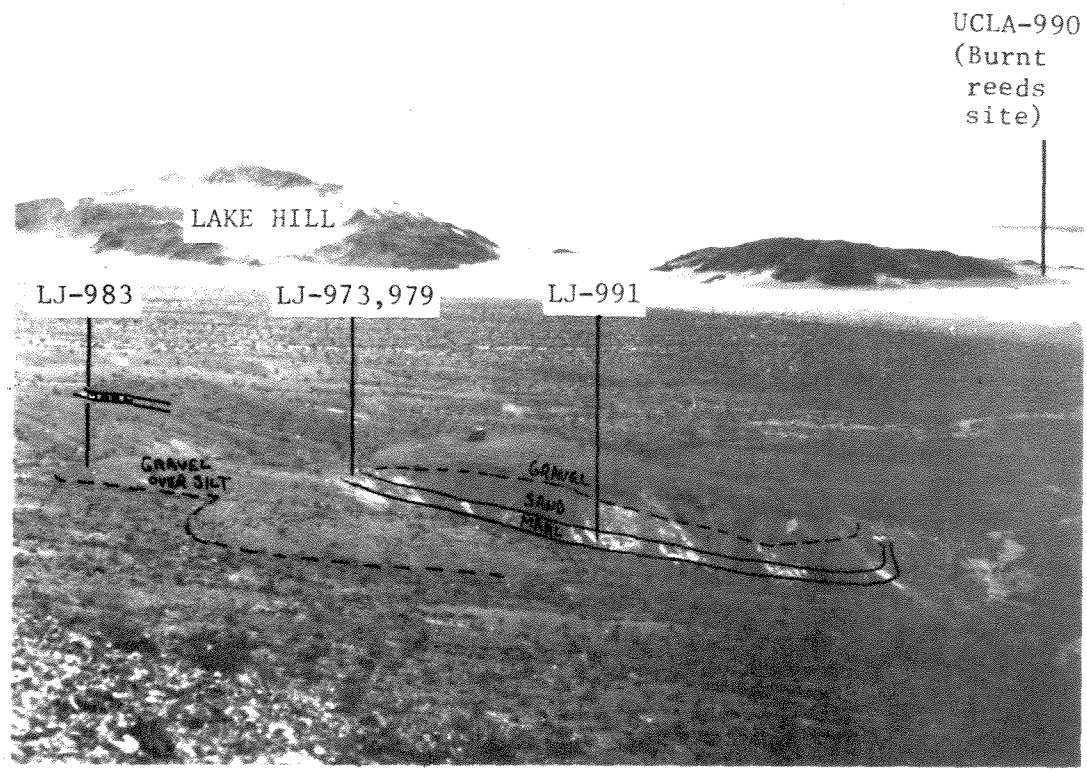

Figure 4-22. Looking south across Station 2 of E.L. Davis. Note the prominent marl bed and the two benches. Vertical lines point to where the C-14 dating samples seem to have been collected.

of the bench, but the underlying sand and silt appear to continue 20 feet farther up the hill, where they underlie lag gravel and are truncated by a small bench (1870±10 feet). The upper margin of a poorly-preserved tufa band lies 23 feet higher (1893±10 feet). This lithoid-to-dendritic tufa forms one-foot-thick rinds on boulders. In the south walls of two major gullies to the north, this tufa band appears to be associated with a poorly-developed beach bench bearing subrounded lag cobbles and boulders overlain by colluvium. This tufa bears some resemblence to the intermediate-level tufas on Lake Hill.

These lake deposits are attributed to Gale Stage even though the shoreline of the lake stand which deposited these sediments has not been identified. The 1893-foot shoreline lies more than 20 feet above the highest sediments, which thus cannot be stratigraphically related to it. The 1850-foot and 1870-foot benches were probably cut along shorelines, but they both truncate the sediments and no tufa has been found along them. All these sediments may have been deposited from a shoreline at the level of the 1870-foot bench and incised by a later high shoreline along the 1850-foot bench. However, where shorelines seem to have been downwarped (as they do here) progressively higher shorelines should be progressively younger (if all formed at the present level of Wingate Pass). This objection could be answered in two ways: 1) early uplift of the block followed by downthrow or 2) misinterpretation of field relationships between deposits at 1850-1870 feet and those below 1850 feet. If

1850-70 deposits overlie those below 1850 feet then progressively-higher benches are progressively younger.

Radiocarbon ages of materials collected from this site by E.L. Davis were reported by Hubbs et al (1965, p. 94-6), are listed on Table 4-2 and discussed in the section after next.

Big Four Mine Road (North)

North of the road, rinds of snail-bearing lithoid tufa six to 18 inches thick reach 1825±10 feet elevation on a prominent beach bench (fig. 4-19). Subrounded to rounded gravel of carbonate clasts extends about seven feet higher and continues along the hill to the south, terminating in a southwest-dipping gravel deposit which bottoms in a gully about 30 feet below the high tufa line. Downgully, about 80 feet below the high tufa line, a marl bed draped onto the gully's north side is overlain by thin colluvium containing float blocks of lithoid and dendritic tufa. No clear relationships between tufa, marl and gravel can be established.

This site seems to be Station 4 of E.L. Davis as recorded by Hubbs et al (1965, p. 94-5), although its listed elevation (549m, 1801 feet) conflicts with my altimeter traverses which place the highest marl at 1742±10 feet and the highest tufa at 1825±10 feet elevation. Radiocarbon ages of materials collected from this site by E.L. Davis were reported by Hubbs et al (1965, p. 94-5). These dates are listed in Table 4-3 and discussed in the next section.

Table 4-2.

Published Radiocarbon Ages from Station 2 of E.L. Davis[1]

Lab No.	Reported Elev. (ft)	Material Dated	Radiocarbon Age (B.P.)	Comments
LJ-979	1854	Marly silt	24,750±1300	2
LJ-973	1854	Snail shells	>50,000	2
LJ-991	ca 1837	Compacted marl	32,900±700	3
LJ-983	ca 1871	Lithoid tufa	17,100±900	4

Comments:

1) Hubbs et al, 1965, p. 94-5.

2) The dated shells were reportedly collected from the dated marly silt and were probably collected from the saddle just east of the broad, 1850-foot bench. Hubbs (1965) explained the discrepancy between marl and snail dates by suggesting that the shells might have been reworked from older lake deposits. The sand and silt beneath the marly silt contain firm shells compared to crumbly shells contained in the marly silt. These two units might have been mixed (both are riddled with animal burrows) to incorporate older shells in younger silt, or the marly silt may have been contaminated by younger carbon to explain the age discrepancy (Appendix A).

3) This marl, collected 5m below the bench, is probably the same unit as the marly silt described in (2). The unit here appears fresh and not burrowed by animals.

4) This tufa was collected "...from the surface of a small level bench ca 5m higher than a larger level area..." (Hubbs et al, 1965, p. 94). This is presumably the 1870-foot bench (fig. 4-22), although no tufa could be found on this bench.

Table 4-3. Published Radiocarbon Ages from Station 4 of E.L. Davis

Lab. No.	Reported Elev (ft)	Probable Elev (ft)	Material Dated	Age (B.P.)	Comments
LJ-986	1801	1742±10	Marly Silt	>40,000	1,2
LJ-987	"	"	Compacted Marl	>40,000	1,2
LJ-981	"	"	Snail Shells (Carnifex sp)	>50,000	1,2
LJ-984	"	"	Lithoid Tufa	32,300± 1600	1,3
UCLA-1123-I	1800	1742±10?	Tufa (inorganic)	15,950± 1000	4,5
1123-O	"	"	Tufa (organic)	12,000± 260	4,6
UCLA-1118-I	1900	1825±20?	Tufa (inorganic)	27,000± 1000	4,5
1118-O	"	"	Tufa (organic)	12,500± 800	4,6

Comments

1) Hubbs et al, 1965, p. 94-5. Reported location: NE 1/4 sec 27, T 17 S, R 24 E (36°25'47"N, 117°24'25"W).

2) The above reference (1) suggests that the snail shells have been reworked and does not specifically state that they were found within the marl.

3) This tufa was reported "...from surface at Station 4..."; (where it is clearly colluvial), but called "...tufa on overlying beach stones..." in LJ-981 comment.

4) Berger & Libby, 1966, p.495. Reported location 36°26'N,117°24'W.

5) These dates were corrected for old lake water in reference 4 by subtracting 2500 years; the values listed here are uncorrected so they may be compared with the LJ dates.

6) These dates from organic residue remaining after dissolving all carbonate in HCl; this may not all be original carbon.

Absolute Age

Published radiocarbon ages of materials collected from high shorelines in northern Panamint Valley are listed in Tables 4-2 and 4-3. The age of deposits attributed to Gale Stage exceeds 50,000 years, based on two shell dates (LJ-973, LJ-981), which are generally thought to yield more reliable radiocarbon ages than other carbonate materials (Appendix A). Dates on these other carbonate materials, particularly tufa, are viewed skeptically and they are considered to represent only minimum ages for the dated materials (Appendix A).

Shallow Lake Stands

During latest Pleistocene time, northern Panamint Valley appears to have been occupied by a shallow lake whose area ranged between seven and 18 square miles--the respective areas now enclosed by the modern playa and the 1570-foot contour. The evidence for this lake is sparse--no cut or depositional shoreline features have been found, but nodose tufa at three places suggest its existence: on the west side of the playa on a knob of Paleozoic carbonate rocks tufa reaches 1570±5 feet elevation (SE 1/4 SE 1/4 SW 1/4 sec 4, fig. 4-19); 2) on the southeast side of Lake Hill at 1550±5 feet elevation, where a low tufa mound rises above an alluvial surface (NE 1/4 SW 1/4 SW 1/4 sec 11, fig. 4-19); and 3) a distinct "bathtub ring" tufa band reaching 1555±5 feet elevation and extending about 500 feet northerly along the steep southwest side of Lake Hill (E 1/2 SE 1/4 sec 10, fig. 4-19).

Published radiocarbon ages indicate that this shallow lake stand persisted until about 10,000 years ago (Table 4-4). Davis (1970, p. 91) noted that these dates suggest the presence of "...at least a seasonal lake about 10,5000 years ago." Hubbs et al (1965, p. 93) suggested that the lake stand which deposited the 1555-foot tufa band "...represents a slight refilling of north Panamint Valley" about 13,000 years ago. Archeological evidence also suggests that the lake was shallow during at least part of the 13,000 to 10,000 B.P. interval. Davis (1970, p. 99, 117, 134-5) collected Clovis-related artifacts on the surface at 1560±10 feet elevation and Clovis and Agate Basin artifacts at 1575±10 feet; elsewhere in the United States, Clovis artifacts are limited to 12,000 to 11,000 B.P. and Agate Basin to 11,000 to 10,000 B.P. (Haynes, 1965, p. 161).

The paleohydrologic implications of the shallow lake stand and its correlation with lake stands in southern Panamint Valley are discussed in Chapter 5 (Paleohydrology).

The Lake Panamint Record in Cores Taken from North Panamint Playa

The logs of four cores taken from north Panamint playa have been published (Smith and Pratt, 1957; Motts and Carpenter, 1968) and are presented graphically on Figure 4-23. The record of core NP-3 is most suitable for reconstructing lake history because of its completeness and depth (162 feet). This record is not correlated with the record of the other deep hole (DH2, 370 feet) because no marker horizons are present in the core logs and because silt and clay facies seem to predominate in core NP-3, whereas sand is abundant at

Table 4-4. Published Radiocarbon Ages of the Shallow Lake in North Panamint Valley.

Lab No.	Elevation (feet)	Material Dated	Reported Age (B.P.)	Comments
LJ-977	1555±5	Nodose tufa	13,000±700	1
UCLA-989	1550±10	Organic mat	10,020±120	2,3
UCLA-990	1542±2	Burnt reeds	10,520±140	2,4

Comments

1) Hubbs et al, 1965, p. 93. This tufa band forms a distinct "bathtub ring" extending 500 feet northerly along the steep southwest side of Lake Hill (E 1/2 SE 1/4 sec 10, fig. 4-19).

2) Berger & Libby, 1966, p. 468.

3) This organic mat was encountered in a trench excavated at the south end of Lake Hill for archeological investigations reported by Davis (1970).

4) These reeds burned in growth position and were encountered in a trench excavated on the northwest margin of Hill 1695 (fig. 4-19) for archeological excavations reported by Davis (1970). The elevation of this site is from her map, figure 4.

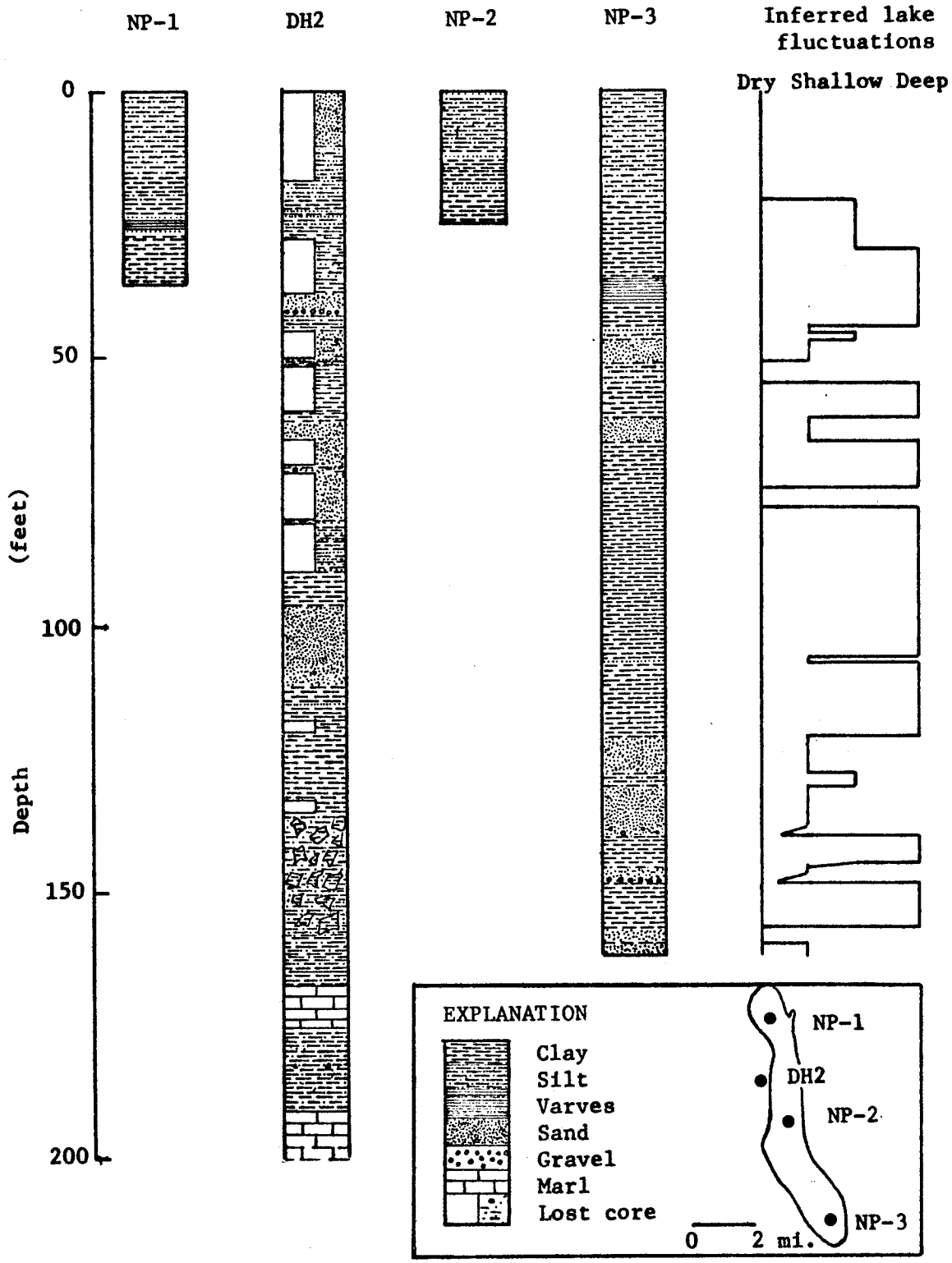

Figure 4-23. Graphic logs of cores from north Panamint playa (after Smith and Pratt (1957) and Motts and Carpenter (1968)).

comparable depths in much of core DH2. The greater abundance of sand in DH2 is tentatively attributed to the location of this hole at the distal edge of the alluvial fan from Darwin Wash, whereas the location of hole NP-3 is in the middle of the south part of north Panamint playa (figs. 4-1, 4-23). Darwin Wash, the largest drainage tributary to Panamint Valley, may have supplied enough sand to Lake Panamint for bottomset sand to reach the lake bottom at the site of DH2 even during high lake stands. Because NP-3 is half again as far from the mouth of Darwin Wash as DH2, much less sand could have reached NP-3 during high lake stands.

A tentative plot of fluctuations in the level of Lake Panamint in north Panamint Valley is based entirely on the record from core NP-3 (fig. 4-23; app. B). Dry or intermittently-dry conditions are inferred from oxidized yellowish and brownish sediments, presumably indicative of at least intermittent subaerial exposure. Periods during which no complete lake desiccation occurred are inferred from greenish sediments, which suggest reducing lake-bottom conditions. Beds of greenish sand and gravel suggest periods of low lake level, shallow enough for waves to transport coarse debris along the lake bottom, but yellowish and brownish sand were probably deposited subaerially. Conditions of rising water level in north Panamint Valley by overflow from south Panamint Valley are inferred from beds of sand and/or gravel grading upward into clay. Deep lake stands are inferred from clay beds of high plasticity.

The pattern of lake fluctuations inferred from the NP-3 core log resembles the pattern of lake fluctuations inferred from core logs from south Panamint playa and from shoreline and stratigraphic

relationships at Pleasant Canyon. Tentative correlation between these patterns is shown on Figure 7-1.

Correlation

The prominent high shorelines on both sides of northern Panamint Valley are probably correlative. The prominence of the shoreline near the Townes Pass Road suggests correlation with these high shorelines, although its tufa is more like tufa on the middle shoreline on the Wildrose segment. The band of dendritic to nodose tufa 25 to 45 feet below the high shoreline on the valley's west side is probably correlative with the middle shoreline on the Wildrose segment, as are the tufa deposits at 1800 to 1820 feet elevation on Lake Hill. This middle shoreline is probably older than the higher shoreline, just as the lower tufa line on the southern Argus Range seems to be older than the prominent, highest shoreline at Bendire and Water canyons. The middle shoreline is tentatively attributed to earliest G_1 substage, when the level of Lake Panamint was stabilized by overflow across the bedrock lip now buried beneath Wingate Pass. The higher shoreline is tentatively attributed to later substages of Gale Stage, when the level of Lake Panamint was stabilized by overflow through the present outlet channel in Wingate Pass.

Both the higher and middle shorelines probably formed during deposition of clay from 84 to 120 feet depth in core NP-3. Marl at 167.5 to 175.0 and 190 to 200 feet depth in core DH2 invites correlation with nearshore marl on the Wildrose and Big Four segments, if marl was deposited simultaneously at widely-separated places along

the bottom and near the shore of Lake Panamint.

Tectonic Deformation

Normal faulting

High shorelines have been offset 30 feet down to the west by normal faulting along the Ash Hill fault at the north end of Ash Hill (fig. 4-3). The higher and middle shorelines on the Wildrose segment have been dropped along both down-to-the-west and down-to-the-east faults (figs. 4-7, 4-9). These faults strike north and have had throws of five to thirty feet since formation of these two shorelines.

The greatest density of fault scarps lies along the east wall of the Wildrose graben, a north- to north-northwest-trending feature about one-half mile wide, four miles long and 100 to 200 feet deep (fig. 4-5). The east wall is step-faulted down to the west and a similar zone of step faulting strikes northwest into the graben's southeast corner. No shoreline remnants have been cut by this faulting, although a head-sized block of tufa was found on one of the scarps at about 2050 feet elevation.

Warping

The prominent high shoreline on both sides of northern Panamint Valley has been tilted northward. On the west side, it descends from about 1980 feet elevation at the south end of Ash Hill to 1820±20 feet 12 miles north; this tilting has the same sense on both sides

of the Ash Hill fault. On the east side, it descends from a high of 2085±10 feet on the central Wildrose segment to a low of 1825±10 feet north of the Big Four Mine Road, 17 miles north. Tilting is fairly uniform on Ash Hill but irregular and interrupted by faults on the Wildrose segment; these are the only two stretches where shoreline remnants are continuously exposed. Some of the difference in the amount of tilting between the middle and higher shorelines on the northern Wildrose segment may have resulted from a local westward component of tilting in addition to the dominant northward component. The middle shoreline, which here lies well to the west of the higher shoreline, appears to cross the axis of a north-striking monocline and to have been tilted west along it (figs. 4-8, 4-9). The higher shoreline, lying entirely east of the monocline's axis, was not noticeably deformed by the monoclinal flexure.

Folding

The monocline which deforms the intermediate high shoreline is the easternmost member of a series of folds which have deformed fan deposits in the high area which forms the divide between the north and south basins of Panamint Valley (fig. 4-8). In the vicinity of the divide, folds strike N 15° W to N 30° W and their flanks dip 10 to 20 degrees, but local dips are as steep as 70 degrees in fanglomerate.

Thrust Faulting

Quaternary thrust movement has occurred along a west-northwest-trending fault zone at the north end of Panamint Valley, where plutonic rocks of Hunter Mountain now overlie deposits of talus shed from the mountain front (figs. 4-24, 4-25, 4-26; R.S.U. Smith, 1974, 1975). A zone of crushed crystalline rock, 50 to 100 feet thick, dips 17 to 35 degrees north and northeast beneath unshattered crystalline rock and overlies talus rubble composed of sound boulders of the same crystalline rock (fig. 4-27). Erosion has locally stripped the crush zone from its rubble sole, and nearby streams have trenched 200 feet into fan deposits which overlie the trace of the crush zone. An irregular, south-facing fault scarp suggests that still younger thrust movement has occurred 1.5 miles southwest of the main thrust zone (fig. 4-26). The probable southeastward continuation of this younger thrust zone is marked by the abrupt southwest margin of a large body of uplifted and dissected gravel of the same unit which forms the sole of the main thrust zone. This gravel dips southwest along the margin at angles steeper than elsewhere. Steeper dips along its southwest margin and uplift of the entire body of gravel between the main and younger thrust zones are both consistent with compressional deformation.

Traced to the northwest, the strike of the main crush zone bends to N 55° W and its dip becomes nearly vertical at Grapevine Pass (between Panamint and Saline valleys), where offset streams and horizontal slickensides suggest right-lateral movement. Mapping by

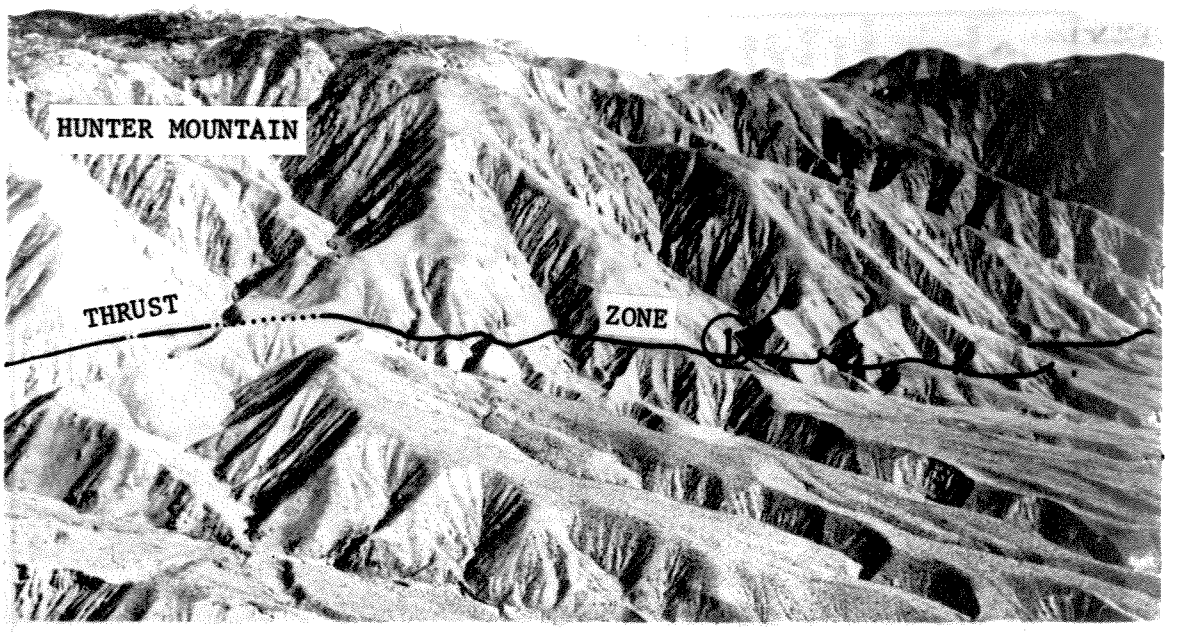

Figure 4-24. Aerial view of Hunter Mountain from the southwest. Note thrust zone.

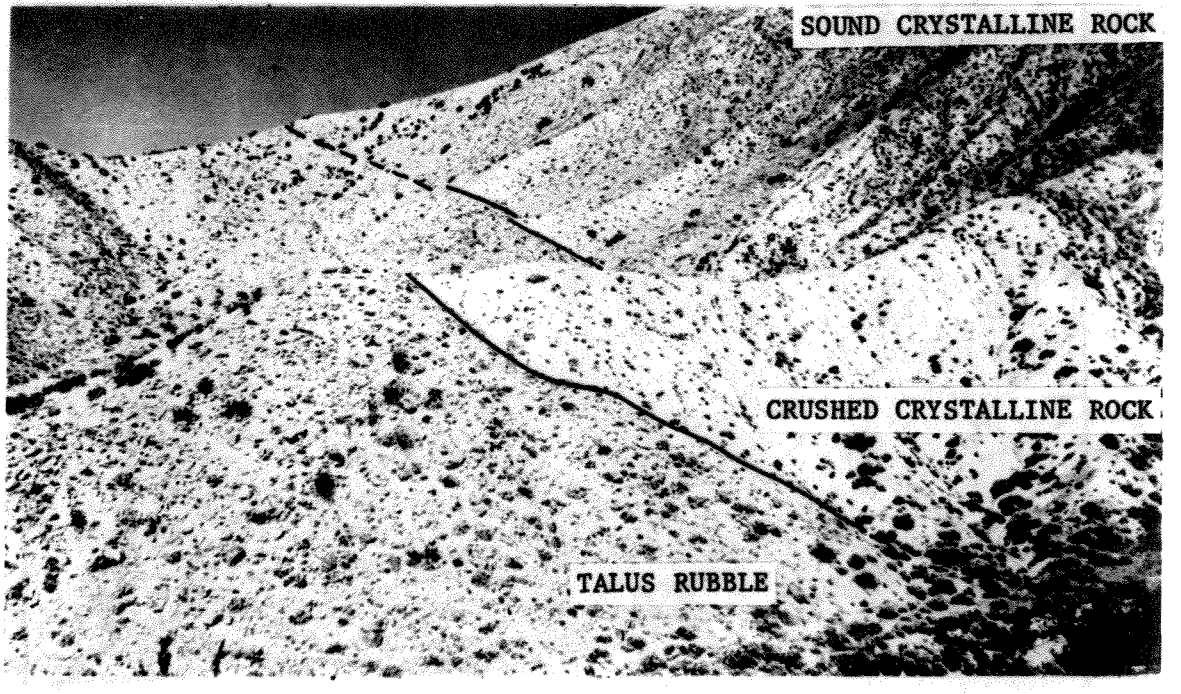

Figure 4-25. Looking west along thrust zone from (1) on figure 4-24.

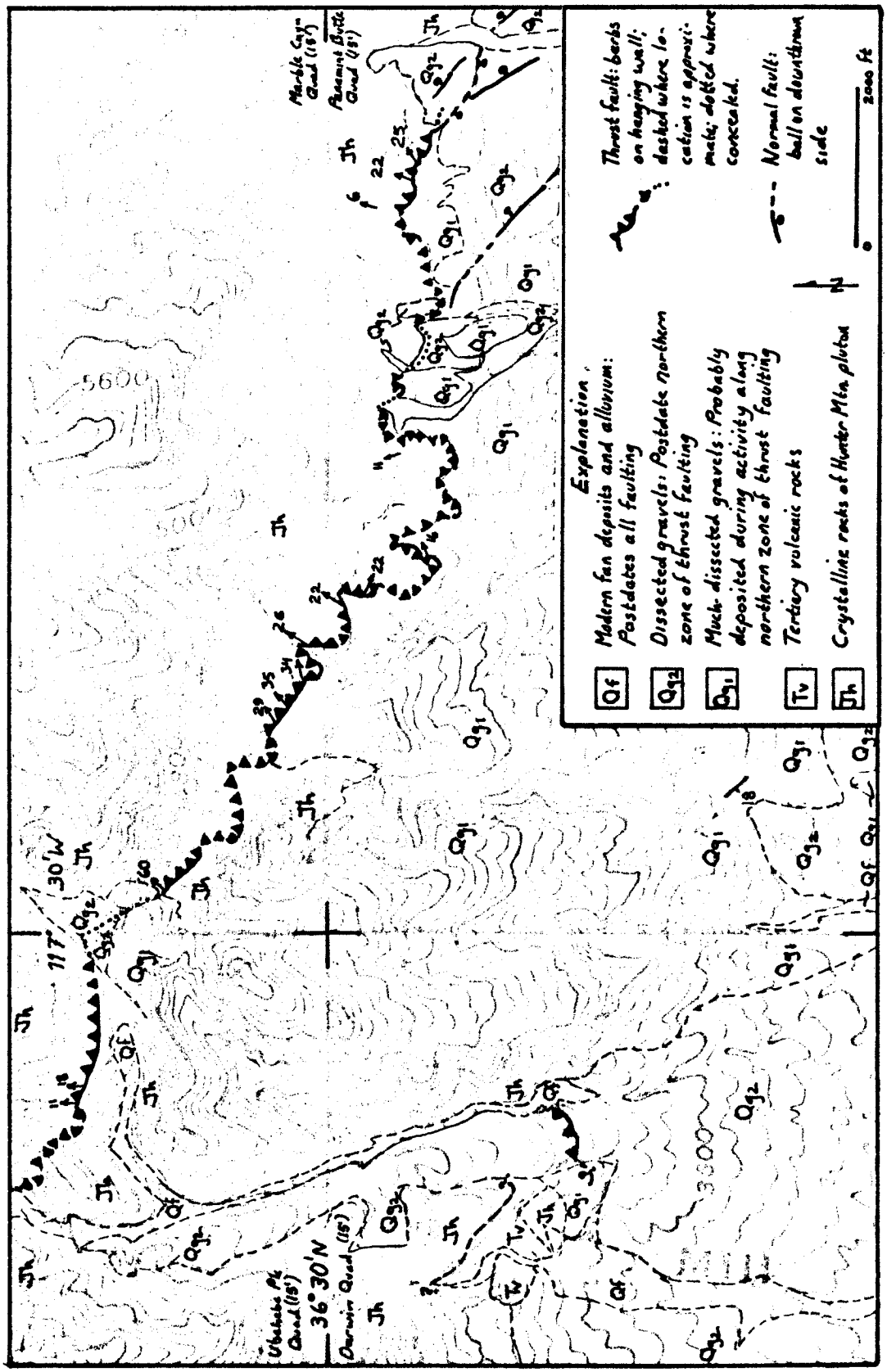

Figure 4-26. Geological map of thrust faults along the southern flank of Hunter Mountain.

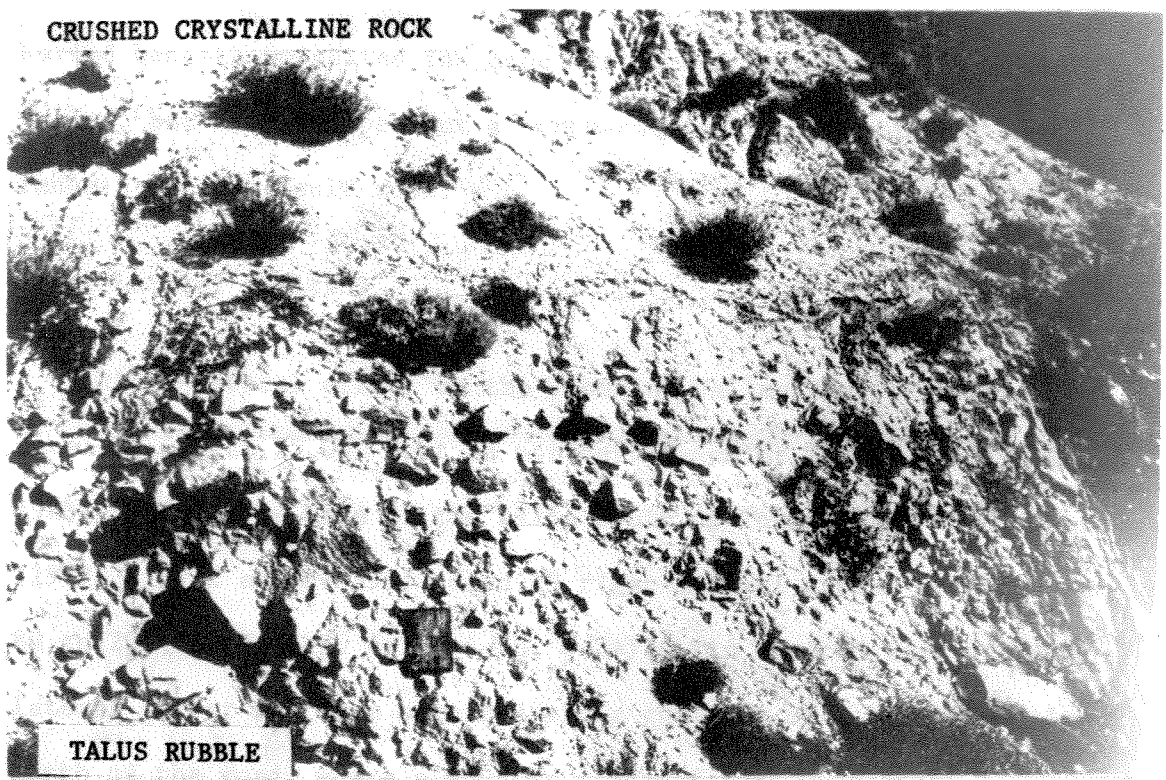

Figure 4-27. Thrust zone marked by crushed crystalline rock overlying talus rubble of sound crystalline boulders.

McAllister (1956) has shown that this fault zone is continuous with the fault zone along the foot of the steep south wall of Saline Valley. The southeastward extent of the thrust zone is unknown because it is buried beneath unfaulted fan deposits in northeasternmost Panamint Valley, but it may represent a northwestward continuation of the Panamint Valley fault zone.

Right-Lateral Faulting

Right-lateral offset on the Panamint Valley fault zone may total 10,000 to 15,000 feet in northern Panamint Valley (R.S.U. Smith, 1975). Along the base of the hills south of Townes Pass Road, Hopper (1947, fig. 2 and p. 399) noted 19 right-lateral stream offsets of 80 to 200 feet (figs. 4-18, 4-28, 4-29). Six hundred feet of right-lateral offset may have occurred along the base of a hill directly north of the road, where a shutter ridge of late-Quaternary fan gravel, rich in clasts of Precambrian and Paleozoic rocks, lies directly opposite the foot of a steep, 200-foot-high hill of Tertiary volcanic rocks (figs. 4-28, 4-29). This fan gravel was probably deposited by the stream which cut the gap now followed by Townes Pass Road. This stream drains a large area of Plio-Pleistocene fanglomerate made up of similar clasts. Right-lateral fault movement has probably displaced the fan gravel northward along the base of the hill.

Two miles southeast of Townes Pass Road, right-lateral offset of similar, but older, fan deposits probably totals 1,000 to 2,000 feet. Here, the prominent high shoreline has been cut into hills

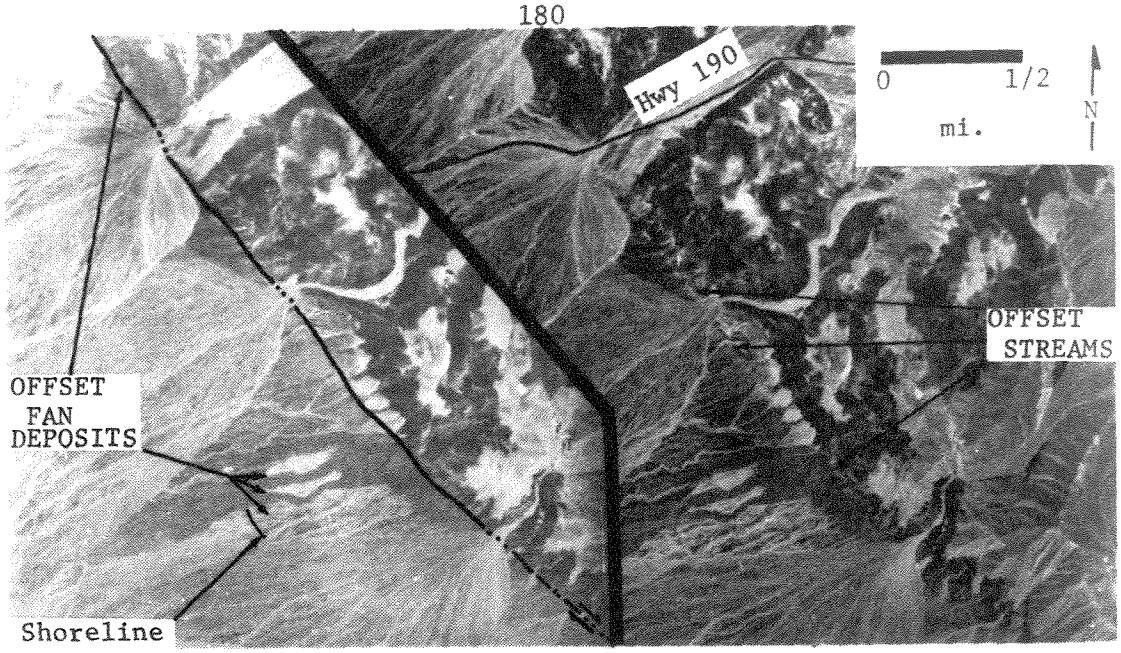

Figure 4-28. Stereogram of right-lateral fault offset near Townes Pass Road (California Highway 190).

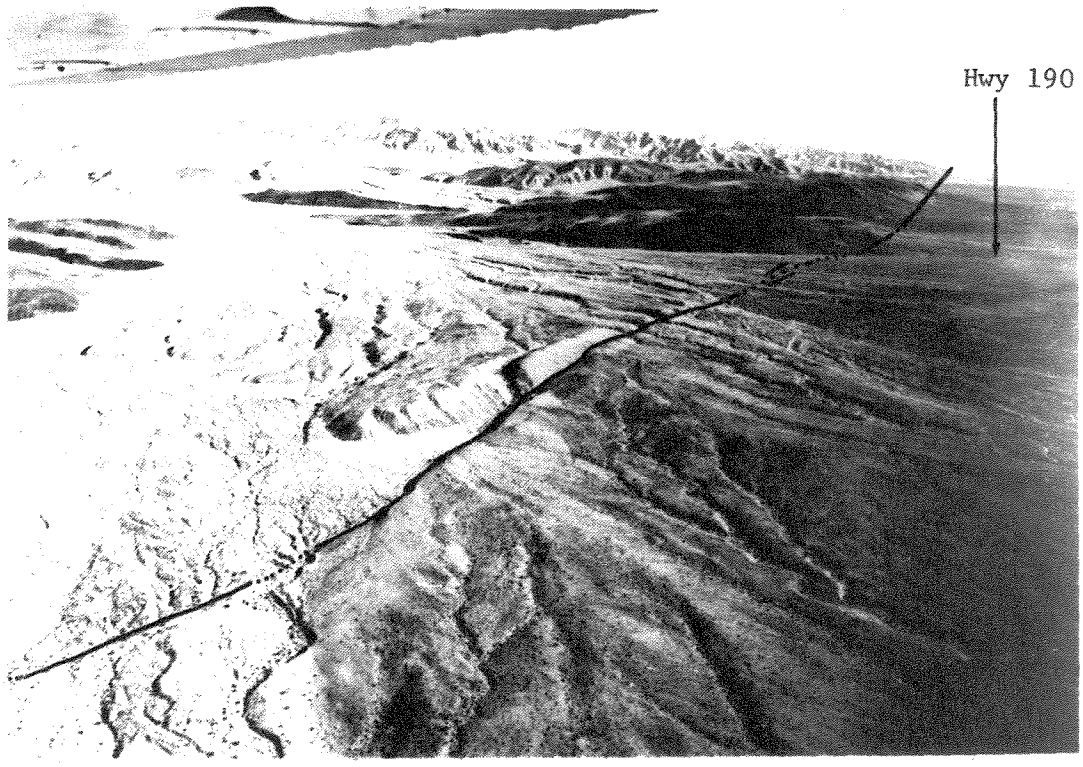

Figure 4-29. Aerial view to the southeast along the Panamint Valley fault zone toward the Townes Pass Road. Note what appear to be offset streams in the left foreground.

of light-toned debris (clasts of Precambrian and Paleozoic rocks) which have been enveloped by dark-toned fans containing clasts of volcanic rocks from the scarp of the Panamint Valley fault zone, upslope and to the east of the hills (fig. 4-28; the probable source canyon for the light-toned debris is in the lower right corner).

In the northern Wildrose segment, a sheet of monolithologic (landslide) breccia appears to have been offset 10,000 to 15,000 feet right-laterally from its probable source area in Wildrose Canyon (figs. 4-1, 4-5). This breccia of crushed metamorphic rocks has an outcrop extent of more than one square mile. It was deposited on eroded fanglomerate and is overlain by fan deposits into which the higher and middle shorelines were cut (fig. 4-8).
This landslide could not have formed from the heterogeneous assemblage of clasts now found in the Plio-Pleistocene fanglomerate which forms the steep hills now upfan from the breccia. If the breccia postdates the fanglomerate in the hills above (as seems likely), right-lateral fault offset is the simplest mechanism for displacing it from the mouth of Wildrose Canyon.

CHAPTER 5

PALEOHYDROLOGY

Modern Hydrology

Introduction

The hydrologic basin tributary to Panamint Valley covers an area of about 1600 square miles (fig. 5-1). It is about 90 miles long in a northerly direction, 25 to 35 miles wide in its northern part and eight to 20 miles wide in its southern part. Although the bordering mountains are high, topographic closure of the basin is less than 1000 feet because of the low level of Wingate Pass (elevation 1977±1 feet) which breaches the basin rim between Panamint Valley and Death Valley (fig. 5-2). The pass between Panamint Valley and Searles Valley is slightly higher (2265 feet).

A low divide (elevation 1715 feet) separates the Panamint Valley hydrologic basin into two topographically-closed subunits: a north basin, with a tributary drainage of about 570 square miles; and a south basin, with a watershed of about 1030 square miles (fig. 5-2). The north basin is floored by a dry playa and the south basin is floored by a predominantly-wet playa*. The elevation of the north playa at 1540 feet is 500 feet higher than the south playa.

Both playas are typically occupied by shallow ephemeral lakes

*See Carranza (1965) and Durgin (in preparation) for detailed studies of the south and north playas, respectively.

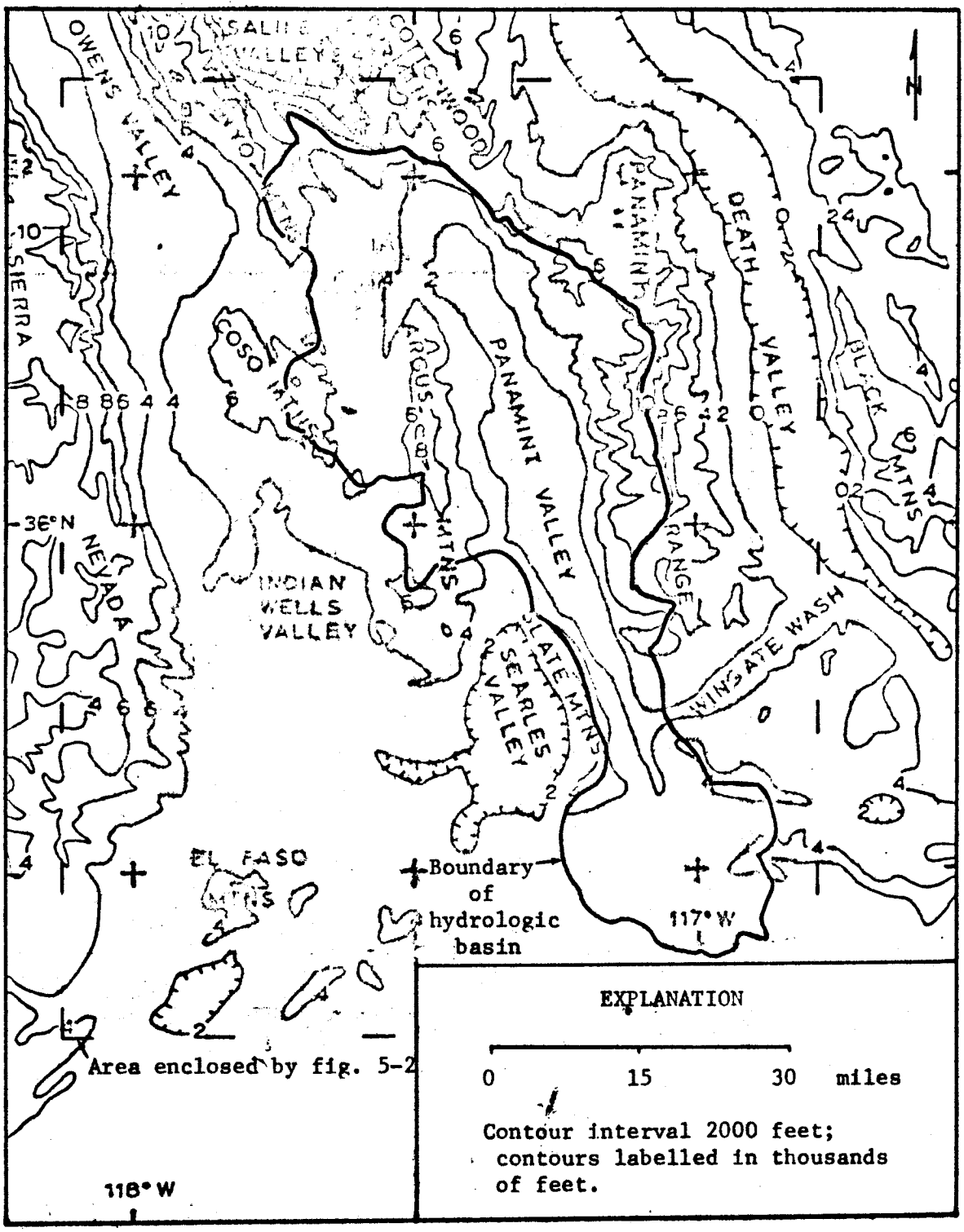

Figure 5-1. Topographic setting of Panamint Valley's hydrologic basin.

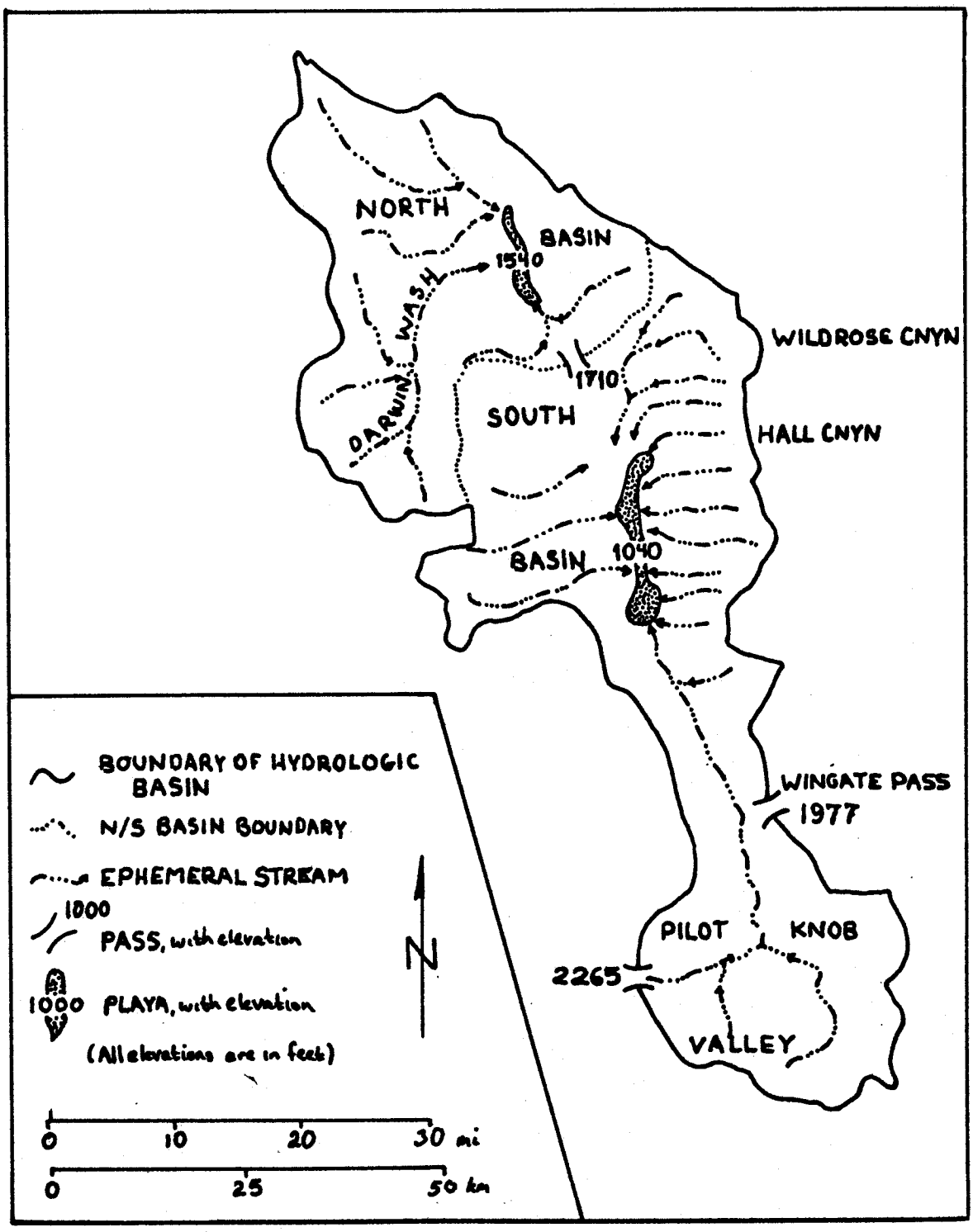

Figure 5-2. Panamint Valley's hydrologic basin.

following major storms. Because these lakes seem to occur more frequently than does runoff from the mountains, some of them may be created by direct precipitation onto the playas and by local runoff and seepage from the alluvial surfaces adjoining the playas. The only perennial lake in Panamint Valley occupies a fault-bounded depression at the north end of the south playa. It is small (< 0.1 mi^2) and receives runoff from the only perennial stream to reach the valley floor, the lower, spring-fed part of Hall Canyon (fig. 5-2).

The streams tributary to Panamint Valley are ephemeral, although those draining the higher mountains commonly have short, spring-fed reaches of perennial surface flow. The streams typically follow narrow canyons along steep gradients (300 to 1000 feet per mile, although some reaches have sustained gradients of 2000 feet per mile, e.g., lower Hall Canyon). Most canyons are narrow over their entire lengths and run directly to the mountain foot without intersecting other canyons. However, canyons draining the highest parts of the central Panamint Range commonly have broad alluviated headwaters above their narrow canyon reaches (Maxson, 1950, p. 102-3, 108-112). The only two extensive drainage systems tributary to Panamint Valley both drain upland basins (Darwin Wash and Pilot Knob Valley).

Surface runoff from all of these streams is infrequent. The stream gage at Wildrose records surface flow about once a year; the one on Darwin Wash records one or two floods per year in excess of its perennial, spring-fed underflow which percolates into gravels of the wash a short distance downstream (fig. 5-3).

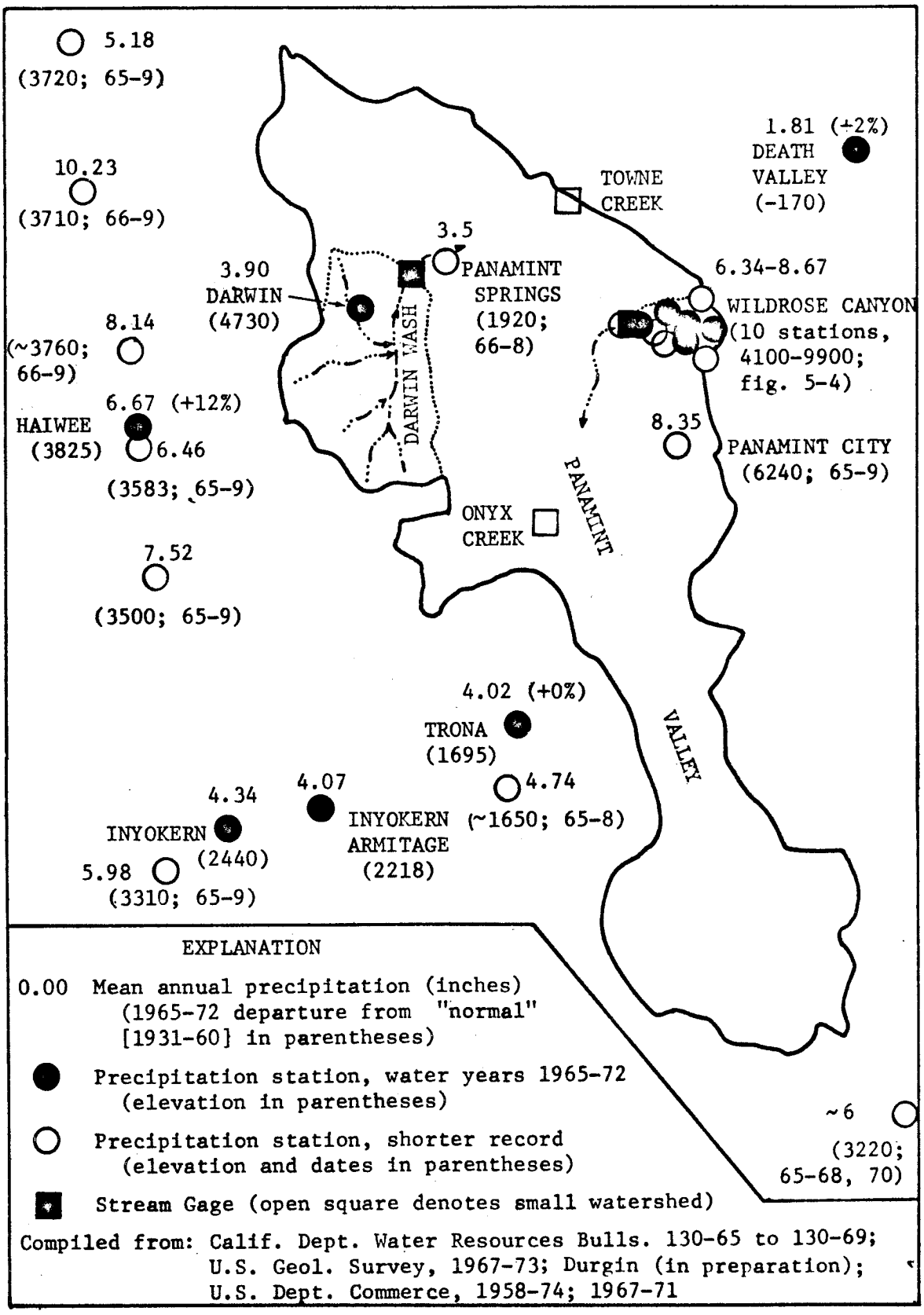

Figure 5-3. Map of precipitation in Panamint Valley and vicinity.

The paucity of surface runoff suggests that ground-water underflow accounts for much of the water reaching the valley floor. Thompson (1929, p. 124-5) noted that basins floored by dry-surfaced playas usually lose ground water to lower basins floored by moist-surfaced playas. He suggested (p. 184-7) that ground water flows from Panamint Valley's higher north basin to its lower south basin, whose moist playa surface is maintained by a shallow ground-water table.

Precipitation

Panamint Valley receives its sparse precipitation from winter frontal storms (60-75%) supplemented by summer convective storms (25-40%) (table 5-1). Precipitation is extremely variable from year to year, but probably averages three to four inches per year on the valley floor and 6 to 12 inches on the higher mountain slopes (figs. 5-3, 5-4, 5-6). The region's aridity is usually attributed to its geographic position within the rain shadow to the lee of the Sierra Nevada (for example, see Morrison, 1965b, p. 267). During winter, those storms which cause the heaviest precipitation, as for example during January and February, 1969, seem to be warm storms which enter the area from the southwest without crossing the highest part of the Sierra Nevada. Additionally, Panamint Valley lies too far west to get a large amount precipitation from thundershowers fed by moist summer air which enters the area from the gulfs of Mexico and California.

The precipitation record from Panamint Valley is short, and all official stations are in the adjoining mountains rather than on the

Table 5-1. Monthly distribution of precipitation in Wildrose Canyon

Station Elev. (ft)	4100	4300	5300	5750	6400	7200	Mean	Per Cent
Period of Record	1-67 to 10-73	7-64 to 9-72	7-64 to 9-72	7-64 to 9-72	7-64 to 9-72	7-64 to 9-72		
Record Length (months)	82	99	99	99	99	99		
Months missing	6	0	0	18	0	5		
January	0.70	0.6	0.44	1.02	0.68	0.73	0.70	9.85%
February	1.64	1.2	0.85	1.32	1.18	1.34	1.26	17.79
March	0.23	0.4	0.19	0.22	0.25	0.52	0.30	4.28
April	0.44	0.6	0.46	0.43	0.72	0.66	0.55	7.82
May	0.23	0.2	0.15	0.21	0.18	0.18	0.19	2.72
June	0.29	0.2	0.18	0.62	0.56	0.76	0.44	6.17
July	0.28	0.6	0.56	1.05	1.10	1.08	0.78	11.03
August	0.40	0.5	0.76	0.97	0.93	0.86	0.74	10.44
September	0.16	0.1	0.25	0.24	0.33	0.26	0.21	3.02
October	0.25	0.1	0.05	0.06	0.09	0.12	0.11	1.58
November	1.15	0.9	0.75	0.68	1.27	1.31	1.02	14.43
December	0.20	0.9	0.77	0.61	1.20	0.92	0.77	10.87
Annual*	6.02	6.3	5.41	7.43	8.49	8.68	7.06	
Summer (May-Sept)	1.36	1.6	1.90	3.09	3.10	3.08	2.36	33.38
Winter (Oct-Apr)	4.66	4.7	3.51	4.34	5.39	5.60	4.70	66.62

*These annual figures do not necessarily correspond to those shown on Fig.5-4 because a) The record for most stations is three months longer than water years 1965-72; and b) the "months missing" here are lumped in those figures.

Compiled from U.S. Geol. Survey Water Resources Data for California, (1965-72) & U.S. Weather Bureau (Environmental Data Service) Climatological Data for California, 1967-73.

valley floor (fig. 5-3). In the plateau region north of the Argus Range, the U. S. Geological Survey has reported precipitation from Darwin (elevation 4730) since 1963. In the Panamint Range, the U. S. Weather Bureau has reported full weather data from Wildrose Ranger Station (elevation 4100) since 1967, and sporadic precipitation data from a storage gage ten miles to the south at the site of Panamint City (elevation 6240) since 1965 (fig. 5-3). Only the Wildrose Canyon watershed in the Panamint Range is well instrumented, having six rain gages at elevations of 4300 to 9990 feet elevation as a result of being designated a hydrologic-benchmark station by the U. S. Geological Survey in 1964 (fig. 5-4).

Annual precipitation has ranged widely from year to year. The difference between minimum and maximum annual precipitation at the six Wildrose stations during the seven-year period was eight to 15 inches, compared to mean annual precipitation of about six to nine inches (table 5-1, fig. 5-4). Although part of this variation may have been due to chance distribution of showers, precipitation was at or above average at five of the six stations during each of the three wettest years (1965-66, 1967-68, 1968-69); likewise, precipitation was substantially less than average at all six stations during the two driest years (1969-70, 1970-71) (fig. 5-6). This suggests that differences from one year to the next are largely caused by systematic year-to-year variations in precipitation over the entire region rather than by random or local effects.

Near to normal precipitation fell on Panamint's neighboring valleys during the period of published data from the Wildrose Canyon

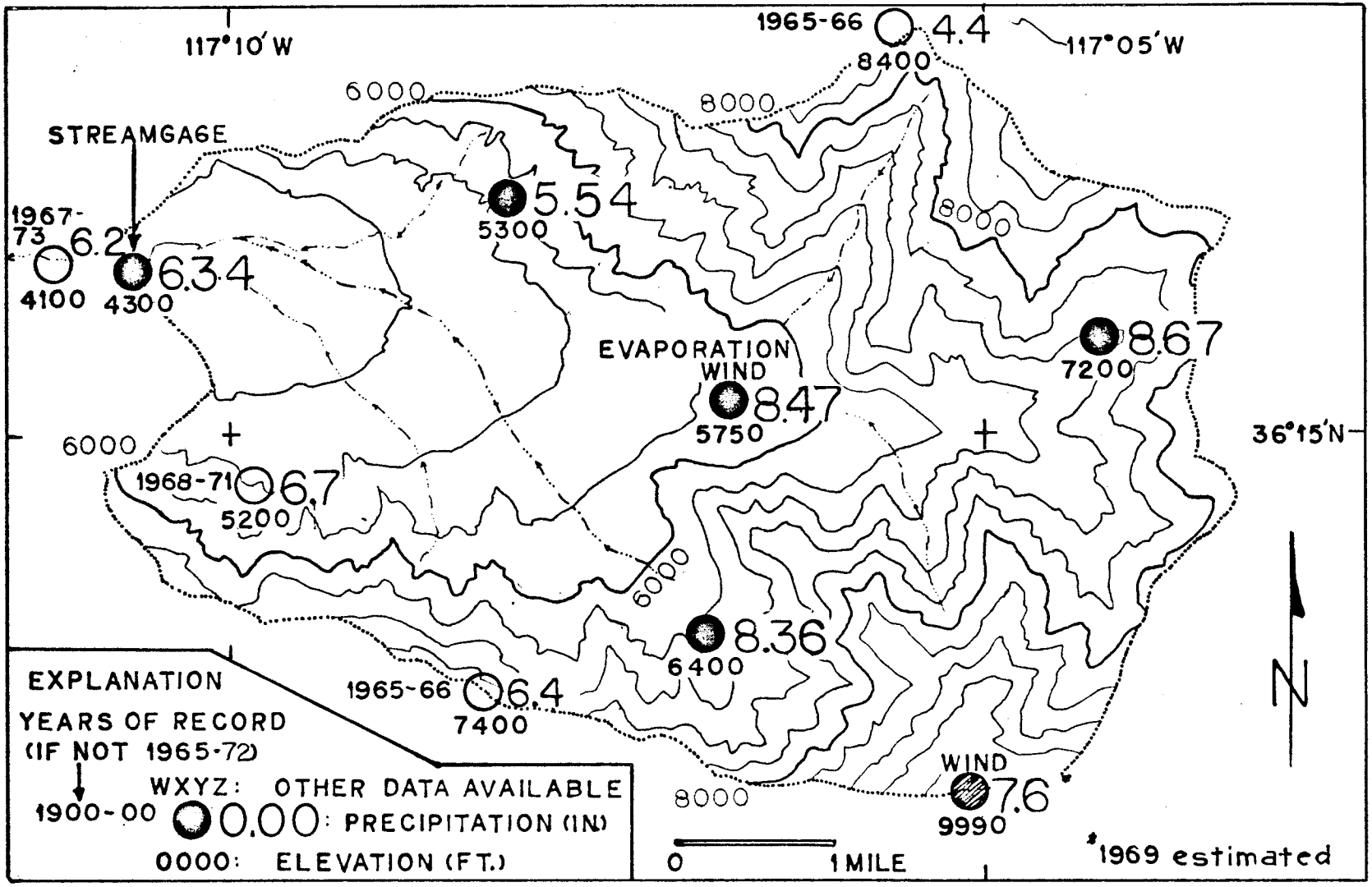

Figure 5-4. Topography of. and precipitation in, the Wildrose Canyon watershed.

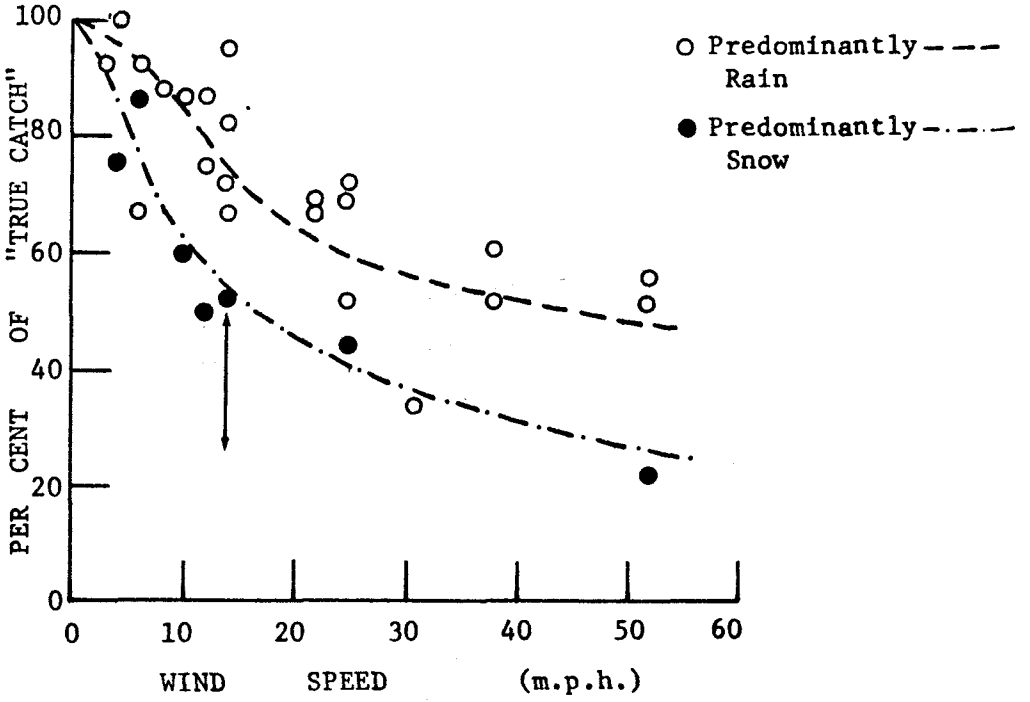

Figure 5-5. Gage capture of incident precipitation as a function of wind speed. (from Wilson, 1954).

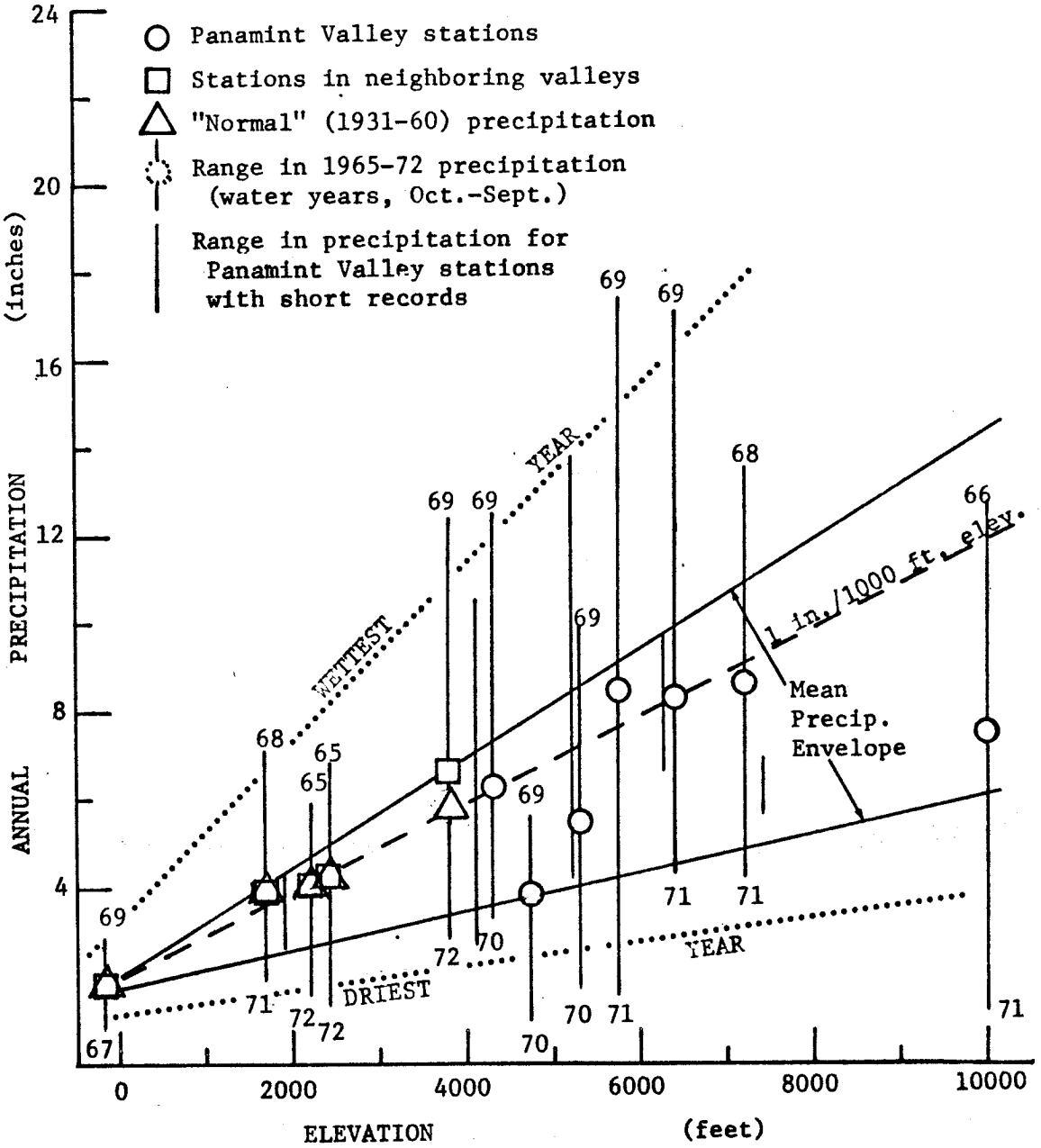

Figure 5-6. Precipitation in Panamint Valley and vicinity as a function of elevation.

watershed (water years 1965-1972, October 1964-September 1972). To the east and south in Death and Searles valleys, precipitation exceeded long-term "normal" (1931-60) values by less than two per cent (fig. 5-3). To the west and northwest, precipitation in the Owens Valley trough was about 12 to 20 per cent above "normal". These comparisons suggest that the eight-year precipitation record from the Wildrose watershed is at least roughly equivalent to long-term "normal" values.

Although precipitation in mountainous regions seems generally to increase with elevation, it also depends on other topographic parameters, and true precipitation tends to be substantially greater than measured precipitation because wind flow over rain gages does not allow full interception of incident precipitation by the gages. Spreen (1947) found that precipitation in western Colorado depended not only on elevation but also on site exposure, orientation and maximum land slope. James (1964) measured ten per cent greater rainfall on the leeward side of a small hill in western Oregon than on the windward side. A much greater variation around a taller, steeper mountain near Santa Barbara, California, was measured by Hovind (1965) : precipitation on the summit was twice that on the windward slope but half that on the leeward slope. Black (1954) estimated that precipitation at Barrow, Alaska, was two to four times that recorded by gages, largely because of strong winds. Wilson (1954) compiled available data on gage interception of actual rainfall and snowfall as a function of wind velocity (fig. 5-5).

Annual precipitation in Panamint Valley and vicinity is plotted as a function of elevation on Figure 5-6. From a base of about two inches at zero elevation (Death Valley), precipitation appears to increase regularly by about one inch per thousand feet, except for two stations which receive substantially less than others: Darwin (elev. 4730) and Rogers Peak (elev. 9990 in Wildrose Canyon). The Darwin anomaly may reflect other factors, but the Rogers Peak one probably reflects the effects of strong winds at its exposed site.

Data on mean wind speed are available for the Wildrose stations at 5750 and 9990 feet elevation (table 5-2). The low wind speeds observed at 5750 feet (about five m.p.h.) seemingly do not greatly affect the accuracy of precipitation measurement, the measured values of rainfall being about five per cent low and those of snowfall being about 20 per cent low (fig. 5-5), with the deficiency in total measured precipitation being perhaps ten per cent since rainfall predominates over snowfall. The effect of wind on recorded precipitation at the 9990-ft station should be much greater, because of its extremely exposed position at the summit of Rogers Peak, one of the highest peaks of the Panamint Range, where mean winter wind speed exceeds ten m.p.h. and summer speeds are about seven m.p.h. (table 5-2,fig. 5-4). Furthermore, storm winds associated with precipitation are probably much stronger than the mean values. If most winter precipitation on the summit comes as snow, Figure 5-5 suggests that only about 60 per cent of it is recorded; likewise, if all summer precipitation comes as rain, about 90 per cent of it is recorded. Because winter

Table 5-2 Seasonal variation in mean wind speed in Wildrose Canyon. (Speeds in miles per hour).

	Station Elevation (ft)	
	5750	9990
Period of record	7-64 to 9-72	7-64 to 9-72
Record Length (Months)	99	99
Months missing	2	34
January	4.8	11.8
February	4.6	12.0
March	5.0	10.3
April	4.8	9.5
May	4.8	7.1
June	4.9	6.7
July	4.4	6.4
August	5.1	6.1
September	5.2	7.3
October	5.1	8.4
November	4.4	9.7
December	4.7	9.8
Annual	4.8	8.8

precipitation predominates over summer, the total annual precipitation could easily be half again as much as has been recorded (about eight inches). This correction would put the 9990-foot data in line with the pattern of precipitation increase with elevation plotted for the lower stations (about one inch per thousand feet). Actually, total precipitation at such an exposed station could be several times that recorded, as noted by Black (1954) for Barrow, Alaska.

Unless the Wildrose precipitation gages intercept a much smaller fraction of incident precipitation than the foregoing discussion suggests, there is no evidence to support a sharp increase in precipitation with elevation above 5000 feet as proposed by Hunt and Robinson (1966, p. B6-7). It seems rather that their estimate of the relationship between precipitation and elevation is too low (0.5 in./1000 ft.) below 5000 feet elevation and too high (2 in./1000 ft.) above 5000 feet. The steady increase in precipitation by one inch per thousand feet plotted on Figure 5-6 seems to fit the available data better than their stepwise increase. Their results may have been perturbed by the storage-gage data from the Spring Mountains (100 miles to the east) used in devising their curve. During the period of Wildrose record, precipitation at any given altitude in the Spring Mountains was one and a half to three times greater than that measured in the Wildrose watershed (see U. S. Dept. Commerce 1967-71).

Sparse observations of precipitation on the valley floor tend to support the validity of the precipitation/elevation relationship shown on Figure 5-6. Durgin (in preparation) reported 3.5 inches annual

precipitation at Panamint Springs (elev. 1920) during August 1966-August 1968. This accords with a value of about four inches predicted from Figure 5-6.

Runoff

Four stream gages are presently active in the Panamint Valley drainage, all installed by the U. S. Geological Survey during the early 1960's. Two of these measure runoff from major drainages: Darwin Wash, with a watershed of 173 square miles, measured just below the point where its underflow is forced to the surface at Darwin Falls; and Wildrose Canyon, draining the 27-square-mile watershed from which precipitation data have been reported in the previous section (fig. 5-4). The Darwin Wash gage has recorded a mean surface flow of 377 acre-feet per year (1963-72) consisting of steady flow of about 0.1 to one cubic foot per second augmented by infrequent floods. The Wildrose gage records no surface flow except for floods every several years (U. S. Geol. Survey). Two other gages measure runoff from very small drainages: Towne Creek (elev. 4800 ft, area 0.05 mi^2) and Onyx Creek (elev. 1750 ft, area 0.52 mi^2) (Waananem, 1971, p. 93).

Discharge at all four gages seems to occur after intense summer thundershowers rather than winter storms. This is consistent with the findings of Kesseli and Beaty (1959) and Beaty (1968) for the White Mountains, which are similar to the Panamint Range in dimensions, bulk and relief, although about 3000 feet higher and somewhat

wetter. These authors found that summer cloudbursts caused more frequent and destructive flooding than either wintertime or snowmelt floods, probably because of their intense, rapid rainfall on small areas.

Storms during early September, 1967, caused severe floods in both Wildrose Canyon and Darwin Wash and caused the only flow ever recorded at the Towne Creek gage (2 ft^3/sec). The Wildrose flood of 4 September totaled 93 acre-feet of water,and reached a peak discharge of 1060 cubic feet per second. It was fed by 0.24 to 1.58 inches of rain that day on the watershed, following upon 0.2 to 0.6 inches which fell during the previous three days (unpub. U. S. Geol. Survey records). Darwin Wash discharged 300 acre-feet of water at a maximum rate of 3130 cubic feet per second. On that day, 0.51 inches of rain fell on Darwin (unpub. U. S. Geol. Survey records) and 0.22 on Panamint Springs (Durgin, in preparation).

Heavy winter precipitation during January and February 1969 totaled 3.08 inches at Darwin and six to ten inches on the Wildrose watershed. Runoff past the Darwin Wash gage totaled 1256 acre-feet discharged at a maximum rate of 4400 cubic feet per second (26 Feb.); this is more than three times mean annual runoff (377 acre-feet per year, 1963-72). Despite the heavy precipitation on the Wildrose watershed, runoff was observed on only one day (25 Feb.) when discharge of 32 acre-feet of water had a peak rate of 204 cubic feet per second. Precipitation on the watershed averaged about three inches on 24-25 February.

Some floods are accompanied by mudflows, although these have not been recorded in the stream-gage data. Murphy (1932, p. 335) described a large mudflow which swept down Surprise Canyon on 26 July 1917. Small mudflows may have occurred in some of the canyons of the Panamint Range during the heavy winter rains of 1969 judging by the freshness of some of the mudflow deposits there and the dislocation of roads by them, although these sites were not seen before the floods. The frequency of mudflows may be similar to that of mudflows in the White Mountains, 100 miles to the northwest. There, Beaty, (1968) documented three major debris flows from the range during the decade 1957-66.

Evaporation

Evaporation from a 24-inch, sunken, screened evaporating pan at 5750 feet elevation in the Wildrose Canyon watershed averaged about 83 inches per year during water years 1965-72; its seasonal distribution is shown on table 5-3. The evaporation rate from this pan corresponds to about 58 inches of evaporation from a hypothetical lake surface at this elevation, using the 0.69 pan coefficient that Hely, Hughes and Irelan (1966, p. 15-17) determined by comparing evaporation from similar pans to the actual evaporation from the surface of the Salton Sea.

The rate of evaporation tends to decrease with elevation, but not at a uniform rate (fig. 5-7). This curve is based on both evaporating-pan studies and measurement of the water budget of actual

Table 5-3 Evaporation rates at 5750 ft. elevation

in Wildrose Canyon, water years 1965-72

Month	Pan Evaporation (inches) per day	Per Month	Lake Evaporation (Pan coefficient=0.69) inches per month
January	0.088	2.72	1.9
February	0.110	3.10	2.1
March	0.137	4.25	2.9
April	0.178	5.33	3.7
May	0.287	8.89	6.1
June	0.346	10.38	7.2
July	0.368	11.40	7.9
August	0.372	11.54	8.0
September	0.352	10.56	7.3
October	0.265	8.21	5.7
November	0.142	4.27	2.9
December	0.090	2.79	1.9
Annual		83.44	57.6

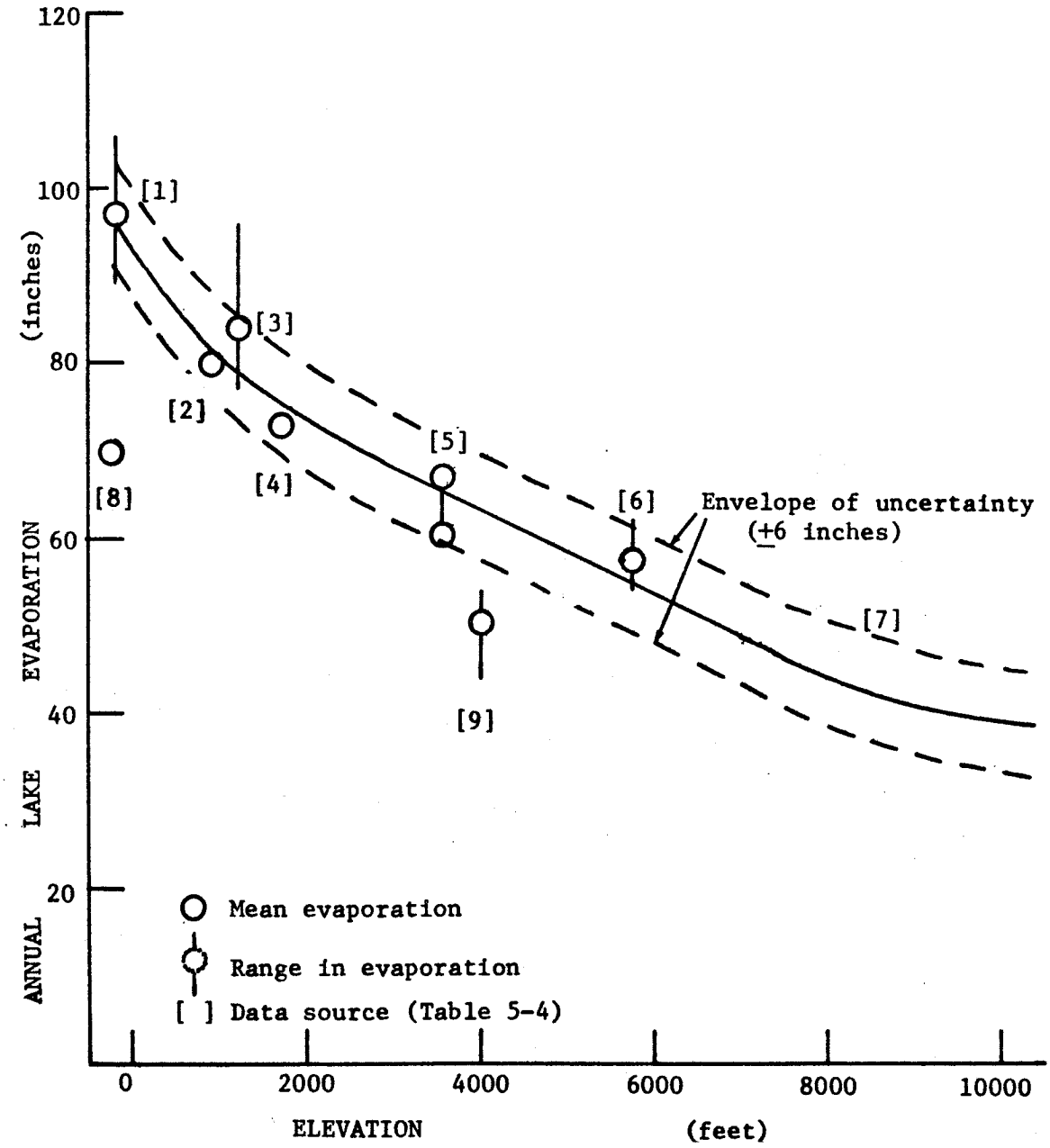

Fig. 5-7 Evaporation in Panamint Valley and vicinity as a function of elevation.

lakes (summarized in table 5-4) and represents an attempt to fit a curve to rather scattered data. The six-inch error envelope which parallels the curve represents an arbitrary attempt to include all data points. Nevertheless, evaporation rates at both Walker Lake and the Salton Sea lie conspicuously below the envelope, and are ignored in considering the evaporation from Panamint Valley.

Because evaporation from the valley floor presently occurs primarily from the surface of a moist playa rather than from standing water, its rate should be much smaller than 75 to 80 inches suggested by fig. 5-7. Feth and Brown (1962) found that evaporation from a salt crust overlying clay at Great Salt Lake, Utah, was roughly one per cent of that from an adjacent pan filled with fresh water. In Death Valley, Hunt and Robinson (1966, p. B8-11) found that the evaporation rate from wet mud and salt was less than ten per cent of that from a similar container of water. These data suggest that evaporation from the entire moist playa surface in southern Panamint Valley (20 mi^2) probably corresponds to that from a lake covering only about 1 mi^2.

Table 5-4. Evaporation data used in plotting figure 5-7.

Place	Elev. (ft)	Gross Lake Evap.(in.)	Method	Pan coef	Dates	Reference
1) Death Valley	-168	97	Class A pan (USWB)	0.60[a]	1959-71	U.S. Dept Commerce
2) Silver Lake	905	79	Water budget		1938	Blaney, 1957
3) L Mead	1200	84	Class A pan Energy budget	.70[a]	1936-53	Harbeck et al, 1958
4) Trona	1623	73	Class A pan	.66[a]	1920-23	Young, 1948
5) Owens L	3570	67.4[b]	Water budget		1906-14	Lee, 1927, 1935
6) Wildrose	5750	57.6	Sunken pan (screened)	.69[c]	1965-72	U.S. Geol. Survey
7) Mt. Whitney	4500-14500	d	22" pan		1905	Lee, 1912 p. 50
8) Salton Sea	-230	79	Mass transfer Energy budget Sunken pan (screened)	.69	1961-62 1948-62	Hely etal, 1966
9)Walker Lake	4030	50	Water budget		1929-34	Harding,1935

Footnotes:

a) Pan coefficients from maps by Kohler, Nordenson & Baker, 1959.

b) Equivalent evaporation of fresh water; actual rate from lake water was 60 inches.

c) Pan coefficient from Hely et al, 1966.

d) Shape of curve only.

Paleohydrology

The Climate during Pluvial Times

The climate during the pluvial episodes of Pleistocene time is generally thought to have been both cooler and wetter than modern climate. Schumm (1965, p. 786-7) has summarized the data on the intensity of this climatic change in the nonglaciated regions of the western U.S. He concluded that pluvial climates were typically 10°F cooler than their modern counterparts and received about ten inches more annual precipitation, regardless of modern precipitation. Runoff should have been more than twenty times greater than modern in arid watersheds (like Panamint Valley) which now receive less than ten inches of precipitation per year and have weighted mean annual temperatures of 50-60°F (Wildrose, 4100 ft, 55.8°, table 5-5). Evaporation should have been less--using Langbein's (1961, p. 3) plot of evaporation as a function of precipitation and temperature, ten degrees of cooling and ten inches more rain should cause 20 to 30 inches less net evaporation (or 10 to 20 inches less gross evaporation) in Panamint Valley and its tributary watershed.

In Panamint Valley, these conditions can be crudely approximated by lowering the modern climatic zones by about 4000 feet in elevation: this decreases temperature by 13 to 15°F (interpolation from table 5-5),increases precipitation by four inches (fig. 5-6), and decreases evaporation by about 19 inches (fig. 5-7). This 4000-foot lowering of climatic zones should roughly correspond to

Table 5-5 Seasonal distribution of mean temperature in Panamint Valley and Vicinity

Station	Death Valley	Trona	Haiwee	Wildrose
Elevation (ft)	-170	1695	3825	4100
Period of Record	"normal" (1931-60)	"normal" (1931-60)	"normal" (1931-60)	1-67 to 1-74
Record Length	30 yrs.	30 yrs.	30 yrs.	85 months
Record Missing				9 months
January	52.0 °F	45.1 °F	34.9 °F	39.5 °F
February	58.2	50.6	43.8	44.7
March	67.3	57.4	49.9	48.9
April	77.0	65.8	58.2	53.1
May	85.1	73.6	65.5	64.3
June	93.9	81.6	73.9	73.0
July	101.6	89.4	81.1	81.0
August	99.1	87.2	79.1	79.0
September	90.9	80.3	73.1	70.1
October	77.0	68.0	70.5	59.2
November	70.5	53.9	49.2	48.7
December	53.1	46.1	41.8	38.3
Annual	77.1	66.6	60.1	58.3
Weighted mean*				55.8

(Compiled from U.S. Weather Bureau & Environmental Data Service Climatological Data for California, 1967-74)

*Using Langbein et al (1949) method:

$$\text{Weighted mean} = \frac{\sum_{i=1}^{12} T_i P_i}{\sum_{i=1}^{12} P_i}$$

where T_i = mean monthly temperature

P_i = mean monthly precipitation

the maximum 4000-foot lowering of vegetation zones during late Wisconsin times (about 10,000 to 24,000 years B.P.).

Martin (1964, p. 68-9) noted that pollen assemblages in the Searles Lake "parting mud" (10,000-24,000 B.P., deposited in a lake whose surface elevation was 1750-2260 feet (G.I. Smith, 1968, p.296, 299)) corresponded to those now found in soil at 6000 to 7000 feet elevation in the Panamint Range, but not to those found below 6000 feet nor above 7000 feet. This suggests that vegetation zones were at least 4000 feet lower than modern during pluvial times. East of the Spring Mountains, Nevada, Mehringer (1967) noted that vegetation zones in the Las Vegas Valley were about 3300 feet lower than their modern counterparts during 13,000 to 14,000 B.P. He interpreted this cool period to be followed by a warming, drying trend interrupted by cooler, wetter episodes at about 10,000-10,500 B.P. and 8,000-8,500 B.P. Earlier (1965, p.186) Mehringer estimated that vegetation zones were lowered by about 4000 feet during the period 11,000 to 20,000 B.P. Data from plant remains found in rat middens indicate at least 2000 feet of vegetation-zone lowering during 9-10,000 B.P. and part of the interval 10,000 to 29,000 B.P. (Wells and Jorgensen, 1964, and Wells and Berger, 1967).

These data suggest that the period 10,000 to 13,000 B.P. represented by the small lake in north Panamint Valley was one of fairly intense pluvial climate, although its intensity may have been exceeded by that of earlier pluvial episodes. If so, the size of this lake can be used to determine the magnitude of pluvial

runoff into Panamint Valley from local sources. The analysis is presented on the following pages indicates that local runoff was far too small to support the deep, overflow stages of Lake Panamint, which must then have been filled by Sierra Nevada water overflowing from Searles Lake.

The Shallow Late-Wisconsin Lake in North Panamint Valley

The evidence for the shallow lake which occupied north Panamint Valley during the interval 10,000 to 13,000 radiocarbon years B.P. has already been given (chapter 4). The area covered by this lake fluctuated between that of the modern playa (7 mi^2) and that enclosed by the 1560-foot contour (15 mi^2). Evaporation on the valley floor (76.5 in/yr, fig. 5-7) is partly offset by precipitation (3.5 in/yr, fig. 5-6), so net evaporation from a lake would total about 73 inches per year. Net evaporation would thus remove about 27,000 acre feet of water per year from a lake covering just the playa, and about 58,500 acre feet from the 1560-foot lake. To sustain the playa lake would require about 0.9 inches of annual runoff from the entire tributary watershed (571 mi^2, fig. 5-2); the 1560-foot lake would need about 1.9 inches. Modern runoff appears to be about 25 to 50 times less than these values.

About 0.04 inches of annual surface runoff drain from Darwin Wash, the basin's largest tributary (173 mi^2), although this is probably supplemented by ground-water underflow. This watershed is representative of the entire basin, although its median elevation

is somewhat higher (5300 feet vs. 4850 feet, fig. 5-8). Although the town of Darwin (4730 ft.) is much drier than comparable elevations in the Wildrose drainage (3.9 vs. 6.5 inches), the Darwin Wash watershed may not be comparably dry because it drains the highest parts of the Argus and Coso ranges, whose rain shadow may cover Darwin.

During late-Wisconsin times, less runoff was needed to sustain the shallow lake than would now be required because of the cooler, wetter climate then prevailing. Figure 5-9 shows the relationship between net evaporation and required runoff for both the playa and 1560-foot lakes, both in inches and as a multiple of modern Darwin-Wash runoff. This figure shows that the lakes needed a minimum of 0.6 to 1.2 inches of annual runoff, even assuming the coolest, wettest pluvial conditions considered likely; this is about 15 to 30 times greater than modern runoff, approximately in accord with Schumm's (1965, table 1) projected pluvial runoff for such a basin. A somewhat drier, warmer pluvial (eg, 2000-ft depression of climatic zones)would require about 0.75 and 1.6 inches of runoff to sustain the respective playa and 1560-ft lakes, or about 20 and 40 times modern runoff. Because this would require more runoff than envisioned by Schumm from a drainage basin both drier and warmer than those he described, these conditions seem less likely to have prevailed during the lake's existence than the cooler, wetter conditions described above.

A simplified version of Snyder and Langbein's (1962) method of

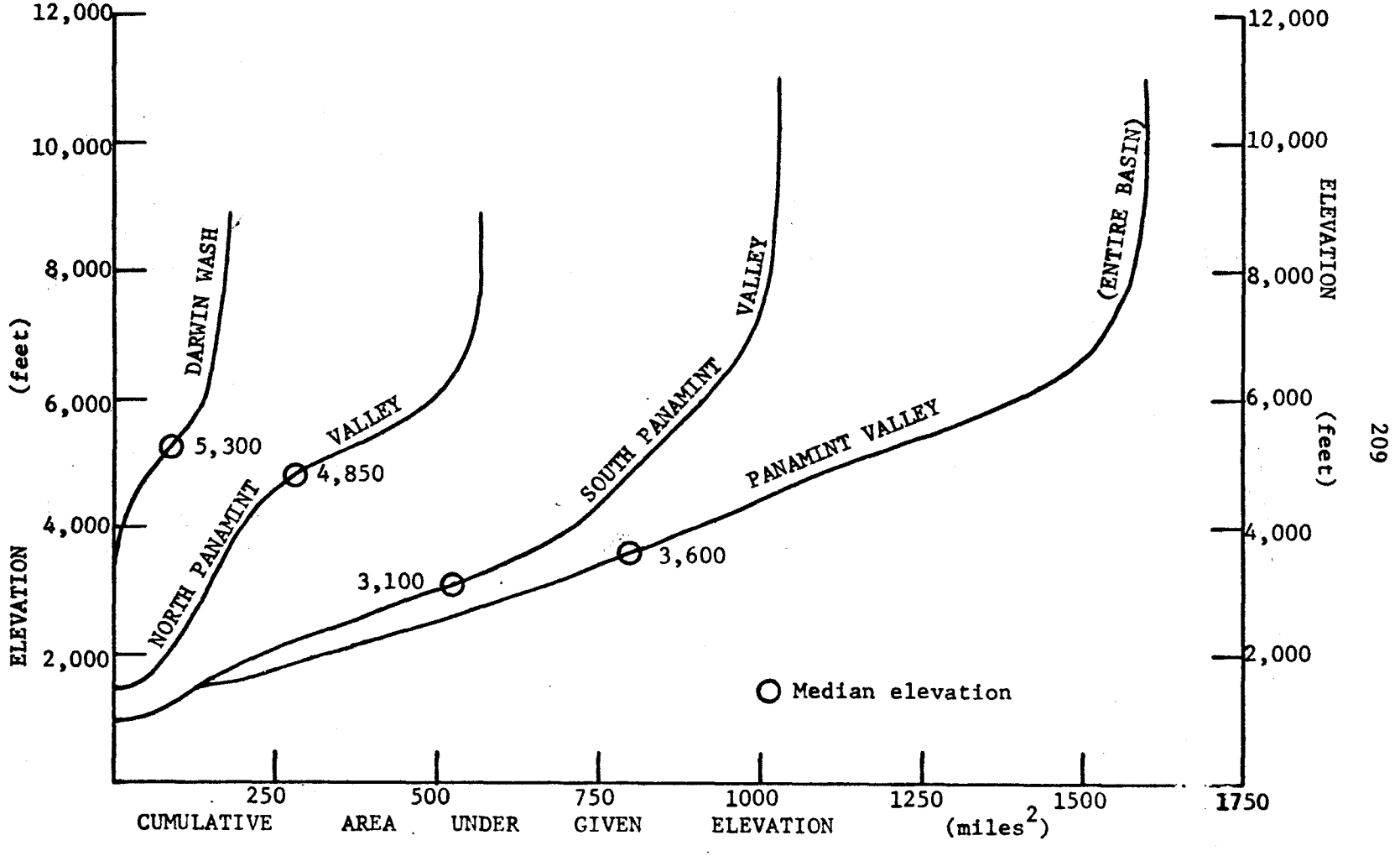

Figure 5-8. The relationship between elevation and enclosed area for Panamint Valley's subbasins.

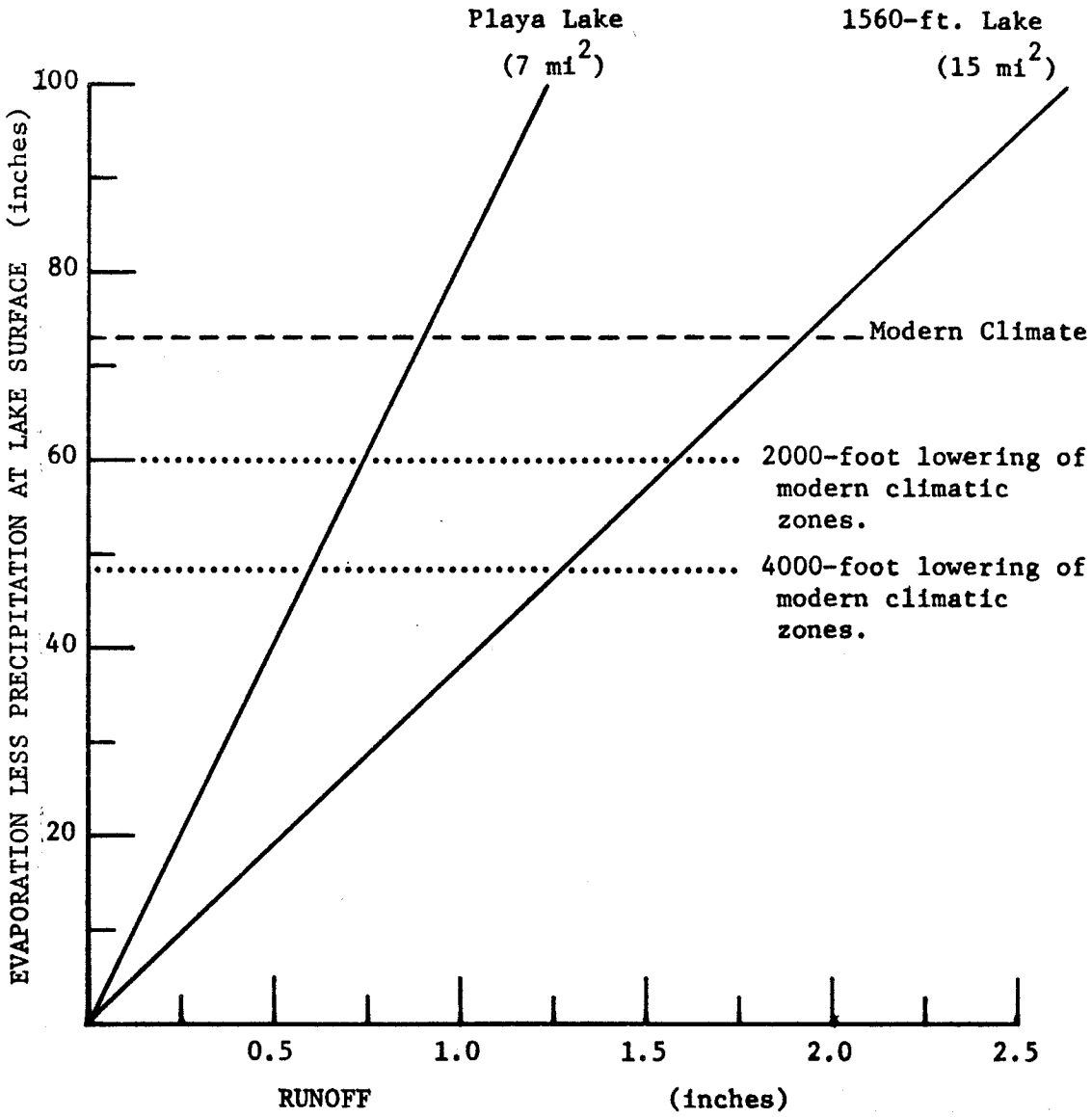

Figure 5-9. The relationship between evaporation and the runoff required to sustain shallow lakes in north Panamint Valley.

analyzing the paleohydrology of pluvial lake basins suggest runoff about one to two times that needed to support the shallow lake. These authors compared present values of the ratio (P/E) between mean basin precipitation (P) and evaporation (E) with their pluvial counterparts for three pluvial lakes in the western Great Basin (lakes Lahontan, Russell and Deep Springs). The calculated pluvial values of P/E (0.63-0.90) were 0.32 to 0.36 higher than present values (0.27-0.57). Modern evaporation at the median elevation (4850) of north Panamint basin is about 60 inches (fig. 5-7), and mean precipitation can be taken either as the Darwin value (4 in.) or the Wildrose value (7 in.,fig. 5-6). These yield modern respective P/E values of 0.07 and 0.12 and pluvial values of 0.39-0.48. Using their plot (fig. 5, p. 2391) of the relationship between P/E values and runoff/evaporation (R/E) values, pluvial R/E was 0.03 to 0.06 assuming no change in the modern seasonal distribution of precipitation. Using 40 inches as mean basin evaporation (from 4000 feet of climatic-zone depression, fig. 5-7), pluvial runoff was 1.2 to 2.4 inches from 16 to 20 inches of precipitation. The lower of the two figures is adequate to sustain the 1560-foot lake, and the higher figure will be taken as the maximum plausible pluvial runoff during the most intense pluvial climates (eg, Tahoe time). The latter runoff could sustain a lake of about thirty square miles in area, but covering only five per cent of the tributary drainage area.

Local Runoff to Southern Panamint Valley during Pluvial Times

Although the highest part of the Panamint Range drains into southern Panamint Valley, the 1030-square-mile watershed also drains large areas of low hills, so its median elevation is substantially lower than north Panamint's (3100 ft vs. 4850 ft). Consequently, the pluvial runoff values just determined for north Panamint Valley should represent upper limits on the pluvial runoff into south Panamint Valley. Assuming 4000 feet of lowering of climatic zones, gross evaporation from a lake in south Panamint would have been 58 inches (fig. 5-7) and precipitation seven inches (fig. 5-6), leaving net evaporation of 51 inches. Alternatively, if precipitation was 10 inches greater than present (three inches), net evaporation would have been 45 inches. The equilibrium lake sizes (A) for 0.6, 1.2 and 2.4 inches of runoff (R) are as follows:

R	A	Surface elev.
0.6	12.1-13.7 mi^2	1040
1.2	24.2-27.5	1055
2.4	48.5-54.9	1100

None of these hypothetical lakes is as large as the highest young, shallow lake in south Panamint Valley (1160 ft elev., 67 mi^2), suggesting that Sierra Nevada water overflowing from Searles Lake was partly to largely responsible for this highest stand of the shallow lake. The lakes fed solely by local runoff should thus have been largely confined to covering the playa surface to depths of less

than ten to 20 feet. Such lakes would have covered two to five per cent of the area of their tributary watershed.

The Dependence of Lake Panamint's Overflow on Sierra Nevada Runoff

The analysis of just presented of equilibrium lake sizes in north and south Panamint Valley indicates that, even during the most intense pluvial periods, local runoff could not sustain lakes covering more than about five per cent of the entire watershed's area (1601 mi^2). Overflow stands of Lake Panamint were much larger, covering about 300 square miles or about 19 per cent of the watershed. Such lake stands would have required 500,000 to 700,000 acre feet of water from sources outside the Panamint Valley watershed, presumably supplied by Sierra Nevada runoff overflowing from Searles Lake. If this supply were curtailed, the lake's surface elevation would have dropped 30 to 44 inches the first year and slightly less each succeeding year as its small equilibrium size was approached. Such sharp drops in level can easily explain the general absence of prominent shore features at levels other than overflow level.

Runoff into Owens Valley during Glacial Times

Before irrigation was practiced in Owens Valley and before Owens River was diverted into the Los Angeles Aqueduct, Owens Lake was a navigable body of water covering 100 to 110 square miles (Gale, 1915, 254-5). During 1906-1914, the lake's inflow averaged about 350,000 acre feet per year, balanced by 60.8 inches of annual

gross evaporation from the lake's surface (Lee, 1927, 1935). The lake's tributary watershed covers 2706 mi^2 (Snyder, Hardman & Zdenek, 1964) including the lake's area, so about 2.5 inches of runoff from the rest of the watershed (about 2600 mi^2) sustained the lake.

The tributary drainage to Owens Valley was probably larger than present during some parts of glacial time and smaller during other parts of glacial time (fig. 5-10). Lake Russell in Mono Basin overflowed into the east fork of Owens River via Adobe Valley during Tahoe time (Putnam, 1949, p. 1295-6; Lajoie, 1968, p. 184, 187-8). Lake Russell covered an area of 267 mi^2 in a basin of 794 mi^2; Lake Adobe covered 20 mi^2 in a basin of 326 mi^2 (Snyder, et al, 1964). Lake Adobe did not overflow during latest Wisconsin times: a rise in level (11,000 to 8,500 B.P.) followed a drier period of unspecified length (Batchelder, 1970). Long Valley Lake (Mayo, 1934) covered about 90 mi^2 of a 385 mi^2 basin (Snyder et al, 1964). Although it seems to have occupied a closed basin during part of Wisconsin time, it was breached, drained, dissected and integrated into Owens Valley drainage, probably during Tahoe time (Rinehart & Ross, 1957; Putnam, 1960, p. 247-9; 1962, p. 199; Cleveland, 1961; 1962, p. 14-15), or possibly during Tioga time (Mayo, 1934). The ensuing discussion of Owens Valley runoff during glacial times will ignore contributions from Mono Basin and Adobe Valley but will consider separately the effects of complete isolation of Long Valley versus complete integra- into Owens Valley.

Mean annual temperature in the Owens Valley watershed should be

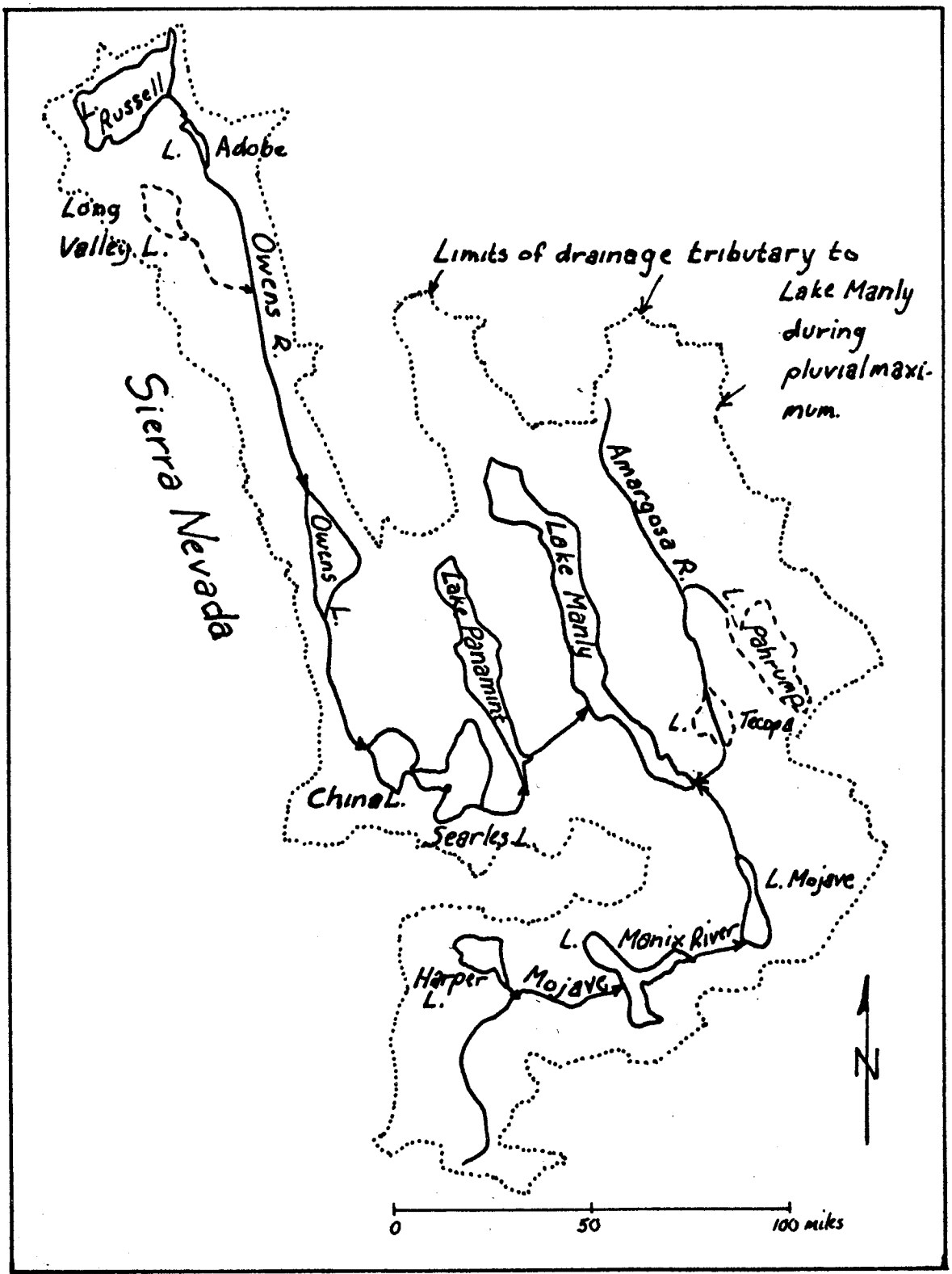

Figure 5-10 The pluvial-lake system which sumped in Death Valley (Modified from Snyder et al, 1964).

about 50°F, based on data reported by Bateman (1965, p. 8) and Rinehart and Ross (1965, p. 5) for the Sierra Nevada and by Kesseli and Beaty (1959, p. 14) for the White Mountains; this is roughly the temperature at the basin's median elevation (about 6,000 feet). Because most precipitation comes during the winter months, the weighted mean temperature (Langbein et al, 1949) should be somewhat lower. Mean basin precipitation is difficult to determine because precipitation increases sharply at higher elevations rather than steadily with elevation as in Panamint Valley (fig. 5-6). Using the curves of Langbein et al (1949, fig. 2) relating precipitation to runoff for various values of weighted mean temperature, 2.5 inches of basin runoff should correspond to 16 inches of precipitation for 40-degree mean temperature or to 20 inches of precipitation for 50-degree temperature. If glacial climates were 10°F cooler and ten inches per year wetter, Schumm's (1965) table 1 predicts five times greater runoff from a watershed whose weighted mean temperature is 50°F and whose annual precipitation is 20 inches; this would yield 12.5 inches of runoff from the Owens Valley watershed. The cooler (40°) climate would experience less runoff enhancement for the same precipitation, but this would be roughly cancelled out by greater runoff enhancement for the lower precipitation. Thus, 12.5 inches seems to represent a reasonable runoff value for glacial times in Owens Valley. A similar figure is reached using rough calculations by the Snyder and Langbein (1962) method.

This runoff appears to have been just about enough to sustain

overflow stands of Owens, Searles and Panamint lakes. Assuming that pluvial climates were ten inches wetter than modern and that the equilibrium size of Searles and Panamint Lakes was five per cent of their respective tributary areas, ten to 12 inches of total Owens Valley runoff was enough to sustain overflow of both lakes. The higher figure represents no contribution from Long Valley, whereas the lower figure represents complete draining of Long Valley Lake and integration of its drainage into Owens Valley. If the equilibrium size of Searles and Panamint Lakes was two per cent, the required runoff was 12 to 14 inches. If the pluvial precipitation increase was not ten but four inches (4000-ft-lowering of climatic zones), the required runoff ranged from 12 inches (5% equilibrium area, Long Valley runoff) to 16 inches (2% equilibrium area, no Long Valley runoff). These runoff values (10 to 16 inches) are in good accord with the predicted runoff from Owens Valley (12.5 inches) based on its modern climate and runoff. This suggests that runoff from the Sierra Nevada was marginally enough to sustain the overflow stands of Lake Panamint during the most intense glacial climates. As such, the record of the overflow stands of Lake Panamint should correspond on a one-for-one basis with the greatest advances of Sierra Nevada glaciers, which cannot all be distinguished in the Searles Lake record because of its nearly continuous overflow during glacial times.

Lake Manly not Sustained by Sierra Nevada Runoff

To sustain the deepest stand of Lake Manly (618 mi^2, Snyder et al, 1964) in addition to overflow conditions in Owens, Searles and

Panamint lakes, 18 to 30 inches of runoff from Owens Valley would have been required. This range in runoff encompasses the full variety of cases discussed in the previous section, but even the lowest value of required runoff is larger than any reasonable value of runoff from Owens Valley, but its companion figure (10 inches for Owens-Searles-Panamint alone) allows Owens Valley to provide about a third of Manly's required inflow. Unless runoff from Lake Russell's overflow stages was quite large, Lake Manly must have been fed primarily by water from the Amargosa and Mojave River systems.

CHAPTER 6

TECTONICS OF PANAMINT VALLEY

Summary of Shoreline Deformation

Vertical deformation in this region is characterized by differential north-south warping of the crustal blocks on both sides of the Ash Hill fault and the Panamint Valley fault zone, the vertical components of offsets on both of which vary considerably along their lengths (R.S.U. Smith, 1973, 1975). The prominent high shoreline of pluvial Lake Panamint, believed to have formed with respect to the basin's modern outlet elevation (1977 feet in Wingate Pass), provides a datum for measuring this deformation (figs. 6-1, 6-3). This once-horizontal shoreline of Gale-Stage age now exhibits structural relief of about 370 feet, from a low elevation of 1820±20 feet near the lake's north end to a high of 2190±20 feet on the central Panamint Range (fig. 6-3). Calculations indicate that less than five per cent of this warping could result from isostatic response to the drying up of Lake Panamint. The Wildrose segment has undergone local westward tilting (figs. 4-8, 4-9), but elsewhere north-south shoreline profiles (fig. 6-3) cannot record possible westward tilting.

Relative vertical displacements along the Ash Hill and Panamint Valley fault zones have generally been down to the west since Gale-Stage time (figs. 6-1, 6-2, 6-3). East-facing scarps are found mainly in zones of complex surface faulting, such as the Wildrose

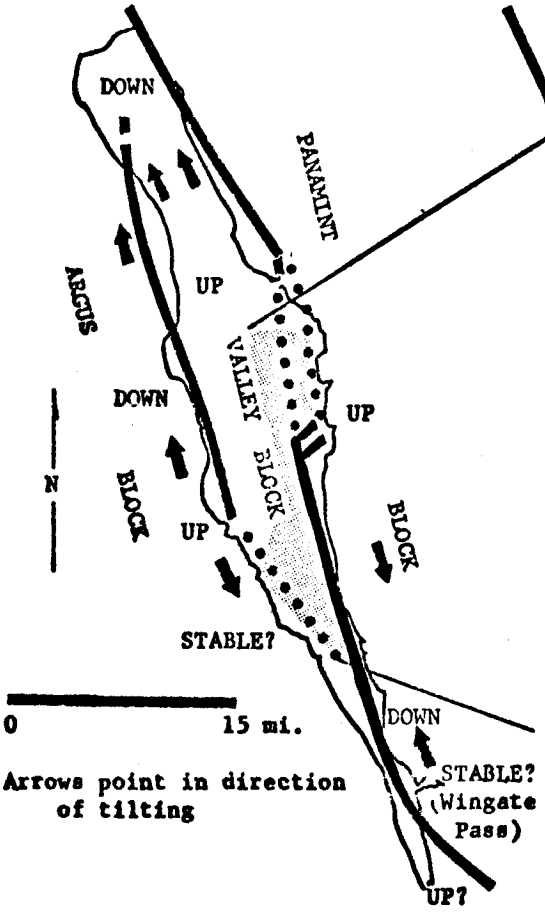

Figure 6-1. Map of high-shoreline deformation.

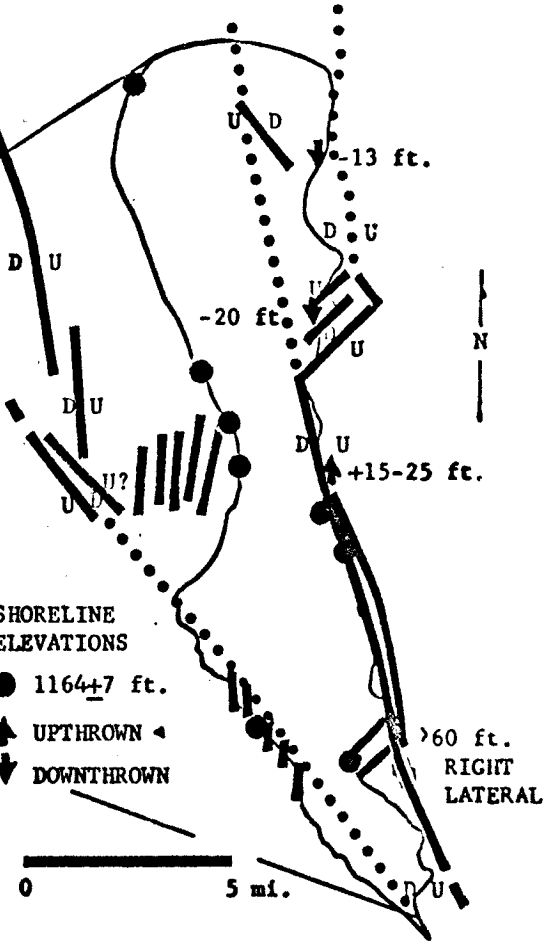

Figure 6-2. Map of low-shoreline deformation.

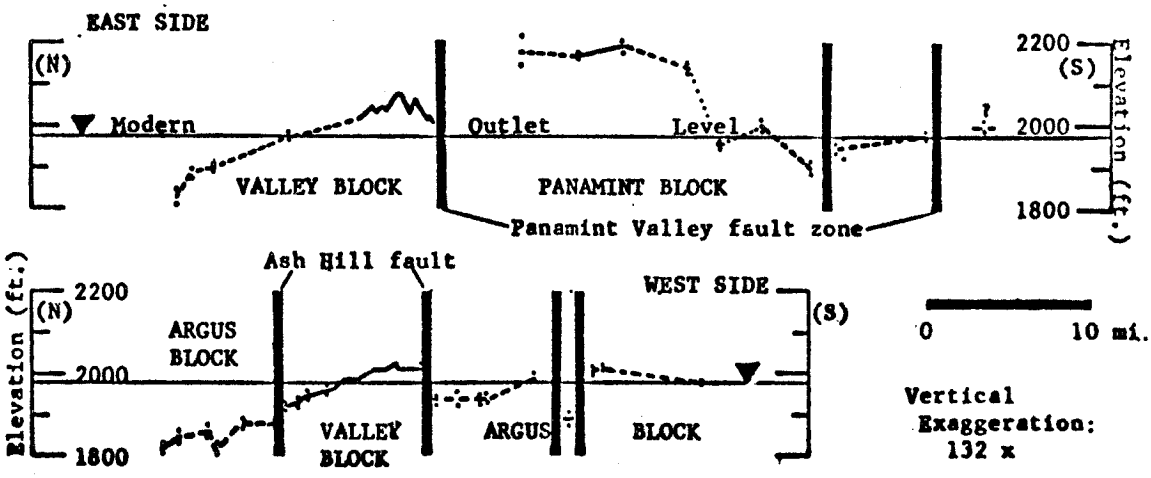

Figure 6-3. North-south profiles of high-shoreline deformation.

graben and the area immediately south of it, where east- and west-facing scarps are usually paired. Single, east-facing scarps are not found along the Ash Hill fault but are common along the Panamint Valley fault zone north of Highway 190, where they are attributed to right-lateral offset of elevated terrain (figs. 4-19, 4-21). No consistent sense of absolute offset characterizes either fault, although the Panamint block appears to have experienced absolute uplift along much of its western margin based on the assumption that the Wingate Pass sill level has been stable. Absolute downthrow has probably occurred along northeast-striking normal faults in the fault-bounded, northwest-facing Ballarat embayment in the front of the Panamint Range, based on the much-lower elevation here of the low shoreline, whose elevation is remarkably uniform at most other places (fig. 6-2). Faults here, and in several other range-front embayments, are en echelon to the trend of the Panamint Valley fault zone.

The Small Magnitude of Isostatic Deformation

Isostatic rebound caused by unloading of the crust following desiccation of Lake Panamint and neighboring lakes was very small compared to tectonic deformation of the shorelines. Calculations, using Crittenden's (1963a, b) criteria for the isostatic response of Lake Bonneville, show that differential rebound between the highest uplifted shorelines and Wingate Pass could not have exceeded six feet because isostasy compensates point loads over a large area

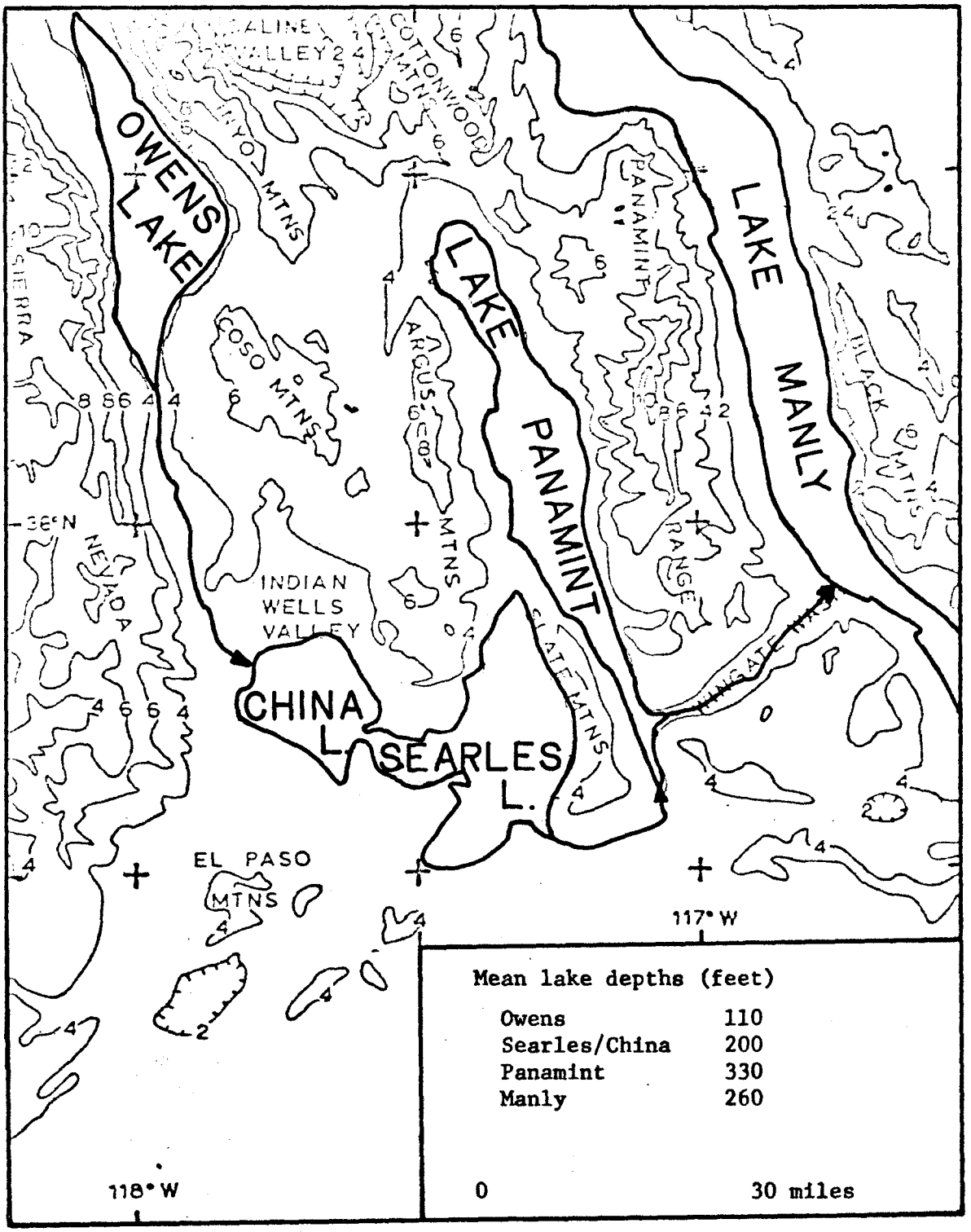

Figure 6-4. The Owens-Searles-Panamint-Manly pluvial lake system.

rather than locally. Thus, the isostatic component of deformation can be ignored because it is small compared to tectonic influences and is also smaller than uncertainties in actual shoreline elevation.

Isostatic crustal rebound following evaporation of a deep pluvial lake was first proposed by G.K. Gilbert (1890, p. 379-83) in his classic monograph on Lake Bonneville, Utah, as an explanation for the progressively higher elevation of both the Bonneville and Provo shorelines toward the center of the ancient lake basin. Crittenden (1963a, b) confirmed Gilbert's interpretation in a more thorough analysis using many new data on shoreline elevation. Isostatic rebound of the shorelines of Lake Lahontan, Nevada, has also been briefly noted by Mifflin and Wheat (1971).

Isostatic response to a group of intermontane lakes should be small because the area of the lakes is small compared with the area of the intervening, unflooded mountains and the water load of each lake can be treated as a point source. As stated by Crittenden (1963b, p. E17), "...because the shear strength of the crust is not zero, the point loads applied at the surface may be effectively distributed over an area materially larger than...25-mile radius..." Empirically he found that a pattern similar to the pattern of observed shoreline uplift could be generated by contouring mean water depth averaged over circles of 25- and 40-mile radius. By interpolation, he decided that circles of 35-mile radius should "...produce a reasonable match." (p. E17).

The method used to compute isostatic readjustment within the Owens-Searles-Panamint-Manly lake system (fig. 6-4), was as follows:

Within the area flooded by each lake, the modern surface elevation of the southwest corner of each section was determined by inspection to the nearest ten feet from U.S. Geological Survey 15-minute topographic quadrangles (contour interval 40 feet, locally 80 feet). When subtracted from the elevation of the modern basin lip, these elevations yielded representative depths of water for one-mile squares centered on each point (lip elevations used (feet): Owens: 3760; Searles: 2260; Panamint: 1977; Manly:300 (non-overflow; Blackwelder, 1933, p. 468; Hooke, 1972, p. 2088)). For ease of computation and conformity with township grids, water depth was averaged over squares 72 miles on a side rather than over the 70-mile-diameter circles suggested by Crittenden. Mean depths of the distributed water load, calculated for a series of squares whose centers are two miles apart along east-west profiles six miles apart, are contoured for the Panamint Valley area on Figure 6-5.

As seen on that figure, Panamint Valley lay within the zone of maximum average water depth because it occupies the approximate geographic center of the Owens-Manly system (fig. 6-4). Mean depths of the distributed water load ranged from 55 feet at the northwestern and southern limits of Lake Panamint to 85 feet on the lake's western shore, so the difference between the maximum and minimum depth of the distributed water load was only 30 feet over the length and breadth of Lake Panamint. The depth differential between any point and Wingate Pass was even less, about 20 feet. Assuming that the density of compensating mantle material was

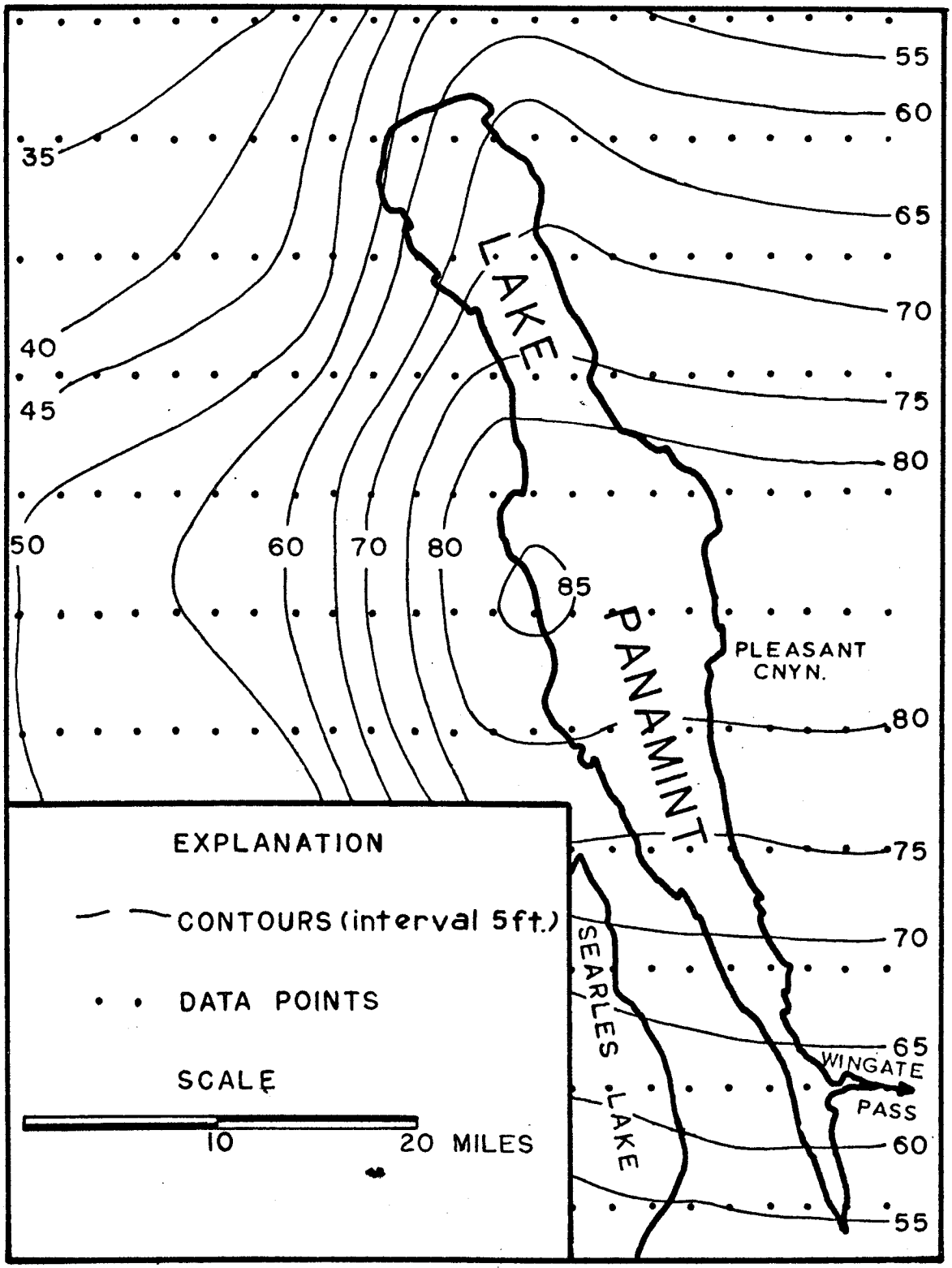

Figure 6-5. Map of Panamint Valley showing mean water depth of the Owens-China-Searles-Panamint-Manly lake system at pluvial maximum averaged over 72-mile squares centered on the shown data points.

about 3.4 and that the response to loading and unloading was instantaneous, the maximum amount of differential rebound amounts to about nine feet over the entire lake and about six feet between Wingate Pass and any other point on the lake's perimeter.

The calculated pattern of isostatic rebound resembles that of observed shoreline deformation (fig. 6-5) but is of much smaller magnitude. The structural relief of the isostatic rebound is about nine feet, but actual structural relief on the most prominent shoreline is about 370 feet. The difference between these two figures is a strong indication that the observed deformation of the lake's shorelines is almost wholly the result of tectonic processes rather than of isostatic origin. These influences probably act independently as suggested by Crittenden (1963b, p. E29) for the Wasatch Range. Because of this, the isostatic effect can be almost entirely ignored in calculating rates of vertical deformation for the high shorelines.

Tectonic Rates

The rate of horizontal movement along the Panamint Valley fault zone exceeds the rate of vertical movement by an unknown amount. Radiocarbon dates previously described indicate the fastest uplift rate of the Panamint Range to be less than 4.8 ± 0.5 feet per thousand years, near Pleasant Canyon, and the fastest downthrow rate to be less than 3.1 ± 0.5 feet per thousand years, at the north end of the Valley and Argus blocks. A minimum rate of right-lateral movement

of six feet per thousand years is indicated by the offset accumulated during part of the time since desiccation of the lake which cut the highest low shoreline in south Panamint Valley, which probably ended about 10,000 B.P. (fig. 2-30). Shoreline data indicate that the Argus Range has been downthrown relative to the Valley block at a rate of less than two feet per thousand years, and that north Panamint Valley has been tilted northward at a rate of less than 0.2 to 0.5 feet per mile per thousand years.

Have Uplift Rates Remained Uniform through Time?

If the rate of uplift of the Panamint Range has been uniform through time, then the ages of two or more uplifted, overflow-stage shorelines should be in the same proportion as their respective elevations above Wingate Pass[1], and the absolute age of each can be found if the absolute age of one is known. Radiometric dating of fault offset at three other California localities suggests uniform uplift rates, and two lines of evidence from within Panamint Valley also suggest uniform uplift rates.

The Sierra Nevada and elsewhere in California

Gilbert et al (1968, p. 310) and Curry (1971, p. 8, 10) noted that the rate of vertical tectonic movement in the Mammoth and Mono basins had remained remarkably constant during the last three million

---

[1] These elevations are above the lip (bedrock, 1930±15 feet) or alluvial (1977±1 feet) at which each lake stand was stabilized by overflow.

years at about one to two feet per thousand years. Clark (1972) questioned the extension of these rates to younger deformation, stating that: "...late Pleistocene and Holocene faulting has been quite irregular in both rate and position along the eastern base of the Sierra Nevada." Curry (1971, p. 38) used relative magnitude of fault offset to establish the proportional ages of Tahoe (25m offset) and Tenaya (15-20m) moraines, but found no offset of Tioga moraines; so the proportional age of the Tioga moraines cannot be established on the basis of its offset relative to Tahoe and Tenaya moraines. Elsewhere along the Sierra Nevada front, Clark (1972 and oral commun., Aug. 1972) has found some canyons whose offsets in Tioga and Tahoe moraines are in roughly the same proportion, but at least in two other canyons no offset of younger moraines is seen, despite large offset of a Mono Basin moraine in one canyon and of a Tahoe moraine in the other. Thus the late-Quaternary rate of faulting along the eastern front of the Sierra Nevada may only locally have been uniform despite the semblence of a uniform rate throughout Quaternary time.

The best California evidence for uniform uplift rates through fairly short time intervals comes from study of a branch of the San Jacinto fault in Borrego Valley. Here, Clark, Grantz and Rubin (1972, p. 120-1) postulated a constant rate of vertical movement along this right-lateral fault during the last 3000 years from radiocarbon dates on shells. At their calculated 200-years recurrence interval between M6-6.5 earthquakes, the 1.7 meters of observed uplift represented about 17 episodes of surface faulting.

In the Los Angeles basin, Bandy and Marincovich (1973) found that uplift of the Baldwin Hills along the right-lateral Newport-Inglewood fault zone has occurred at a rate of 5.7 to 5.9 meters per thousand years since about 28,000 B.P., and at five to eight meters per thousand years since about 36,000 B.P. These data permit, but do not require, that the Baldwin Hills have been uplifted at a constant rate for the last 36,000 years.

Panamint Valley

Throughout Panamint Valley, vertical tectonic deformation during Gale Stage was in remarkably constant proportion (0.26/1.00) to tectonic deformation since Gale Stage (fig. 6-6). This constant proportionality holds thre in areas of shoreline downwarp as well as in areas of shoreline uplift. It fails in only one area, where the later shoreline on the northern Wildrose block lies along the hinge line of monoclinal westward tilting of the earlier shoreline. The uniformity of deformation is best seen on a plot of the modern elevation of the earlier Gale-Stage shoreline (earliest G_1) as a function of the modern elevation of the later Gale-Stage shoreline (G_5). The line plotted by inspection on Figure 6-6 passes within the error limits of all elevation pairs except for the six Wildrose pairs (discussed above) which lie well to its right (see also fig. 4-9). The earlier Gale-Stage shoreline is attributed to a lake stand stabilized by overflow across the bedrock lip 47±16 feet below the modern level of Wingate Pass. The later Gale-Stage shoreline

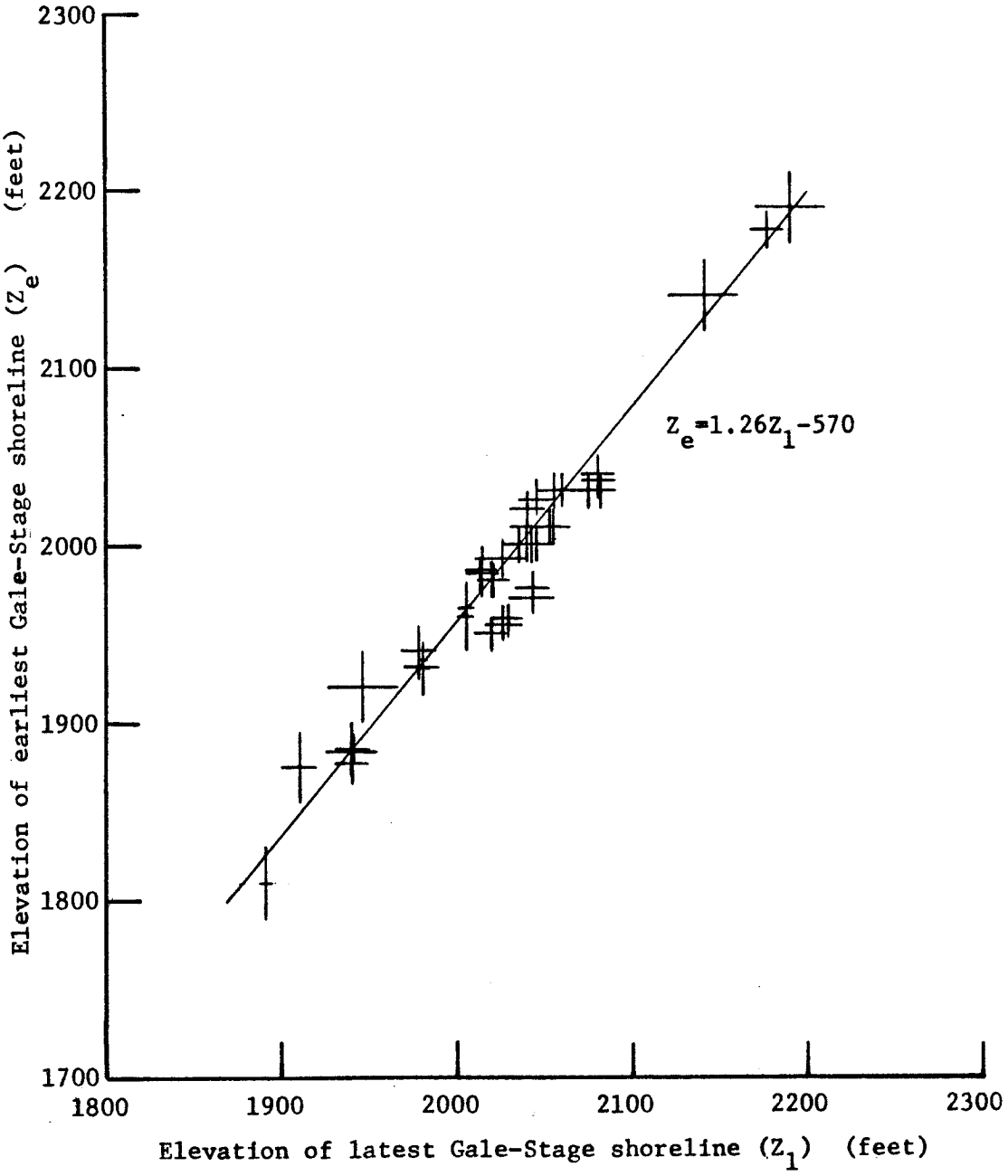

Figure 6-6. Elevation of earliest Gale-Stage shoreline as a function of elevation of latest Gale-Stage shoreline.

is attributed to a lake stand stabilized by overflow through the outlet channel in the modern pass. In downwarped areas, the later shoreline is more than 47 feet above the earlier one; in uplifted areas, the later shoreline is less than 47 feet above the earlier one. In the most uplifted part of the Panamint Range (Pleasant, South Park and Redlands canyons) the later shoreline appears to have been superposed onto the earlier one (fig. 3-30).

The uniform proportion between Gale-Stage and post-Gale-Stage vertical deformation, regardless of sense, style or magnitude of deformation, argues strongly for uniform rates of vertical deformation since the beginning of Gale-Stage time, and, by extrapolation, argues for uniform deformation rates since formation of the oldest recognized (E_1) shoreline. This allows use of uplift as a valid temporal scale for the pluvial chronology of Lake Panamint. The unlikely alternative explanation for the observed proportionality of deformation magnitudes requires that tectonic rates have increased or decreased synchronously and uniformly throughout the valley.

Other evidence for a constant rate of uplift comes from correlation of the uplifted shorelines at Pleasant Canyon with the ostracod zones recognized in core DH1,1a by Smith and Pratt (1957) (fig. 6-7). If the youngest unequivocal overflow shoreline (H_1) is normalized to the highest observed ostracod zone in the cores and the depth of these zones is plotted to scale with the uplifted shorelines, a remarkable similarity appears between the two patterns (fig. 6-7). These ostracod zones should reasonably represent deep lake stands,

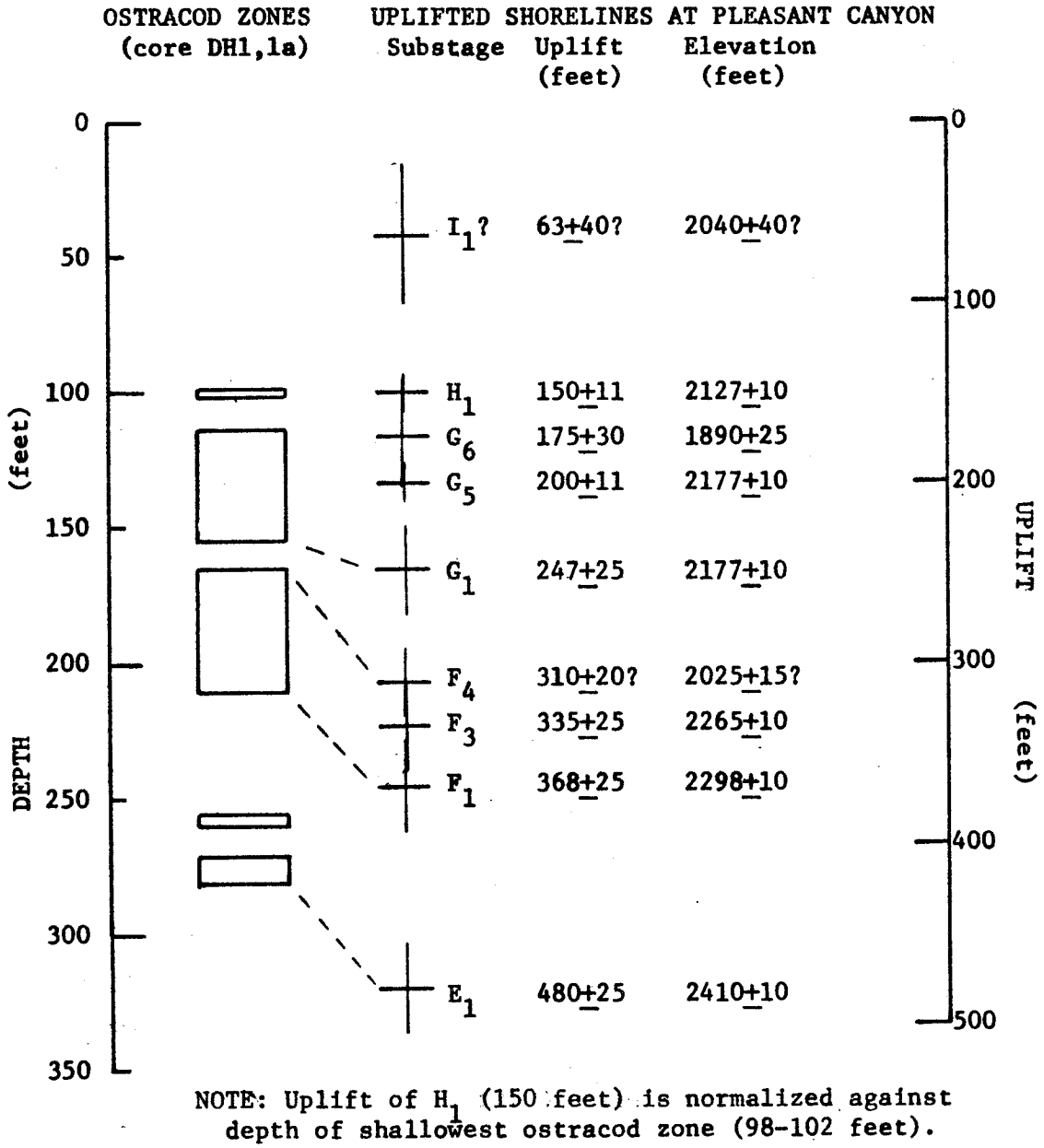

Figure 6-7. Comparison between the pattern of uplifted Pleasant Canyon shorelines and the pattern of ostracod zones in core DH1,1a as logged by Smith and Pratt (1957).

and each is succeeded by a fetid zone which suggests lake desiccation and eutrophication (fig. 3-29). It seems unlikely that the patterns of the ostracod zones and the uplifted shorelines would be so similar unless the lake-sediment depositional rate were constantly proportional to the uplift rate.

Hooke (1972, p. 2094-6) presents arguments from the history of fan segmentation and the record of pluvial Lake Manly in Death Valley, suggesting an exponentially-increasing rate of eastward tilting of the Panamint Range-Death Valley block. However, I believe that his arguments are not applicable to the western Panamint Range and Panamint Valley. Hooke's analysis assumes simple, planar, eastward tilting of the Panamint Range and ignores north-south tilting of the western range front. His assumed age of the highest (Gale-Stage) shoreline at South Park Canyon (his Blackwelder Stage, 10,000-11,000 B.P.) is much younger than H_1 deposits (>31,150±1400 B.P.) which overlie the youngest deposits attributed to the Gale-Stage shoreline at Pleasant Canyon. These relationships seemingly invalidate his solution of six equations in six unknowns to determine the exponent of uplift rate (exponent equals zero at uniform uplift rate).

Quaternary Right-Lateral Tectonics of Panamint Valley

The tectonics of Panamint Valley have been dominated by the Panamint Valley fault zone during much of Quaternary time. The north-south warping of shorelines, local east-west folding, thrust

faulting, en echelon normal faulting and large vertical fault movements can all be considered secondary manifestations of a regional right-lateral shear which has its primary manifestation in the observed right-lateral movement along the Panamint Valley fault zone. The modern trend of the fault zone is largely parallel to the trend of the Panamint Range and of the Tertiary dip-slip faults which blocked out the range. Toward the valley's north end, the fault zone either dies out against Hunter Mountain or bends sharply to the west along the zone of thrust faulting which marks Hunter Mountain's base. The probable continuation of this thrust zone bends to the northwest,and its dip steepens, as the divide between Panamint and Saline valleys is approached. Right-lateral movement here is suggested by stream offsets and by subhorizontal slickensides on the near-vertical, northwest-striking fault surface. The fault zone continues on to the northwest, where it appears to form the steep southern wall of Saline Valley (McAllister, 1956). It seems to end at the southwest corner of Saline Valley, where continuity of mapped geologic units (Ross, 1967) does not permit its continuation into the Inyo Range.

The segment of this fault zone extending from the northeast corner of Panamint Valley to the southwest corner of Saline Valley was interpreted as a scissors fault by McAllister (1956), but it may instead be a small intracontinental transform fault which formed as a consequence of differential extension between the two valleys and the mountains which bound Panamint Valley on its north end and

Saline Valley on its south end (fig. 6-8). The east side of Saline Valley had to move relatively eastward to allow the valley floor to drop; this movement was right lateral relative to the Nelson Range at its south end (Lombardi, 1964). Similarly, the west side of Panamint Valley, including the Darwin upland and the Nelson Range, had to move westward relative to Hunter Mountain in a right-lateral sense for northern Panamint Valley to open. Whether this transform(?) fault was parallel to the orientation of regional right-lateral shear is conjectural. If it were, both valleys could have formed in the "pull-apart" manner proposed by Burchfiel and Stewart (1966) for the origin of Death Valley and by Hamilton and Myers (1966, p. 532-3) for basins west of Death Valley. In this model, a northern right-lateral fault would have been paired with a right-lateral fault of similar trend at the valley's south end. In Panamint Valley, range-front grabens, striking in azimuth acutely clockwise relative to the trend of the Slate Range, suggest right-lateral shear along the northeast range margin, where no continuous fault trace can be found (fig. 6-6). Confirmation of right-lateral faulting along the front of the Slate Range would support the pull-apart hypothesis for the origin of Panamint Valley.

The azimuth of modern regional right-lateral shear trends more northerly than the northwest-bearing fault between Panamint and Saline valleys. Reorienting of this azimuth may have allowed right-lateral movement to be imposed onto older, north-trending normal faults of Tertiary age and normal faults along which the modern

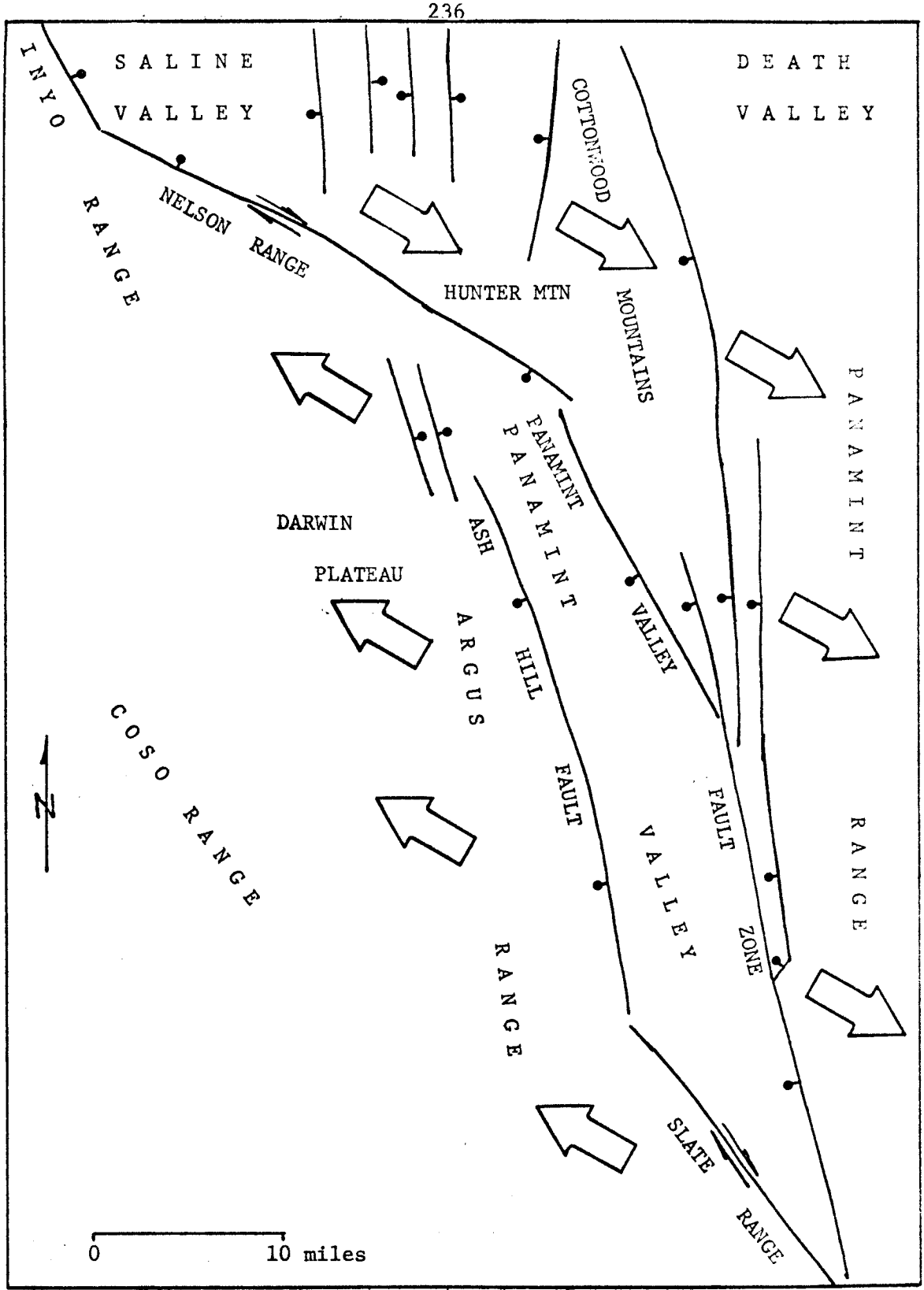

Figure 6-8. Diagrammatic map showing possible opening of Panamint Valley as a right lateral "pull-apart".

valley was blocked out at the initiation of transform (?) faulting. The modern trace of the Panamint Valley fault zone probably follows older normal faults of both ages, and its late-Quaternary offset rate allows a maximum likely offset of two to three miles to accumulate in 0.8 to 2.6 million years.

For right-lateral movement to continue along the northwest-trending transform (?) fault and to establish a new trace for the Panamint Valley fault zone along older, north- to north-northwest-trending normal faults, the sharp bend between these two trends in northeastern Panamint Valley had to be cut off, or northern Panamint Valley had to be thrust under Hunter Mountain in an amount similar to the right-lateral displacement (fig. 6-8). Observations suggest a combination of these two behaviors. The older zone of thrust faulting probably follows the deformed plane of the eastern part of the transform (?) fault, and large cumulative offset in the crystalline rocks is suggested by the 100-foot-thickness of the crush zone in the upper plate of the thrust fault (fig. 4-25). Panamint Valley's northeast corner has been cut off, as indicated by the inactive, dissected trace of the older thrust zone, and by the sparse distribution and degraded character of fault scarps in northeastern Panamint Valley. Most fault traces here have probably been buried beneath fanglomerate. Younger faulting probably migrated valleyward as the fault trace straightened itself, but as it did so, it was forced to abandon the old transform (?) zone of weakness which had localized the earlier thrust movement while being

deformed by it. The toe of an uplifted berm below the dissected trace of the older, inactive thrust zone may be the surface expression of another thrust fault which converges at depth with the old transform (?) fault. The abundant, irregular scarps which cut the old alluvium below this toe may be the surface expression of thrust faulting which was not localized by older zones of weakness.

The northward tilting of shorelines in northern Panamint Valley is consistent with a compression associated with the bending in the direction of right-lateral movement and with underthrusting of Panamint Valley beneath Hunter Mountain. The north-south warping of shorelines along the rest of Panamint Valley may indicate differing response of the three structural blocks to the right-lateral shear imposed on the area. Similar deformation along parallel right-lateral faults on the San Francisco peninsula, California, has been described by Lajoie, Weber and Tinsley (1972).

Right-lateral movement around a major bend of the Panamint Valley fault zone may have caused folding and uplift of fan deposits exposed within the bend near the divide between the north and south basins of Panamint Valley (fig. 6-8). North of here, the fault zone strikes N 35° W, but south of here it strikes N 15° W. Paradoxically, the trend of the Wildrose graben (N 20° W) is parallel to the strike of folds (N 15° W to N 30° W) in fan deposits which lie just three to five miles to the northwest. The graben lies within a major bend in the range front, but probably lies on the <u>outside</u> of the actual

bend in the Panamint Valley fault zone. Alluviation of the range front and the absence of fresh fault scarps along much of the range front for 15 miles south to Ballarat suggest that the active trace may lie one to three miles west of the range front. This trace is largely obscured beneath modern fan and playa deposits, but the northwest- and northeast-trending faults which bound the Ballarat embayment and other range-front embayments do not cross this trace to the west side of the Valley block. The Wildrose graben's west wall may well mark the active trace of the Panamint Valley fault zone, the graben itself having formed in response to extension along the outside of the bend.

Right-lateral shear may be responsible for zones of en echelon normal faulting at embayments in the front of the Panamint Range (fig. 6-2). Individual faults strike at acute angles clockwise from the trend of the Panamint Valley fault zone, which is consistent with extension related to right-lateral shear, and absolute downthrow at Ballarat confirms continuing extension oblique to the fault zone. Tension gashes similarly-oriented relative to the Ash Hill fault suggest that it has a component of right-lateral offset.

CHAPTER 7

PLUVIAL CHRONOLOGY AND CORRELATION

History of Lake Panamint

Bases for Reconstruction

The history of Lake Panamint is reconstructed from two types of records to which an implicit time scale can be assigned; a) the succession of shorelines and lake deposits at Pleasant Canyon, with a time scale based on shoreline uplift rates, and b) logs of cores from three holes drilled in Panamint Valley and logged by Smith and Pratt (1957) and Motts and Carpenter (1968), with a time scale based on estimated sedimentation rates. Two holes (DH1,1a and DH3) were drilled into south Panamint playa and one (NP-3) into north Panamint playa figs. 3-29, 4-23; app. B). The core and shoreline records were correlated by inspection, and plotted in scales adjusted to bring the high stands into alignment (fig. 7-1).

The composite record of fluctuations in the level of Lake Panamint plotted at the top of Figure 7-1 is based on the shoreline record and the three core records plotted below. The "time" scale of the composite record is in units of net shoreline uplift at Pleasant Canyon. Net uplift probably reflects age in years, but such ages are not shown on Figure 7-1 because uplift rates are not precisely known; estimated ages of lake stages are listed on Table 7-1. Uplift rates are prefered over lake-bottom sedimentation

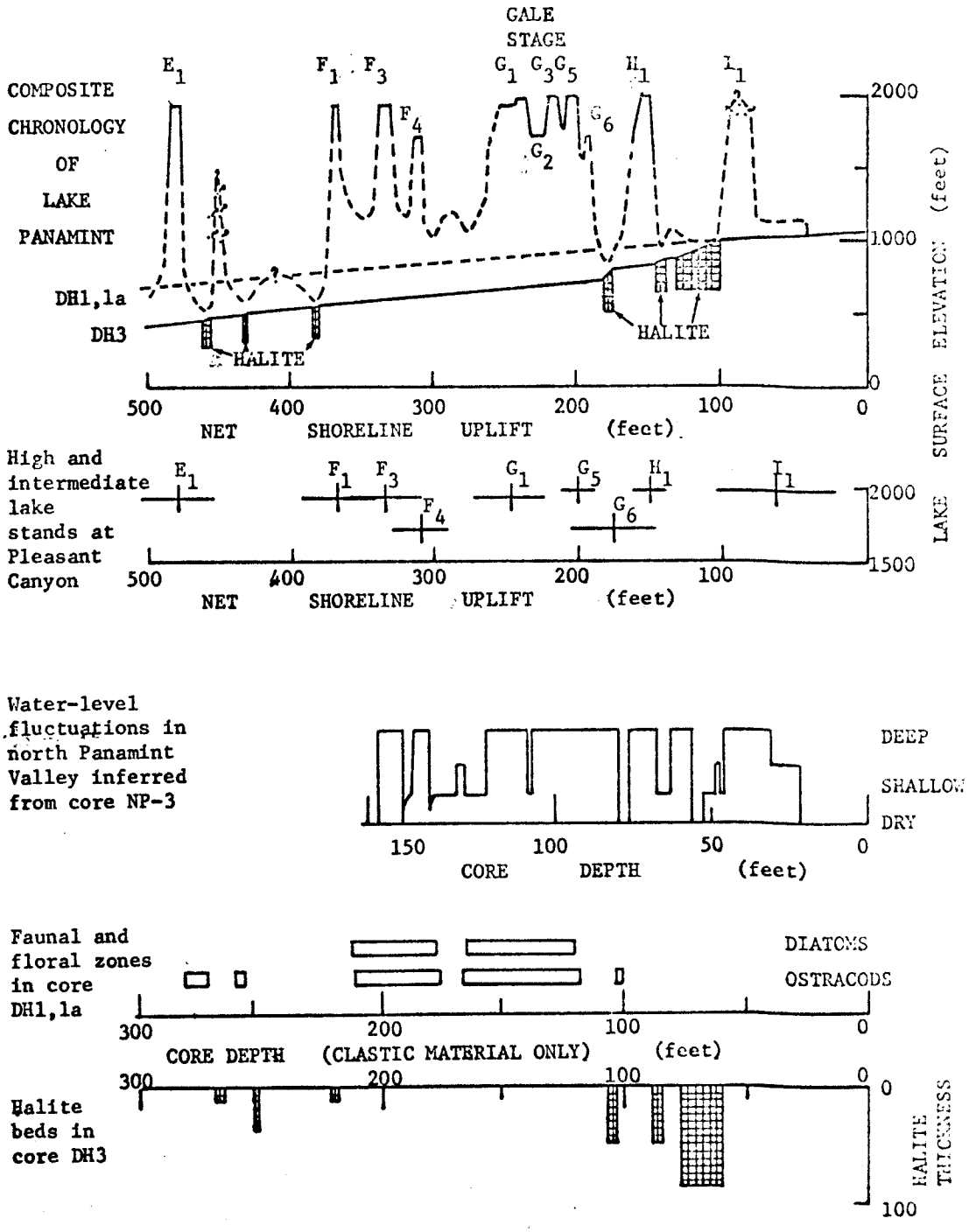

Figure 7-1. Construction of the composite pluvial chronology of lake Panamint (top) from high-shoreline and core records (below).

rates for constructing the "time" scale because uplifted shorelines provide a record of lake stands whose levels were controlled by overflow but such stands cannot be inferred from the core record.

In determining net uplift of high shorelines, the following assumptions are made: 1) High shorelines formed since G_1 time were cut by lakes stabilized at the level of the modern outlet channel through Wingate Pass (1977±1 feet); 2) High shorelines formed prior to G_1 time were cut by lakes stabilized at the level of the bedrock lip beneath Wingate Pass (1930±15 feet); 3) A mud-flow during early G_1 time blocked Wingate Pass, raising the outlet level to 1985±5 feet, and erosion during the rest of Gale-Stage time lowered the outlet to its present level (1977±1 feet); 4) Intermediate-level shorelines were formed by lakes stabilized at the level of the modern divide (1715±5 feet) between the south and north basins of Panamint Valley; and 5) Isostatic deformation can be ignored in calculating shoreline uplift. The error bars on the uplift of each lake substage shown on Figures 7-1 and 7-2 represent the sum of the uncertainties in each shoreline's modern elevation and in the level at which the shoreline formed.

The record of deep, overflowing lakes is determined mostly from the succession of shorelines and nearshore deposits at Pleasant Canyon, supplemented by similar information from elsewhere in Panamint Valley. Periods when the lake maintained moderately high levels, whether it overflowed or not, are determined largely from the published core logs. Ostracod and diatom zones in core DH1,1a

recognized by Smith and Pratt (1957) are correlated with periods of generally-high lake level as recorded at Pleasant Canyon (fig. 3-19). Varves and greenish, plastic clay in core NP-3 as logged by Motts and Carpenter (1968) are also similarly correlated (fig. 4-23). The relative temporal position of the last high stand (I_1) of Lake Panamint is based on the record from NP-3.

Dry or intermittently dry conditions in north Panamint Valley are inferred from oxidized yellowish and brownish sediments in the core from NP-3, presumably indicative of at least intermittent subaerial exposure. Intervals of greenish sand and/or gravel in the NP-3 core suggest periods of low lake level, shallow enough for wave action to transport coarse debris along the lake bottom. Intervals of yellowish and brownish sand were probably deposited subaerially. Conditions of rising water level in north Panamint Valley are suggested by intervals of sand and/or gravel grading upward into clay. Beds of sodium chloride logged in the core from DH3 in south Panamint Valley provide the principal evidence for desiccation and very low stands of Lake Panamint. As correlated, salt-rich layers in DH3 occupy positions between ostracod and diatom zones in DH1,1a, and arrangement consistent with high and low water stages.

Composite Lake History

Panamint Valley was occupied by deep lakes during four pluvial episodes deparated by periods of desiccation intense enough to cause

sodium chloride deposition (fig. 7-1). The first pluvial episode (E-Stage), although brief, was wet enough to cause Lake Panamint to overflow into Death Valley. Inspection of the DH1,1a and DH3 core logs suggests that two high E-Stage lake stands were separated by a short period of salt deposition, but only one E-Stage shoreline has been recognized. The succeeding interpluvial period (EF) was twice as long as the next-longest interpluvial (HI). The lowest water levels during the EF interpluvial probably occurred at its beginning and end, the only parts of this interpluvial marked by salt beds. The second pluvial episode (F and Gale stages) lasted four times longer than any other pluvial episode (E, H, I). The combined duration of overflowing lake stands was shorter during the first half (F Stage) than during the second half (Gale Stage) of the second pluvial episode, as judged by the greater prominence of the Gale-Stage shoreline and larger bulk of Gale-Stage deposits. The F-Stage lake probably spilled into Death Valley for short periods on two occasions, whereas the Gale-Stage lake probably overflowed during much of its duration. A period of low lake level separated F Stage from Gale Stage, as indicated by the absence of ostracods and diatoms from this interval on core DH1,1a, but complete desiccation did not occur, for salt is lacking in this interval in core DH3. A brief episode of salt deposition separated the end of Gale Stage from the beginning of H Stage, when Lake Panamint once again spilled briefly into Death Valley. H Stage was followed by a period of almost-continuous salt deposition, totalling 130 feet in

thickness in core DH3, excluding enclosed clastic material. This indicates more complete desiccation than during the two previous interpluvial periods (EF and GH), even though the EF interpluvial period was longer. The salt deposited during the HI interpluvial period was probably introduced into the lake mostly during F and Gale stages, but complete desiccation did not occur until the HI interpluvial period. The I-Stage lake may have overflowed briefly into Death Valley, but evidence for overflow is equivocal. Firm evidence does indicate that the lake rose at least to within 150 feet of overflow level. During much of I Stage, the lake's level was below 1560 feet in north Panamint Valley and below 1165 feet in south Panamint Valley. These or still lower levels were probably maintained until final desiccation of the lake.

Radiometric and Extrapolated Ages of Lake Stages

Youngest Possible Ages

The discernible record indicates that Panamint Valley filled to overflowing more than 80,000 years ago. This conclusion is based on extrapolation from radiocarbon dates showing minimum ages for deposits attributed to Gale Stage (G_1?,>50,000 B.P.) and to H Stage (H_1,>31,150±1400 B.P.). If youngest possible age is plotted as a linear function of shoreline uplift at Pleasant Canyon, then a line defined by the origin, H_1 and G_1 (fig. 7-2) defines the youngest possible age of other lake substages whose shoreline uplift is known. Two assumptions underlie Figure 7-2; 1) uplift rates have

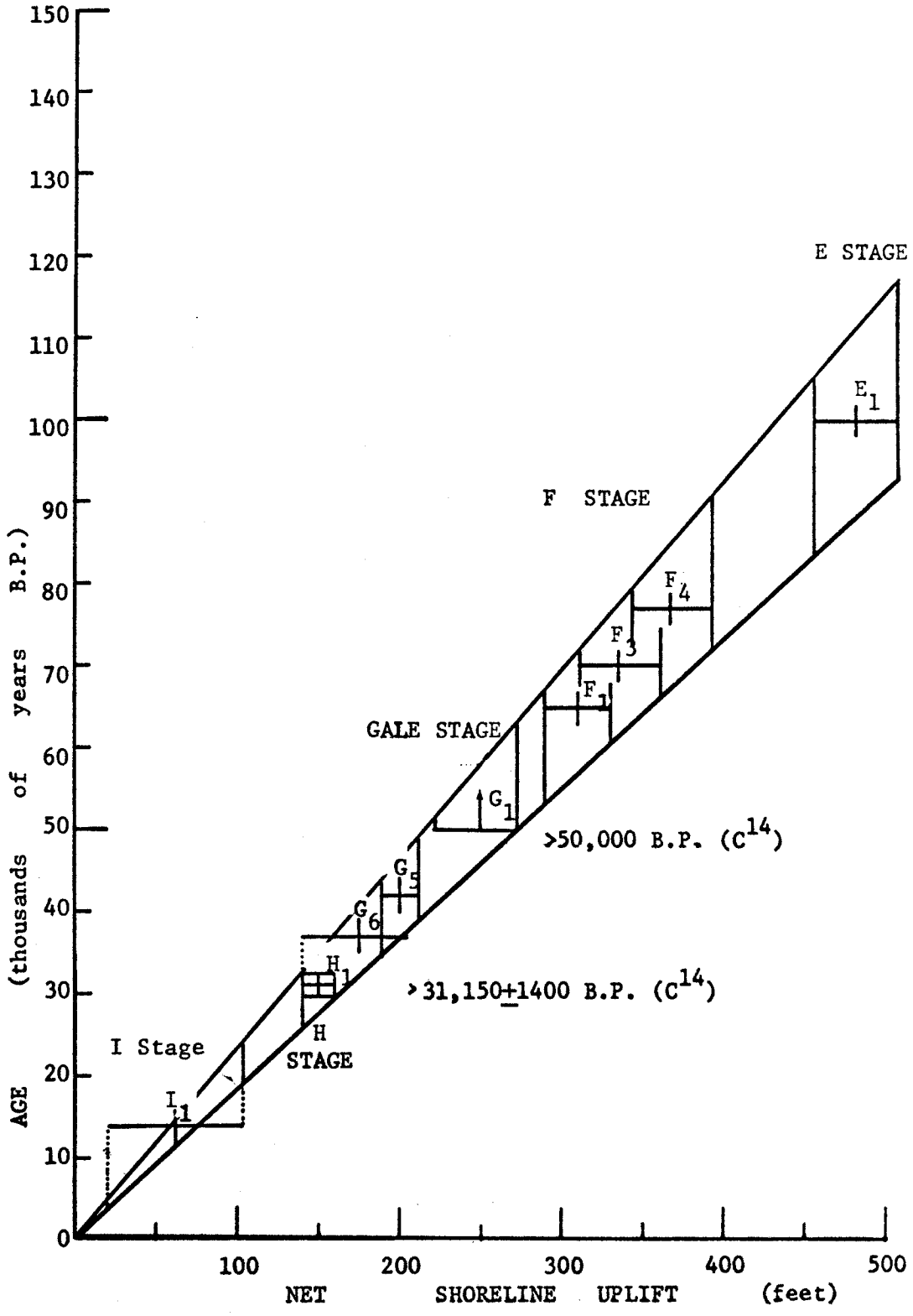

Figure 7-2. Youngest possible ages of lake stages.

been constant; and 2) of all carbonate materials, shells yield the most reliable radiocarbon dates. However, any carbonate date greater than 25,000 B.P. must be considered indicative of minimum age because young carbon has probably contaminated the sample (Thurber, 1972; app. A). Only one date (I-6543, 31,150±1400) is on shells collected by this author from deposits (H_1) in the Pleasant Canyon section. Three dates from the published literature (Hubbs et al, 1965, p. 93-6) are on snail shells from deposits in northern Panamint Valley attributed to Gale Stage (Tables 4-1, 4-2, 4-3). One of these dates LJ-985 (>45,000 B.P.) is from snails in marl which postdates the early G_1 substage on the northern Wildrose segment. Another date (LJ-973, >50,000 B.P.) is from snails in marl near the base of Gale-Stage deposits on the southern Big Four segment, and the third date (LJ-981, >50,000 B.P.), from the northern Big Four segment, is on snails from marl uncertainly attributed to Gale Stage.

These dates indicate that Gale Stage was initiated more than 50,000 years ago and that the mudflow which raised the level of Wingate Pass during G_1 substage occurred more than 45,000 years ago. The youngest possible ages of other lake stages, extrapolated from these dates, supercede the tentative ages reported earlier (R.S.U. Smith, 1972). These last were computed by shoreline uplift using a preliminary radiocarbon age of 30,000 to 40,000 B.P. provided by James Buckley of Teledyne Isotopes (oral communication, July, 1972) for the same sample of shells from H_1 substage which later yielded

the 31,150±1400-year age (I-6543). As shown by Table 7-1, the youngest possible age for each lake stage is substantially younger than its probable age.

Probable Ages

Lake Panamint probably filled to overflowing about 120,000 years ago (E Stage). This conclusion is reached by comparing the chronologies of Lake Panamint, based on constant rate of shoreline uplift, and Searles Lake, based on extrapolated sedimentation rates calibrated by radiocarbon dating (G.I. Smith, 1968). The results are presented in Figure 7-3, and the probable age and duration of each lake stage is listed on Table 7-1. Bases for this comparison will be discussed in the next section.

The episode of generally-interpluvial conditions between E and F stages probably lasted 25,000 to 30,000 years. The combined F and Gale stages lasted about 45,000 years until about 48,000 B.P., without any episode of desiccation intense enough for salt to be deposited on the lake bottom. Subsequently, the lake level rose at about 38,000 B.P. to overflow briefly into Death Valley (H Stage). Water levels were probably very low during the next 15,000 years when 130 feet of halite were deposited on the lake bottom. This interpluvial period was followed by the I-Stage pluvial, which lasted about 15,000 years. The lake was possibly deep enough only during the earliest part of this period to overflow into Death Valley. Lake levels were low during the rest of this interval, which ended

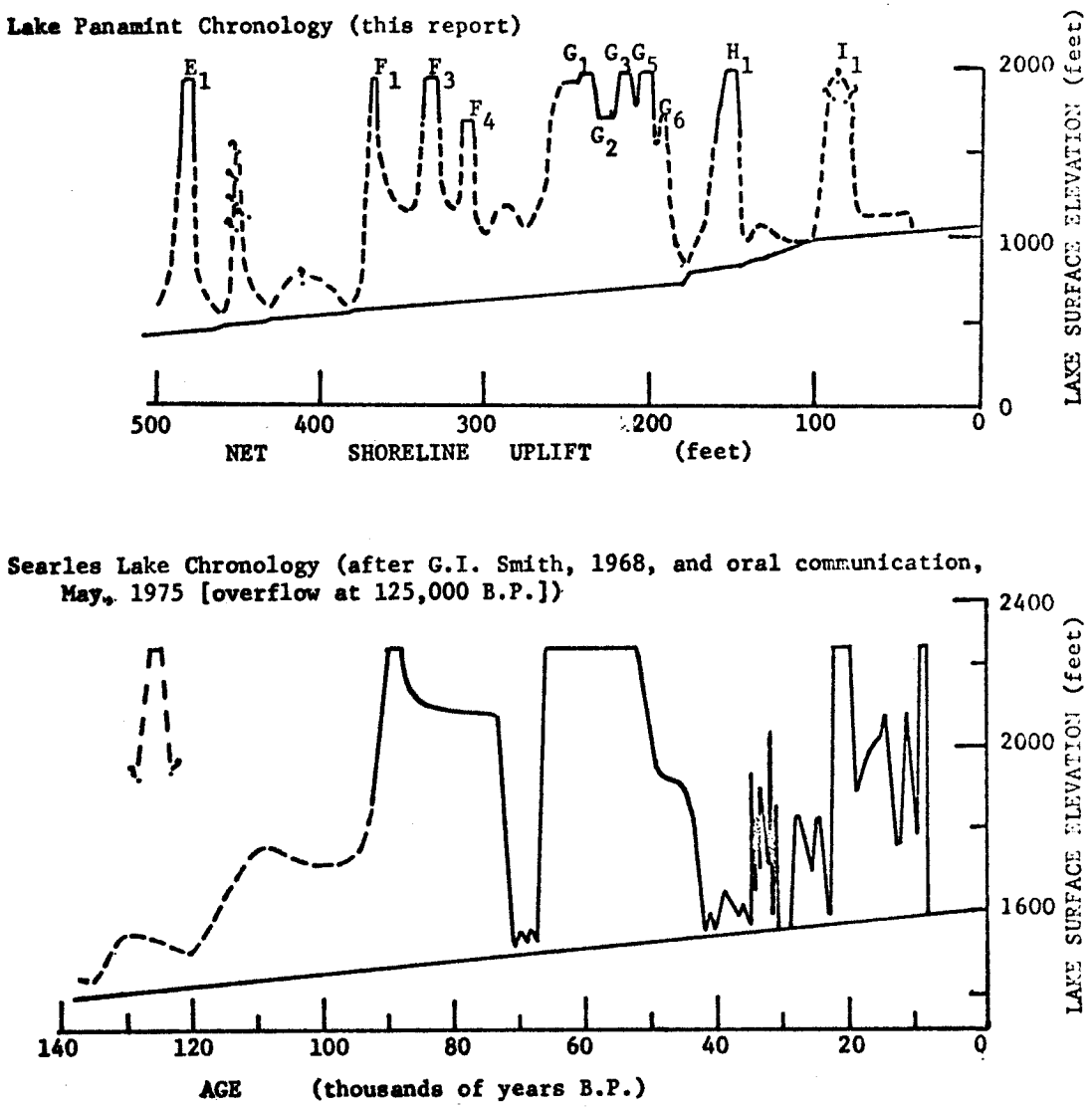

Figure 7-3. Correlation of the pluvial chronologies of Lake Panamint and Searles Lake.

Table 7-1

Youngest possible, and probable, ages of stages of Lake Panamint.

Stage	Youngest Possible Age (Years B.P.)	Probable Age (Years B.P.)	Probable Duration (Years)
I (?)	14,000±10,000 (?)	23,000±10,000 (?)	--
H	31,150±1400	38,000±6,000	--
Gale Stage			About 20,000
G_6	37,000±11,000	48,000±10,000	
G_5	42,000±7,000	52,000±10,000	
G_1	50,000 (C^{14})	65,000±13,000	
F Stage			About 15,000
F_4	65,000±12,000	78,000±15,000	
F_3	70,000±13,000	83,000±15,000	
F_1	77,000±14,000	92,000±15,000	
E	100,000±17,000	120,000±20,000	

NOTE: These ages apply to recognized high and intermediate lake stands defined by shorelines at Pleasant Canyon, except for I Stage. Because the shorelines were being cut as the range underwent uplift, erosion destroyed part of the evidence for the uplift. Thus age, calculated in uplift, is younger than it would be otherwise, and most ages are probably biased towards a younger age rather than greatest age. The age given for G_1 substage probably dates the youngest part of that substage prior to raising of the outlet level of Wingate Pass. The probable ages of G_1 and G_5 substages are consistent with the proportion (1.26) relating magnitude of G_1 deformation to magnitude of G_5 deformation throughout Panamint Valley (fig. 6-6).

about 10,000 B.P., as determined from the only radiocarbon dates on plant material collected from Panamint Valley (Berger and Libby, 1966; Table 4-4).

Comparison with other Pluvial-Lake Chronologies

Searles Lake

Since Lake Panamint overflowed only when overflow from Searles Lake supplied the necessary water, each high stand of Lake Panamint should synchronize with a high stand of Searles Lake. G.I. Smith (1968, and oral communications March and May, 1975) has constructed an absolute chronology for Searles Lake by means of exhaustive field mapping, examination of cores and nearly 100 radiocarbon dates on materials in cores and nearshore deposits.

Correlation of pluvial events in Panamint and Searles basins is based on the spacing, sequence and relative duration of periods of high and low water levels (fig. 7-3). Smith assigned ages within the older part of the Searles record by extrapolating sedimentation rates established in radiocarbon-dated part of cores. Recent refinement of these data inclines Smith (oral communications, March and May, 1975) to think that the base of the dated section approaches 150,000 years rather than the 130,000 years earlier calculated (Smith, 1968; fig. 7-3). Using the temporal spacing of Lake Panamint water-level stages derived from the assumed constant uplift rate, an empirical matching with the stages in Searles Lake is attempted (fig. 7-3). The match is good for four of the five recognized Lake Panamint

stages (E,F,G,I). Only H stage has no obvious counterpart in the Searles Lake record, as no Searles overflow during the period 52,000 to 24,000 B.P. has been recognized. Smith (oral communication, March, 1975) accepts the possibility that a brief, undetected overflow of Searles Lake may have occurred between 52,000 and 28,000 B.P., as his chronology for the interval, 43,000 to 33,000 B.P., was constructed entirely from the lake-bottom core record of the mineralogy of salts precipitated from lake water.

Smith (oral communication, May, 1975) now feels that an episode of overflow from Searles Lake occurred about 125,000 years ago. Interestingly, this episode was not shown in the chronology (G.I. Smith, 1968) used in establishing the correlations shown in Figure 7-3, but the temporal position of this early overflow corresponds well with the E Stage in Panamint Valley. This correspondence of early overflow episodes for both lakes strengthens the proposed correlation of pluvial events in the two basins. G.I. Smith (1968) earlier estimated that late-Pleistocene pluviation of the western Great Basin began at least 130,000 years ago, but an overflow at 125,000 years ago is not incompatible with his revised estimate that this pluviation began about 150,000 years ago. Pluvial conditions simply may not have become intense enough to cause Searles Lake overflow until 25,000 years after the onset of pluviation.

Lake Manly

Significant fluctuations in the level of pluvial Lake Manly in Death Valley should reflect episodes of overflow from Lake Panamint,

provided that a large proportion of Lake Manly's water was derived from this source. Water also flowed into Lake Manly from the Amargosa and Mojave river drainages. Blackwelder (1933) described and named Lake Manly and later (1941, 1954) suggested that lake depth was 600 feet during Tahoe time and 400 feet during Tioga time. He concluded that the Amargosa River provided most of Lake Manly's water because he found evidence for Tahoe overflow from Lake Panamint but not of Tioga overflow. Correlation of pluvial events with Sierra Nevada glaciations (later section, this chapter) supports Blackwelder's impression that Lake Panamint overflowed into Lake Manly during much of Tahoe time but only briefly (if at all) during Tioga time. Tahoe overflow of Lake Panamint may have provided enough additional water to increase the depth of Lake Manly by 200 feet. Paleohydrologic calculations (Chapter 5) suggest that overflow from Lake Panamint could never have provided a larger proportion of Lake Manly's water. In any case, Gale Stage, and maybe F Stage, of Lake Panamint probably correspond to the 600-foot stand of Lake Manly, and I Stage (and maybe H Stage) may correspond to the 400-foot stand.

Hooke (1972) proposed that the 600-foot stand of Lake Manly be named "Blackwelder Stage" and suggested an age of 10,000 to 11,000 B.P. from radiocarbon dates on disseminated organic material in shallow cores from the floor of Death Valley. Shoreline features of this stage were visited with Hooke during the earliest part of this study (March, 1970). These features are only locally preserved, and their

degree of degradation seems comparable to, if not greater than, that of Gale-Stage shoreline features in Panamint Valley. This suggests that Hooke's Blackwelder Stage may be five or six times older than he thought. Hooke's radiocarbon-dated material may possibly have come from deposits comparable to those formed by the shallow, and separate, lakes in north and south Panamint Valley about 10,000 years ago. A relationship between lake-floor sediments and shoreline features is not easily established and an extended sequence of deposits and features may be required, rather than single events.

Lakes Lahontan and Bonneville

Correlation of pluvial events in Panamint Valley with those in the Lahontan and Bonneville basins is tenuous and no specific correlation is proposed at this time. This difficulty stems from two sources; 1) discrepancies between the Lake Bonneville chronology determined from shorelines and nearshore deposits (Morrison, 1965b, p. 273-9; Morrison and Frye, 1965) and the chronology determined from core date (Eardley et al, 1973); and 2) uncertainties in the absolute age and duration of the Lahontan and Bonneville lake stages. Chronologies of these lakes are presented on Figure 7-4 along with the Lake Panamint chronology for purposes of comparison.

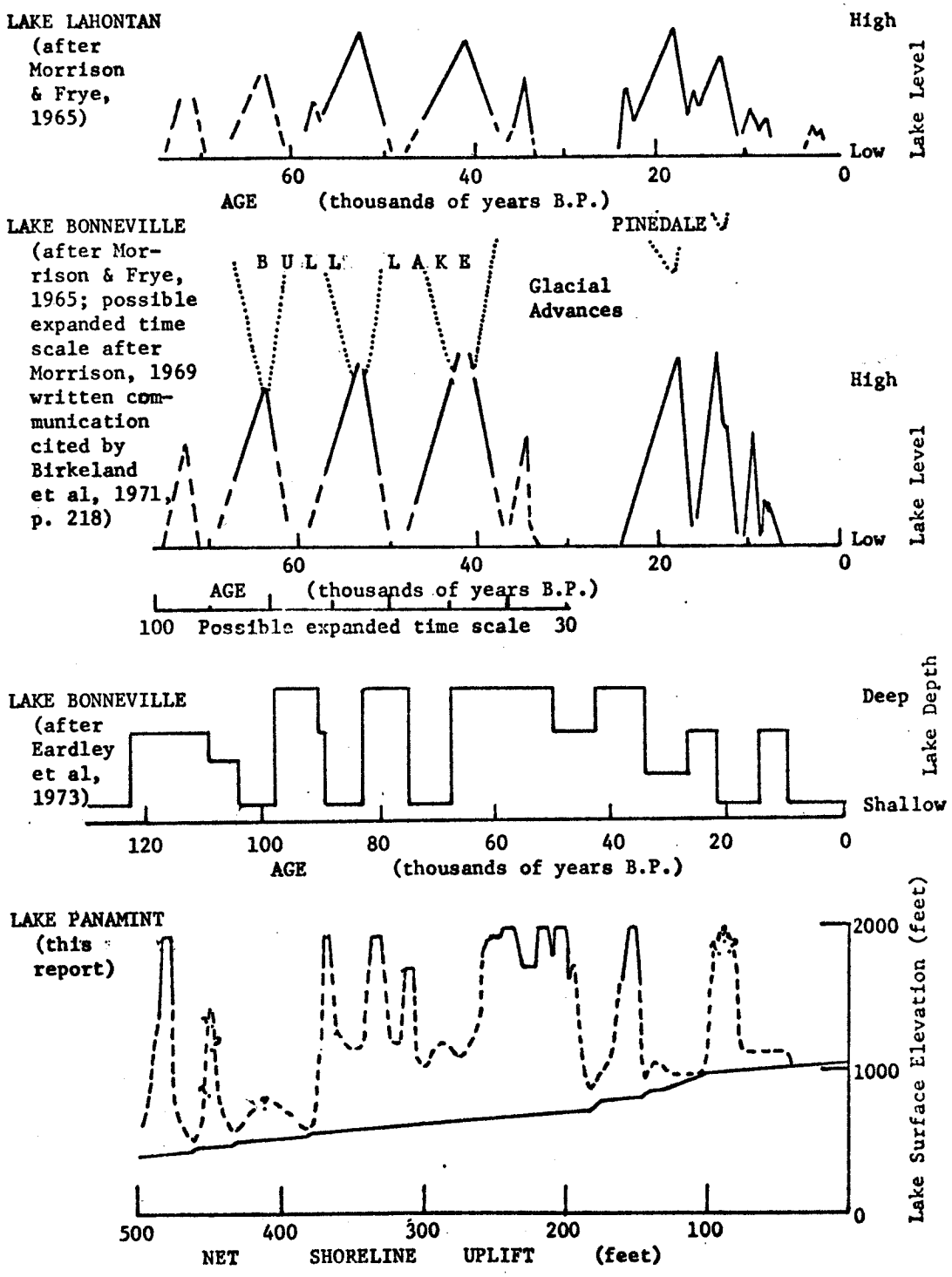

Figure 7-4. Comparison of pluvial chronologies of lakes Lahontan, Bonneville and Panamint.

Correlation with Sierra Nevada Glaciations

Introduction

Absolute dates for late-Pleistocene Sierra Nevada glaciations are essentially nonexistent. Dalrymple (1964) obtained Potassium-Argon dates of 90,000±90,000 and 60,000±50,000 from a basalt flow which underlies a Tahoe moraine in Sawmill Canyon south of Big Pine. Bailey et al (in press) reported Potassium-Argon dates of 126,000± 25,000 and 62,000±13,000 from basalt flows respectively underlying and overlying Curry's (1971) type Casa Diablo till near Mammoth. They correlated Casa Diablo till with Mono Basin till. Adam (1967) obtained a radiocarbon date of 9,990±800 on organic material above rock flour in a lake ponded by a Tioga terminal moraine south of Lake Tahoe. These ages clearly do not define very satisfactorily the ages of the Sierra Nevada glaciations.

Relative Duration of Glaciations

In his classic work defining glacial stages on the east side of the Sierra Nevada, Blackwelder (1931, p. 889) noted that "...moraines of the Tahoe stage are commonly so large and massive that they overshadow the rather diminutive moraines of the Tioga stage." In addition (p. 891), "The moraines of the Tahoe stage were much more extensive than those of the Tioga stage and they terminated at elevations averaging about 500 feet lower." Later authors subscribe to the general validity of these observations,

but Curry (1968, p. 36x) and Sharp (1969, p. 83-5) suggest that the unusual bulk of some Tahoe moraines possibly partly reflects large underlying bodies of earlier tills, such as the Mono Basin. At Bloody Canyon, Sharp and Birman's (1963) type locality for the Mono Basin glaciation, however, outermost parts of Tahoe laterals cannot be banked upon earlier moraines because the Tahoe glacier followed a path divergent from that of the earlier Mono Basin glacier. Even so, the bulk of the outermost Tahoe moraines far exceeds that of Tenaya or Tioga moraines (see Sharp and Birman's map, p. 1083).

The greater bulk of Tahoe compared to Tioga moraines indicates either 1) A longer period of deposition; 2) A faster rate of deposition; or 3) A greater volume of available debris produced by the preceding interglacial (or interstadial?) period. Since Mono Basin moraines seem to be no larger than Tahoe moraines and the weathering interval preceding the Mono Basin glaciation was probably as long if not longer than the pre-Tahoe interval, possibility (3) seems unlikely.

Among other things, rates of glacial erosion depend on ice thickness and flow velocity, which itself increases with ice thickness (Glen and Lewis, 1961; Paterson, 1969, p. 89-93; Flint, 1971, p. 113-4). The somewhat greater height of Tahoe lateral moraines than Tioga laterals on valley walls in the lower parts of canyons shows greater ice thickness there, but the crests of Tioga lateral moraines locally ascend farther upstream to meet Tahoe crests (Birman, 1964, p. 61), so Tahoe ice in the glaciers' source areas

was probably not substantially thicker than Tioga ice (Janda, 1966, p. 130). Nonetheless, the fact that the Tahoe glaciers extended farther out from the range front than the Tioga glaciers indicates a greater supply of ice, higher velocity perhaps, and more vigorous erosion, but probably not enough to account for the difference in morainal bulk, contrary to possibility (2). This elimination leaves possibility (1), that the greater bulk of Tahoe moraines reflects a considerably greater duration of the Tahoe glaciation than of the Tioga glaciation.

Birman (1964, p. 39) applied the name Tenaya to a set of small moraines nested within Tahoe laterals but beyond Tioga terminals. Tenaya moraines are characterized by a degree of dissection and weathering of surficial boulders intermediate between that found on Tioga and Tahoe moraines. Near the type area, Tenaya laterals truncate Tahoe laterals from other canyons (Birman, 1964, p. 40), and in Bridgeport Basin pass under a Tioga terminal "...with a distinct topographic unconformity." (Sharp and Birman, 1963, p. 1080). Tenaya deposits are not recognized in all glaciated canyons along the eastern Sierra Nevada escarpment (Birkeland, 1964, p. 824; Sharp, 1969, p. 88-90), but "Qualitative relations and semiquantitative data indicate that the Tenaya is a valid and distinct glaciation between Tahoe and Tioga, although the small moraines suggest that it was a relatively short-lived event." (Sharp, 1972, p. 2233). Presumably he means "short-lived" with respect to both Tioga and Tahoe, whose moraines are large by comparison. Thus Tenaya was

apparently substantially shorter in duration than Tioga, just as Tahoe was apparently substantially longer than Tioga, judging by the bulk of morainal material.

Tentative Correlation

Pluvial events in Panamint Valley are correlated with phases of Sierra Nevada glaciations on the basis of sequence and duration (R.S.U. Smith, 1972). Just as the bulk of a moraine reflects the duration of the glaciation which deposited it, the bulk of near-shore lake deposits should reflect the duration and stability of the water level along which they were deposited. Gale-Stage deposits at Pleasant Canyon have far greater bulk and broader distribution than deposits of any other lake stage, indicating that the total duration of high water stands during Gale Stage was greater than for any other lake stage and possibly greater than for all other lake stages combined. The dominating bulk of Gale-Stage deposits suggests correlation with bulky moraines of the Tahoe glaciation. The less-bulky H-Stage deposits, and their younger stratigraphic position than Gale-Stage deposits, suggest correlation with the smaller moraines of the Tenaya glaciation. No high lakeshore deposits attributable to I Stage have been identified in Panamint Valley, probably because the I-Stage lake overflowed only very briefly if at all. The reduced water supply for I Stage seems consistent with the reduced size of Tioga glaciers compared to Tahoe and Tenaya ice streams.

Pre-Tahoe glaciations cannot be correlated with pluvial stages on the basis of bulk of deposits. Mono Basin moraines are largely obscured by the overriding Tahoe moraines, and are clearly seen only where the Tahoe glaciers followed a different path than Mono Basin glaciers. The time required for a divergent valley to become sufficiently developed for a later glacier to follow it suggests that the interval between the Mono Basin and Tahoe glaciations was of significant duration. The longest interpluvial, by about two times, in the Lake Panamint record is between E and F stages, so possibly the E-Stage lake in Panamint Valley correlates with the Mono Basin glaciation. This would mean that high stands of the F-Stage lake are early Tahoe in age. The two or three high stands of the F-Stage lake suggest two or three distinctly separate glacial advances during this early Tahoe period, but moraines of these early advances were probably overriden by still more advanced later phases of the Tahoe glacier. The Tahoe glacier probably maintained its most advanced position for a large part of the late-Tahoe interval. This is surmised from the behavior of the Gale-Stage lake in Panamint Valley, whose level seemingly seldom dropped far below the sill into north Panamint Valley. The assumption implicit in the foregoing discussion is that rises in pluvial lakes are synchronous with glacial advances, as they appear to have been along the front of the Wasatch Range in Utah (Richmond, 1964, p. 35-7; Morrison, 1965a, p. 53-5, and 1965b, p. 276). Tentative correlation between pluvial and glacial events is shown on Table 7-2.

Table 7-2.

Tentative ages of late-Pleistocene Sierra Nevada glaciations compared with published ages.

Glacial Stage	Age (Thousands of years B.P.)			
	This Report (Equivilent lake stage in parentheses)	Curry[1] (1971)	G.I. Smith[2] (1968)	Others
Tioga	23±10 (I) [3]	about 20	10-24	
Tenaya	38±6 (H) [3]	about 45	24-28	
Tahoe	48±10-92±15(F,G)	60-75	33-70	90±90 [4] 60±50
(late)	48±10-65±13(G)			
(early)	78±15-92±15(F)			
Mono Basin	120±20 (E) [3]	about 130	75-130	62±13 [5] 126±25
				110-120 [6]

[1]Curry (1971, p. 8, 38) estimated these ages from the available radiometric dates, relative magnitude of fault offset on moraines of different ages, and possible correlation with deep-sea cores and radiocarbon-dated deposits of continental glaciations. He recognized (p. 38) that "Tahoe may represent cold pulses culminating about 65,000 years ago but possibly including advances of about 90,000 and about 110,000 B.P. also."

[2]G.I. Smith (1968) estimated these ages by correlation with the pluvial record of Searles Lake (fig. 7-3).

[3]Age of greatest glacial advance.

[4]Dalrymple, 1964.

[5]Bailey et al (in press). Based on correlation of Casa Diablo till with Mono Basin till.

[6]Richmond and Obradovich, 1972. Based on correlation of early Bull Lake till in Yellowstone National Park with Mono Basin till.

Tentative Ages of Glaciations

Because age limits of late-Pleistocene Sierra Nevada glaciations are not well defined by absolute dates on moraines and other deposits, recourse can be had to defining such limits from correlated phases of pluvial lakes, as attempted in Table 7-2. These correlations suggest that the first major late-Pleistocene glacial advance (Mono Basin) occurred about 120,000 years ago, and that the Tahoe glaciation lasted from about 92,000 to 48,000 years ago. These ages suggested from the pluvial stages of Lake Panamint agree fairly well with Curry's (1971, p. 8, 38) ages estimated from fault offset of moraines, except that they suggest a three-times-greater duration of the Tahoe glaciation (Table 7-2). The ages derived from the Panamint Valley chronology are not in agreement with glaciation ages suggested by G.I. Smith (1968) from the Searles Lake record, even though that record was used in calibrating the Lake Panamint chronology (Table 7-2). The differences involves the age of the Tenaya glaciation and correlation of the pluvial period extending from about 92,000 B.P. to about 78,000 B.P. I assign the Tenaya to a pluvial period (H) immediately following Tahoe, whereas G.I. Smith places the Tenaya close to the Tioga. Smith places the 78,000 to 92,000 B.P. pluvial in the Mono Basin, while I assign it to the Tahoe because of; 1) the great bulk of Tahoe moraines, and 2) the long interpluvial between E and F stages, which is correlated with the interglacial (or interstadial) between the Mono Basin and Tahoe glaciations. Smith recognizes no interpluvial period in the

Searles Lake record during this time.

Richmond and Obradovich (1972) suggested correlation between glacial stages in the Sierra Nevada and Yellowstone National Park, where glacial deposits are interbedded with volcanic rocks dated by Potassium-Argon methods. They correlated the Mono Basin till with early Bull Lake till (110,000 to 120,000 years old) and Tahoe till with late Bull Lake till, underlain by interglacial rhyolite (about 105,000 years old) and overlain by interglacial rhyolite (about 70,000 years old). Their suggested age for the Mono Basin glaciation accords well with my suggested age, and their Tahoe age is accordant with my early Tahoe phase. These ages for both the early Tahoe and Mono Basin glaciations fall within the upper (126,000$\pm$ 25,000) and lower (62,000$\pm$13,000) limits set by Bailey et al (in press) for the Potassium-Argon age of the Mono Basin glaciation (Table 7-2).

A growing body of evidence suggests that late-Pleistocene mountain glaciation in the western United States and the accompanying pluviation of the Great Basin began before 100,000 years ago, which is earlier than dates assigned the earliest Wisconsin midcontinental glaciation, variously set at 94,000 B.P. (Mörner, 1972) and about 70,000 B.P. (Dreimanis and Karrow, 1972). Mörner's age corresponds to my suggested age for the onset of the Tahoe glaciation. Perhaps the Mono Basin and early Bull Lake glaciations represent the effects of glacial climates restricted to the western United States or at least not felt in midcontinental regions. The alternatives are that

these glaciations are not Wisconsin at all, or that they were less extensive than later Wisconsin ice advances, hence overridden and not yet recognized in the midcontinent.

APPENDIX A

VALIDITY OF RADIOCARBON DATES ON CARBONATE MATERIALS

Radiocarbon age determinations on carbonate materials from pluvial lakes must be used with caution. Thurber (1972) provides the most recent and succinct summary of the two principal considerations affecting such dates; 1) contamination through incorporation of old "dead" (no C^{14}) carbon, and 2) contamination by introduction of young (high C^{14} activity) carbon after deposition. Contamination of shells by old carbon is greatest in pluvial lakes containing high concentrations of bicarbonate ion, and initial radiocarbon "ages" of 500 to 2200 years have been calculated for carbonate materials deposited in Lakes Lahontan and Bonneville and in Searles Lake, respectively (Broecker and Kaufman, 1965, p. 539, 554). Contamination by old carbon is considered a serious problem only for young materials, in which the initial "age" may be a large fraction of the measured radiocarbon age.

Contrawise contamination of carbonate materials by young carbon is a more serious problem in dating old materials. The radiocarbon "age" of a 40,000-year-old sample contaminated by one per cent modern carbon will be 32,000 years (8,000 years younger than actual), but the radiocarbon "age" of a 10,000-year-old sample contaminated by one per cent modern carbon will be 9,800 years, only 200 years younger than actual (Thurber, 1972, Table 1). Contamination by young carbon can occur before the sample is collected, during collection,

during storage, or during preparation for dating. Exchange of atmospheric or water-dissolved carbon dioxide with sample carbonate seems to occur rapidly on all exposed surfaces, which contain a significant percentage (1% to 3-5%) of the sample's total carbon (Thurber, 1972, p. 9; Stuiver, 1964, p. 384). The effect of such contamination is great enough so that Thurber (1972, p. 9) "...suggests that all ages of carbonate material over 25,000 years should be considered minimum ages unless careful studies show that the contamination is less than 1 per cent of the total carbon." Olsson (1968, p. 215) concurs with this injunction for shell dates older than 25,000 years.

A true radiocarbon age of >31,150 for H_1 deposits is derived by applying this injunction to the 31,150±1400 B.P. radiocarbon date (I-6543) on snail shells from H_1 deposits at Pleasant Canyon. The shells dated were all fresh-looking specimens of the genera Carnifex and Lymneae which retained pearly luster on interior surfaces. All shells were broken into large flakes so that their spires and all adhering dirt could be removed. These flakes were etched in dilute hydrochloric acid until their weight was diminished by half, then rinsed in distilled water and dried under an infrared lamp. The infrared absorbance spectrum of this shell material indicates that its composition was predominantly aragonite, not calcite which forms when exchange occurs. The procedure used may have been inadequate to prevent significant contamination by modern carbon. Thurber (1972, p. 9) suggests that acid etching is

"...perhaps not sufficient, especially for older samples, because the acid may not be able to reach a high percentage of the surfaces available to gas." Olsson (1968, p. 215; Olsson and Eriksson, 1965; Olsson et al, 1968) cautions against sample contamination by young carbon after acid etching both from exchange with modern carbon dioxide present in the atmosphere and dissolved in distilled water. These factors, plus ignorance about how the sample was treated after submission to Isotopes laboratory for dating, suggest that the 31,150 B.P. radiocarbon age for H_1 stage be regarded as a minimum age.

Radiocarbon dates in the published literature on materials from Lake Panamint should likewise be used with caution. Sampling procedures, and the condition, composition and treatment of samples, are unknown. Many samples are of tufa, which has yielded dates inconsistent with stratigraphic relationships in the Lahontan Basin (Morrison, 1965c; Morrison and Frye, 1965, p. 16-18) and in Searles Basin (G.I. Smith, oral communication, 1975).

APPENDIX B

PUBLISHED CORE LOGS USED IN THIS STUDY

South Panamint Valley

SP-1 (as logged by Motts and Carpenter, 1968; 83 feet deep).

Depth (feet)	Unit thickness (feet)	Description
3	3	Silt, clayey, dark yellowish brown 10YR4/2 to brown 10YR5/3, dry to slightly moist, with gypsum crystals at .5 feet.
13	10	Interbedded clay, silt and sand, brownish yellow 10YR6/6.
15	2	Silt, very dark grayish brown 10YR3/2, with some fine sand lens.
16	1	Silt, coarse grained, with abundant muscovite flakes.
		[No description logged for 16-23-ft. interval]
33	10	Silt, clayey, fine grained, light brown 5YR5/6, with blotches of medium light gray N6, slightly salty, sand lenses at 25 and 32 feet.
41	8	Alternating layers of clay and sand, pale blue 5B7/2 to grayish yellow green 5GY7/2.
43	2	Sand, silty, very fine grained, grayish yellow green 5GY7/2, grading into coarser sediment.
53	10	Silt, sandy, grayish olive 10Y4/2 to grayish olive green 5GY3/2, with black pebbles at 53 feet.
58	5	Silt, light olive gray 5Y5/2, with sand lens at 58 feet.
61	3	Clay, light olive gray 5Y5/2, with stringers of brownish gray 5YR4/1 and black N1.
64	3	Silt, sandy, light olive gray 5Y5/2 with coarse sand lens at 63 feet.
68	4	Interbedded clay and silt, dusty yellow green 5GY4/2, with sand lens at 65 feet.
73	5	Interbedded clay, silt and sand, grayish olive green 5GY3/2.
78	5	Clay, dusty yellow green 5GY5/2, with bands of black N2, silt lenses at 75 and 78 ft.

SP-1 (continued)

Depth (feet)	Unit thickness (feet)	Description
83	5	Silt, clayey to sandy, grayish olive green 5GY3/2, with black bands to 79 ft.

DH1,1a (as logged by Smith and Pratt (1957; DH1 surface to 450 ft., DH1a 450 to 500 feet; sixty per cent of core recovered.)

Depth (feet)	Unit thickness (feet)	Description
6.0	6.0	No core.
40.5	34.5	Silt, dusky-yellow (5Y6/4), very well sorted, calcareous. Apparent bedding defined by color changes.
50.8	10.3	Silt, clayey, to clay, grayish yellow (5Y8/4), well sorted, massive, calcareous.
55.0	4.2	Clay and some silt, yellowish-gray (5Y7/2) to pale-olive (10Y6/2).
59.0	4.0	Silt, clayey, yellowish-gray (5Y7/2) to dusky-yellow (5Y6/4); fine laminar bedding; calcareous; fine beds of gypsum interspersed.
64.0	5.0	Silt, clay, and a little gypsum* interbedded; color ranges from medium light gray (N6) to greenish gray (5GY6/1) to light greenish gray (5GY8/1). Gypsum is in thin beds.
65.0	1.0	Clay, silty; contains nodules of limestone; light greenish gray (5G8/1); massive.
71.0	6.0	Clay, silty; pockets of gypsum crystals; light greenish gray (5G8/1); thinly bedded; calcareous.
98.5	27.5	Clay and a little silt, light greenish-gray (5GY8/1), thinly laminated, calcareous. Thin silt and clay beds are very carbonaceous, core had strong odor of H_2S when fresh.
99.5	1.0	Clay and a little silt, greenish-gray (5GY8/1). Similar to unit above. Ostracodes, two species, observed in 98 to 101 ft interval.
105.0	5.5	Clay and a little silt, light greenish-gray (5GY8/1), thinly laminated, calcareous; very carbonaceous beds.
153.0	48.0	Clay and a very small amount of silt, light greenish-gray (5GY8/1) to (5G8/1). Carbonaceous bedding lines, laminar, in top 20 ft; bedding is less pronounced and thicker (maximum about 1 in.) in lower part. Ostracodes observed from about 112 ft to bottom of unit; diatoms in some zones; chara at 150 ft.
155.0	2.0	Silt and a little fine sand; greenish gray (5GY6/1) to light greenish gray (5GY8/1) in lower part; massive; very calcareous. Ostracodes.
165.0	10.0	Clayey silt and silty clay, light greenish-gray (5GY8/1); no distinct bedding planes except near top where the bedding is thin; calcareous.
185.0	20.0	Clay and silty clay, greenish-gray (5GY6/1), thinly bedded, calcareous; slightly carbonaceous. Diatoms and ostracodes visible.

DH1,1a (continued)

Depth (feet)	Unit thickness (feet)	Description
210.0	25.0	Clay and silty clay, light greenish-gray (5GY8/1), massive, calcareous; salty. Contains ostracodes and diatoms.
210.5	.5	Gypsum* crystal aggregate, yellowish-gray (5Y8/1).
228.8	18.3	Silt and clay; color ranges from yellowish gray (5Y8/1) to light greenish gray (5G8/1); massive; calcareous. Gypsum crystals diminish downward from 2 to 0 percent of the material. One inch of very fine sand at 227.3 ft.
230.0	1.2	Sand, very fine, and silt; light olive gray (5Y6/1); massive; calcareous.
246.6	16.6	Silt and clay, yellowish-gray (5Y7/2), massive, calcareous.
255.0	8.4	Clay and silty clay, light greenish-gray (5GY8/1), fine laminations, calcareous; carbonaceous.
259.5	4.5	Silt, yellowish-gray (5Y7/2), massive, calcareous. Visible ostracodes.
269.0	9.5	Silt, with much clay, very light gray (N8), thinly bedded. At 259.9 ft there were laminae of bassanite*, calcite*, and gypsum*.
270.0	1.0	Sand, very fine, to silt, yellowish gray (5Y7/2), laminar bedding.
280.0	10.0	Silt to clay, yellowish-gray (5Y7/2); massive except for bottom 3 in. which are laminar; very calcareous. Ostracodes abundant.
287.6	7.6	Silt, moderate grayish-yellow (5Y7/4), massive, calcareous.
310.0	22.4	Silt; greenish gray (5GY6/1) in upper part grading to light olive gray (5Y6/1) in lower part; calcareous; gypsiferous, locally as much as 15 percent but overall average is 2 percent.
315.0	5.0	Silt, greenish-gray (5GY6/1), massive, slightly mottled; calcareous; carbonaceous(?).
339.8	24.8	Silt, dusky-yellow (5Y6/4), massive, calcareous.
350.0	10.2	Sand, medium, to clay; average is fine sand; very light gray (N8) to light greenish gray (5GY8/1); massive; bottom 2 in. finer grained; calcareous in silt and clay zones.
358.0	8.0	Silt, moderate grayish-yellow (5Y7/4), massive, calcareous.
360.0	2.0	Silt to fine sand, light-gray (N7). Bedding laminar to 1 in.; irregular pods (10 percent of total volume) of pure fine-grained calcite.
370.0	10.0	Silt to fine sand, greenish-gray (5GY6/1), massive. Up to 5 percent calcite in upper part diminishing downward. Bottom foot is conglomeratic; pebbles, up to 1 in. in size of metamorphic rocks.
378.4	8.4	Silt, yellowish-gray (5Y7/2), massive, calcareous.
386.0	7.6	Silt to fine sand; light olive gray (5Y6/1) grading to white (N9) in highly calcareous zones, massive. At 380 ft there is a pebble of subangular metamorphic rock 1 in. in diameter; may be from zone above.
408.0	22.0	Silt, a little clay, light olive-gray (5Y6/1), massive, calcareous.
417.0	9.0	Clay, silty, to silt; pale olive (10Y6/2); massive; calcareous.
418.7	1.7	Clay, silty; mottled colors averaging greenish gray (5GY6/1); calcareous.
420.0	1.3	Clay, silty; pods of limestone; light greenish gray (5GY8/1); fine laminar bedding.

DH1,1a (continued)

Depth (feet)	Unit thickness (feet)	Description
430.0	10.0	Silt to fine sand, light greenish-gray (5GY8/1), massive, calcareous.
440.0	10.0	Carbonate, silty, white (N9) to light greenish-gray (5GY8/1), massive.
442.0	2.0	Silt to very fine sand; light greenish gray (5GY8/1) to greenish gray (5GY6/1) in mottled patterns; massive; pods of carbonate.
450.0	8.0	Silt, pale-olive (10Y6/2), calcareous, massive. (End of Panamint drill hole 1.)
470.0	20.0	Silt and a little clay, grayish-yellow (5Y8/4), generally massive, calcareous.
471.0	1.0	Silt and a little clay, yellowish-gray (5Y7/2), with pods of white (N9) limestone; massive.
494.7	23.7	Silt and a little clay, grayish-yellow (5Y8/4), generally massive, calcareous.
495.0	.3	Silt and a little clay, yellowish gray (5Y7/2), and few pods of white (N9) limestone.
500.0	5.0	Silt and a little clay, grayish-yellow (5Y8/4), massive, calcareous.

DH3 (as logged by Smith and Pratt, 1957; 995 feet deep; 47 per cent of core recovered.)

Depth (feet)	Unit thickness (feet)	Description
40.0	40.0	Silt, clayey; pale orange (10YR8/4) average color, but varies locally to medium yellowish brown (10YR5/4) forming variegated pattern; massive. Angular fragments of mica, hornblende(?). Calcareous.
50.0	10.0	Clay, silty; moderate brown (5YR3/4) to dark yellowish-brown (10YR4/2), massive. Fragments of iron oxide; about 1 percent gypsum at 50.0 ft. Calcareous. Bottom 2 ft has many angular fragments (up to 10 mm in diameter) of light grayish orange (10YR8/4) clay and fine sand.
59.7	9.7	Calcium carbonate, silty; pale greenish yellow (10Y8/2) to white (N9) forming variegated color pattern; massive.
60.0	0.3	Silt and halite, calcareous*, grading down to halite; pale olive (10Y6/2) to colorless. Crystals in upper part are euhedral; in lower part form solid mass.
69.0	9.0	Silt, grayish-orange (10YR7/4), massive. Crystals of halite dispersed through silt; also blebs of greenish clay up to 2 mm wide. Poor core.
70.0	1.0	Clay, grayish-yellow green (5GY7/2), massive. Euhedral crystals of halite (up to 10 percent of core) throughout. Calcareous.
80.0	10.0	Halite, with about 40 percent silt to very fine sand; grayish yellow green (5GY7/2). Local laminar bedding. Halite is both euhedral and fragmentary. Thin bed of gypsum* and halite* at 78.0 ft; pure halite between 79.0 and 79.5 ft.

DH3 (continued)

Depth (feet)	Unit thickness (feet)	Description
90.0	10.0	Halite and silt, grayish-orange (10YR7/4). Core is about 60 percent halite; a little gypsum; calcareous. Poor core.
159.0	69.0	Halite, generally colorless, but some included silt gives yellowish or grayish coloring; massive. Thin interbeds of silt at 105.0 ft (0.2 ft thick), 124.0 ft (0.3 ft thick), and 133.0 ft (0.2 ft thick). A little gypsum* and calcite*. Core from 135.0 to 159.0 ft is missing; drilling characteristics suggest same material as 90.0 to 135.0 ft interval.
160.0	1.0	Silt, pale-orange (10YR8/4), massive. Halite crystals form about 1 percent of core. Calcareous.
164.5	4.5	Clay, silty, to clay. Average color is yellowish gray (5Y7/2) with patches that are more orange or green thus giving an overall mottled effect. Poor laminar bedding in upper part, excellent laminar bedding in lower part. Halite crystals form about 5 percent of total. Solid beds of halite at 162.0 ft (0.3 ft thick) and 162.9 ft (0.2 ft thick).
173.5	9.0	Halite*, colorless. Bedding, if any, destroyed by drilling. Crystals are encased in yellowish-gray (5Y7/2) clay. Halite probably formed about 90 percent of unit. A little calcite* and gypsum*.
174.0	.5	Clay and silty clay, yellowish-gray (5Y7/2); laminar bedding. Halite crystals make up about 5 percent of core.
205.0	31.0	Halite, colorless. Bedding, if any, destroyed by drilling. Crystals encased in clay.
224.4	19.4	Clay, silty, yellowish-gray (5Y7/2), massive. Beds of solid halite* at 211.5 to 212.5 ft, 214.5 to 215.0 ft, and 220.5 to 221.5 ft; a little calcite* and gypsum*.
265.0	40.6	Halite*; generally colorless or tinted gray or tan by included clay; massive(?). A little gypsum and calcite. This section cored very poorly and the resulting "core" consists of wafers of halite and piles of broken halite crystals.
273.5	8.5	Clay, silty, to clay; pale greenish yellow (10Y8/2) to yellowish gray (5Y7/2); massive. Contains small amounts of halite and gypsum; calcareous.
275.0	1.5	Clay, a little silt and sand; yellowish gray (5Y7/2) with mottled patches of darker material; massive. Calcareous.
330.0	55.0	Clay, a little silt, a very little fine sand. Color ranges between yellowish gray (5Y7/2) and grayish yellow (5Y7/4); local lenses of pale olive (10Y6/2). From 275.0 to 298.0 ft the color emphasizes the beds (the coarser sediments are greener, the finer are more yellow); from 298.0 to 330.0 ft the unit is massive. Calcareous, increasing downward.
345.0	15.0	Clay, a little silt, a very little fine sand. Colors range between yellowish gray (5Y7/2), pale greenish yellow (10Y8/2), and pale olive (10Y6/2); average is toward pale olive. Color banding but no apparent lithologic bedding. Noncalcareous except for bottom ft.
354.4	9.4	Clay, pale greenish-yellow (10Y8/2), massive; very calcareous; 1-in. beds of gypsum* at 351.0 and 352.0 ft.
365.0	10.6	Silt, calcareous, and gypsum; greenish gray (5GY6/1) to white (N9); massive. Megascopic crystals of gypsum* (from 10 to 50 percent of core) in a matrix of calcareous silt; the calcite content is between 30 and 90 percent.

DH3 (continued)

Depth (feet)	Unit thickness (feet)	Description
375.0	10.0	Clay, with pods of calcium carbonate. Dark greenish gray (5G4/1) and moderate brown (5YR4/4) mixed with some streaks and pods of white (N9), still damp. Texture is contorted; may have been bedded.
384.0	9.0	Silt, light greenish-gray (5G8/1) to very light gray (N8), massive; very calcareous; a few crystals of gypsum up to 4 mm long.
385.0	1.0	Gypsum and calcite, very light gray (N8), massive. Crystals of gypsum up to 1 mm long.
395.0	10.0	Gypsum and halite, silty, light greenish-gray (5GY8/1); massive. Gypsum and halite form up to 90 percent of core; average is about 70 percent.
401.0	6.0	Clay with pods of calcite*, dark greenish-gray (5G4/1) and moderate-brown (5YR4/4), still damp. Texture contorted. Poor core.
401.3	.3	Halite and silt, colorless crystals.
408.0	6.7	Clay, silty, light dusky-yellow (5Y7/4), massive. Some isolated halite crystals; calcareous.
412.0	4.0	Silt, grayish-olive (10Y4/2), still damp; massive. May be cuttings, not core.
415.0	3.0	Clay, silty, light dusky-yellow (5Y7/4); laminar bedding. A little halite; calcareous.
418.0	3.0	Silt, grayish-olive (10Y4/2), massive. May be cuttings, not core.
424.3	6.3	Clay and a little silt interbedded. Dusky-yellow (5Y6/4) clay and yellowish-gray (5Y7/2) silt. Bedding of two types: one is laminar; the other is about 20 mm thick. Section about 90 percent clay. Calcareous.
449.3	25.0	Halite; colorless crystals (usually covered with clay); massive. A little gypsum* and calcite*. Some beds of silt included in the core are probably cuttings, not core.
450.0	.7	Sand, very fine, yellowish-gray (5Y7/2). Bedding faint, about 5 mm average thickness. Well sorted, well indurated. Calcareous.
454.0	4.0	Clay and a little silt interbedded. Dusky-yellow (5Y6/4) clay and yellowish-gray (5Y7/2) silt. Well bedded. Calcareous. Top foot is still damp; presumably cuttings, not core.
456.6	2.6	Silt. Between yellowish gray (5Y7/2), light olive gray (5Y5/2), and pale olive (10Y6/2); average is toward pale olive. Laminar bedding. Carbonaceous partings. Calcareous; salty.
460.0	3.4	Clay and a little silt in upper half grading to silt in lower half. Dusky yellow (5Y6/4) and yellowish gray (5Y7/2) in upper half; pale olive (10Y6/2) in lower half. Entire unit well bedded. Carbonaceous partings. Calcareous.
461.0	1.0	Clay and a little halite. Clay is dusky blue (5PB3/2), still damp. Halite forms about 10 percent of core.
474.0	13.0	Halite*, colorless; tan or gray clay coating on crystals; massive. A 1-in. silt bed at 464.5 ft. Upper two-thirds about 20 percent, clay; lower one-third about 2 percent clay.
479.7	5.7	Silt and clay, pale-olive (10Y6/2). Bedding 1 to 10 mm thick; defined by color banding. Pods of white (gypsum ?).
485.0	5.3	Clay and halite. Clay is pale olive (10Y6/2); halite is colorless. Fine bedding. Ratio of halite to clay is 1 to 1. A little calcite.

DH3 (continued)

Depth (feet)	Unit thickness (feet)	Description
531.0	46.0	Halite; a little clay. Halite is colorless. Massive(?). A little calcite and gypsum. Top contact is gradational; basal contact is sharp. Core is very poor and bedding is not recognizable; the section drilled as if massive salt.
545.0	14.0	Clay, yellowish-gray (5Y7/2) to pale-olive (10Y6/2). Bedding is distinct, units 1 to 10 mm thick; some partings appear carbonaceous. Calcareous.
555.0	10.0	Silt; yellowish-gray (5Y7/2), darker where core is still damp; massive to mottled texture. Fragments of halite and gypsum, the percentage increasing downward; calcareous.
556.0	1.0	Calcite and gypsum encased in mud, greenish-gray (5GY6/1). Core is about 90 percent crystals.
557.0	1.0	Silt, yellowish-gray (5Y8/1), massive, slightly calcareous.
559.5	2.5	Halite; a little clay. Colorless halite; clay is greenish gray (5GY6/1). Massive.
569.5	10.0	Clay, yellowish-gray (5Y8/1) to light greenish-gray (5GY8/1), mottled coloring; generally massive, local thin bedding; calcareous.
585.3	15.8	Clay grading down to silt, yellowish-gray (5Y8/1). Bedding fine up to 10 mm. Calcareous. Fine sand, 576.0 to 577.0 ft.
590.0	4.7	Clay, yellowish-gray (5Y8/1) to very pale orange (10YR8/2), massive, calcareous.
596.5	6.5	Silt to fine sand; yellowish gray (5Y7/2) to pale olive (10Y6/2), patches of white (N9); massive. Pods and small lenses of gypsum and halite at 596.0 ft.
601.0	4.5	Clay, yellowish-gray (5Y8/1) to very pale orange (10YR8/2), generally massive, calcareous.
610.0	9.0	Silt grading downward to very coarse sand with silt matrix, yellowish-gray (5Y7/2) to (5Y8/1), massive, calcareous and gypsiferous, from 603.0 to 604.0 ft gypsum forms up to 30 percent of core.
624.0	14.0	Silt and fine sand grading down to fine sand, light olive-gray (5Y6/1), massive, slightly calcareous. Poor core.
624.3	.3	Tuff, mixed with very fine sand; very light gray (N8). Fine bedding defined by black streaks of carbon or biotite. Very well indurated.
656.0	31.7	Sand, very fine, yellowish-gray (5Y7/2), massive. Calcareous.
785.0	129.0	Silt to very fine sand, yellowish-gray (5Y7/2); very faint bedding to massive; very well sorted. Calcareous; a 1-ft bed of calcareous silt at 724.0 ft. Many flakes of mica, up to 0.5 mm wide.
794.0	9.0	Clay, silty, yellowish-gray (5Y7/2), massive(?), slightly calcareous. Poor core.
795.0	1.0	Sand, very fine, yellowish-gray (5Y7/2), massive. A little gypsum; calcareous.
801.0	6.0	Silt; very little fine sand; dark yellowish gray (5Y6/2). Bedding in top ft 1 to 10 mm thick; appears to be at an angle of about 60° to the sides of the core; probably a result of drilling pressures.
805.0	4.0	Silt to very fine sand, dark grayish-yellow (5Y7/4), massive, very slightly calcareous.
814.2	9.2	Silt to very fine sand, dark-yellowish-gray (5Y8/2), massive. A little gypsum.
815.0	.8	Silt to very fine sand, dark grayish-yellow (5Y7/4); faint bedding; slightly calcareous.

DH3 (continued)

Depth (feet)	Unit thickness (feet)	Description
829.3	14.3	Silt to very fine sand, yellowish-gray (5Y7/2) to dark-grayish-yellow (5Y7/4). Some faint laminar bedding but generally massive. Slightly (about 0.5 percent) gypsiferous; calcareous; flakes of mica common.
835.0	5.7	Clay, gypsiferous, silty, dark grayish-yellow (5Y7/4), mottled coloring. Gypsum forms 5 to 20 percent of core, average 10 percent; found as bladed crystals up to 10 mm long. Very slightly calcareous.
844.5	9.5	Clay and a little silt. Dusky-yellow (5Y6/4) clay and yellowish-gray (5Y7/2) silt. Massive.
845.0	.5	Silt, gypsiferous(?); very light greenish gray (5GY9/1), lenses of white (N9).
855.0	10.0	Silt, greenish-gray (5Y7/1). Locally shows faint bedding up to 10 mm thick but is generally massive. Lenses of anhydrite* and gypsum*; very slightly calcareous*.
865.0	10.0	Clay, silty, yellowish-gray (5Y7/2); massive, generally, with local laminar bedding; calcareous, a little gypsum*.
875.0	10.0	Core lost; estimated to be the same as previous 10 ft.
895.0	20.0	No core; solid bit used; the material is presumably similar to that at 865.0 ft.
913.0	18.0	Clay, very little silt and very fine sand; dark grayish yellow (5Y7/4). Very well bedded; laminar to 20 mm thick in upper part, grades down to massive. Black partings of carbon or biotite in upper part. Calcareous, a little anhydrite(?)*.
914.6	1.6	Clay; yellowish gray (5Y7/2), to light olive gray (5Y5/2) in lower part. Lenses (up to 1 mm thick) of biotite(?). Excellent laminar bedding. Calcareous.
915.0	.4	Sand, fine, dusky-yellow (5Y6/4), poorly sorted, massive.
931.4	16.4	Silt to very fine sand, yellowish-gray (5Y7/2). Massive in upper half grading to very faint bedding in lower half. Calcareous; gypsiferous.
935.0	3.6	Silt, yellowish-gray (5Y7/2). Excellent laminar bedding; partings of black biotite(?). Calcareous.
945.0	10.0	Clay, silty,to silt; light greenish gray (5GY8/1); massive. Gypsum at 937.0 ft.
965.0	20.0	Clay to silt, yellowish-gray (5Y8/1) to light olive-gray (5Y6/1). Fine bedding; laminar to 15 mm thick. Some partings of biotite silt. Small lamellae of gypsum(?) and anhydrite*.
985.0	20.0	Silt with thin beds of gypsum(?) and anhydrite(?); yellowish gray (5Y8/1). Silt beds are well sorted and well indurated. Gypsum(?) and anhydrite(?) form about 10 percent of the core. No core recovered from 965 to 973 ft but drilling characteristics indicate a well-indurated material similar to the recovered core.
995.0	10.0	No core; drilled as if very hard material, like unit above.

North Panamint Valley

NP-1 (as logged by Motts and Carpenter, 1968; 36 feet deep.)

Depth (feet)	Unit thickness (feet)	Description
1	1	Silt, clayey, yellowish gray 5Y7/2, very dry, poor plasticity.
12	11	Silt, clayey, grayish orange 10YR7/4, moderate plasticity, some salt.
15	3	Silt, clayey, pale yellowish brown 10YR4/2, moderate to poor plasticity.
18	3	Clay, silty, dark yellowish brown 10YR4/2.
20	2	Silt, clayey, dark yellowish brown 10YR4/2, with fine sand lens at 19 ft.
23	3	Clay, silty, dark yellowish brown 10YR4/2, with stringers of pale olive 10Y6/2, moderate to good plasticity.
23	-	Sand lens.
26	3	Varves, silt and clay, with sand lens at 25.5 ft.
27	1	Clay, silty to sandy, pale olive 10Y6/2, good plasticity.
35	8	Clay, pale olive 10Y6/2, good plasticity, with sand lens at 35 ft.
36	-	Bottom of test hole.

NP-2 (as logged by Motts and Carpenter, 1968; 24 feet deep.)

Depth (feet)	Unit thickness	Description
0.5	0.5	Sand, silty, yellowish gray, 5Y7/2, very dry, poor plasticity.
4	3.5	Silt, clayey, light brown 7.5YR6/4, poor plasticity.
10	6	Silt, clayey, dark brown 10YR4/3, poor to moderate plasticity.
12	2	Clay, silty, brown, 10YR5/3, moderate plasticity, with sand lens at 12 ft.
24	12	Clay, silty, pale olive 10Y6/2, with lenses of silt and sand, some black specks at 14-17 ft., sand lens, coarse to fine grained, at 18 ft.
24	-	Bottom of test hole.

NP-3 (as logged by Motts and Carpenter, 1968; 162 feet deep.)

Depth (feet)	Unit thickness (feet)	Description
4	4	Silt, clayey, light yellowish brown, 10YR6/4, poor plasticity, some salt.
13	9	Silt, clayey, pale brown 10YR6/3, poor plasticity, granulated.
20	7	Silt, clayey, light yellowish brown, 10YR6/4, moderate plasticity, increased clay content at 13 ft.
30	10	Clay, silty, pale olive 10Y6/2, moderate plasticity with some sand and gravel.
35	5	Clay, silty, grayish green 10GY5/2, with some stringers of dark yellowish orange 10YR6/6.
40	5	Varves, clay and silt, light olive gray 5Y5/2.
45	5	Clay, light olive 5Y5/2, becomes sandy at 43 ft.
46	1	Sand, very coarse, grayish yellow green 5GY6/2.
48	2	Silt, clayey, grayish yellow green 5GY6/2.
51	3	Sand, medium to fine grained, grayish yellow green 5GY6/2.
55	4	Silt, clayey, pale brown 5YR5/2.
62	7	Clay, silty, grayish green 10GY5/2, with some black specks at 57 ft.
66	4	Sand, very fine grained, grayish yellow green 5GY7/2, with silt and large calcareous fragments at 65 ft.
75	9	Clay, pale olive 10YG/2, plastic, with white fragments at 75 ft.
79	4	Clay, silty, pale brown 10YR5/2, moderate plasticity, crumbly texture.
84	5	Clay, silty, pale blue green 5BG7/2, moderate to good plasticity.
		[No description logged for 84-89-ft. interval.]
90	1	Clay, pale olive 10Y6/2, plastic.
107	17	Clay, very pale green 10G8/2, plastic.
108	1	Sand, coarse to fine grained, light olive gray 5Y5/2, with layer of white and black pebbles at 108 ft.
122	14	Clay, pale olive 10Y6/2, clay broken into hard aggregates.
128	6	Sand, medium grained, pale grayish olive 10Y5/2, with traces of moderate brown 5YR4/4.
131	3	Silt, clayey, moderate brown 5YR4/4, with gradation to stones.
132	1	Sand, pebbly, medium grained, light olive gray 5Y5/2, white, angular fragments.
138	6	Sand, medium grained, light olive 10Y5/4, coherent.

NP-3 (continued)

Depth (feet)	Unit thickness (feet)	Description
140	2	Sand, pebbly, medium to coarse grained, moderate yellowish brown 10YR5/4, with igneous rock, black, 140 ft.
144	4	Clay, very pale orange, 10YR8/2.
149	5	Clay to gravel, gradation, light olive 10Y5/4.
158	9	Clay, silty, pale olive 10Y6/2 to dark yellowish brown 10YR4/2, plastic.
161	3	Sand, fine grained, dark yellowish brown 10YR4/2, with streaks of clay, light brown 5YR5/6.
162	1	Sand, coarse to very coarse grained.
162	-	Bottom of test hole.

DH2 (as logged by Smith and Pratt, 1957; 375 feet deep; 58 per cent of core recovered.)

Depth (feet)	Unit thickness (feet)	Description
10.0	10.0	No core; probably all sand, coarse to fine.
17.0	7.0	No core; probably sand to silt.
19.8	2.8	Sand to silt, greenish-yellow (10Y7/2), massive. Sand grains of quartz (about 90 percent of sand), feldspar, biotite (euhedral, bleached to a golden color), iron oxide-coated quartz, possibly some pyroxene and hornblende. Calcareous.
21.5	1.7	Clay, fragments of rounded feldspar crystals, and euhedral biotite; yellowish gray (5Y8/1); massive. Streaks (1 mm average width) of hematite* generally parellel to bedding but some are perpendicular. Spots of black flakes (may be iron or manganese oxides). Irregular patches (up to 1 in. long) of brown stains, darker than hematite stains.
21.9	.4	Sand, coarse to fine, pale greenish-yellow (10Y8/2). Subangular quartz and feldspar, about 5 percent mica; streaks of reddish iron oxide. Calcareous.
22.4	.5	Clay, yellowish-gray (5Y8/1). Scattered flakes of biotite, some zones of iron oxide. A few stringers of coarse sand. Calcareous. Massive.
22.7	.3	Sand, similar to sand at depth of 21.9 ft.
23.2	.5	Clay containing about 5 percent quartz- and feldspar-sand fragments, yellowish-gray (5Y8/1), massive, calcareous.
23.7	.5	Sand, medium, yellowish-gray (5Y7/2), well-sorted, subangular; about 10 percent biotite flakes; calcareous.
26.8	3.1	Clay; contains about 1 percent subangular fragments of fine to coarse sand; pale greenish yellow (10Y8/2); much biotite, generally euhedral; calcareous.
30.0	3.2	No core.

DH2 (continued)

Depth (feet)	Unit thickness (feet)	Description
38.0	8.0	Core destroyed while being removed from core barrel; sludge fragments indicate most of core was clay, yellowish gray (5Y8/1), with fragments of coarse sand forming about 5 percent of total. Some layers of coarse to very coarse sand.
40.7	2.7	Sand, fine to very fine, yellowish-gray (5Y7/2), massive, well-sorted. Many biotite flakes up to 1 mm diameter. Very calcareous.
41.2	.5	Pebble gravel, light greenish-gray (5GY8/1). Matrix of clay. Fragments are of large crystals(?) of feldspar and quartz, and fine-grained volcanic(?) rocks. Ratio of pebbles to matrix is 1 to 3. Calcareous.
44.8	3.6	Silt, some beds of fine to very fine sand; yellowish gray (5Y8/1). Sand beds up to 2 in. thick.
50.0	5.2	No core; probably fine sand, pebbly sand, and some clay.
51.6	1.6	Granule and clay mixture, yellowish-gray (5Y8/1). Granules up to 3 mm in diameter, subrounded to subangular, composed of basalt and individual minerals. May be cuttings, not core.
51.8	.2	Sand, very fine, light greenish-gray (5GY8/1). Contains larger fragments of quartzite and limonite(?). Massive. Calcareous.
60.0	8.2	No core; cuttings indicate much clay.
61.8	1.8	Silt to clay, pale greenish-yellow (10Y8/2). Contains some subangular fragments of dolomite(?) and some small flakes of biotite.
62.0	.2	Clay, pale greenish-yellow (10Y8/2). Contains a 1-in. rounded fragment of vesicular volcanic rock.
65.0	3.0	Sand, fine to medium, some fragments of very coarse grained sand; pale olive (10Y6/2). Fragments about 97 percent feldspar and quartz(?); some biotite, olivine, iron oxide, and rock fragments. Slightly bedded. Calcareous.
70.0	5.0	No core; drilled as if sand.
72.4	2.4	Sand and clay intermixed, pale-olive (10Y6/2). Sand similar to sand at 65.0 ft. Contains rounded fragments of dolomite, intrusive rock, and volcanic rock up to 10 mm in diameter. Average size about 5 mm. Poor core.
80.0	7.6	No core; drilled as if loose sand.
80.7	.7	Clay; contains fragments up to 1 mm long of feldspar and biotite; pale olive (10Y6/2). Bottom 2 in. is coarse sand, mainly feldspar.
90.0	9.3	No core. Drilled as if sand and clay interbedded; interval between 84 and 86 ft mostly clay.
97.6	7.6	Clay, pale greenish-yellow (10Y8/2), massive, homogeneous; core breaks with conchoidal fracture. Contains fragments of biotite up to 0.5 mm in diameter, some feldspar(?).
111.7	14.1	Sand, coarse to very fine, pale-olive (10Y6/2), massive. Fragments angular to subangular, many are crystal shaped. Approximate composition: 90 percent feldspar, 6 percent quartz, 3 percent biotite, 1 percent iron oxide, pyroxene(?), amphibole(?). Entire section is very calcareous.
114.5	2.8	Clay, pale greenish-yellow (10Y8/2). Lower half shows fine bedding (1 to 5 mm thick); upper half shows no bedding. Breaks with a conchoidal fracture. Clay contains 1 mm biotite fragments, some pyroxene(?), hornblende(?), and feldspar. Very calcareous.

DH2 (continued)

Depth (feet)	Unit thickness (feet)	Description
114.8	.3	Sand, very coarse, white (N9), well-sorted. Contains fragments of biotite and quartz(?), possibly gypsum. Noncalcareous.
117.8	3.0	Clay, greenish-yellow (10Y7/2); conchoidal fracture. Contains biotite flakes, some iron-oxide stains.
120.0	2.2	No core.
132.4	12.4	Clay, greenish-yellow (10Y7/2); conchoidal fracture. Contains flakes of biotite.
135.0	2.6	No core.
158.2	23.2	Clay and silt breccia; pale greenish-yellow (10Y8/2) clay fragments in matrix of light-brown (5YR6/4) silt. Fragments are angular, range in width up to diameter of core (2 in.). Ratio of fragments to matrix is about 2 to 1.
162.5	4.3	Silt and clay, yellowish-gray (5Y8/1), massive, calcareous. Very few biotite flakes. Contains moderate orange-pink (5YR8/4) stringers of silt, similar to the matrix in the unit above.
167.5	5.0	Silt and clay, white (N9) to grayish-orange (10YR7/4). Contains fragments of feldspar and biotite.
175.0	7.5	Marl, pinkish-gray (5YR8/1). From 50 to 90 percent calcite, average about 70. Contains fragments of feldspar and biotite.
180.0	5.0	Silt and clay; very pale orange (10YR8/2) grading downward to grayish orange (10YR7/4); massive; calcareous*.
184.0	4.0	Silt and clay, generally very pale orange (10YR8/2); stringers of moderate orange-pink (5YR8/4) silt; massive; calcareous. At 182.3 ft a 1-in. fragment of vein quartz and smaller pebbles of volcanic rocks were found. This unit may be cuttings, not core.
190.0	6.0	Silt and clay, some beds of fine to medium sand; grayish orange (10YR7/4). Well bedded; sand beds up to 2 in. thick, finer sediments laminar. Sand fragments largely quartz and feldspar, with some biotite (bleached), iron oxides, and pyroxene(?). Calcareous.
200.0	10.0	Marl, mottled white (N9) and very pale orange (10YR8/2). Mainly $CaCO_3$ with irregular patches of silt. Ratio of carbonate to silt is generally about 2 to 1; some zones about 98 percent carbonate. Transition to unit above is gradational.
208.2	8.2	Clay and a little silt, pale greenish-yellow (10Y8/2), massive. Irregular patches and vertical "dikes" of iron oxide stains. Visible minerals: biotite, pyroxene(?), feldspar, iron oxides, possible some iddingsite after olivine. Transition to unit above is gradational over about 2 in.
217.7	9.5	Clay and a little silt, pale grayish-orange (10YR7/2). Vertical streaks of light-brown (5YR6/4) finer clay.
219.8	2.1	Gravel, pale grayish-orange (10YR7/2). Matrix of fine to medium sand; fragments of subangular to subrounded pebbles (2 to 15 mm; average size about 5 mm) of volcanic rocks (andesitic and basaltic; pumiceous) and limestones (dusky blue (5 PB3/2) and medium gray (N6)).
225.8	6.0	Clay and a little silt, yellowish-gray (5Y7/2). Vertical streaks of light-brown (5YR6/4) finer clay.
227.4	1.6	Sand, fine to medium, pale grayish-orange (10YR7/2).
230.0	2.6	Clay, silt, and fine sand, pale grayish-orange (10YR7/2).

DH2 (continued)

Depth (feet)	Unit thickness (feet)	Description
240.0	10.0	Gravel, pale grayish-orange (10YR7/2). Matrix is fine to medium sand; fragments of volcanic rocks and limestones have a maximum diameter of about 5 mm.
250.0	10.0	No core; sludge cuttings indicate gravel only.
260.0	10.0	No core; gravel(?).
265.0	5.0	No core; solid-bit drill used.
270.0	5.0	Silt and clay, yellowish-gray (5Y7/2), massive. Some subangular fragments of limestone, 2 to 10 mm in diameter.
276.0	6.0	Silt, pale grayish-orange (10YR7/2), massive. A very few pebbles scattered throughout. Calcareous. Some darker streaks (carbon?).
277.0	1.0	Silt, pebbly, pale grayish-orange (10YR7/2). Pebbles between 2 and 15 mm wide, averaging about 5 mm; composed of volcanic rocks (cinder basaltic rocks and limestone). Ratio of pebbles to silt is about 1 to 10.
279.0	2.0	Sand, very fine, and silt; pale orange (10YR7/2); very well sorted. Fine bedding averaging about 1 mm between bedding planes; bottom 6 in. is crossbedded, as if windblown.
279.4	.4	Gravel, pale-orange (10YR7/2). Pebbles form about 80 percent of the unit; rounded to subrounded, between 2 and 20 mm wide, averaging about 8 mm: consist of basaltic rocks, cinder, and quartzite(?).
282.6	3.2	Clay and silt, pale-orange (10YR7/2), well-sorted. At 281.3 ft and 282.0 ft there are well-cemented 2 in. beds of very coarse sand fragments in a matrix of solid calcite* and silt; sand consists of angular fragments of feldspar*, quartz*, amphibole*, pyroxene*, hematite*, and volcanic rocks*.
290.0	7.4	Sand, fine to very fine, light brownish-gray (5YR6/1), massive. Contains a few pebbles of andesitic rocks, cinder, and dolomite; round to subround; up to 20 mm long.
356.0	66.0	No core; drilled as if gravel.
359.2	3.2	Clay, very pale orange (10YR8/2), massive.
359.5	.3	Clay, grayish-orange (10YR7/4).
365.0	5.5	Sand, fine, grading into coarse sand at base; grayish orange (10YR7/4). Contains pebbles of limestone ranging in size from 2 to 10 mm, averaging about 5 mm; subangular.
375.0	10.0	No core; tricone bit used. Cuttings and drilling characteristics indicate lithology similar to the nearby outcrops of Paleozoic limestone.

REFERENCES CITED

Adam, D.P., 1967, Late-Pleistocene and Recent palynology in the central Sierra Nevada, California: p. 275-301 in Cushing, E.J., and Wright, H. E., Jr., eds., 1967, Quaternary paleoecology: New York and London, Yale Univ. Press.

Albee, A.L., ed., 1971, Telescope Peak quadrangle, California: geology by Arden L. Albee, Marvin A. Lanphere, and S. Douglas McDowell (1960-1970), compiled for use at 1:250,000 scale (unpublished).

Babcock, J.W., 1975, Volcanic rocks in the Coso Mountains, California [abs]: Geol. Soc. America Abs. with Programs, v. 7, no. 3, p. 291-2.

Bailey, G.E., 1902, The saline deposits of California: Bull. Calif. State Mining Bureau, v. 24, 216p.

Bailey, R.A., Dalrymple, G.B., and Lanphere, M.A., 1975, Volcanism, structure and geochronology of Long Valley caldera, Mono County, California: Jour. Geophys. Research, (in press).

Ball, S.H., 1907, A geologic reconnaissance in southwestern Nevada and eastern California: U.S. Geol. Survey Bull. 308, 218p.

Bandy, O.L., and Marincovich, Louis, Jr., 1973, Rates of Cenozoic uplift, Baldwin Hills, Los Angeles, California: Science, v. 181, p. 653-5.

Batchelder, G.L., 1970, Post-glacial fluctuations of lake level in Adobe Valley, Mono County, California [abs]: American Quaternary Assoc., 1st Meeting, Abs., p. 7.

Bateman, P.C., 1961, Willard D. Johnson and the strike-slip component of fault movement in the Owens Valley, California, earthquake of 1872: Bull. Seismol. Soc. America, v. 51, no. 4, p. 483-493.

_____ 1965, Geology and tungsten mineralization of the Bishop district, California: U.S. Geol. Survey Prof. Paper 470, 208p.

_____ , and Wahrhaftig, Clyde, 1966, Geology of the Sierra Nevada: p. 107-172 in: Bailey, E.H., ed., 1966, Geology of northern California: Calif. Div. Mines and Geol. Bull. 190, 507p.

Beaty, C.B., 1968, Sequential study of desert flooding in the White Mountains of California: U.S. Army Natick Labs. Tech. Rept. 68-31-ES, 96p.

Berger, Rainer, and Libby, W.F., 1966, U.C.L.A. radiocarbon dates V: Radiocarbon, v. 5, p. 467-497.

Birkeland, P.W., 1964, Pleistocene glaciation of the northern Sierra Nevada, north of Lake Tahoe, California: Jour. Geology, v. 72, p. 810-825.

_____ , Crandell, D.R., and Richmond, G.M., 1971, Status of correlation of Quaternary stratigraphic units in the western coterminous United States: Quaternary Research, v. 1, no. 2, p. 208-227.

Birman, J.H., 1964, Glacial geology across the crest of the Sierra Nevada, California: Geol. Soc. America Spec. Paper 75, 80p.

Black, R.F., 1954, Precipitation at Barrow, Alaska, greater than recorded: American Geophys. Union Trans., v. 35, no. 2, p. 203-206.

Blackwelder, Eliot, 1931, Pleistocene glaciation in the Sierra Nevada and basin ranges: Geol. Soc. America Bull., v. 42, p. 865-922.

_____ , 1933, Lake Manly: an extinct lake of Death Valley: Geog. Rev., v. 23, p. 464-471.

_____ , 1941, Lakes of two ages in Searles Basin, California [abs]: Geol. Soc. America Bull., v. 52, p. 1943-1944.

_____ , 1954, Pleistocene lakea and drainage in the Mojave Desert region, southern California: ch. 5, p. 35-45 in Jahns, R.H., ed., 1954, Geology of southern California: Calif. Div. Mines Bull. 170, 671p..

Blaney, H.F., 1957, Evaporation studies at Silver Lake in the Mojave Desert, California: American Geophys. Union Trans., v. 38, no. 2, p. 209-215.

Broecker, W.S., and Kaufman, Aaron, 1965, Radiocarbon chronology of Lake Lahontan and Lake Bonneville II, Great Basin: Geol. Soc. America Bull., v. 76, p. 537-566.

Burchfiel, B.C., and Stewart, J.H., 1966, "Pull-apart" origin of the central segment of Death Valley, California: Geol. Soc. America Bull., v. 77, p. 439-442.

California Dept. Water Resources, 1965-1971, Bulls. 130-63, 130-64, 130-65, 130-66, 130-67, 130-68, 130-69.

Campbell, M.R., 1902, Reconnaissance of the borax deposits of Death Valley and Mohave Desert: U.S. Geol. Survey Bull. 200, 23p.

Carranza, Carlos, 1965, Surficial geology of a part of south Panamint Valley, Inyo County, California: Univ. Massachusetts M.S. thesis (unpublished).

Clark, M.M., 1972, Range-front faulting: case of anomalous relations among moraines of the eastern slope of the Sierra Nevada, California [abs]: Geol. Soc. America Abs. with Programs, v. 4, no. 3, p. 137.

_____ , 1973, Map showing recently active breaks along the Garlock and associated faults, California: U.S. Geol. Survey Misc. Geol. Inv. Map I-741.

_____ , Grantz, Arthur, and Rubin, Meyer, 1972, Holocene activity of the Coyote Creek fault as recorded in sediments of Lake Cahuilla: U.S. Geol. Survey Prof. Paper 787, p. 112-130.

Cleveland, G.B., 1961, Economic geology of the Long Valley diatomaceous earth deposit, Mono County, California: Calif. Div. Mines and Geology Map Sheet 1.

_____ , 1962, Geology of the Little Antelope Valley clay deposits, Mono County, California: Calif. Div. Mines and Geology Spec. Rept. 72, 28p.

Crittenden, M.D., Jr., 1963a, Effective viscosity of the Earth derived from isostatic loading of Pleistocene Lake Bonneville: Jour. Geophys. Res., v. 68, p. 5517-5530.

_____ , 1963b, New data on the isostatic deformation of Lake Bonneville: U.S. Geol. Survey Prof. Paper 454-E, 31p.

Curry, H.D., 1938, Strike-slip faulting in Death Valley, California [abs]: Geol. Soc. America Bull., v. 49, p. 1874-1875.

Curry, R.R., 1966, Glaciation about 3,000,000 years ago in the Sierra Nevada: Science, v. 154, p. 770-771.

_____ , 1968, Quaternary climatic and glacial history of the Sierra Nevada, California: Univ. California [Berkeley] Ph.D. thesis, 204p.

_____ , 1971, Glacial and Pleistocene history of the Mammoth Lakes Sierra--a geologic guidebook: Univ. Montana Dept. Geology, Geol. Ser. Pub. 11, 49p.

Dalrymple, G.B., 1963, Potassium-argon dates of some Cenozoic volcanic rocks in the Sierra Nevada, California: Geol. Soc. America Bull., v. 74, p. 379-390.

_____ , 1964, Potassium-argon dates of three Pleistocene interglacial basalt flows from the Sierra Nevada, California: Geol. Soc. America Bull., v. 75, p. 753-758.

_____ , Cox, Allan, and Doell, R.R., 1965, Potassium-argon age and paleomagnetism of the Bishop Tuff, California: Geol. Soc. America Bull., v. 76, p. 665-674.

Davis, E.L., 1970, Archaeology of the north basin of Panamint Valley, Inyo County, California: Nevada State Mus. Anthropol. Papers no. 15, p. 83-141.

Dibblee, T.W., Jr., 1967, Areal geology of the western Mojave Desert, California: U.S. Geol. Survey Prof. Paper 522, 153p.

Dreimanis, A., and Karrow, P.F., 1972, Glacial history of the Great Lakes-St. Lawrence region, the classification of the Wisconsin (an) Stage, and its correlatives: Internat. Geol. Cong., sess. 24, sec. 12, p. 5-15.

Durgin, P.B., [in preparation], Surficial geology of north Panamint Valley, Inyo County, California: Univ. Massachusetts M.S. thesis.

Eardley, A.J., Shuey, R.T., Gvosdetsky, V., Nash, W.P., Picard, M.D., Grey, D.C., and Kukla, G.J., 1973, Lake cycles in the Bonneville basin, Utah: Geol. Soc. America Bull., v. 84, p. 211-216.

Evernden, J.F., Savage, D.E., Curtis, G.H., and James, G.T., 1964, Potassium-argon dates and the Cenozoic mammalian chronology of North America: Am. Jour. Sci., v. 262, p. 145-198.

Feth, J.H., and Brown, R.J., 1962, Method for measuring upward leakage from artesian aquifers using rate of salt-crust accumulation: U.S. Geol. Survey Prof. Paper 450-B, p. B-100-B-101.

Flint, R.F., 1971, Glacial and Quaternary geology: New York: John Wiley and Sons, 892p.

_____, and Gale, W.A., 1958, Stratigraphy and radiocarbon dates at Searles Lake, California: Am. Jour. Sci., v. 256, p. 689-714.

Free, E.E., 1914, The topographic features of desert basins of the United States with reference to the possible occurrence of potash: U.S. Dept. Agr. Bull. 54.

Gale, H.S., 1915, Salines in the Owens, Searles, and Panamint basins, southeastern California: U.S. Geol. Survey Bull. 580-L, p. 251-323.

Gilbert, C.M., Christensen, M.N., Al-Rawi, Yehya, and Lajoie, K.R., 1968, Structural and volcanic history of Mono Basin, California-Nevada: Geol. Soc. America Mem. 116, p. 275-329.

Gilbert, G.K., 1890, Lake Bonneville: U.S. Geol. Survey Mon. 1, 438p.

Glen, J.W., and Lewis, W.V., 1961, Measurements of side-slip at Austerdalsbreen, 1959: Jour. Glaciology, v. 3, no. 30, p. 1109-1122.

Gray, C.H., Jr., 1962, Limestone resources of southern California, part 2: Calif. Div. Mines and Geology Mineral Inf. Service, v. 15, no. 6, p. 4-7.

Hall, W.E., 1971, Geology of the Panamint Butte quadrangle, Inyo County, California: U.S. Geol. Survey Bull. 1299, 67p.

_____, and MacKevett, E.M., Jr., 1962, Geology and ore deposits of the Darwin quadrangle, Inyo County, California: U.S. Geol. Survey Prof. Paper 368, 87p.

_____, and Stephens, H.G., 1963, Economic geology of the Panamint Butte quadrangle and Modoc District, Inyo County, California: Calif. Div. Mines and Geology Spec. Rept. 73, 39p.

Hamilton, Warren, and Myers, W.B., 1966, Cenozoic tectonics of the western United States: Rev. Geophys., v. 4, no. 4, p. 509-549.

Hanna, G.D., 1963, Some Pleistocene and Pliocene freshwater Mollusca from California and Oregon: Calif. Acad. Sci. Occasional Paper 43, 20p.

Harbeck, G.E., Jr., Kohler, M.A., Koberg, G.E., et al, 1958, Water-loss investigations: Lake Mead studies: U.S. Geol. Survey Prof. Paper 298.

Harding, S.T., 1935, Evaporation from large water-surfaces based on records in California and Nevada: Am. Geophys. Union Trans., 1935, p. 507-511.

Haynes, C.V., Jr., 1965, Carbon-14 dates and early man in the New World: p. 145-164 in: Proc. 6th Internat. Conf. Radiocarbon and Tritium Dating: Pullman, Wash.: Washington State Univ., 784p. (U.S. Atomic Energy Comm. CONF-650652).

Hely, A.G., Hughes, G.H., and Irelan, Burdge, 1966, Hydrologic regimen of Salton Sea, California: U.S. Geol. Survey Prof. Paper 486-C, 32p.

Hileman, J.A., Allen, C.R., and Nordquist, J.M., 1973, Seismicity of the southern California region: Pasadena, Calif.: Calif. Inst. Technology Seismol. Lab.

Hill, M.L., 1954, Tectonics of faulting in southern California: chap. 4, p. 5-13, in: Jahns, R.H., ed., 1954, Geology of southern California: Calif. Div. Mines Bull. 170.

_____, and Troxel, B.W., 1966, Tectonics of Death Valley region, California: Geol. Soc. America Bull., v. 77, p. 435-438.

Hooke, R. LeB., 1972, Geomorphic evidence for late-Wisconsin and Holocene tectonic deformation, Death Valley, California: Geol. Soc. America Bull., v. 83, p. 2073-2098.

Hopper, R.H., 1947, Geologic section from the Sierra Nevada to Death Valley, California: Geol. Soc. America Bull., v. 58, p. 393-423.

Hovind, E.L., 1965, Precipitation around a windy mountain peak: Jour. Geophys. Research, v. 70, no. 14, p. 3271-3278.

Hubbs, C.L., Bien, G.S., and Suess, H.E., 1965, La Jolla natural radiocarbon measurements IV: Radiocarbon, v. 7, p. 66-117.

Hunt, C.B., Robinson, T.W., Bowles, W.A., and Washburn, A.L., 1966, Hydrologic basin, Death Valley, California: U.S. Geol. Survey Prof. Paper 494-B, 138p.

Hutchinson, G.E., 1957, A treatise on limnology: New York: John Wiley and Sons, v. 1, 1015p.

Jahns, R.H., 1951, The epsom salts line-monorail to nowhere: Eng. and Sci., v. 14, no. 7, p. 18-21.

James, J.W., 1964, The effect of wind on precipitation catch over a small hill: Jour. Geophys. Research, v. 69, no. 12, p. 2521-2524.

Janda, R.J., 1966, Pleistocene history and hydrology of the upper San Joaquin River, California: Univ. California [Berkeley] Ph.D. thesis, 425p.

Jennings, C.W. ed., 1958, Death Valley sheet: Calif. Div. Mines and Geology Map of California, Olaf P. Jenkins Edition, Scale 1:250,000.

_____, Burnett, J.L., and Troxel, B.W., eds., 1962, Trona sheet: Calif. Div. Mines and Geology Map of California, Olaf P. Jenkins Edition, Scale 1:250,000.

Johnson, B.K., 1957, Geology of a part of the Manly Peak quadrangle, southern Panamint Range, California: Univ. Calif. Pubs. Geol. Sci., v. 30, no. 5, p. 353-424.

Kesseli, J.E., and Beaty, C.B., 1959, Desert flood conditions in the White Mountains of California and Nevada: U.S. Army Quatermaster Research and Eng. Center [Natick, Mass.] Tech. Rept. EP-108, 107p.

Knox, R.E., 1963, Cenozoic deposits of the Emigrant Canyon area, Panamint Range, California: Univ. Southern Calif. M.A. thesis, 101p. [unpub.].

Kohler, M.A, Nordenson, T.J., and Baker, D.R., 1959, Evaporation maps for the United States: U.S. Weather Bur. Tech. Paper 37, 13p.

Lahee, F.H., 1952, Field Geology, 5th ed.: New York: McGraw-Hill, 883p.

Lajoie, K.R., 1968, Late Quaternary stratigraphy and geologic history of Mono Basin, eastern California: Univ. Calif. [Berkeley] Ph.D. thesis, 379p.

_____, Weber, G.E., and Tinsley, J.C., 1972, Marine terrace deformation: San Mateo and Santa Cruz counties: p. 100-113 in: U.S. Geol. Survey Staff and Cummings, J.C., eds., 1972, Progress report on the U.S.G.S. Quaternary studies in the San Francisco Bay area: an informal collection of preliminary papers: Guidebook for Friends of the Pleistocene, October 6,7,8, 1972, 164p.

Langbein, W.B., et al, 1949, Annual runoff in the United States: U.S. Geol. Survey Circ. 52, 14p.

_____, 1961, Salinity and hydrology of closed lakes: U.S. Geol. Survey Prof. Paper 412, 20p.

Lanphere, M.A., 1962, Geology of the Wildrose area, Panamint Range, California: Calif. Inst. Technology Ph.D. thesis.

_____, Dalrymple, G.B., and Smith, R.L., 1975, K-Ar ages of Pleistocene rhyolitic volcanism in the Coso Range, California: Geology, v. 3, no. 6, p. 339-341.

Lee, C.H., 1912, An intensive study of the water resources of a part of Owens Valley, California: U.S. Geol. Survey Water-Supply Paper 294, 135p.

_____, 1927, Evaporation on United States reclamation projects: discussion: Am. Soc. Civil Engineers Trans., v. 90, p. 330-343.

_____, 1935, Discussion of "Evaporation from large water-surfaces based on records in California and Nevada: Am. Geophys. Union Trans., 1935, p. 511-512.

Lee, W.T., 1906, Geology and water resources of Owens Valley, California: U.S. Geol. Survey Water-Supply Paper 181, 28p.

Lombardi, O.W., 1964, Extreme deformation in Saline Valley, California, as related to the general deformation of the western United States [abs]: Geol. Soc. America Spec. Paper 76 [Abs. for 1963], p. 281.

Martin, P.S., 1964, Pollen analysis and the full-glacial landscape: p. 66-73 in: Hester, J.J., and Schoenwetter, J., eds., 1964, The reconstruction of past environments: Taos, N.M.: Fort Bergwin Research Center Pub. 3.

Maxson, J.H., 1950, Physiographic features of the Panamint Range, California: Geol. Soc. America Bull., v. 61, p. 99-114.

Mayo, E.B., 1934, The Pleistocene Long Valley Lake in eastern California: Science, v. 80, p. 95-96.

McAllister, J.F., 1956, Geologic map of the Ubehebe Peak quadrangle, California: U.S. Geol. Survey Geol. Quad. Map GQ-95.

McDowell, S.D., 1967, The intrusive history of the Little Chief granite porphyry stock, Panamint Range, California: Calif. Inst. Technology Ph.D. thesis.

_____, 1974, Emplacement of the Little Chief stock, Panamint Range, California: Geol. Soc. America Bull., v. 85, p. 1535-1546.

McKee, E.H., 1968, Age and rate of movement of the northern part of the Death Valley-Furnace Creek fault zone, California: Geol. Soc. America Bull, v. 79, p. 509-512.

Mehringer, P.J., Jr., 196 , Late Pleistocene vegetation in the Mohave Desert of southern Nevada: Jour. Arizona Acad. Sci., v. 3, no. 3, p. 172-188.

_____, 1967, Late Quaternary vegetation in the Mohave Desert (U.S.A.): Rev. Paleobotany and Palynology, v. 2, p. 319-320.

Michael, E.D., 1966, Large lateral displacement on Garlock Fault, California, as measured from offset fault system: Geol. Soc. America Bull., v. 77, p. 111-114.

Mifflin, M.D., and Wheat, M., 1971, Isostatic warping in Lahontan basin, northwestern Great Basin [abs]: Geol. Soc. America Abs. with Programs, v. 3, no. 7, p. 647.

Moore, S.C., 1974, Syn-batholithic thrusting of Jurassic? age in the Argus Range, Inyo County, California [abs]: Geol. Soc. America Abs. with Programs, v. 6, no. 3, p. 223.

Mörner, N.A., 1972, World climate during the last 130,000 years: Internat. Geol. Cong., sess. 24, sec. 12, p. 72-79.

Morrison, R.B., 1965a, Lake Bonneville: Quaternary stratigraphy of eastern Jordan Valley, south of Salt Lake City, Utah: U.S. Geol. Survey Prof. Paper 477, 77p.

_____, 1965b, Quaternary geology of the Great Basin: p. 265-285 in: Wright, H.E., Jr., and Frey, D.G., eds., 1965, The Quaternary of the United States: a review volume for the VII Congress of the International Association for Quaternary Research: Princeton, N.J.: Princeton Univ. Press, 922p.

_____, 1965c, Radiocarbon chronologies of lakes Lahontan and Bonneville: a stratigraphic evaluation [abs]: Internat. Assoc. Quaternary Research, 7th Internat. Cong. (Boulder and Denver, Colo., U.S.A.), Abstracts, p. 347.

_____, and Frye, J.C., 1965, Correlation of the middle and late Quaternary successions of the Lake Lahontan, Lake Bonneville, Rocky Mountain (Wasatch Range), southern Great Plains, and eastern Midwest areas: Nevada Bur. Mines, Rept. 9, 45p.

Motts, W.S., and Carpenter, David, 1968, Report of test drilling on Rogers, Coyote, Rosamond and Panamint playas in 1966: p. 31-57 in: Neal, J.T., ed., 1968, Playa surface morphology: miscellaneous investigations: Air Force Cambridge Research Lab. Environmental Research Papers, no. 283, 150p.

Moyle, W.R., Jr., 1969, Water wells and springs in Panamint, Searles, and Knob valleys, San Bernardino and Inyo Counties, California: Calif. Dept. Water Resources Bull. 91-17, 110p.

Muehlberger, W.R., 1954, Geology of the Quail Mountains, San Bernardino County, California: Map Sheet 16 in: Jahns, R.H., ed., 1954, Geology of southern California: Calif. Div. Mines Bull. 170, 671p.

Murphy, F.M., 1930, Geology and ore deposits of a part of the Panamint Range, California: Calif. Inst. Technology M.S. thesis [unpub.].

_____, 1932, Geology of a part of the Panamint Range, California: Calif. Div. Mines, Rept. State Mineralogist, v. 28, p. 329-355.

Noble, L.F., and Wright, L.A., 1954, Geology of the central and southern Death Valley region, California: ch. 2, p. 143-160 in: Jahns, R.H., ed., 1954, Geology of southern California: Calif. Div. Mines Bull. 170, 671p.

Olsson, I.U., 1968, Modern aspects of radiocarbon dating: Earth Sci. Rev., v. 4, p. 203-218.

_____, and Eriksson, K.G., 1965, Remarks on C^{14} dating of shell materials in sea sediments: Prog. Oceanography, v. 3, p. 253-266.

Olsson, I.U., Göksu, Yeter, and Stenberg, Allan, 1968, Further investigations of storing and treatment of foraminifera and mollusks for C^{14}-dating: Geol. Fören. i Stockholm Förh., v. 90, p. 417-426.

Pakiser, L.C., Jr., Kane, M.F., and Jackson, W.H., 1964, Structural geology and volcanism of Owens Valley region, California-- a geophysical study: U.S. Geol. Survey Prof. Paper 438, 68p.

Paterson, W.S.B., 1969, The physics of glaciers: Oxford: Pergamon Press, 250p.

Porter, S.C., 1971, Fluctuations of late Pleistocene alpine glaciers in western North America: p. 307-329 in: Turekian, K.K., ed., 1971, The late Cenozoic glacial ages: New Haven and London: Yale Univ. Press, 606p.

Putnam, W.C., 1949, Quaternary geology of the June Lake district, California: Geol. Soc. America Bull., v. 60, p. 1281-1302.

_____, 1960, Origin of Rock Creek and Owens River gorges, Mono County, California: Univ. Calif. Pubs. Geol. Sci., v. 34, no. 5, p. 221-280.

_____, 1962, Late Cenozoic geology of McGee Mountain, Mono County, California: Univ. Calif. Pubs. Geol. Sci., v. 40, no. 3, p. 181-218.

Richmond, G.M., 1964, Glaciation of Little Cottonwood and Bells canyons, Wasatch Mountains, Utah: U.S. Geol. Survey Prof. Paper 454-D, 41p.

_____, and Obradovich, J.D., 1972, Radiometric correlation of some continental Quaternary deposits: a review [abs]: American Quaternary Assoc., 2nd Nat. Conf., Abs., p. 47-49.

Richter, C.F., 1958, Elementary Seismology: San Francisco: W.H. Freeman and Co., 768p.

Rinehart, C.D., and Ross, D.C., 1957, Geology of the Casa Diablo Mountain quadrangle, California: U.S. Geol. Survey Geol. Quad. Map GQ-99.

_____, and Ross, D.C., 1964, Geology and mineral deposits of the Mount Morrison quadrangle, Sierra Nevada, California: U.S. Geol. Survey Prof. Paper 385, 106p.

Ross, D.C., ed., 1967, Generalized geologic map of the Inyo Mountains region, California: U.S. Geol. Survey Misc. Geol. Inv. Map I-506.

Russell, I.C., 1885, Geological history of Lake Lahontan, a Quaternary lake of northwestern Nevada: U.S. Geol. Survey Mon. 11, 288p.

Saint-Amand, Pierre, Lombardi, O.W., and Shuler, H., 1963, Earthquakes of the western United States: Bol. Bibliog. de Geofisica y Oceanografia Americanas, v. 3, p. 40-105.

Schumm, S.A., 1965, Quaternary Paleohydrology: p. 783-794 in: Wright, H.E., Jr., and Frey, D.G., eds., 1965, The Quaternary of the United States: a review volume for the VII Congress of the International Association for Quaternary Research: Princeton, N.J.: Princeton Univ. Press, 922p.

Scholl, D.W., 1960, Pleistocene algal pinnacles at Searles Lake, California: Jour. Sed. Petrology, v. 30, no. 3, p. 414-431.

Sharp, R.P., 1968, Sherwin till-Bishop tuff geological relationships, Sierra Nevada, California: Geol. Soc. America Bull., v. 79, p. 351-364.

_____, 1969, Semiquantitative differentiation of glacial moraines near Convict Lake, Sierra Nevada, California: Jour. Geology, v. 77, p. 68-91.

_____, 1972, Pleistocene glaciation, Bridgeport Basin, California: Geol. Soc. America Bull., v. 83, p. 2233-2260.

_____, and Birman, J.H., Additions to the classical sequence of Pleistocene glaciations, Sierra Nevada, California: Geol. Soc. America Bull., v. 1079-1086.

Shelton, J.S., 1966, Geology illustrated: San Francisco and London: W.H. Freeman and Co., 434p.

Smith, G.I., 1962, Large lateral displacement on Garlock Fault, California, as measured from offset dike swarm: Am. Assoc. Petroleum Geologists Bull., v. 46, p. 85-104.

_____, 1968, Late-Quaternary geologic and climatic history of Searles Lake, southeastern California: p. 293-309 in: Morrison, R.B., and Wright, H.E., Jr., eds., 1968, Means of correlation of Quaternary successions: Salt Lake City: Univ. Utah Press, 631p. [Internat. Assoc. Quaternary Research, Proc. 7th Cong., v. 8].

_____, and Ketner, K.B., 1971, Lateral displacement on the Garlock Fault, southeastern California, suggested by offset sections of similar metasedimentary rocks: U.S. Geol. Survey Prof. Paper 700-D, p. D1-D9.

Smith, G.I., and Pratt, W.P. 1957, Core logs from Owens, China, Searles and Panamint basins, California: U.S. Geol. Survey Bull. 1045-A, 62p.

_____, Troxel. B.W., Gray, C.H., Jr., and von Huene, Roland, 1968, Geologic reconnaissance of the Slate Range, San Bernardino and Inyo counties, California: Calif. Div. Mines and Geology Spec. Rept. 96, 33p.

Smith, R.S.U., 1972, Tentative correlation of pluvial events in Panamint Valley, California, with Sierra Nevada Pleistocene glaciations [abs]: Geol. Soc. America Abs. with Programs, v. 4, no. 7, p. 671-672.

_____, 1973, Tectonic deformation of pluvial-lake terraces along the Panamint Valley fault zone, eastern California [abs]: Geol. Soc. America Abs. with Programs, v. 5, no. 1, p. 108-109.

_____, 1974, Quaternary thrust movement on a boundary fault at the north end of Panamint Valley, western Basin-and-Range province, California [abs]: Geol. Soc. America Abs. with Programs, v. 6, no. 3, p. 256-257.

_____, 1975, Guide to selected examples of Quaternary tectonism in Panamint Valley, California: p. 112-115 in: Slemmons, D.B., ed., 1975, A field guide to Cenozoic deformation along the Sierra Nevada province and Basin and Range province boundary: California Geology, v. 28, no. 5, p. 99-119.

Snyder, C.T., Hardman, George, and Zdenek, F.F., 1964, Pleistocene lakes in the Great Basin: U.S. Geol. Survey Misc. Geol. Inv. Map I-416.

_____, and Langbein, W.B., 1962, The Pleistocene lake in Spring Valley, Nevada, and its climatic implications: Jour. Geophys. Research, v. 67, p. 2385-2394.

Spreen, W.C., 1947, A determination of the effect of topography on precipitation: Am. Geophys. Union Trans., v. 28, no. 2, p. 285-290.

Stewart, J.H., 1967, Possible large right-lateral displacement along fault and shear zones in the Death Valley-Las Vegas area, California and Nevada: Geol. Soc. America Bull., v. 78, p. 131-142.

_____, Albers, J.P., and Poole, F.G., 1968, Summary of regional evidence for right-lateral displacement in the western Great Basin: Geol. Soc. America Bull., v. 79, p. 1407-1414.

Stewart, J.H., Albers, J.P., and Poole, F.G., 1970, Summary of regional evidence for right-lateral displacement in the western Great Basin: reply: Geol. Soc. America Bull., v. 81, p. 2175-2180.

Stuiver, Minze, 1964, Carbon isotopic distribution and correlated chronology of Searles Lake sediments: Am. Jour. Sci., v. 262, p. 377-392.

Thompson, D.G., 1929, The Mohave Desert region, California: a geographic, geologic and hydrologic reconnaissance: U.S. Geol. Survey Water-Supply Paper 578, 759p.

Thompson, J.H., 1963, Precambrian geology of the Emigrant Canyon area, Panamint Range, California: Univ. Southern California M.S. thesis [unpub.].

Thurber, D.L., 1972, Problems of dating non-woody material from continental environments: p. 1-17 in: Bishop, W.W., and Miller, J.A., eds., 1972, Calibration of hominoid evolution: recent advances in isotopic and other dating methods applicable to the origin of man: Edingurgh: Scottish Academic Press, 478p.

Townley, S.D., and Allen, M.W., 1939, Descriptive catalog of earthquakes of the Pacific coast of the United States 1769-1928: Bull. Seismol. Soc. America, v. 29, p. 1-297.

U.S. Dept. Commerce, 1959-1974, Climatological data for California: annual summary [1958-1973]: Asheville, N.C.: Environmental Data Service.

_____, 1967-1971, Storage-gage precipitation data for the western United States, v. 11-15 [1965-6 to 1969-70]: Asheville, N.C.: Environmental Data Service.

U.S. Geol. Survey, 1967-1973, Water resources data for California-part 1. Surface water records, v. 1: Colorado River basin, southern Great Basin, and Pacific slope basins excluding Central Valley [1965-71]: Menlo Park, Calif.: Water Resources Div.

Waananem, A.O., 1971, Floods from small drainage areas in California: a compilation of peak data, October 1958 to September 1970: U.S. Geol. Survey Open File Rept., 134p.

Wells, P.V., and Jorgensen, C.D., 1964, Pleistocene wood rat middens and climatic change in Mohave Desert: a record of juniper woodlands: Science, v. 143, p. 1171-1173.

_____, and Berger, Rainer, 1967, Late Pleistocene history of Coniferous woodland in the Mohave Desert: Science, v. 155, p. 1640-1647.

Wilson, W.T., 1954, Precipitation at Barrow, Alaska, greater than recorded: discussion: Am. Geophys. Union Trans., v. 35, no. 2, p. 206-207.

Wahrhaftig, Clyde, and Birman, J.H., 1965, The Quaternary of the Pacific mountain system in California: p. 299-340 in: Wright, H.E., Jr., and Frey. D.G., eds., 1965, The Quaternary of the United States: a review volume for the VII Congress of the International Association for Quaternary Research: Princeton, N.J.: Princeton Univ. Press, 922p.

Wornardt, W.W., Jr., 1964, Pleistocene diatoms from Mono and Panamint lake basins, California: Calif. Acad. Sci. Occasional Paper 46, 27p.

Wright, L.A., and Troxel, B.W., 1954, Western Mojave Desert and Death Valley region: Geologic Guide no. 1 in: Jahns, R.H., ed., 1954, Geology of southern California: Calif. Div. Mines Bull. 170.

_____, and Troxel, B.W., 1967, Limitations on right-lateral, strike-slip displacement, Death Valley and Furnace Creek fault zones, California: Geol. Soc. America Bull., v. 78, p. 933-950.

_____, and Troxel, B.W., 1970, Summary of regional evidence for right-lateral displacement in the western Great Basin: discussion: Geol. Soc. America Bull., v. 81, p. 2167-2174.

Young, A.A., 1948, Evaporation from water surfaces in California: basic data: Calif. Div. Water Resources Bull. 54-A, 205p.